COMBATING *PSEUDOMONAS AERUGINOSA* LUNG INFECTIONS USING SYNTHETIC HOST DEFENSE PEPTIDES

by

Kelli Wuerth

B.S., Washington State University, 2009

A THESIS SUBMITTED IN PARTIAL FULFILLMENT OF

THE REQUIREMENTS FOR THE DEGREE OF

DOCTOR OF PHILOSOPHY

in

THE FACULTY OF GRADUATE AND POSTDOCTORAL STUDIES

(Microbiology and Immunology)

THE UNIVERSITY OF BRITISH COLUMBIA

(Vancouver)

August 2017

Abstract

Pseudomonas aeruginosa is a Gram negative bacterium found frequently in the environment. It can infect immunocompromised patients and is a major cause of nosocomial infections. Of particular concern are its roles in lung infections as a causative agent for pneumonia and in respiratory infections in patients with cystic fibrosis and chronic obstructive pulmonary disease. Treatment of *P. aeruginosa* lung infections is difficult due to its formation of biofilms and the development of multi-drug resistant *P. aeruginosa* strains. Synthetic derivatives of host defense peptides (HDPs) called innate defense regulators (IDRs) are alternatives to antibiotics that modulate the immune response rather than directly targeting the bacteria, thus limiting the development of antibiotic resistance. IDRs have shown success against many bacteria but had not previously been tested in *P. aeruginosa* lung infection models. In this work, IDR-1002 reduced the production of inflammatory cytokines by macrophages in response to *P. aeruginosa* lipopolysaccharide. IDR-1002 also limited the toxicity caused by live *P. aeruginosa* to macrophages and bronchial epithelial cells. Importantly, IDR-1002 did not show any toxic effects in vitro, unlike the HDP LL-37. In an acute in vivo *P. aeruginosa* lung infection model, IDR-1002 significantly decreased the bacterial burden as well as the concentrations of MCP-1, KC, and IL-6 in the lungs. In another in vivo *P. aeruginosa* lung infection model using alginate to mimic a chronic infection, IDR-1002 decreased the infiltration of cells to the infection site and significantly decreased IL-6 levels in the lungs. To improve drug delivery, peptide IDR-1018, which has a strong aggregation propensity, was tested with various formulations, and its combination with a hyperbranched polyglycerol reduced the production of inflammatory cytokines in vitro and trended towards reducing cytokines in vivo in the acute *P. aeruginosa* lung infection model. Finally, RNA-Seq and downstream bioinformatics were performed on both lung and blood samples from the acute *P. aeruginosa* lung infection model, providing insights into the impact of *P. aeruginosa* during infection and the protective mechanisms of IDR-1002 via its anti-inflammatory effects. These data suggest the strong potential of IDR-1002 for the treatment of *P. aeruginosa* lung infections.

Lay Summary

Antibiotic resistance is expected to be one of the most serious health crises of the 21st century. One type of bacterium that is already demonstrating resistance to multiple antibiotics is *Pseudomonas aeruginosa*. This bacterium is a frequent cause of pneumonia and other lung infections, particularly in patients with cystic fibrosis and chronic obstructive pulmonary disease. Treatment of *P. aeruginosa* lung infections is difficult due to both inherent and acquired resistance. In this thesis, I examined an alternative to traditional antibiotics, called IDR-1002, for use against *P. aeruginosa* infections. In two types of cells and in two models of lung infection in mice, I demonstrated that IDR-1002 reduces inflammation and can also decrease the number of bacteria in the lungs. I also examined formulations to improve drug delivery and the host responses to both bacteria and IDR-1002. Overall, this thesis demonstrates the potential of IDR-1002 for use against *P. aeruginosa* infections.

Preface

All research was conducted at the University of British Columbia (UBC), Vancouver, in accordance with the ethics approval from the UBC Office of Research Services Clinical Research Ethics board for human subject research under ethics certificate H04-70232 and from the UBC Animal Care Committee for mouse experiments under protocol number A13-0227.

Dr. R.E.W. (Bob) Hancock was the thesis supervisor and provided guidance on manuscripts and thesis concepts.

Portions of the experiments in Chapter 2 are included in the following manuscript in preparation: **Wuerth, K.**, Falsafi, R., and Hancock, R.E.W. Synthetic host defense peptide IDR-1002 reduces inflammation in multiple models of *Pseudomonas aeruginosa* lung infection. I designed, performed, analyzed, and wrote up all experiments in the chapter, with Mr. Reza Falsafi providing technical assistance in sample collection for the experiments shown in Figures 2.18-2.21.

In Chapter 3, I designed, performed, analyzed, and wrote up all experiments in the chapter with the following acknowledgments: Dr. Anthony Boey and Dr. Nazila Safaei Nikouei at the Centre for Drug Research and Development provided the formulated peptide, and Dr. Evan Haney provided assistance in experimental design and technical assistance for some of the cell culture experiments.

Experiments in Chapter 4 are included in the following manuscript in preparation: **Wuerth, K.**, Lee, A., Falsafi, R., Gill, E.E., and Hancock, R.E.W. Characterization of host responses during *Pseudomonas aeruginosa* acute lung infection in the lungs and blood and the effects of synthetic immunomodulatory peptide IDR-1002. I designed, performed, analyzed, and wrote up all experiments in the chapter with the following acknowledgments: Mr. Reza Falsafi isolated the RNA and performed the RNA-Seq; Dr. Amy Lee aligned the RNA-Seq results and generated count tables; and both Dr. Amy Lee and Dr. Erin Gill provided guidance on differential expression analysis.

Table of Contents

List of Tables

List of Figures

List of Abbreviations

AHL – N-acyl-homoserine lactone

AMP – antimicrobial peptide

APC – antigen-presenting cell

AQ – 2-alkyl-4-quinolone

ASL – airway surface liquid

BALF – bronchoalveolar lavage fluid

BMDM – bone marrow-derived macrophage

CDC – Centers for Disease Control and Prevention

CF – cystic fibrosis

CFTR – cystic fibrosis transmembrane conductance regulator

CFU – colony-forming unit

CMC – carboxymethyl cellulose

COPD – chronic obstructive pulmonary disease

CRAMP – cathelin-related antimicrobial peptide

DC – dendritic cell

DE – differentially expressed

ECM – extracellular matrix

EF-2 – elongation factor-2

FBS – fetal bovine serum

F-moc – N-(9-fluorenyl) methoxycarbonyl

GO – gene ontology

H&E – hematoxylin and eosin

HA – hyaluronic acid

HAP – hospital-acquired pneumonia

hBD – human beta-defensin

HBE cells – 16HBE14o- cells (human bronchial epithelial cell line)

HDP – host defense peptide

HKPA103 – heat-killed *P. aeruginosa* strain PA103

HKPAO1 – heat-killed *P. aeruginosa* strain PAO1

HNP – human neutrophil peptide

HPG – hyperbranched polyglycerol

HPMC – hydroxypropyl methyl cellulose

ICU – intensive care unit

IDR – innate defense regulator

IN – intranasal / intranasally

IP – intraperitoneal / intraperitoneally

IT – intratracheal / intratracheally

IV – intravenous / intravenously

LBP – lipopolysaccharide binding protein

LDH – lactate dehydrogenase

LPS – lipopolysaccharide

LTA – lipoteichoic acid

MDR – multi-drug resistance / multi-drug resistant

MIC – minimum inhibitory concentration

MMP – matrix metalloproteinase

MOI – multiplicity of infection

NLR – Nod-like receptor

ORA – overrepresentation analysis

PAS – periodic acid-Schiff

PBMC – peripheral blood mononuclear cell

PCA – principal component analysis

Poly I:C – polyinosinic:polycytidylic

PRR – pattern recognition receptor

QS – quorum sensing

RAW cells – RAW264.7 cells (mouse macrophage cell line)

RLR – RIG-I-like receptor

RNS – reactive nitrogen species

ROS – reactive oxygen species

T3SS – type 3 secretion system

TBS – Tris-buffered saline

TFA – trifluoroacetic acid

TLR – Toll-like receptor

UTI – urinary tract infection

VAP – ventilator-associated pneumonia

WT – wild-type

Acknowledgements

I would like to thank my supervisor, Dr. Bob Hancock, for bringing me into the laboratory and giving me the opportunity to undertake graduate studies. Thank you for your guidance and support over the years and the freedom to develop this thesis work as an independent researcher.

I also want to thank my committee members, Dr. Mike Gold, Dr. Marc Horwitz, and Dr. Bruce Vallance, for their suggestions and guidance during this project.

Thank you to the Hancock lab members who have supported me during graduate school. I am especially grateful to Mr. Reza Falsafi and Dr. Shaan Gellatly for their encouragement and advice.

I also wish to thank the Modified Barrier Facility staff for all of their hard work—none of the in vivo work would have been possible without you.

Thank you to Cystic Fibrosis Canada for providing funding in the form of a doctoral studentship award for my thesis work.

Finally, thank you to my parents; my sister, Michelle; and Rashid for their endless support over these many years, I could not have done this without you.

Dedication

To my family

Chapter 1: Introduction

1.1 *Pseudomonas aeruginosa*

Pseudomonas aeruginosa is a Gram negative, rod-shaped bacterium in the gammaproteobacteria family. It is ubiquitous in the environment and has been isolated from water and soil samples worldwide. It can also occasionally be found as part of the normal human flora on the skin, in the gastrointestinal tract, and in the lungs (1, 2). As such, it does not normally cause problems in healthy individuals, but in immunocompromised patients, or in cases where it has been introduced into new sites, it can lead to infections that can be fatal. Indeed, *P. aeruginosa* is one of the leading causes of death from lung infections. Antibiotics are typically the first medical response to a *P. aeruginosa* infection, but intrinsic and adaptive resistance mechanisms and the rise of acquired multi-drug resistance (MDR) have reduced their effectiveness in treating *Pseudomonas* infections. Unsurprisingly, *P. aeruginosa* is one of the leading resistant pathogens in a hospital setting, and the United States Centers for Disease Control and Prevention (CDC) classified *P. aeruginosa* as a serious threat, the second highest level, in their report on antibiotic resistance (3). Therefore, understanding the pathogenesis of *Pseudomonas* and exploring alternative treatment methods are critical for reducing the morbidity and mortality caused by its infection.

1.1.1 Virulence factors

P. aeruginosa has numerous virulence factors that promote infection (4-6). Pyocyanin and pyoverdine, which are responsible for its characteristic green-blue color, serve multiple roles in infection (7-10). Pyoverdine, along with pyochelin, acts as a siderophore and acquires iron for growth, while pyocyanin inactivates catalase and interferes with the redox system in eukaryotes, leading to the production of inflammatory reactive oxygen species (ROS) (4, 8, 11).

P. aeruginosa produces several toxins, most notably exotoxin A, which is released by the type 2 secretion system and inhibits elongation factor-2 (EF-2) in eukaryotes, thus stopping polypeptide production (12). Depending on the strain of *P. aeruginosa*, it can also produce the exoenzymes ExoS,

ExoT, ExoU, and/or ExoY, all secreted by the type 3 secretion system (T3SS), a needle-like apparatus that is used to inject toxins into neighboring cells and cause necrosis (13-15). ExoU causes the most cellular damage due to its phospholipase A2 activity, which is an activity also induced by the peptide melittin that is found in snake and insect venom (14, 16, 17). *P. aeruginosa* can also produce phospholipase C and many proteases, including elastase (4, 18). These enzymes can be used to break down intercellular tight junctions and host-produced immune mediators to enable the bacteria to spread through the host and blunt the resulting host immune response (19, 20). As with all Gram negative bacteria, *P. aeruginosa* has lipopolysaccharide (LPS) in its outer membrane, which strongly induces immune responses that are highly inflammatory. It is also the major serotype antigen (20). *P. aeruginosa* has type IV pili and a single polar flagellum for motility, although these can be lost in some strains, particularly those found in chronic infections (21-24). Although motility is not strictly necessary for infection, it enhances *P. aeruginosa* virulence (21).

One of the critical aspects of many *P. aeruginosa* infections is its formation of biofilms (25, 26). These are organized multi-cellular structures, held together by a matrix consisting of exopolysaccharides and extracellular DNA, which serve to protect the bacteria from host immunity and antibiotics (26, 27). The major exopolysaccharides in the biofilm matrix are Psl and Pel (28, 29). Another exopolysaccharide that can be found in *P. aeruginosa* biofilms is alginate, which is a linear polymer made of (1,4)-linked β-D-mannuronate and α-L-guluronate subunits that is analogous to the alginate found in seaweed (30, 31). It is estimated that between 65-80% of microbial infections are caused by bacteria growing in biofilms (32). The major steps of biofilm formation involve 1) initial surface attachment, 2) formation of microcolonies, 3) formation of macrocolonies, and 4) dispersal. The formation of biofilms can be directed in part through quorum sensing (QS), a process in which bacteria at sufficient concentrations release signaling molecules above a minimum threshold that signal neighboring bacteria to alter their behavior (33). In *P. aeruginosa*, the QS molecules include N-acyl-homoserine lactones (AHLs) and 2-alkyl-4-quinolones (AQs) (34). When a minimum number of

bacteria are present and producing sufficient levels of specific AHLs or AQs, the bacteria can be directed to form a structured biofilm. QS is also involved in other processes including iron uptake, the production of virulence factors that impact the effectiveness of the host immune system, and certain types of surface motility, such as swarming motility that involves the coordinated movement of multiple bacteria (34).

1.1.2 Antibiotic resistance

P. aeruginosa antibiotic resistance falls into one of three categories: 1) intrinsic, 2) adaptive, or 3) acquired. Intrinsic resistance mechanisms that are inherent in all *P. aeruginosa* include low outer membrane permeability, as well as the presence of a chromosomal AmpC β-lactamase and multiple efflux pumps to destroy and quickly remove antibiotics from within the cell, respectively (4, 35). Porins, which are channels in the outer membrane, are typically reduced in overall number and effectiveness in *P. aeruginosa* (4, 36), thus slowing the entry of antibiotics into *P. aeruginosa* cells.

Adaptive resistance is activated in response to specific environmental conditions, such as a change in pH, decrease in cations such as Ca^{2+} or Mg^{2+}, or the presence of antibiotics or certain carbon sources (36, 37). Growth in biofilms or swarming motility can also act as triggers. This resistance is largely due to alterations in multiple resistance mechanisms including increases in efflux pump expression, reduction in the negative charge of LPS to limit the interaction of positively charged molecules such as polymyxin antibiotics, and increases in β-lactamase production (37). Importantly, this adaptive resistance only lasts while the environmental stimulus is present; once it is removed, the resistance mechanisms are downregulated.

Finally, acquired resistance is genetically encoded resistance, either attained from external sources by DNA transfer from other species of bacteria or other strains of *P. aeruginosa*, or occurring through the selection of mutations that increase drug resistance (4, 36). Examples include acquiring plasmid-encoded β-lactamases or aminoglycoside-modifying enzymes or mutations upregulating efflux pumps that increase their effectiveness in expelling antibiotics (36, 38). This form of resistance

is the most critical for the development of MDR strains (35), although adaptive resistance also contributes to MDR (37).

1.2 *P. aeruginosa* infections in humans

P. aeruginosa infects numerous epithelial locations, including burns, wounds, the urinary tract, the conjunctiva of the eyes, and the lungs. Due to its role as an opportunistic pathogen, it is a frequent cause of nosocomial (hospital-acquired) infections. *P. aeruginosa* accounts for almost 10% of the isolates found in either hospital-wide pneumonia or urinary tract infections (UTIs), which increases to nearly 20% when only intensive care unit (ICU) cases are considered (39). It colonizes catheters and other in-dwelling medical implants, aided by its formation of biofilms, and is the third most common cause of catheter-associated UTIs (40). It is also found in 19.3% of burn infections, second only to *Staphylococcus aureus* (41). However, lung infections are one of the most critical forms of *P. aeruginosa* infection in terms of both morbidity and mortality.

1.2.1 *P. aeruginosa* lung infections and the immune response

The respiratory tract is constantly exposed to microbes during inhalation. In immunocompetent patients, microbes can be removed through mechanical or immunological activity. However, in immunocompromised patients or in those with damage to the respiratory tract, microbes may enter the lungs and cause infection. Cystic fibrosis (CF), chronic obstructive pulmonary disease (COPD), and pneumonia are diseases in which *P. aeruginosa* infections play a key role in disease pathogenesis (42, 43).

CF is an autosomal recessive genetic disorder caused by mutations or deletions in the cystic fibrosis transmembrane conductance regulator (CFTR) gene. Changes in CFTR affect the secretion of mucus and liquids due to its role as a cAMP-regulated chloride ion channel (44-46). This can affect numerous secretory organs, including the respiratory tract, gastrointestinal tract, pancreas, and the male reproductive organs (47). The effects of CF in the lungs are some of the most serious as they

prevent proper clearance of the airways and usually lead to bronchiectasis. In childhood, most CF patients are infected by *S. aureus*, although studies have indicated that 21-29% of infants with CF still acquire *P. aeruginosa* within the first 6-12 months of life (48, 49). However, by late adolescence *S. aureus* has been largely displaced by *P. aeruginosa*, with 80% of CF patients infected by *P. aeruginosa* before reaching their mid-twenties (48). Colonization by *P. aeruginosa* is associated with increased morbidity and mortality (50), and while advances in treatment have greatly extended the average lifespan and quality of life of CF patients, the median lifespan is still only around 40 years (44).

COPD is a progressive lung disease characterized by breathing difficulties. It has multiple risk factors, although cigarette smoking is often an underlying cause. Patients have frequent lung infections, and *P. aeruginosa* has been isolated from patient samples in numerous studies (43). As with CF, *P. aeruginosa* infection in COPD is associated with the later stages of the disease and with exacerbations, although its overall contribution to COPD symptoms is debated (43, 51). Overall, COPD results in 3 million deaths annually worldwide (52).

Pneumonia is inflammation in the lungs, often accompanied by a buildup of fluid and occasionally by bronchiectasis. Two common forms are hospital-acquired pneumonia (HAP) and ventilator-associated pneumonia (VAP), which together are the second most common form of nosocomial infection and result in 30-62% mortality (53, 54). Although most HAP cases are caused by viruses or *Streptococcus pneumoniae*, *P. aeruginosa* is a common cause of pneumonia in late-onset and ICU cases, being found in 18.1% of ICU pneumonia cases (39). Pneumonia also frequently affects people outside of the hospital environment, with risk factors including having COPD or CF. However, it can also occur in otherwise healthy individuals.

P. aeruginosa lung infections begin when the bacteria enter the respiratory tract through aspiration from the gastrointestinal tract or from inhalation through the nose and initial colonization of the sinuses (44). The environment in the respiratory tract is affected by the presence of the airway surface liquid (ASL) interface. The ASL is composed of two thin layers, with the bottom aqueous

periciliary (sol) layer adjacent to the ciliated epithelial surface and the top layer containing mucus (45, 55). In a healthy respiratory tract, the ASL has a watery consistency and can contain neutrophils, macrophages, surfactants, mucins, host defense peptides such as β-defensins and LL-37, and larger antimicrobial proteins such as lactoferrin and lysozyme (45, 56). Microbes can become trapped in the top layer of the mucus, which is then moved by the beating action of cilia on epithelial cells in the lower watery layer, a process called mucociliary clearance (45, 57). This allows the removal of most microbes. However, this process is often compromised in patients at risk for lung infections. In CF patients, the ASL is viscous due to the dysregulation of ion movement and has increased acidity, both of which limit the antimicrobial activities of the ASL, the beating of cilia, and the function of epithelial cells (45, 46, 58). In addition, other factors have been suggested as being involved in the mechanism of initial colonization, including increased receptor expression and decreased epithelial cell phagocytosis (59). In COPD, cilia function is often damaged from smoke exposure, which thus hampers mucociliary clearance (60, 61).

As the initial barriers are breached, *P. aeruginosa* can be detected by pattern recognition receptors (PRRs) on host cells. PRRs are divided into several structural families, with the most critical being the Toll-like receptors (TLRs), Nod-like receptors (NLRs), and RIG-I-like receptors (RLRs). For *P. aeruginosa*, key PRRs include TLR4, which binds LPS with the help of MD2, CD14, and LPS binding protein (LBP), as well as TLR5, which detects the structural component of the flagellum called flagellin (62-65). Additionally, the TLR1/2 complex that detects triacylated lipopeptides and the internal TLR9, which detects unmethylated CpG DNA motifs, can recognize these motifs in *P. aeruginosa* (62, 66). ExoS has also been reported to activate TLR2 and TLR4 (67). For the NLRs, NOD1 (also called NLRC1) detects *P. aeruginosa* peptidoglycan while NLRC4 (also called IPAF) in combination with NAIP5 detects flagellin (68-70). NLRC4 also detects the T3SS, although the T3SS product ExoU can also inactivate NLRC4 (71). Other receptors include asialylated glycolipids containing GalNAcβ1-4Gal, notably asialoGM1, which recognizes *P. aeruginosa* pili and flagellin

(59, 72, 73). Human neutrophils have also been shown to detect a *P. aeruginosa* QS molecule, the AHL N-(3-oxododecanoyl)-L-homoserine lactone, through the bitter taste receptor T2R38 (74), and the neutrophils use CR3 or CD14 to phagocytose the bacteria (75).

Recognition of *P. aeruginosa* by the above TLRs and NOD1 leads to the recruitment of adaptor proteins, most critically MyD88, TRIF, TRAM, and TIRAP for the TLRs, and consequent activation of the NF-κB pathway and the activation of the MAPKs ERK1/2, JNK, and p38 (62, 76). This leads to the upregulated transcription of hundreds of genes as well as the production and release of multiple inflammatory cytokines, including IL-6, TNF-α, and IFN-γ (62, 77). NLRC4 also activates caspase-1, which promotes the maturation and release of IL-1β (69, 71).

Additionally, the release of chemokines such as Gro-α (CXCL1), IL-8, MCP-1, RANTES, and IP-10 leads to the recruitment of immune cells to the site of infection. These cells include neutrophils, which attempt to phagocytize and kill the microbes and also produce ROS and reactive nitrogen species (RNS) (77). However, ExoS and ExoT can limit both neutrophil recruitment and phagocytosis, whereas other virulence factors such as ExoU and elastase are cytotoxic to neutrophils (14, 15). The complement system is also activated during *P. aeruginosa* infection, with roles for C5a and C3a described in the recruitment and opsonization of immune cells (78).

Antigen-presenting cells (APCs) such as dendritic cells (DCs) and macrophages are also present in the lungs and/or can be recruited after infection. These cells are critical for presenting antigens to T cells and activating the adaptive immune response. However, while antibody titers increase in CF patients as the *P. aeruginosa* infection progresses, the adaptive immune system is insufficient for clearing the infection (49).

While the immune system undergoes numerous changes in response to infection, *P. aeruginosa* also adapts to its new environment. During the initial stages, the infection is acute and *P. aeruginosa* produces numerous virulence factors including the exoenzyme toxins, exotoxin A, and proteases. Elastase, which is secreted by both *P. aeruginosa* and host neutrophils, can disrupt tight junctions and

allow bacteria to spread (18, 79). *P. aeruginosa* also induces the shedding of a heparan sulfate proteoglycan, syndecan-1, from epithelial cells, which enhances *P. aeruginosa* virulence (80). Additionally, in vivo evidence in a burn model indicates that *P. aeruginosa* begins to form biofilms as early as eight hours after infection (81). Over time, if the infection is not cleared by the immune system or antibiotic treatment, there is progression to a chronic infection, which is characterized by changes in *P. aeruginosa* cells that allow them to evade the immune response (82). For example, *P. aeruginosa* can turn off the production of flagellin to evade detection by TLR5 and it can also reduce pili expression, rendering many chronic strains non-motile (59). Similarly, LPS loses its O-antigen polysaccharide, making the organism less susceptible to antibody-mediated clearance (83). Additionally, other virulence factors, such as QS and toxins, are dampened (44). Biofilm formation becomes more pronounced, with increasing production of alginate and/or Psl and the development of a mucoid colony phenotype (28, 34, 44). Although there is a massive infiltration of neutrophils into the lungs, the biofilm protects the bacteria from ROS, phagocytosis, and other anti-infective elements (44). As the chronic infection proceeds, the strains of *P. aeruginosa* present also become increasingly antibiotic resistant, and hypermutator mutations speed up the acquisition of resistance and other adaptations that promote chronic bacterial growth (34, 44, 84). In CF and COPD, the host continues to produce inflammatory mediators in response to the infection, but they are usually unsuccessful in clearing it. Intriguingly, in these chronic infections it is usually the host response, rather than the *P. aeruginosa* itself, that causes the most damage to the lungs and the associated morbidity and mortality. Since the host immune system in immunocompromised patients is ineffective at removing the bacteria in chronic lung infections, it is necessary to turn to external treatments.

1.2.2 Treatment options for *P. aeruginosa* lung infections and rise of multi-drug resistant strains

1.2.2.1 Antibiotics

While *P. aeruginosa* infections can occur in a variety of tissues and may involve different forms, such as mucoid strains or biofilms, the major treatment option is inevitably antibiotics. There are four major classes of antibiotics used for *P. aeruginosa*: 1) β-lactams, 2) aminoglycosides, 3), fluoroquinolones, and 4) polymyxins.

There are several variations of β-lactams including carbapenems such as imipenem or meropenem; penicillins such as ticarcillin or piperacillin; cephalosporins such as ceftazidime, cefepime, or ceftobiprole; and monobactams including aztreonam (85-88). These drugs work by inhibiting the production and/or stability of peptidoglycan, a component of the bacterial cell wall (89). Due to intrinsic *P. aeruginosa* resistance to β-lactams through the production of the inducible chromosomal β-lactamase AmpC, these antibiotics are often paired with a β-lactamase inhibitor, such as tazobactam or clavulanic acid, in order to increase effectiveness, or used in combination with an aminoglycoside (90, 91). Modifications in *P. aeruginosa* efflux pumps also increase bacterial resistance to β-lactams.

Anti-pseudomonal aminoglycosides include tobramycin, gentamicin, and amikacin. They bind the bacterial ribosome and inhibit protein synthesis, but unlike many other ribosome inhibitors they are bactericidal. *P. aeruginosa* resistance to aminoglycosides can involve the production of plasmid-mediated aminoglycoside-modifying enzymes that adenylate or phosphorylate the antibiotic (92, 93). However, much of the resistance is due to efflux pump improvement to quickly remove the antibiotics (92, 93). Aminoglycosides have been associated with nephrotoxicity and ototoxicity, but their use for lung infections has expanded due to aerosolized delivery, which allows beneficial effects in the respiratory tract but limits the systemic concentration and thus toxicity (92, 94, 95).

The fluoroquinolones, such as ciprofloxacin and levofloxacin, act on topoisomerase IV and DNA gyrase (96, 97). Resistance can occur frequently through efflux pump upregulation or modification of the targeted enzymes (93).

Polymyxins are cationic lipopeptides that disrupt the bacterial membrane. Polymyxin B and polymyxin E (colistin) are the members used for *P. aeruginosa* infections (98). However, these drugs are also reported to have high nephrotoxicity and neurotoxicity, including neuromuscular blockade, and for many years were only used for topical applications. This toxicity has been partially reduced by chemical modification of the primary amines with methane sulfonate to create a pro-drug (99). The lack of alternative options has led to their more frequent use as inhalation antibiotics in CF in recent years and they are now considered "last resort" antibiotics (4, 91).

For chronic *P. aeruginosa* lung infections, treatment is much more difficult and rarely completely successful. In CF, airway clearance to remove the buildup of mucus is a key part of infection control, which can be done to some extent through treatment with recombinant human DNase I or mucus rehydration (47). Other options in CF include lung transplantation or therapy correcting the *CFTR* product, but due to costs and limited availability and, in the case of CFTR-directed therapy, a limited number of targeted mutants, these treatments are infrequent. For pneumonia and COPD, draining mucus from the lungs is common, but usually only provides temporary relief. COPD is also treated with bronchodilators, steroids, and in some cases lung transplantation. However, when bacterial lung infections occur in COPD patients these treatments are limited due to immunosuppressive side effects. Therefore, the treatment of *P. aeruginosa* lung infections for all of these diseases usually involves the use of antibiotics. In CF, antibiotics are used beginning at an early age in an attempt to prevent, or at least delay, the onset of chronic infection (100). Treatment usually involves a β-lactam in combination with a drug from one of the three other categories, with aerosolized tobramycin, colistin, amikacin, and levofloxacin as common options (91, 101). For COPD, while *P. aeruginosa* infections occur, they are usually not the target of antibiotic treatment, although evidence

is emerging that these infections cause exacerbations and should be treated in a manner similar to CF (43, 51, 102). In the case of pneumonia, usually a combination of a β-lactam and an additional antibiotic from the fluoroquinolone or aminoglycoside classes is recommended, with colistin used for drug-resistant infections (103).

1.2.2.2 Emergence of drug resistance

Treating *P. aeruginosa* lung infections with antibiotics is often met with challenges. This can be attributed to multiple drug-resistance mechanisms, including those due to the formation of biofilms (4, 104). Critically, MDR is on the rise, with studies indicating up to 32% of isolated *P. aeruginosa* strains demonstrating resistance to three or more drugs (105). However, the discovery of new antibiotic classes has stalled. β-lactams were the first antibiotic described, with the discovery of penicillin by Alexander Fleming in 1928, and the aminoglycosides and polymyxins were identified in the 1940s (89, 98, 106). The quinolones are the newest class of antibiotics discovered that can be used against *P. aeruginosa* infections; however, their discovery occurred in 1962 (107). While some new drugs in these four classes have been discovered, such as the β-lactam carbapenems in the 1980s (85), the lack of new antibiotic classes for over fifty years makes the rise of MDR strains a growing health crisis. In the United States, the CDC attribute 51,000 infections to *P. aeruginosa* annually, and 6700 of these are MDR (3). It is therefore critical to find alternative options for combating *P. aeruginosa* infections.

1.3 New therapies against *P. aeruginosa* lung infections: Potential of host defense peptides

Although the development of new antibiotics has stalled in the past two decades, one promising area of research is finding naturally occurring antimicrobials from previously unculturable species (108). A screen of previously unculturable soil microbes found a new antibiotic, teixobactin, that is effective against many Gram positive and some Gram negative species (108). Although the minimum

inhibitory concentration (MIC) for *P. aeruginosa* was >32 µg/ml with teixobactin (108), this method could reveal new antibiotics for use against *P. aeruginosa*.

Another idea is the use of bacteriophages to lyse bacteria, which was used in human medicine in the Soviet Union in the early to mid-twentieth century and is still occasionally used in Russia and Georgia (109). One aspect of phage therapy that is both a benefit and a limitation is that most bacteriophages will attack only specific strains of a bacterial species (109). On one hand, this limits effects on both the host and the host microflora; on the other, this makes it difficult to use against an infection without isolating the bacterial strain. In vitro and in vivo phage treatments have shown effectiveness against *P. aeruginosa*, and the commencement of new clinical trials in humans should provide further information about the viability of phage therapy (109, 110).

Anti-biofilm therapies have also been proposed (111, 112). One drug in phase II clinical trials is OligoG, an alginate oligosaccharide, which has shown effectiveness in disrupting biofilms (101). However, no therapies are currently approved.

An alternative idea is to focus on targeting the host immune system rather than on treatments that directly attack the bacteria. The advantage of this strategy, as opposed to using antibiotics, is that, by harnessing the power of the host immune system, the bacteria would be less likely to develop resistance as they would be attacked via multiple mechanisms by an immune system that has evolved over millennia precisely to deal with microbial infections. One example is using vaccines along with adjuvants. However, despite testing potential vaccines against *P. aeruginosa* since 1970, no vaccine has been approved or recommended for use (113, 114). Some successes were seen with vaccines against flagella in human trials, with a bivalent flagella vaccine advancing to phase III trials in humans, but the vaccine did not reach its benchmarks and its production was terminated (113-116).

Another example is using components of the immune system itself. Intravenous (IV) immunoglobulin has been used for immunodeficiencies and autoimmune diseases (117). Type I interferons are used as therapies for multiple sclerosis, cancer, and hepatitis B and C, usually in

combination with other drugs. The Type II interferon, IFN-γ, has been approved for use against chronic granulomatous disease and osteopetrosis, and has been prescribed off-label for atopic dermatitis (118). Both G-CSF and GM-CSF are used for treating neutropenia (119), and GM-CSF has also been approved as an anti-fungal agent (120).

Although other components produced by the host immune system could be used against infections, a key issue is their potential for creating a cytokine storm and overwhelming the host with inflammatory mediators. For instance, cytokines such as TNF-α, IL-1β, and IL-6 are critical for the response against infection but are also implicated in the immune dysregulation that can lead to septic shock (121). Ultimately, it is necessary to examine potential anti-infection treatments for both pro- and anti-inflammatory influences and find a balance between these effects.

1.3.1 Host defense peptides

Host defense peptides (HDPs) are one component of the immune system that show promise as immunomodulatory agents during infections. HDPs are typically defined as small peptides (10-50 amino acids in length) that are amphipathic. While anionic HDPs exist, cationic HDPs (typically +2 to +9 charge) are the most widely studied and are the focus of this thesis (122). Cationic amphipathic peptides have been found in all three domains of life, and include the polymyxins from bacteria (123). However, the term HDP is usually reserved for ones from the Eukarya domain. HDPs are also often called antimicrobial peptides (AMPs) due to their direct antimicrobial activities against microbes. This can occur by binding of the positively-charged AMP to the negatively-charged bacterial membrane, with multiple peptides assembling to form a pore in the membrane, thus causing the cell to lyse (122, 124, 125). Alternatively, AMPs can also enter the cell and interact with bacterial nucleic acids and proteins (122). Indolicidin, a bovine HDP, inhibits nucleic acid synthesis, whereas pyrrhocidin from insects targets chaperone-assisted protein folding (122). However, many of these direct antimicrobial activities are lost under physiological salt conditions or in the presence of serum (126-128). For example, the human cathelicidin LL-37 loses its antimicrobial activity against methicillin-resistant *S.*

aureus, *Proteus mirabilis*, and *Candida albicans* in the presence of 100 mM of sodium chloride (129), and increasing concentrations of sodium chloride also drastically increase the MIC of LL-37 against *Escherichia coli* (127). Human β-defensin (hBD)-1 was also shown to be unable to kill bacteria in the CF lung, and other β-defensins have shown sensitivity to salt or acidic pH (130-133).

Despite the loss of this antimicrobial activity, these peptides still show effectiveness in infection models (134). It is now understood that this can be attributed to their effects on the host immune system. The immunomodulatory effects of HDPs are numerous and include modifying cytokine or chemokine production and thus recruiting and/or activating leukocytes and modifying inflammation in response to bacterial products; altering the production of ROS and RNS; increasing angiogenesis and wound healing; degranulating mast cells; and binding directly to LPS (134-139). Some cationic peptides have been reported to show anti-cancer activity while others have a role in immunometabolism (134, 135). Importantly, not every HDP possesses all of these effects, and the exact nature of the response can vary according to HDP concentration, location, and the model being used. Therefore, while AMP and HDP are sometimes used interchangeably, HDPs usually refer to cationic peptides with activities that are not due to direct antimicrobial killing, while AMP is reserved for cationic peptides that are acting through bactericidal mechanisms.

In humans, there are several AMPs and HDPs, including hepcidin, LEAP-2, and the histatins (135, 140-144). Other human cationic amphipathic peptides that may also play roles in host defense include hormones such as the natriuretic peptides, certain neuropeptides such as substance P and derivatives of pro-opiomelanocortin, and various gastrointestinal-associated peptides (135, 145-150). However, the most abundant and well-studied human HDPs are the defensins and LL-37, the only human cathelicidin (151-156). The defensins are classified as α- or β-defensins based on the disulfide linkages between six cysteines used for their characteristic three disulfide bonds. There are six well-studied α-defensins, human neutrophil peptides (HNP) 1-4, found mostly in the azurophilic (primary) granules in neutrophils, and HD5 and HD6, which are mostly produced by the Paneth cells in the

intestine (135, 153, 154). There are four prominent β-defensins expressed in humans, human β-defensin (HBD) 1-4, which are largely produced by epithelial cells in multiple locations, including the respiratory tract (131, 153, 154). LL-37 is produced by numerous cells including epithelial cells in the respiratory tract, keratinocytes in the skin, and both circulating and resident leukocytes including neutrophils, monocytes, macrophages, DCs, T cells, and B cells, and is present in tissues, fluids, and secretions (127, 135, 157). Both the defensins and LL-37 are originally translated as a prepropeptide, which is processed into a propeptide that is often stored in granules and then processed into the mature peptide by specific proteases in response to appropriate stimuli such as microbial infection (158).

As mentioned above, HDPs are produced by leukocytes and epithelial cells in the lungs and are also found in the ASL (45, 127). They are involved in the innate immune response to lung infections. The effects of HDPs can be both pro- and anti-inflammatory and vary according to the conditions present (159, 160). Thus, their roles in lung disease are complex. For example, in a xenograft model using rat tracheas seeded with primary human bronchus cells from CF or non-CF patients and then implanted into the flanks of mice, the ASL collected from the CF patient xenografts failed to kill *P. aeruginosa* (161). However, when an adenovirus expressing LL-37 was added, the ASL from the CF xenografts was bactericidal against *P. aeruginosa* in diluted broth (161). The acidic pH of the CF ASL can impair HDP killing of *P. aeruginosa*, as seen with LL-37 and hBD-3 (130). Although these studies focused on direct antimicrobial activity, it has been proposed that the HDP response to bacterial infection in CF is impaired due to high salt content, even though HDP activities are less affected by physiological salt conditions (47). While high concentrations of LL-37, hBD-1, and hBD-2 have been found in CF bronchoalveolar lavage fluid (BALF), those patients still had lung infections, and the presence of the HDPs actually correlated with disease severity, with increased LL-37 associated with inflammation and poor lung function and decreased hBD-2 correlating with decreased lung function (162).

Defensins and LL-37 have shown effectiveness against *P. aeruginosa* when overexpressed, and thus have been proposed to have key roles in lung immunity. In a rat model of *P. aeruginosa* lung infection, the delivery of adenovirus expressing rat β-defensin-2, 48 h prior to infection, decreased the bacterial burden, neutrophil infiltration, and lung pathology (163). The murine homologs of hBD-1, hBD-2, and hBD-3 are involved in the immune response to *P. aeruginosa* keratitis in vivo, with hBD-2 having a critical role (164, 165).

LL-37 and its murine orthologue, cathelin-related antimicrobial peptide (CRAMP) have also been extensively studied for activity against *P. aeruginosa* infections. LL-37 prevents the formation of *P. aeruginosa* biofilms in vitro (166). In an acute *P. aeruginosa* murine lung infection model using the PAO1 strain, which is a commonly used laboratory strain derived from a wound isolate (167), delivery of an adenovirus expressing LL-37 four days prior to infection decreased TNF-α levels and bacterial burden (168). In another acute PAO1 lung infection model, the colony-forming unit (CFU) burden in the lungs and the BALF was significantly reduced for the mice given concomitant intranasal (IN) delivery of LL-37 (169). No significant changes were seen in the expression of TNF-α, IL-6, MIP-2, KC, or MCP-1, and the effects of LL-37 were attributed to early neutrophil recruitment (169). Mice lacking CRAMP showed increased *P. aeruginosa* burden compared to wild-type (WT) controls, but the bacterial numbers could be reduced by adding LL-37 (169). Delayed neutrophil recruitment was also seen in another study for acute *P. aeruginosa* lung infections using mice lacking CRAMP (170). The knockout mice had increased IL-17, MIP-2, and KC compared to WT mice, but no difference in TNF-α; there was also no difference between knockout and WT mice in the dissemination of the *P. aeruginosa* from the lungs or survival (170). In addition to lung infection models, mice lacking CRAMP also showed decreased corneal recovery in a *P. aeruginosa* keratitis model (171). Finally, LL-37 alone or in combination with G-CSF and/or imipenem, all delivered IV, improved survival in a neutropenic intraperitoneal (IP) *P. aeruginosa* sepsis model (172). Overall, *P. aeruginosa* infection models using mice that do not produce CRAMP show increased inflammation and bacterial

numbers and decreased survival. The use of exogenous LL-37 or CRAMP decreases inflammation and improves infection outcomes.

In response to subinhibitory concentrations of LL-37, polymyxin B, and other cationic peptides, *P. aeruginosa* increases adaptive resistance and QS signals (173-176). However, these results were observed in vitro and monitored the direct antimicrobial effects of the peptides, whereas the roles of cationic peptides in vivo are more complex and involve coordination with the host immune system, thereby limiting the development of resistance (177).

Despite these encouraging results, neither the defensins nor LL-37 have entered clinical trials for the treatment of *P. aeruginosa*. Factors that may be responsible include uncharacterized toxicities and the cost of synthesis. The defensins and LL-37, and even some of their derivatives, have shown toxicity both in vitro and in vivo. LL-37 causes hemolysis and other cytotoxic effects at higher concentrations (178), and it promotes apoptosis of epithelial cells and degranulation of mast cells (179, 180). In a *P. aeruginosa* sinusitis model in rabbits, a 24-amino acid LL-37 derivative reduced CFUs but also caused inflammation around the sinus mucosa (181). A 32-mer LL-37 derivative caused edema on its own in a murine *P. aeruginosa* intratracheal (IT) model, and, despite concomitant delivery with the bacteria, it did not reduce bacterial load or increase survival (182). Furthermore, an IT delivered mixture of HNP-1, -2, and -3 induced pro-inflammatory TNF-α in mice (183). Notwithstanding these results, LL-37 has been used successfully in a chronic venous leg ulcer model, the first human trial for LL-37 administration (184). This study used a topical application of LL-37 in sodium acetate and saline that was diluted with polyvinyl alcohol to make a viscous solution that would remain in the wound bed, thus limiting potential systemic toxicity (184). LL-37 has also entered a phase I/II clinical trial for the treatment of melanoma (NCT02225366), with the goal of targeting cancerous cells directly using an intratumoral injection, which will ideally limit any toxic effects on non-cancerous cells. However, no trials using systemic administration of LL-37 are scheduled.

The cost of HDPs can be an issue, with HDPs costing up to hundreds of US$ per gram (126). Longer HDPs or ones with complex chemistry, such as the disulfide bonds in defensins, can increase both the cost and difficulty of manufacturing. Due to direct antimicrobial effects that occur when the HDP reaches a very high concentration, creating recombinant HDPs in bacteria requires protecting the bacteria from the HDP, for example, by connecting the HDP to glutathione transferase or another large protein, then cleaving the fusion for the final product (185). Therefore, most HDPs are made through N-(9-fluorenyl) methoxycarbonyl (F-moc) chemistry, in which individual amino acids are added as a chain to a tethered amino acid, with the growing amino acid chain protected and unprotected by changing the acidity. When the HDP is complete, it is removed from the solid phase by the addition of a counter-ion such as trifluoroacetic acid (TFA).

Due to these issues with HDPs, many researchers have worked on creating new HDPs that have improved toxicity profiles against eukaryotic cells and that are shorter in length in order to reduce the cost of synthesis. While some of these HDPs have been created by semi-random design, many new HDPs are created by truncating the sequence of HDPs or proteins occurring in nature. These include derivatives of LL-37 and an HDP made from the antimicrobial protein lactoferrin that is called hLF1-11 (181, 182, 186). Other HDPs are made by substituting amino acids in a naturally occurring HDP. Our laboratory has used the cyclic bovine HDP bactenecin as a backbone and performed amino acid substitutions and scrambled sequences to create hundreds of new HDPs that are linear but still contain twelve amino acids as with the parent peptide (187-189). These peptides, called innate defense regulators (IDRs), are then screened in vitro to identify the lead peptide candidates (**Table 1.1**).

Table 1.1: Sequences of HDPs and IDRs. LL-37 and bactenecin are naturally occurring HDPs. Bac2a is the linearized version of bactenecin. IDR-1, -1018, and -1002 are derivatives of Bac2a created through amino acid substitution arrays.

Name	Origin	Sequence
LL-37	Natural (human)	LLGDFFRKSKEKIGKEFKRIVQRIKDFLRNLVPRTES
bactenecin	Natural (bovine)	RLCRIVVIRVCR (Disulfide bridge 3-11)
Bac2a	Synthetic	RLCRIVVIRVCR
IDR-1	Synthetic	KSRIVPAIPVSLL
IDR-1018	Synthetic	VRLIVAVRIWRR
IDR-1002	Synthetic	VQRWLIVWRIRK

1.4 Innate defense regulators

Hundreds of IDRs have been tested in vitro for their antimicrobial, anti-biofilm, and immunomodulatory activities (187, 190-198). One peptide, IDR-1018, has emerged as the best candidate in terms of overall activity.

IDR-1018 was isolated from a large screen of synthetic peptides as being the most potent in inducing chemokines. It increased MCP-1 production in human peripheral blood mononuclear cells (PBMCs), whereas in cells exposed to TLR agonists such as LPS, polyinosinic:polycytidylic (poly I:C), Pam3CSK4, and CpG it decreased the production of inflammatory cytokines such as TNF-α or IL-1β (195, 199, 200). It also affected neutrophil activation and promoted their killing of *E. coli* (201). When used on differentiating monocytes, IDR-1018 induced the production of macrophages with both pro- and anti-inflammatory functions, showing an intermediate between the classical M1 macrophages that are considered pro-inflammatory and the alternative M2 macrophages that are associated with anti-inflammatory functions (202). It also helped to resolve a pro-inflammatory autophagy defect in CF epithelial cells that contain a *CFTR* mutation (203). Importantly, it has shown very little cytotoxic activity while producing these numerous immunomodulatory effects (204, 205).

Due to its promising results in vitro, IDR-1018 has also been tested in several in vivo models. In a murine model of cerebral malaria it improved survival when delivered prophylactically through IV injection or when given therapeutically with anti-malarial drugs (200). It also showed success as a

prophylactic in an IP *S. aureus* model (200). Moreover, it promoted better wound healing than LL-37 in mice as well as in *S. aureus*-infected porcine wounds, although it did not improve bacterial clearance (205). In a murine lung infection used to model tuberculosis, it reduced lung inflammation and bacterial burden for both drug susceptible and MDR strains when delivered IT (206). IDR-1018 has also been used successfully in vivo for treatment in a murine neonatal hypoxia/endotoxin challenge model and in *S. aureus*-infected implants (207, 208).

In addition to these activities, IDR-1018 is an excellent broad spectrum anti-biofilm peptide. In a flow cell system designed to model the formation of biofilms on surfaces exposed to the movement of liquid, such as in catheters or in blood vessels, IDR-1018 inhibited the formation of *P. aeruginosa* biofilms and caused the dispersal and killing of bacteria in mature biofilms (209). For example, when *P. aeruginosa* was grown in the flow cell for two days to form a biofilm and then 100 times the MIC of ciprofloxacin was added there was little damage to the biofilm or the bacteria themselves (209). However, adding IDR-1018 to the ciprofloxacin killed most of the bacteria and destroyed the biofilm (209). This synergy also occurred when the combination was added prior to biofilm development (209). IDR-1018 was also effective against biofilms formed by several other strains, including drug-resistant strains such as methicillin-resistant *S. aureus* and various Gram negative bacteria, as well as multispecies biofilms (209, 210). The anti-biofilm activity of IDR-1018 was determined to be due to IDR-1018 affecting the stringent response of bacteria that is used to respond to growth conditions under stress, such as when the bacteria are exposed to antibiotics or the host immune system (211). Despite its anti-biofilm activity, IDR-1018 showed only modest activity against planktonic bacteria, with an MIC of 19 µg/ml against *P. aeruginosa* strain PAO1 (204).

Based on its ability to improve outcomes in infection models, including reducing inflammation and bacterial numbers in a lung model of tuberculosis, as well as its antibiofilm activities, IDR-1018 is a promising candidate for treating *P. aeruginosa* lung infections. However, IDR-1018 is not without its limitations. It has not been effective in other in vivo models, including healing wounds in diabetic

mice and reducing inflammation in a murine arthritis model (205, 212). It was also unsuccessful prophylactically when delivered IP in the malaria model or therapeutically without anti-malarial drugs, and in the tuberculosis model it was ineffective when administered IP (200, 206). Additionally, IDR-1018 aggregates rapidly in most solutions, including water, PBS, and saline, making in vivo delivery difficult (Dr. Evan Haney, unpublished results). Furthermore, this aggregation might affect the bioavailability of the peptide and could hinder its ability to address an infection in the lungs. Therefore, it is desirable to examine alternatives for IDR-1018 use against *P. aeruginosa*.

One alternative to IDR-1018 is through designing a peptide with similar activities as IDR-1018 but that does not aggregate in solution. For IDR-1018, the aggregation is believed to be due to a sequence of five hydrophobic amino acids in the middle of the peptide (LIVAV) (**Table 1.1**). An alternative peptide is IDR-1002. While IDR-1002 also has a sequence of five hydrophobic amino acids (WLIVW), two of those are tryptophans, which are aromatic but zwitterionic and able to pi stack and thus bind to the interfacial regions of membranes, which might be influential in its potential to aggregate. Also, IDR-1002 has an additional polar amino acid, glutamine, in its sequence to increase its polarity. IDR-1002 has demonstrated immunomodulatory activity in vitro by improving monocyte adhesion and chemotaxis towards chemokines, inducing the release of chemokines from PBMCs, inducing both pro- and anti-inflammatory effects in IL-1β-stimulated synovial fibroblasts, and activating neutrophils to improve *E. coli* killing while also reducing their production of inflammatory mediators (192, 201, 206, 213-215). IDR-1002 also showed success in vivo against IP infections with *S. aureus* or *E. coli*, although it was ineffective in the tuberculosis model (192, 206).

Another option for overcoming IDR-1018 aggregation is through the use of formulation. Many drug delivery systems have been designed to improve drug targeting in vivo (216). These include nanoparticles, polymers, and liposomes. Using IDR-1018 with these systems could prevent aggregation, improve bioavailability, and make it more suited for use in vivo.

In conclusion, while IDRs have shown success as anti-infective agents in vitro and in vivo, they have not been previously examined against *P. aeruginosa* lung infections, which desperately require novel therapeutic agents. The concept of immunomodulation by IDR peptides represents a new idea for these infections. There have been a limited number of other synthetic HDPs used against *P. aeruginosa* lung infections in vivo. Derivatives of the bovine cathelicidin BMAP-27 showed encouraging in vitro results, but in an acute *P. aeruginosa* lung infection the lead peptide candidate did not reduce CFU burden and also caused some toxicity, with one mouse dying due to the peptide (217). In a rat model of a chronic *P. aeruginosa* infection in which PAO1 is embedded in agar beads and then left in the lungs for three days, four peptides showed modest reductions in CFU burden when given as a daily treatment for three days, although no statistical analysis of significance was included (218). However, these peptides are longer than the IDRs discussed here, ranging from 18 to 30 amino acids in length, and their effects on inflammation in the lung model were not reported (218). The most successful synthetic peptide against *P. aeruginosa* lung infections has been the sheep HDP derivative novispirin G10, which reduced *P. aeruginosa* burden and inflammatory cytokines in a chronic infection model in rats using a mucoid *P. aeruginosa* strain mixed with alginate (219). However, this peptide is also longer than IDRs, with a length of 18 amino acids, and it was given at 0 h and 3 h relative to infection, meaning the 0 h dose may have killed some of the bacteria directly if they were delivered at the same time (219). Most importantly, novispirin showed toxicity at 1, 5, and 20 mg/ml in the rats (219, 220). Similarly, in a *Klebsiella pneumoniae* lung infection model in mice novispirin G10 showed significant toxicity (219, 220).

Therefore, the need for a new immunomodulatory therapy for *P. aeruginosa* has not been met by previous synthetic HDPs. Based on the existing evidence for immunomodulatory, anti-infective, and anti-biofilm properties of IDR-1002 and IDR-1018, I believe they warrant evaluation as novel anti-pseudomonal drugs.

1.5 Hypothesis and research aims

P. aeruginosa lung infections are found in pneumonia, COPD, and CF, but treating them is difficult due to the rise of MDR strains and the formation of biofilms. As such, *P. aeruginosa* lung infections kill thousands of people each year. The lack of new antibiotics necessitates the use of novel therapeutics, especially since *Pseudomonas* has proven recalcitrant to most newly introduced antibiotics. One strategy is the use of derivatives of HDPs, since these are small, amphipathic peptides with profound immunomodulatory effects that help to fight against microbial infections while limiting excessive inflammation. However, one caveat with HDPs is that they can sometimes cause toxicity to the host. Additionally, some HDPs may be expensive or difficult to make due to their relatively longer sequences and complex secondary structures. Therefore, synthetic HDPs called IDRs have been developed. They have not been tested in models of *P. aeruginosa* lung infection, but IDRs have shown effectiveness in recent years in multiple in vitro and in vivo models against a variety of organisms, including, during the course of this thesis, against *P. aeruginosa* biofilms in vitro (209). Therefore, I **hypothesized** that IDR peptides can be used to prevent and treat *P. aeruginosa* lung infections due to their immunomodulatory properties.

This thesis focused on two IDRs, IDR-1002 and IDR-1018, and looked at their potential for use against *P. aeruginosa* lung infections with three research aims: 1) to determine the effects of IDR-1002 in vitro and in vivo against *P. aeruginosa* infections, 2) to test different formulations of IDR-1018 for optimization of delivery against *P. aeruginosa* infections, and 3) to examine the host pathways involved in a *P. aeruginosa* acute in vivo lung infection and the effects of IDR-1002.

Chapter 2: IDR-1002 is effective at preventing and treating both in vitro and in vivo models of *P. aeruginosa* infections

2.1 Introduction

P. aeruginosa is a frequent cause of lung infections, but treatment is challenging due to *P. aeruginosa* drug resistance and its ability to evade the host immune system by forming biofilms and/or limiting its expression of flagellin.

HDPs are small, naturally occurring peptides that have shown profound effects in many conditions, including a critical role in the host response to microbial infections (134). However, their use as exogenous agents has been limited due to toxicity and cost. Therefore, synthetic versions, called IDRs, have been developed with similar properties but with reduced toxicity and cost (187-189). IDR-1002 has been tested in vivo against *S. aureus* and *E. coli* and shown to have anti-infective properties (192). These effects suggest that IDR-1002 may also be beneficial against *P. aeruginosa* infections.

In this chapter, I examine the potential of IDR-1002 as an anti-infective agent against *P. aeruginosa* lung infections. First, IDR-1002 and the human HDP LL-37 were tested in in vitro cultures of bronchial epithelial cells and macrophages, two key cell populations for the immune response during a lung infection, and the effects of peptide on toxicity and cytokine and chemokine release were evaluated with peptide alone or in the presence of *P. aeruginosa* or its components. Next, two murine lung models were developed for testing IDR-1002. The acute *P. aeruginosa* lung model used IN administration of *P. aeruginosa* PA103, a highly virulent strain that produces ExoU and ExoT but is a weak biofilm former (221-224). It was originally isolated from human sputum and is considered non-motile due to a lack of flagellum, and it also shows a reduced twitching ability, indicating dysfunctional type IV pili (23, 223, 225). It has also been used in numerous rabbit and murine *P. aeruginosa* infection models (221, 226, 227).

While the initial stages of *P. aeruginosa* lung infection are acute and can be examined through this model, in diseases such as CF the *P. aeruginosa* infection transitions to a chronic state that is characterized by ongoing inflammation while the bacteria are protected by biofilms. However, *P. aeruginosa* does not normally cause a chronic infection in mice, therefore the bacteria are often embedded in agar or agarose beads and then delivered IT (228, 229). Alternatively, a model was developed using a clinical isolate of *P. aeruginosa* mixed with alginate isolated from the same strain (230-232). While both models provide the *P. aeruginosa* with some protection from the host immune system, using an actual biofilm component, alginate, instead of agar better reflects the interactions of the host immune system with the bacteria during a chronic infection. To improve the throughput and make the model more representative of the typical route of lung infection, I used alginate isolated from seaweed and used IN administration of the *P. aeruginosa* and alginate mixture. I also used the CF patient isolate LESB58, which is now considered to be the first isolated Liverpool Epidemic Strain, a group of highly virulent strains that have increased antibiotic resistance and are associated with increased morbidity and transmission among CF patients (233-235). LESB58 is a strong biofilm producer, and although it has flagellum it shows decreased motility compared to other *P. aeruginosa* strains (236).

The in vitro and in vivo results showed that IDR-1002 was effective against preventing *P. aeruginosa* lung infections and could lower CFU burden and limit the release of pro-inflammatory cytokines. Additionally, while IDR-1002 did not affect the lung CFUs in the alginate model, it still decreased infection-induced cytokine production and tissue damage in the lungs. Overall, the data indicate that IDR peptides could be novel therapeutic or prophylactic agents against *P. aeruginosa* lung infections.

2.2 Materials and methods

2.2.1 Mice and ethics statement

C57Bl/6J mice were ordered from Jackson Laboratory or were bred at the Modified Barrier Facility (University of British Columbia). Female mice were used between 6-8 weeks of age. All experiments were approved by the UBC Animal Care Committee.

2.2.2 Reagents

LL-37 (LLGDFFRKSKEKIGKEFKRIVQRIKDFLRNLVPRTES-NH_2) was purchased from CPC Scientific (Sunnyvale, California, USA) and IDR-1002 (VQRWLIVWRIRK-NH_2) was purchased from Kinexus (Vancouver, British Columbia, Canada). Both peptides were synthesized by F-moc chemistry and purified by HPLC to greater than 95% purity. Peptides were stored as desiccated powders at -20°C, then resuspended in endotoxin-free water for experiments and stored at -20°C unless otherwise noted. LPS from *P. aeruginosa* PAO1 (strain H103) was isolated in the laboratory by the Darveau-Hancock method as previously described (237). Briefly, *P. aeruginosa* was grown to an OD_{600} reading of 0.6-0.8, then the bacteria were centrifuged and lyophilized (237). The dried bacterial cells were then resuspended and subjected to a series of purification steps to remove contaminating material, then the LPS concentration was quantified by determining the concentration of the LPS component 2-keto-3-deoxyoctonate (237). *S. aureus* lipoteichoic acid (LTA) was purchased from InvivoGen (San Diego, California, USA).

2.2.3 Cell culture

16HBE14o- (HBE) cells were grown in MEM with Earle's salts (Gibco 11090) and RAW264.7 (RAW) cells were grown in DMEM (Gibco 10313), each with the addition of 10% (v/v) heat-inactivated fetal bovine serum (FBS) and 2 mM L-glutamine (Gibco 25030). Cells were maintained at 37°C with 5% carbon dioxide and passaged by removing media, washing with PBS (Gibco 10010), and adding 0.05% trypsin (Gibco 2520) to detach the cells. Cells were centrifuged, the supernatant was removed, and the cells were resuspended and transferred to new flasks.

For experiments, HBE cells were passaged into 48-well plates (1 x 10^5 cells/ml, 0.5 ml per well) and allowed to grow for approximately two days to achieve greater than 80% confluency in a monolayer. At approximately 2 h before experiments, the medium was removed, cells were washed with PBS, and fresh medium supplemented with L-glutamine and 1% FBS was added. The cells were rested for 2 h, then used for experiments. RAW cells were passaged into 48-well plates (1.5 x 10^5 cells/ml, 0.5 ml per well) and allowed to grow overnight before being used for experiments. For treatments, samples received equivalent volumes of the diluents unless otherwise noted. Culture supernatants were collected and then stored at -20°C.

2.2.4 Bacterial culture and heat-killed bacteria

Bacterial strains *P. aeruginosa* PA103, LESB58, and PAO1 (strain H103) were streaked onto LB plates from frozen stocks and grown overnight at 37°C. The following day individual CFUs were used to make overnight cultures in LB and grown overnight at 37°C with shaking. Overnight cultures were diluted 1:50 (PA103 and PAO1) or 1:10 (LESB58) and grown to an OD_{600} reading of approximately 0.5. Bacteria were washed with endotoxin-free 0.9% sodium chloride solution (saline), centrifuged, supernatant discarded, and the pellet resuspended in endotoxin-free saline to an OD_{600} of 0.5. Bacteria were then diluted to the appropriate concentration based on previous experiments relating OD_{600} reading to CFU/ml, and serial dilutions were plated on LB to check the final concentration.

For heat-killed bacteria, 10-15 ml of the bacterial suspension in endotoxin-free saline was centrifuged, resuspended in a small volume of endotoxin-free saline, then heated in a 65°C water bath for 1 h. After heating, the bacteria were tested for viability by plating a small volume on LB agar.

2.2.5 *Pseudomonas* lung infection models

P. aeruginosa PA103 or LESB58 was prepared as described above, except LESB58 was resuspended in a 11 mg/ml sodium alginate (Sigma-Aldrich) solution that was prepared in endotoxin-free saline. Mice were anesthetized with 2-5% isoflurane and placed on an intubation stand (BrainTree Scientific, Massachusetts, USA). IDR-1002, *P. aeruginosa*, or appropriate controls were instilled

dropwise using a micropipette into the left nostril of each mouse. *P. aeruginosa* was in a 20 µl volume, while the peptide volume was approximately 10-20 µl depending on the weight of the mouse. Isoflurane was periodically applied to keep the mouse at a steady respiratory rate. After instillation, mice were kept on the stand under isoflurane for 2-3 minutes to ensure absorption of the liquid. Once they were fully recovered, they were returned to their cages.

For sample collection, mice were euthanized with 120 mg/kg of IP injected sodium pentobarbital. Blood was collected from the inferior vena cava and allowed to clot, then centrifuged and the serum was collected. For BALF collection, the chest cavity and trachea were exposed and an incision was made in the trachea. A cannulated needle was then inserted and used to slowly fill the lungs with sterile PBS (600 µl), which was then slowly withdrawn through the cannulated needle and saved. This procedure was repeated twice for a total of three washes. The first BALF wash was used for CFU enumeration by spread-plating undiluted BALF or ten-fold dilutions made in PBS onto LB agar plates in duplicate. Plates were incubated overnight at 37°C and CFUs were enumerated the following day. The remaining first BALF wash was centrifuged and the supernatant saved for ELISAs. The pellet from the first BALF wash was combined with the pellet from BALF washes 2 and 3 and resuspended in PBS, then leukocytes were counted on a hemocytometer using Turk's stain.

For lung homogenates, the lungs were collected and the lobes separated and placed in 300 µl of PBS. The lungs were then homogenized on a Mini-Beadbeater-96 (BioSpec, Bartlesville, Oklahoma, USA) for 1 minute. The homogenates were filtered (40 µm filter, #431750, Corning) and the filtrate was used for plating on LB as described above. The remaining liquid was stored at -20°C for use in ELISAs.

2.2.6 Cell differential counts and lung histology

In some experiments, the leukocytes were also used in a StatSpin Cytofuge 2 (Beckman-Coulter) and the resulting slides were air-dried overnight, stained with the Diff-Quik Staining Kit (VWR, Radnor, PA) according to the manufacturer's protocol, and then 200 cells/slide were counted.

For histology, a cannulated needle was used to deliver 4% paraformaldehyde (PFA) into the lungs, then the trachea was tied off with string to prevent leakage and the lungs were placed in a container of 4% PFA. After two days, the samples were washed with 70% ethanol. Wax-It Histology Services (Vancouver, British Columbia, Canada) embedded the samples in paraffin, sectioned them, and then stained the slides with hematoxylin and eosin (H&E), periodic acid-Schiff (PAS), or Alcian blue.

2.2.7 ELISAs

Samples were stored at -20°C until use in ELISAs. The levels of cytokines and chemokines were measured using eBioscience (San Diego, California, USA) antibodies for murine TNF-α and IL-6 and human IL-6. MCP-1 antibodies were from eBioscience or R&D Systems (Minneapolis, Minnesota, USA). KC (CXCL1) antibodies were from Fitzgerald (Acton, Massachusetts, USA) or R&D Systems. Human IL-8 antibodies were from Invitrogen (Waltham, Massachusetts, USA). Standards were purchased from the same sources. The ELISAs were performed by following the manufacturer protocols with optimization of antibody and sample dilutions, washes, and incubation times. They were developed using TMB (eBioscience) and the reactions were stopped with 2 N sulfuric acid. The plates were read on a Power Wave X340 plate-reader (Bio-Tek Instruments, Winooski, VT) and data were fitted to a 4-parameter standard curve using KC4 software (Bio-Tek).

2.2.8 Lactate dehydrogenase (LDH) assay

Supernatants collected from cell cultures were combined at a 1:1 (v/v) ratio with complete LDH assay reagent (Roche Diagnostics, Basel, Switzerland). After incubating for 15-25 minutes in the dark, the plates were read on a Power Wave X340 plate-reader (Bio-Tek Instruments, Winooski, VT). Results were normalized to the control sample (0% toxicity) and to a sample in which 2% (v/v) Triton X-100 had been added to cause complete lysis of the cells (100% toxicity).

2.2.9 Statistical analysis

Data were analyzed using Microsoft Excel 2013 and GraphPad Prism version 7. GraphPad Prism was used to perform an unpaired t-test, one-way ANOVA, or two-way ANOVA as appropriate. Tukey's and Dunnett's multiple comparisons tests were used when comparing the means of all samples or when comparing to only to a control sample, respectively. A value of $p \leq 0.05$ was considered statistically significant.

2.3 Results

2.3.1 IDR-1002 is not toxic in vitro

HBE cells and RAW cells were exposed to a range of either LL-37 or IDR-1002 concentrations (5 x 10^{-4} µM to 50 µM) for 24 h, then supernatants were collected and cytotoxicity measured by assessing the release of cytosolic LDH. IDR-1002 showed less than 5% toxicity compared to the Triton X-100 control for both HBE cells and RAW cells, whereas LL-37 showed almost 50% cytotoxicity at the highest dose in RAW cells and nearly 100% cytotoxicity at 25-50 µM in HBE cells (**Figure 2.1**). Based on these results, the maximum doses of LL-37 used in future experiments were 3 µM for HBE cells and 25 µM for RAW cells, as these doses caused less than 20% cytotoxicity. This 20% limit has been used for evaluating HDPs and IDR peptides in order to balance between limiting any effects caused by cell death while also allowing for some experimental variability.

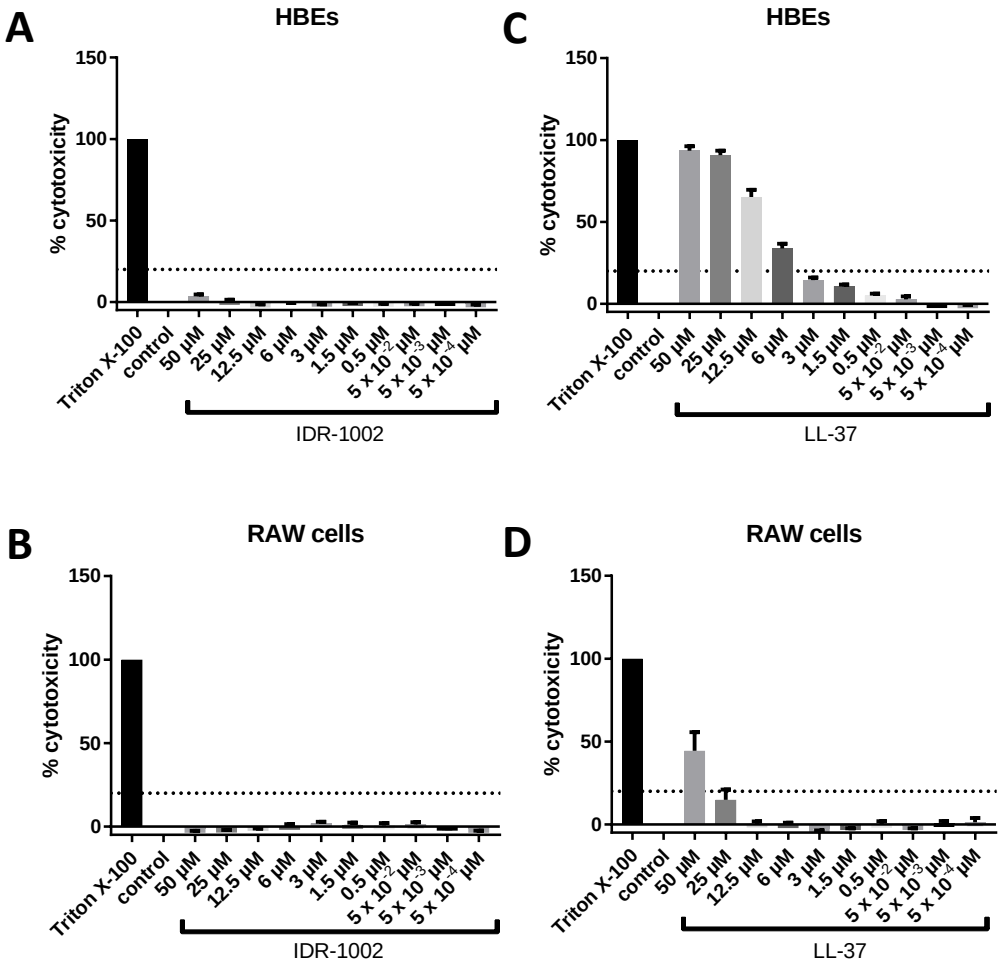

Figure 2.1: IDR-1002 is not toxic in HBE cells or RAW cells, whereas LL-37 demonstrates cytotoxicity. The listed concentrations of IDR-1002 (A, B) or LL-37 (C, D) were added to cells, then supernatants were collected after 24 h and used in an LDH cytotoxicity assay. The horizontal line represents 20% cytotoxicity. Data represent mean ± SEM from four (HBE cells) or five (RAW cells) independent experiments.

2.3.2 IDR-1002 is not pro-inflammatory and it suppresses inflammatory cytokines induced by *P. aeruginosa* lipopolysaccharide

IDR-1002 (5 x 10^{-4} µM to 50 µM) or LL-37 (5 x 10^{-4} µM to 3 µM for HBE cells or 25 µM for RAW cells) was added to HBE cells or RAW cells at the same time as *P. aeruginosa* LPS (10 ng/ml), then supernatants were collected after 24 h and used for ELISAs to measure the production of cytokines and chemokines in response to peptide alone or the combination of peptide and LPS. Both

HBE cells and RAW cells showed similar cytotoxicity results as the samples shown in Fig. 2.1 without LPS.

In HBE cells, IL-6 and IL-8 production showed a slight but significant dose-dependent increase in response to IDR-1002 and LL-37 (**Figure 2.2**). HBE cells did not demonstrate changes in IL-6 or IL-8 in response to LPS, but the combinations of IDR-1002 or LL-37 with LPS showed virtually identical results to those with peptide alone, with both peptides showing a dose-dependent increase.

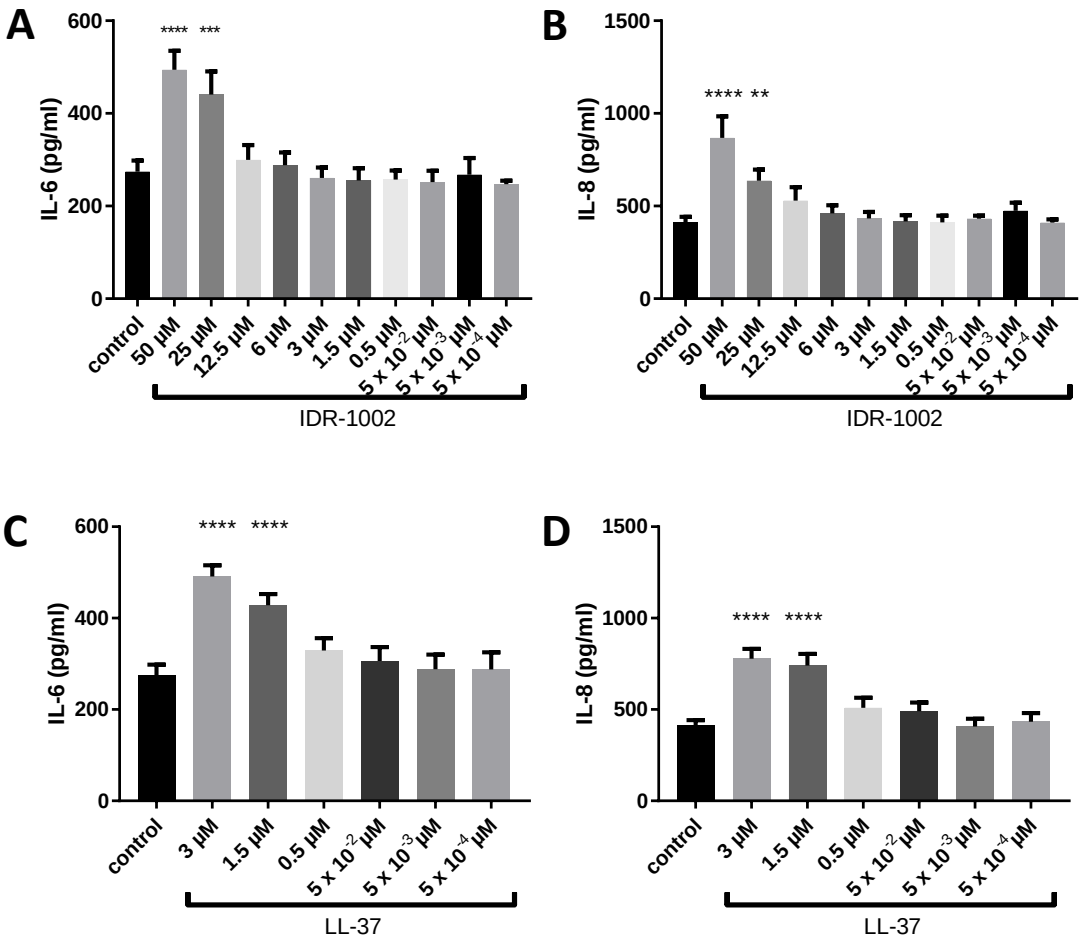

Figure 2.2: HBE cells show increases in IL-6 and IL-8 in response to peptide. Peptide was added to the cells, then supernatants were collected after 24 h for ELISAs. IDR-1002 significantly increased IL-6 (A) and IL-8 (B), and LL-37 significantly increased IL-6 (C) and IL-8 (D). Data represent mean ± SEM from four independent experiments and were analyzed using two-way ANOVA and Dunnett's multiple comparisons test. **: $p \leq 0.01$, ***: $p \leq 0.001$, ****: $p \leq 0.0001$ compared to control.

In RAW cells, the levels of pro-inflammatory cytokines TNF-α and IL-6 in the supernatant were below the detectable limit for all doses of IDR-1002 and LL-37 (**Figure 2.3**). MCP-1 production

was not increased in response to either peptide. RAW cells showed significant increases in IL-6, TNF-α, and MCP-1 levels in response to LPS, but when higher doses of IDR-1002 or LL-37 were used in conjunction with LPS, the levels returned to the baseline seen in the control without LPS. The decreases in cytokine or chemokine concentration were dose-dependent, with higher concentrations of peptide producing a greater reduction in the LPS-induced response. However, lower concentrations of LL-37 actually increased the production of cytokines in combination with LPS, with IL-6 showing a significant increase compared to LPS alone.

To further examine the effects of IDR-1002 on LPS exposure, RAW cells were treated with 12.5, 25, or 50 μM IDR-1002 at 24 or 4 hours prior to LPS exposure, 2 hours after LPS exposure, or at the same time as LPS as in the previous experiment, with each time point also having an LPS control and a control without LPS. Samples were collected 24 h after LPS addition and used in ELISAs (**Figure 2.4**). Intriguingly, IDR-1002 significantly reduced IL-6, TNF-α, and MCP-1 production at all times points of application relative to LPS treatment and at most concentrations, with the exception being 12.5 μM IDR-1002 given 24 h prior to LPS. Even when given 2 h after the addition of LPS, IDR-1002 still reduced IL-6, TNF-α, and MCP-1 production in a dose-dependent manner with less than half of the cytokines and chemokine produced relative to that due to LPS alone. The results with LPS suggests that IDR-1002 has the potential to limit inflammatory mediators as a prophylactic or therapeutic agent.

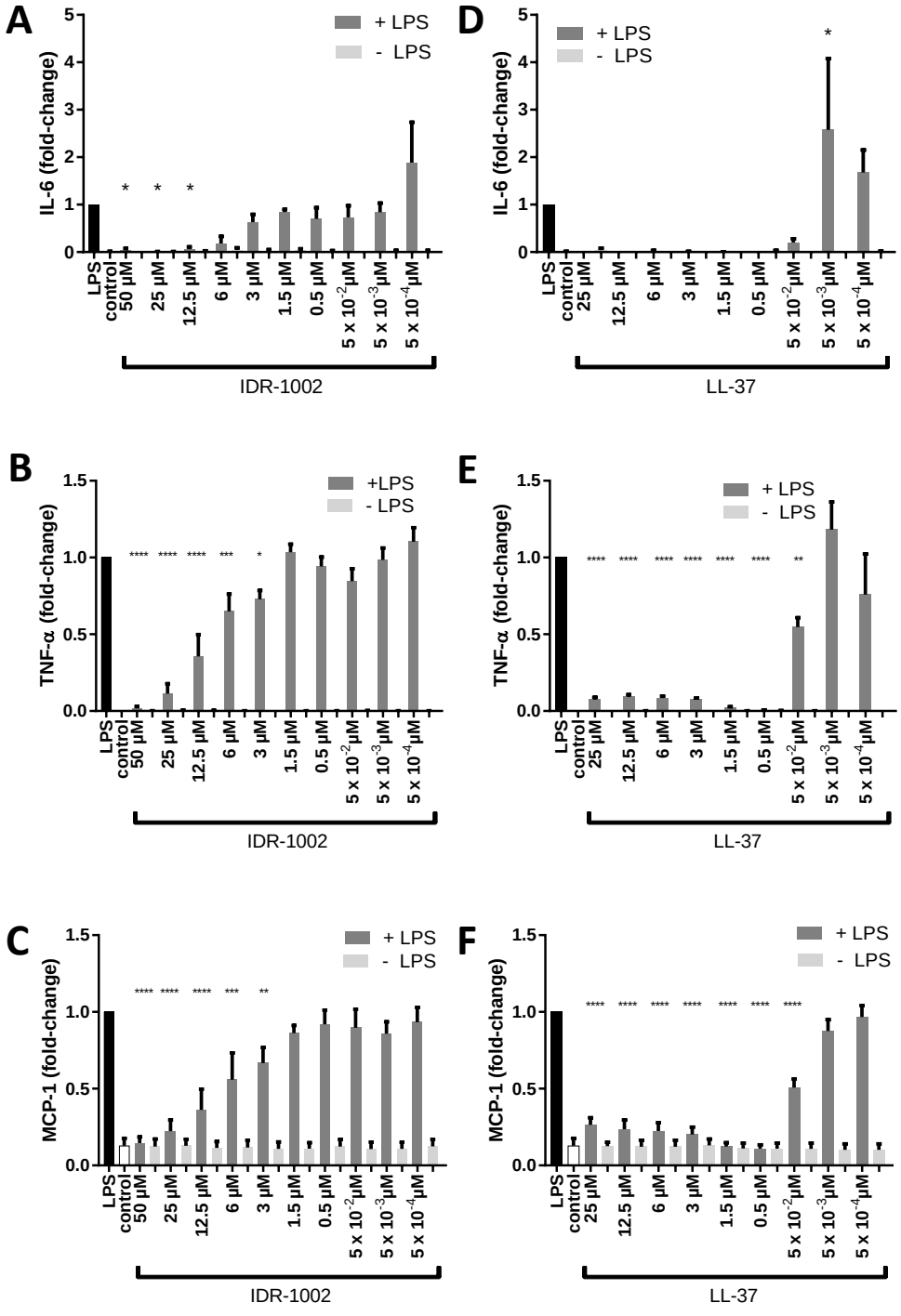

Figure 2.3: IDR-1002 and LL-37 reduce LPS-induced cytokines and chemokine in RAW cells. The listed concentrations of IDR-1002 or LL-37 were added with or without *P. aeruginosa* LPS (10 ng/ml), then supernatants were collected after 24 h. Without LPS, IDR-1002 and LL-37 did not induce any of the cytokines or chemokine. IDR-1002 decreased LPS-induced IL-6 (A), TNF-α (B), and MCP-1 (C). LL-37 also decreased LPS-induced IL-6 (D), TNF-α (E), and MCP-1 (F). Data represent mean ± SEM relative to LPS from four independent experiments and were analyzed using two-way ANOVA and Dunnett's multiple comparisons test and expressed as fold-change relative to LPS. Only the significance for samples given LPS is displayed. *: $p \leq 0.05$, **: $p \leq 0.01$, ***: $p \leq 0.001$, ****: $p \leq 0.0001$ compared to LPS.

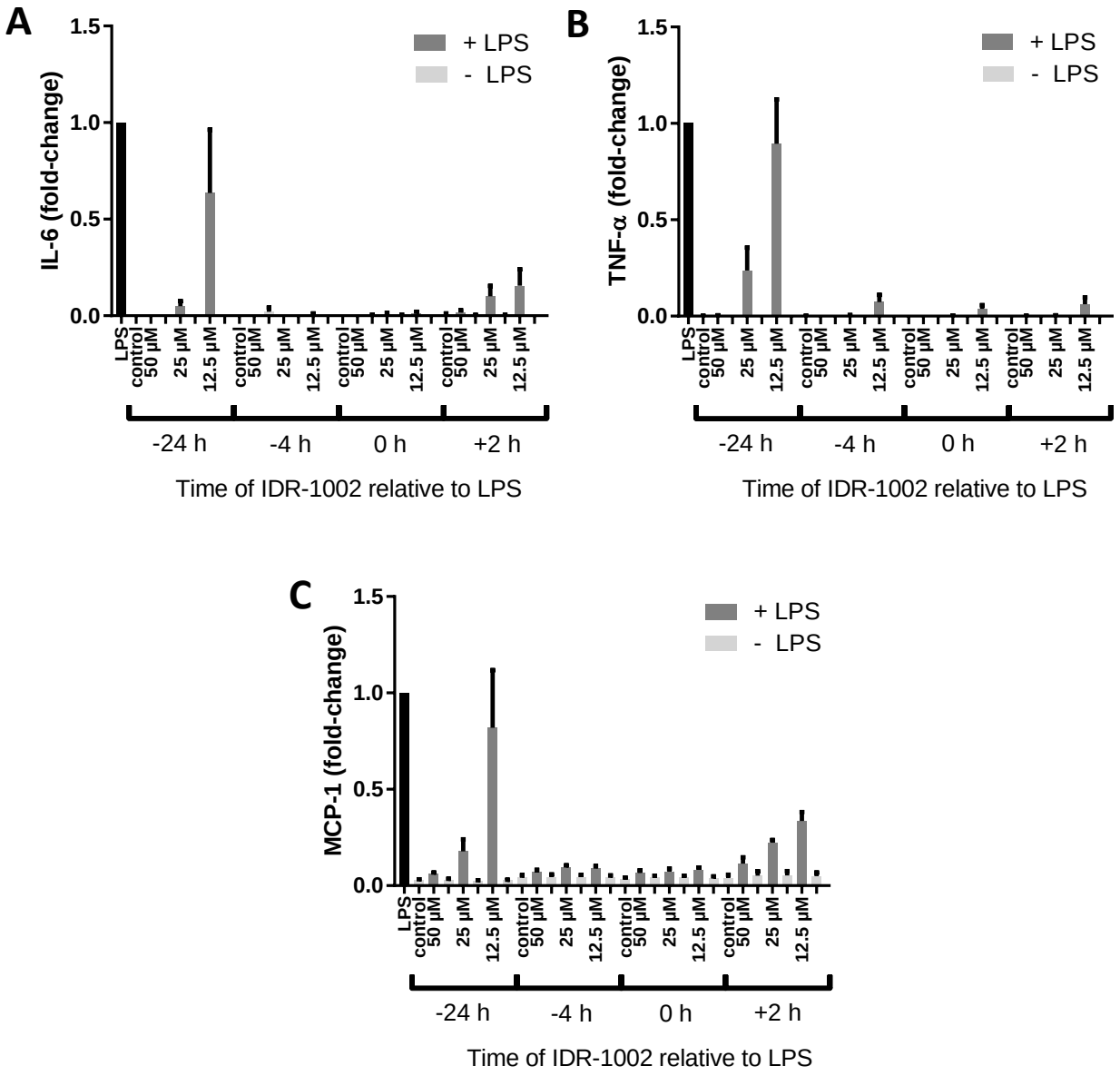

Figure 2.4: IDR-1002 reduces LPS-induced inflammatory cytokines and chemokine when added before or after the addition of LPS. IDR-1002 at 12.5, 25, or 50 µM was added 24 or 4 h prior to *P. aeruginosa* LPS, at the same time as LPS (0 h), or 2 hours after LPS. Supernatants were collected 24 h after the addition of LPS for use in ELISAs for IL-6 (A), TNF-α (B), and MCP-1 (C). Data represent mean ± SEM from three independent experiments, relative to LPS at each time point.

2.3.3 IDR-1002 has more limited effects on inflammatory mediators induced by heat-killed *P. aeruginosa*

Although LPS is a factor in the innate immune response to *P. aeruginosa*, other moieties are present in whole bacteria. Therefore, whole *P. aeruginosa* PAO1 (strain H103) or PA103 were grown,

resuspended in saline, heat-killed, and added to HBE cells or RAW cells at multiplicities of infection (MOIs) of 1, 10, 50, or 100, based on original seeding density of the cells. *P. aeruginosa* PAO1 (strain H103) LPS resuspended in water was added at 1, 10, or 100 ng/ml for comparison. Controls were treated with equivalent volumes of water or saline, or contained only medium. An LDH cytotoxicity assay showed that none of the conditions used was toxic.

RAW cells showed a significant increase in IL-6, TNF-α, and MCP-1 in response to heat-killed PAO1 (HKPAO1) and heat-killed PA103 (HKPA103) compared to the medium control (**Figure 2.5**).

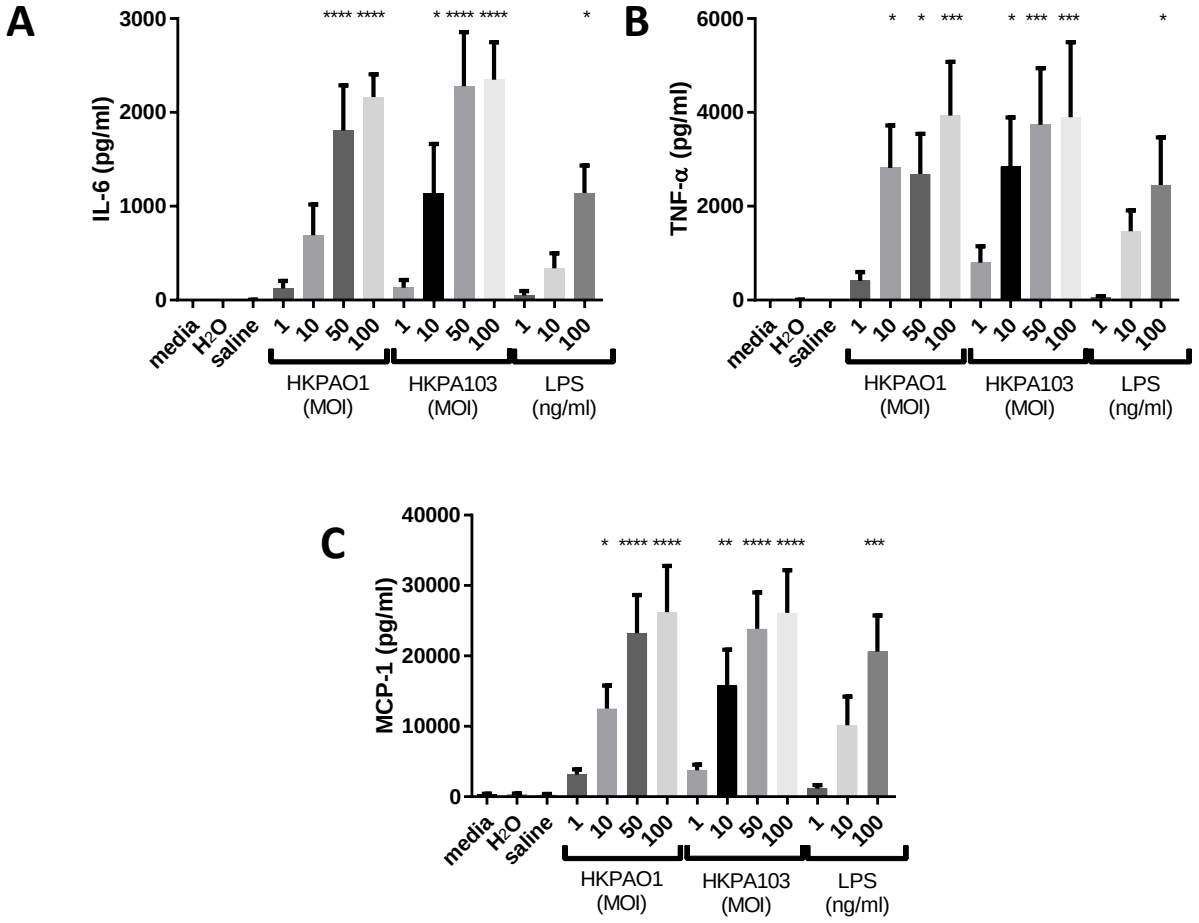

Figure 2.5: Heat-killed *P. aeruginosa* induces inflammatory mediators in RAW cells. Heat-killed *P. aeruginosa* PAO1 (HKPAO1) or PA103 (HKPA103) in saline at MOIs of 1, 10, 50, or 100, or PAO1 LPS at 1, 10, or 100 ng/ml in water was added to RAW cells at 0 h. Controls received equivalent volumes as the treatments of either saline or water, or received only medium. Supernatants were collected after 24 h for use in ELISAs for IL-6 (A), TNF-α (B), and MCP-1 (C). Data represent mean ± SEM from four independent experiments and were analyzed using two-way ANOVA and Dunnett's multiple comparisons test. *: $p \leq 0.05$, **: $p \leq 0.01$, ***: $p \leq 0.001$, ****: $p \leq 0.0001$ compared to media control.

Increases in IL-6, TNF-α, and MCP-1 were also seen after LPS exposure. MOIs of 50 and 100 produced similar results, possibly indicating the inflammatory response had attained a maximum effect at these MOIs. Therefore, it was decided to use an MOI of 10 for HKPA103 treatment of RAW cells to test the effects of peptides. This also gave comparable results to LPS at 10 ng/ml, which was the concentration of LPS used in previous experiments. In HBE cells, the responses to HKPAO1 and HKPA103 in IL-6 and IL-8 production were slight and, as described above, LPS did not produce a response.

In RAW cells, HKPA103 at MOI 10 was added at 0 h and immediately followed by IDR-1002 or LL-37 at a range of doses from 5 x 10^{-4} μM to 25 μM. LDH cytotoxicity assessments indicated that LL-37 at 25 μM with HKPA103 was very toxic (>40% compared to Triton X 100 control), therefore, this dose of LL-37 was not included in the ELISAs. In contrast to its ability to decrease LPS-induced inflammatory cytokines, IDR-1002 had no significant influence on IL-6 and MCP-1 production induced by HKPA103, while LL-37 reduced the HKPA103-induced IL-6 and MCP-1 in a manner similar to the results with LPS (**Figure 2.6**). LL-37 also reduced TNF-α at 12.5 and 6 μM, but at lower doses it slightly, although not significantly, increased TNF-α in the presence of HKPA103. Similarly, IDR-1002 also slightly increased TNF-α in the presence of HKPA103. The results with only IDR-1002 or LL-37 without HKPA103 were similar to the previous results in Figure 2.3 in showing no induction of these cytokines.

To see if the lack of IDR-1002 response to HKPA103 could be attributed to a particular TLR agonist, the TLR2 agonists Pam3CSK4 and *S. aureus* LTA were tested in RAW cells at various concentrations. In an initial experiment, LTA induced responses similar to those seen with HKPA103, whereas Pam3CSK4 showed a weaker induction than LTA for the cytokine output. Therefore, LTA was chosen as the TLR2 agonist.

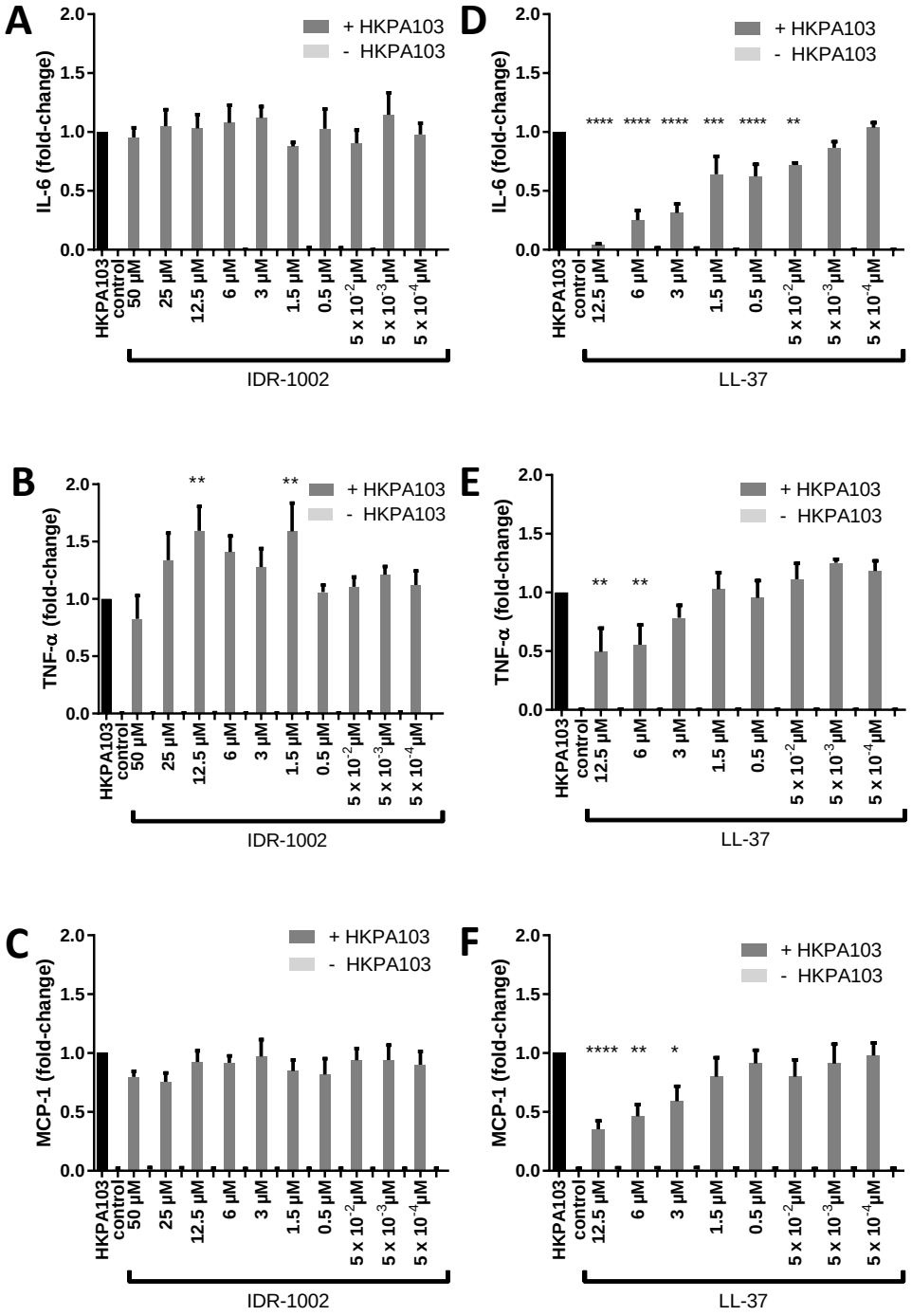

Figure 2.6: LL-37 decreases responses to HKPA103 in RAW cells, but IDR-1002 does not decrease responses. At 0 h, RAW cells were given HKPA103 at MOI 10 with or without IDR-1002 or LL-37 at the listed concentrations, then supernatants were collected after 24 h for use in ELISAs. The effects of IDR-1002 were evaluated for HKPA103-induced IL-6 (A), TNF-α (B), or MCP-1 (C), and, similarly, the effects of LL-37 were evaluated for HKPA103-induced IL-6 (D), TNF-α (E), and MCP-1 (F). Data represent mean ± SEM from three independent experiments and were analyzed using two-way ANOVA and Dunnett's multiple comparisons test and expressed relative to HKPA103. Only the significance for samples given HKPA103 is displayed. *: $p \leq 0.05$, **: $p \leq 0.01$, ***: $p \leq 0.001$, ****: $p \leq 0.0001$ compared to HKPA103.

LTA (10 µg/ml) was added to RAW cells at 0 h and immediately followed by 12.5, 25, or 50 µM of IDR-1002, then supernatants were collected and used for LDH cytotoxicity assessment and ELISAs after 24 h. None of the treatments caused toxicity. IDR-1002 significantly reduced the IL-6 and MCP-1 induced by LTA, and also showed a reduction, albeit not significant, in TNF-α (**Figure 2.7**).

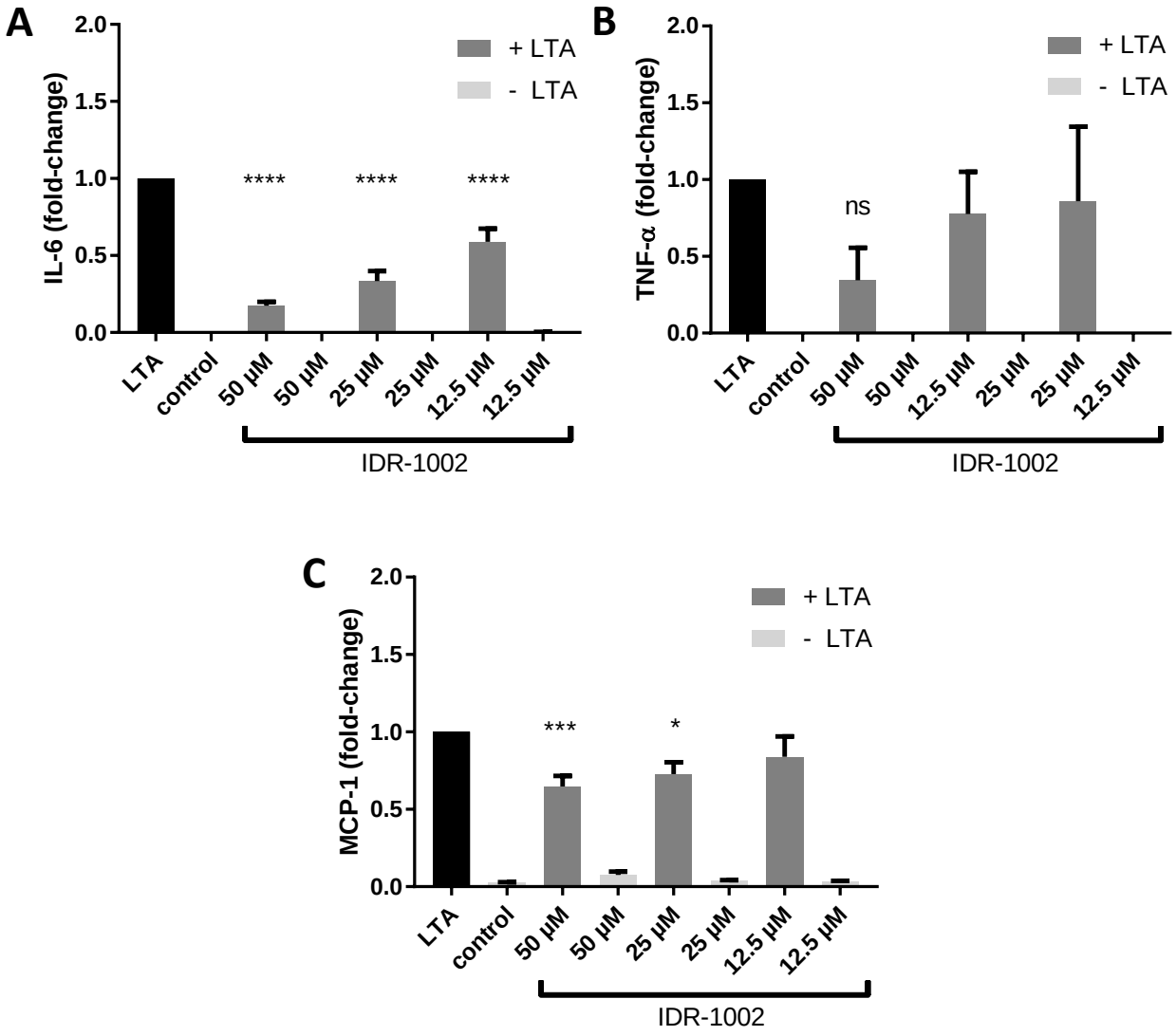

Figure 2.7: IDR-1002 reduces LTA-induced cytokines and chemokine. At 0 h, RAW cells were given LTA (10 µg/ml) and IDR-1002 at the indicated concentrations. Supernatants were collected at 24 h and used for ELISAs for IL-6 (A), TNF-α (B), and MCP-1 (C). Data are expressed as fold-change relative to LTA. Data represent mean ± SEM from five or six independent experiments and were analyzed using two-way ANOVA and Dunnett's multiple comparisons test and expressed as fold-change relative to LTA. Only the significance for LTA-treated samples is shown. *: $p \leq 0.05$, ***: $p \leq 0.001$, ****: $p \leq 0.0001$ compared to LTA.

2.3.4 IDR-1002 reduces toxicity caused by *P. aeruginosa* in vitro

Although dead bacteria and bacterial components, such as LPS, can cause inflammation, it is also important to examine the effects of living bacteria. Therefore, live *P. aeruginosa* strain PA103 was added to HBE cells or RAW cells at MOIs of 4, 2, 1, or 0.5 based on the cell seeding density. Triton X-100 (2%) was added to control wells at the same time in order to have controls with 100% cell lysis for comparison. At 2, 4 and 6 h, samples were collected, along with an uninfected control and a Triton X-100 control at each time point, and used for LDH cytotoxicity assays and ELISAs. In HBE cells, little toxicity was seen at 2 or 4 h, but at 6 h PA103 caused almost 50% cell death, with toxicity increasing as the MOI increased (**Figure 2.8**). In RAW cells, the toxicity was accelerated, with around 50% toxicity at 4 h for MOI 4 and 2, and all MOIs showing greater than 90% toxicity at 6 h post-infection. Therefore, an MOI of 4 at 6 h was selected for HBE cells and an MOI of 1 at 4 h selected for RAW cells as these were the greatest MOIs and longest time points tolerated without causing more than 50% cytotoxicity.

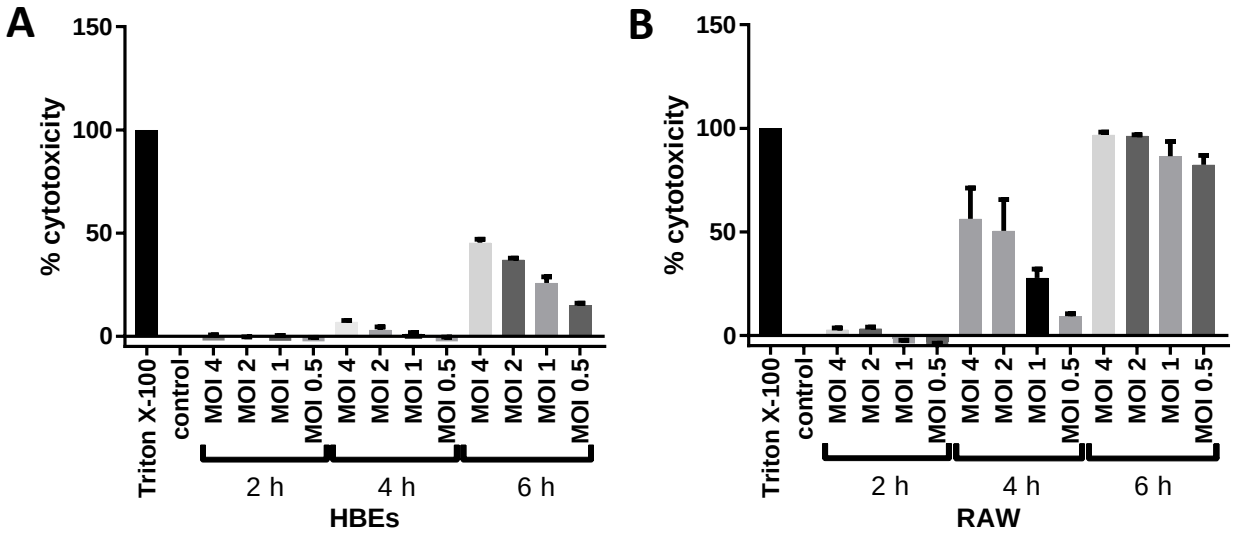

Figure 2.8: *P. aeruginosa* causes toxicity in HBE cells and RAW cells. Live *P. aeruginosa* PA103 at MOIs of 0.5, 1, 2, or 4 was added to HBE cells (A) or RAW cells (B) at time 0 h at the same time as control and Triton X-100 samples. Samples were collected at 2, 4, or 6 h and compared to a control and Triton X-100 for each time point in an LDH cytotoxicity assay. Data represent mean ± SEM from three (RAW cells) or four (HBE cells) independent experiments.

Next, the effects of peptides on the live PA103 were tested. In HBE cells, PA103 (MOI 4) was added at 0 h, and either IDR-1002 (50 µM) or LL-37 (3 µM) was added to the wells at -1 h or 0 h in relation to infection with PA103. Triton X-100 was also added at 0 h to control wells in order to have controls with 100% cell lysis for comparison. Samples were collected at 6 h post-infection and used for LDH cytotoxicity assays and ELISAs. For RAW cells, the design was similar except PA103 was used at an MOI of 1, LL-37 was used at 12.5 µM, and all samples were collected at 4 h post-infection. In HBE cells, IDR-1002 blocked the cytotoxic effects of PA103, instead showing cytotoxicity levels near those of the control or IDR-1002 by itself (**Figure 2.9**). The combination of LL-37 and PA103 induced a synergistic effect in increasing cytotoxicity as opposed to reducing the toxicity or simply having an additive effect.

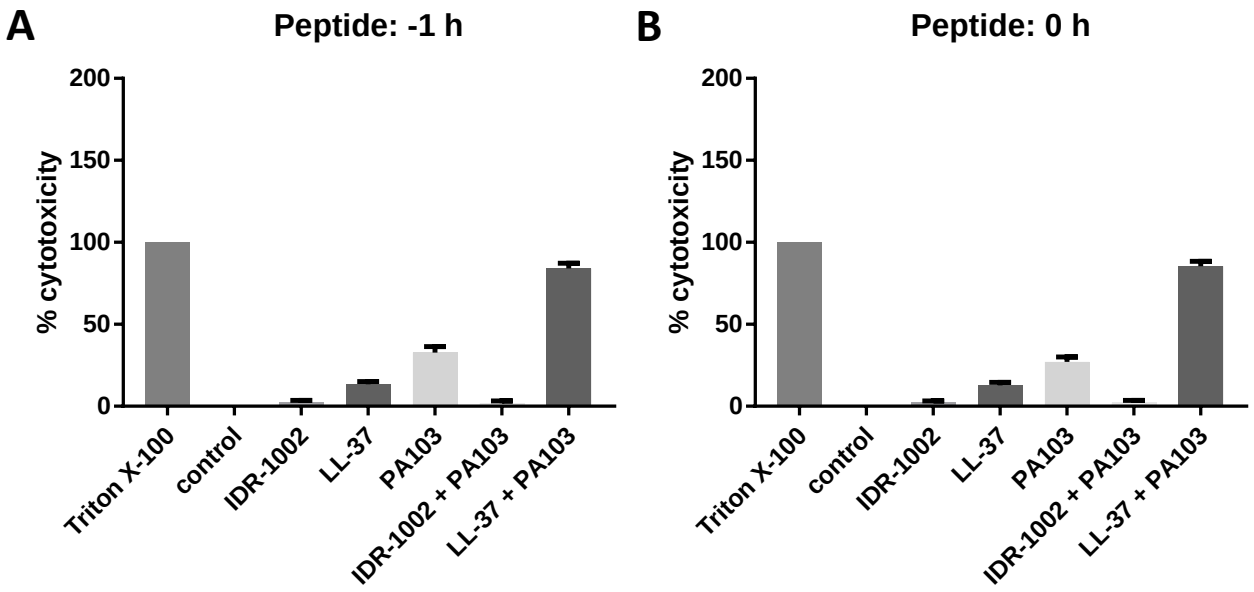

Figure 2.9: IDR-1002 limits cytotoxicity of *P. aeruginosa* in HBE cells, while LL-37 increases it. Live *P. aeruginosa* PA103 (MOI 4) was added at 0 h, and IDR-1002 (50 µM) or LL-37 (3 µM) was added at -1 h (A) or 0 h (B). Triton X-100 was added at 0 h. Samples were collected at 6 h and compared to a control and Triton X-100 for each time point in an LDH cytotoxicity assay. Data represent mean ± SEM from four independent experiments.

In RAW cells, IDR-1002 showed a similar blocking effect for PA103 cytotoxicity, but the combination of PA103 and LL-37 showed similar cytotoxicity levels to those of PA103 alone (**Figure**

2.10). For each of the cell lines, the cytotoxicity results were similar regardless of the time the peptide was added.

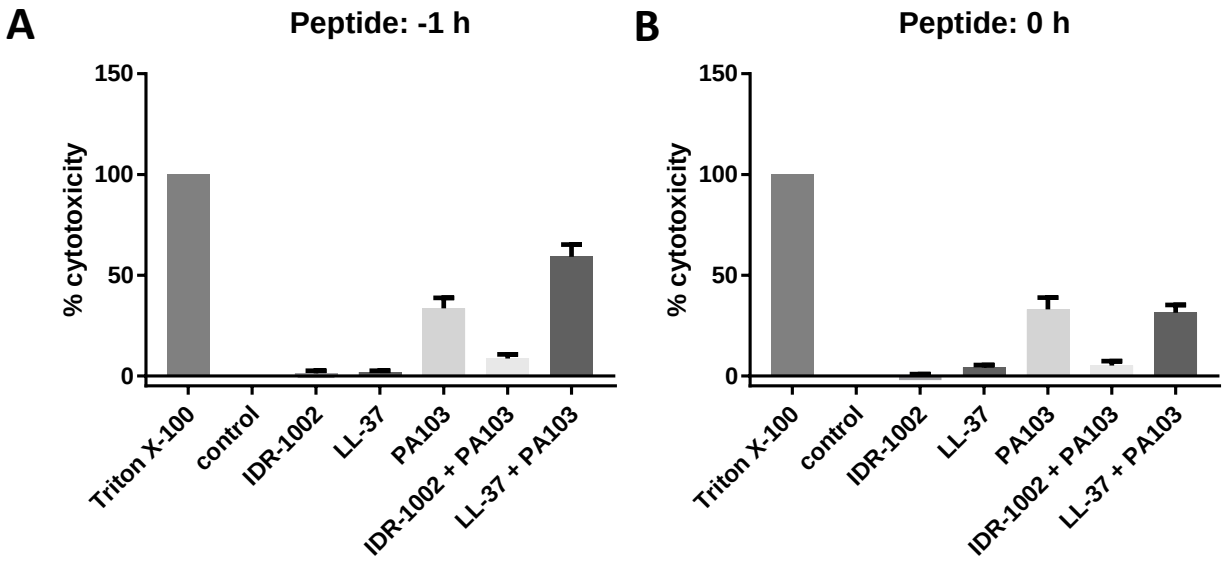

Figure 2.10: IDR-1002 limits cytotoxicity of *P. aeruginosa* in RAW cells. Live *P. aeruginosa* PA103 (MOI 1) was added at 0 h, and IDR-1002 (50 µM) or LL-37 (12.5 µM) was added at -1 h (A) or 0 h (B). Triton X-100 was added at 0 h. Samples were collected at 4 h and compared to a control and Triton X-100 for each time point in an LDH cytotoxicity assay. Data represent mean ± SEM from four independent experiments.

Cytokine and chemokine levels in the supernatants were also examined. In HBE cells, IL-6 and IL-8 showed slight increases when either peptide or PA103 was added, but the combination of LL-37 and PA103 showed significant increases in both markers (**Figure 2.11**). IL-6 and TNF-α were below the detectable limit in RAW cell samples, while MCP-1 concentrations were mostly undetectable and all were below 200 pg/ml, compared to the results seen at 24 h with LPS or HKPA103 inducing approximately 10 ng/ml of MCP-1.

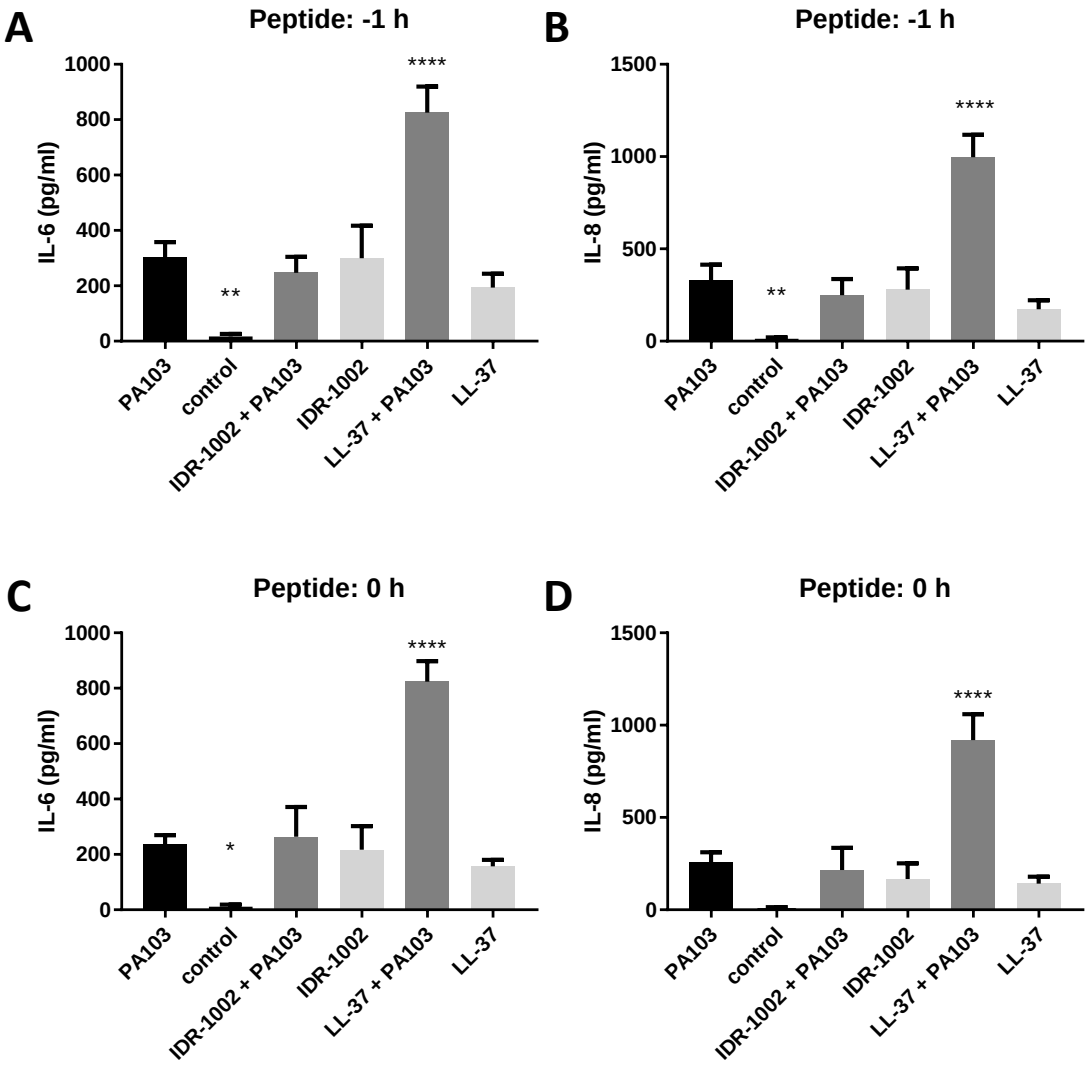

Figure 2.11: IL-6 and IL-8 production in HBE cells in response to live *P. aeruginosa* PA103. PA103 (MOI 4) was added at 0 h, then IDR-1002 (50 µM) or LL-37 (3 µM) was added at -1 h (A, B) or 0 h (C, D). Samples were collected at 6 h and used for ELISAs for IL-6 (A, C) or IL-8 (B, D). Data represent mean ± SEM from four independent experiments and were analyzed using two-way ANOVA and Dunnett's multiple comparisons test. *: $p \leq 0.05$, **: $p \leq 0.01$, ****: $p \leq 0.0001$ compared to PA103.

2.3.5 *P. aeruginosa* strain PA103 produces an acute lung infection in mice

To establish an acute *P. aeruginosa* infection model, female C57Bl/6J mice of 6-8 weeks of age were instilled IN with 2, 4, or 6 x 10^5 CFUs of *P. aeruginosa* PA103 per mouse. Mice were monitored at 3 and 18 h post-infection and scored on a scale of 1-4 for the appearance of fur, eyes, and hunching, and a scale of 1-5 for categories of warmth, activity, and respiration, with a total score

of 20 or more or a score of 5 in any category indicating a humane endpoint (Appendix 1). Mice were euthanized at 18 h and BALF and serum were collected. CFU counts from the BALF showed increasing CFUs as the original instillation dose increased (**Figure 2.12**). Interestingly, total leukocytes in the BALF increased in the mice administered 2 x 10^5 CFU compared to those given 4 x 10^5 CFU, but then dropped again for the mice given 6 x 10^5 CFU. By 18 h, the mice given 2 x 10^5 CFU had no visible signs of infection, the mice administered 4 x 10^5 CFU had a wide range of health scores, and the mice administered 6 x 10^5 CFU were all noticeably sick.

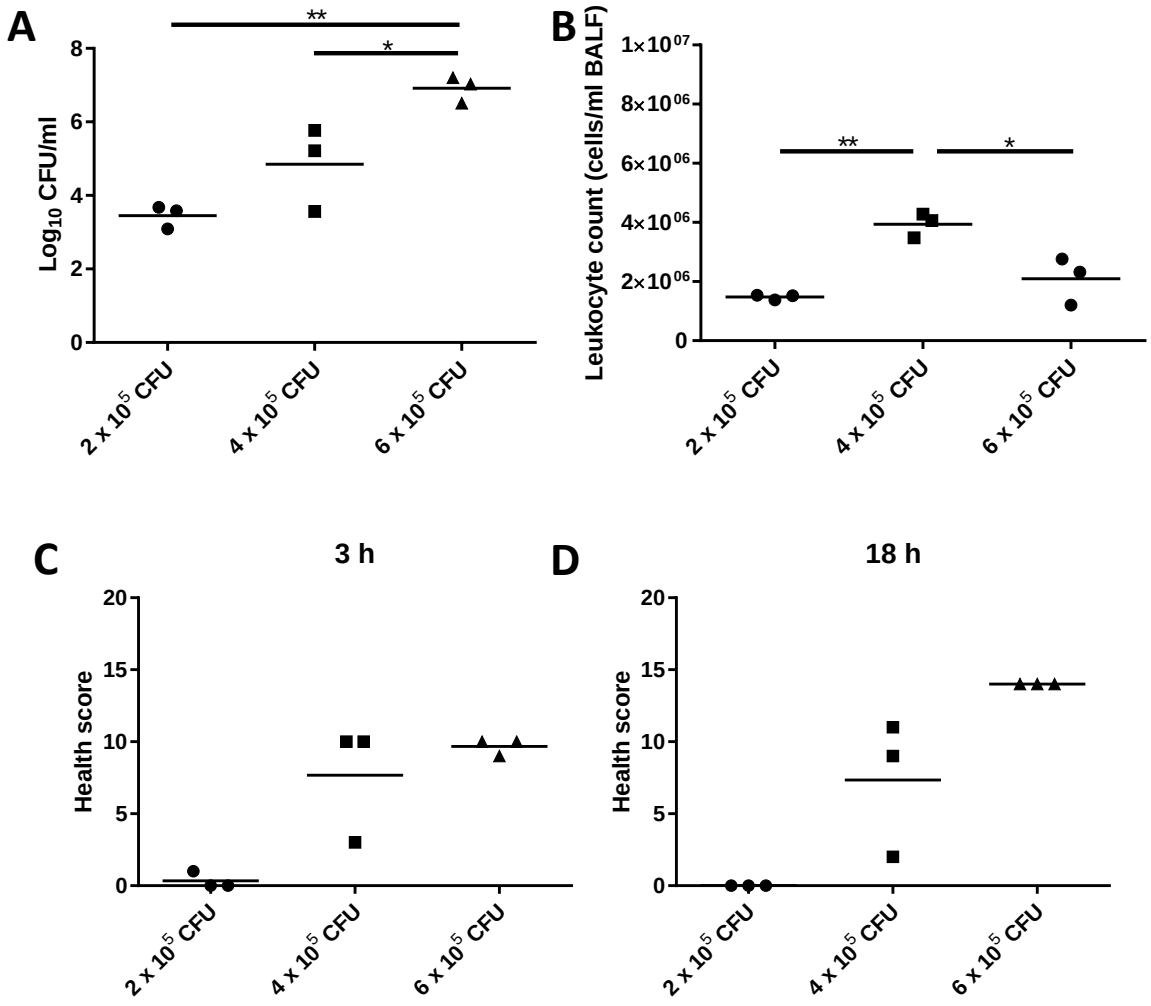

Figure 2.12: *P. aeruginosa* PA103 causes an acute lung infection in mice. Mice were instilled IN with 2, 4, or 6 x 10^5 CFUs, then euthanized and samples processed at 18 h. (A) CFU counts from the BALF. (B) Leukocyte counts in the BALF. (C) Health scores at 3 h post-infection. (D) Health scores at 18 h post-infection. Data represent n = 3 mice per condition from one experiment and were analyzed using one-way ANOVA and Tukey's multiple comparisons test. *: $p \leq 0.05$, **: $p \leq 0.01$.

The BALF and serum from these mice were used for ELISAs (**Figure 2.13**). IL-6, KC, and MCP-1 all showed significant increases in both the BALF and serum for the mice given 6 x 10^5 CFU compared to those given 2 x 10^5 CFU, and also showed significant increases relative to mice given 4 x 10^5 CFU mice (with the exception of KC in the serum). No detectable TNF-α was found in the serum, while TNF-α in the BALF increased with initial CFU concentration, although not significantly.

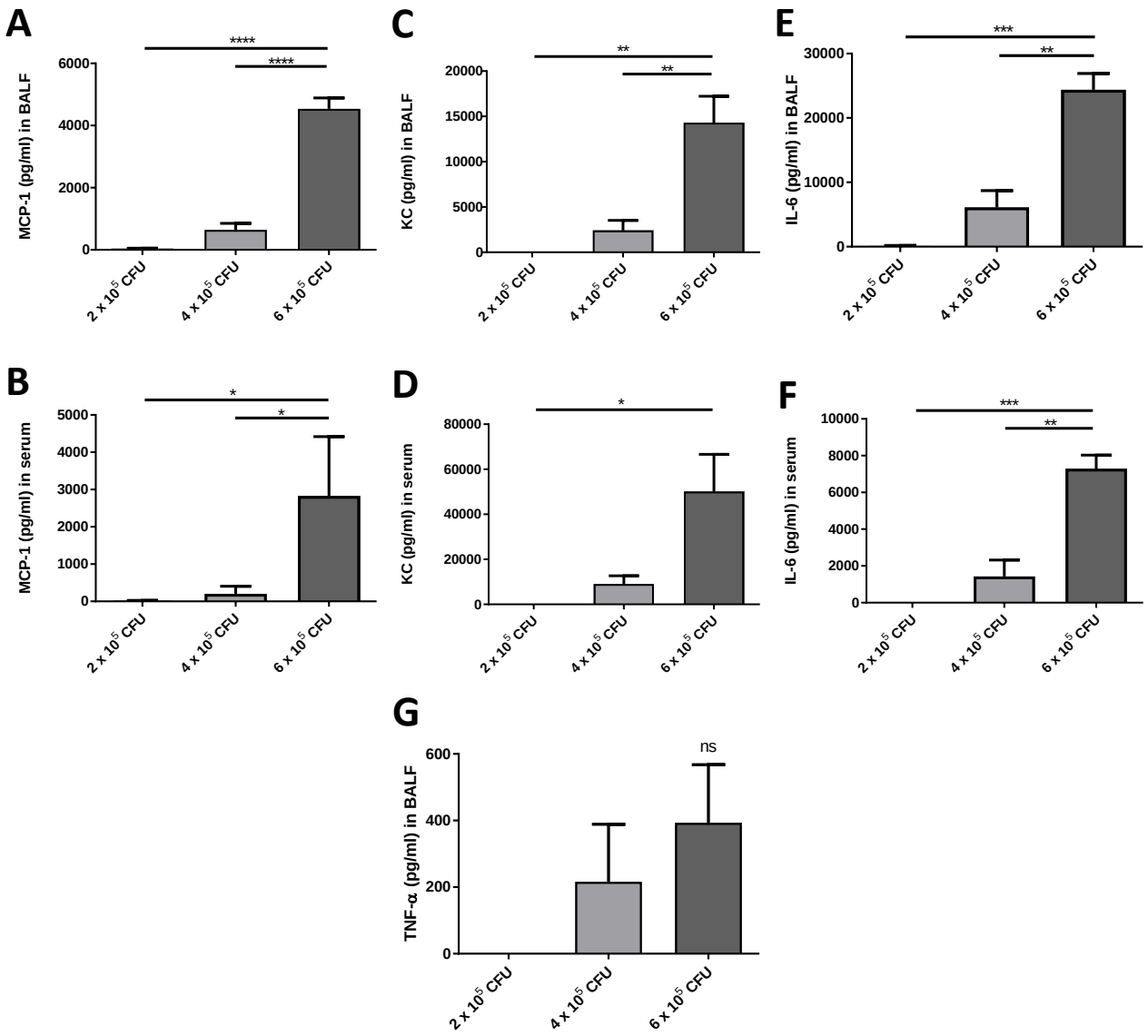

Figure 2.13: *P. aeruginosa* PA103 increases the levels of cytokines and chemokines in the BALF and serum of infected mice. Mice were instilled IN with 2, 4, or 6 x 10^5 CFUs, then euthanized and samples processed at 18 h. ELISAs were performed for MCP-1 in BALF (A) and serum (B); KC in BALF (C) and serum (D); IL-6 in BALF (E) and serum (F); and TNF-α in BALF (G). Data represent mean ± SEM for n = 3 mice per condition from one experiment and were analyzed using one-way ANOVA and Tukey's multiple comparisons test. *: $p \leq 0.05$, **: $p \leq 0.01$, ***: $p \leq 0.001$, ****: $p \leq 0.0001$.

2.3.6 Intraperitoneally-delivered IDR-1002 does not reduce *P. aeruginosa* burden in the lungs

Mice were injected IP with IDR-1002 resuspended in in vivo grade saline at 2 mg/kg or 4 mg/kg, and controls were injected with saline. After 4 hours, mice were infected IN with 4 x 10^5 CFU/mouse, then were monitored, euthanized, and processed as described previously. No differences were seen in the CFU counts, number of leukocytes in the BALF, or health scores between the control mice and the IDR-1002 mice (**Figure 2.14**).

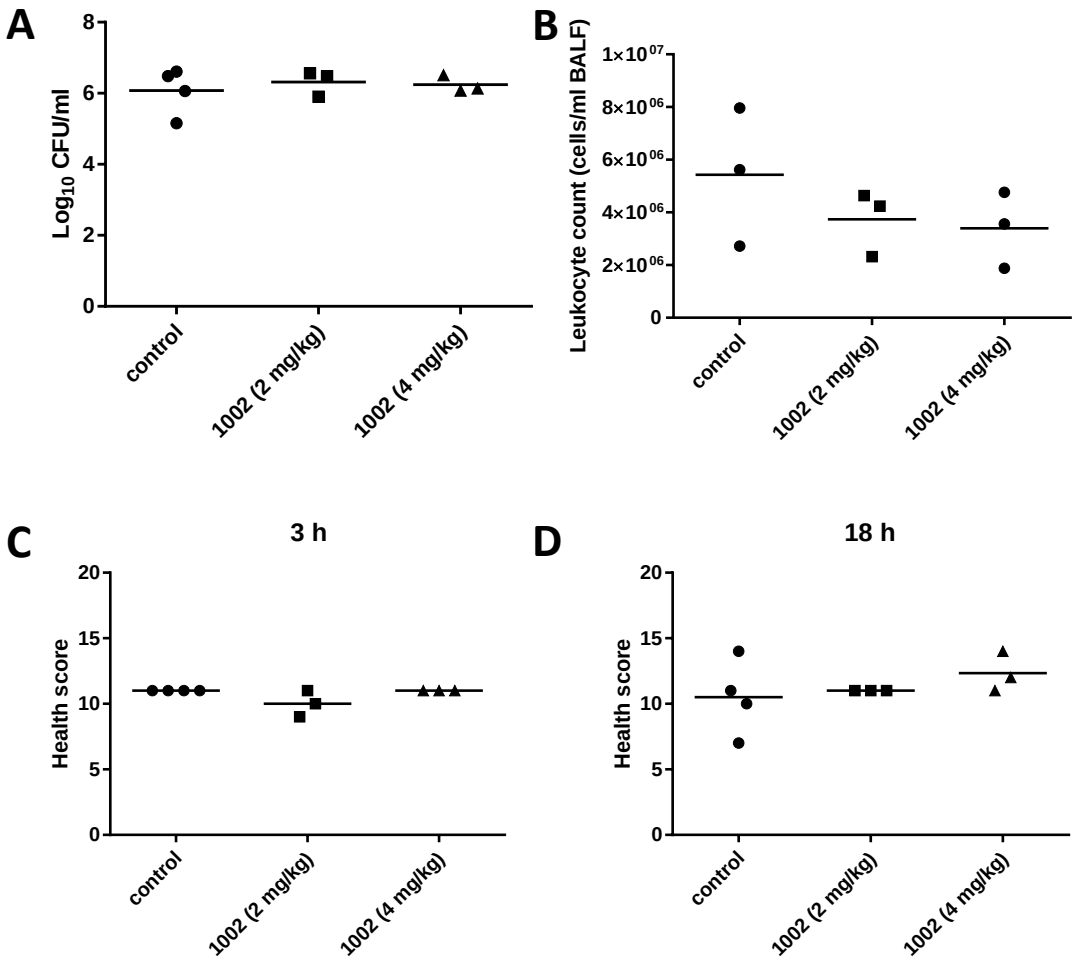

Figure 2.14: IDR-1002 delivered intraperitoneally does not change CFU burden, total leukocytes in the BALF, or signs of infection. Mice were injected IP with saline or IDR-1002 (2 or 4 mg/kg) at -4 h, instilled IN with 4 x 10^5 CFUs of *P. aeruginosa* PA103 at 0 h, then euthanized and samples processed at 18 h. (A) CFU counts from the BALF. (B) Leukocyte counts in the BALF. (C) Health scores at 3 h post-infection. (D) Health scores at 18 h post-infection. Data represent n = 3 or 4 mice per condition from one experiment and were analyzed using one-way ANOVA and Dunnett's multiple comparisons test. There were no statistically significant differences.

The BALF and serum were also used in ELISAs for MCP-1, KC, IL-6, and TNF-α (**Figure 2.15**). Interestingly, MCP-1 in the serum showed a small but significant increase at the 2 mg/kg concentration of IDR-1002. The other cytokines and chemokines had similar concentrations for both the control and the IDR-1002 mice. TNF-α in the serum was below the detectable limit.

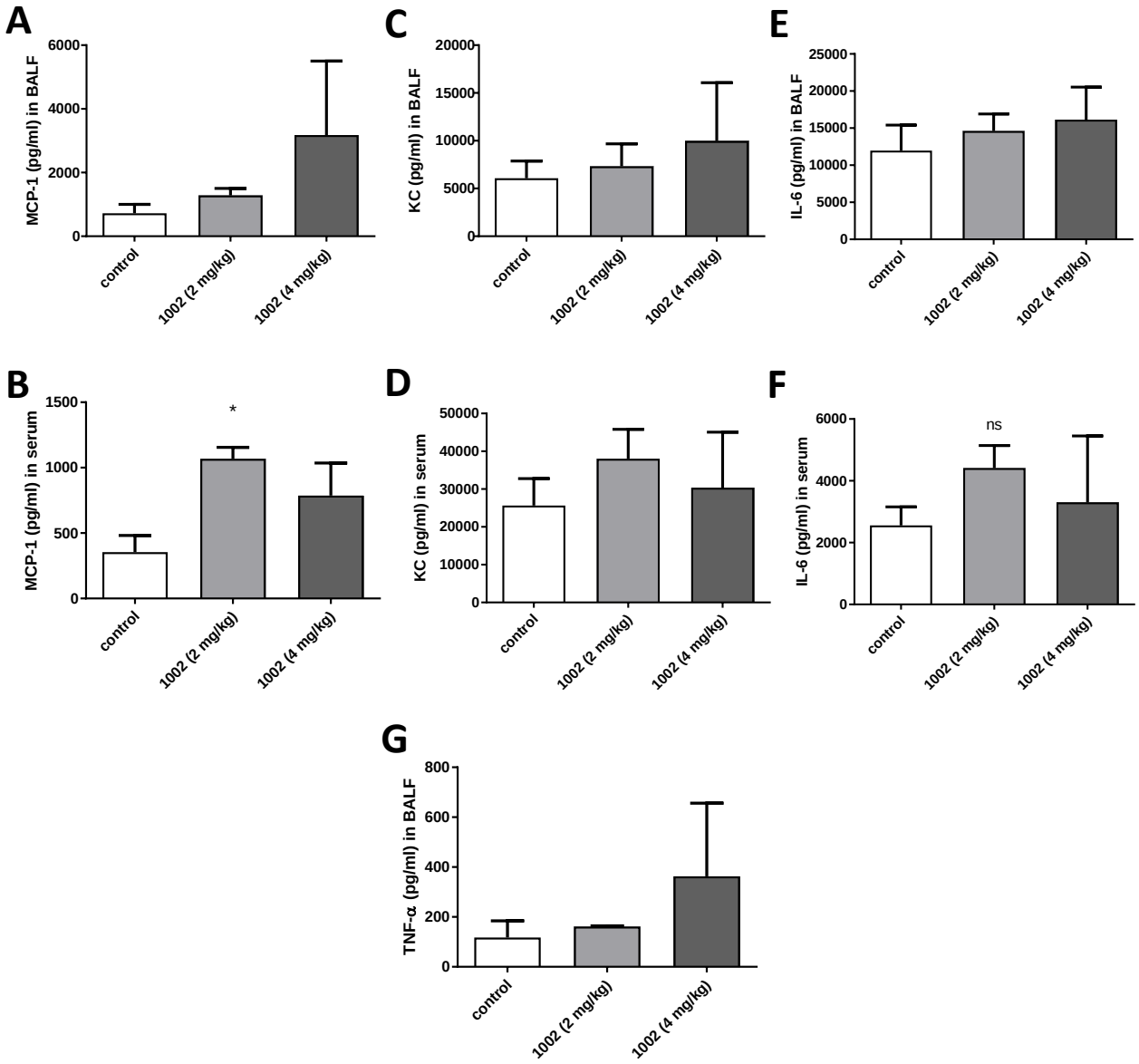

Figure 2.15: IDR-1002 delivered intraperitoneally does not affect cytokines, but infected mice given IDR-1002 show increased serum MCP-1. Mice were injected IP with saline or IDR-1002 (2 or 4 mg/kg) at -4 h, instilled IN with 4 x 10^5 CFUs of *P. aeruginosa* PA103 at 0 h, then euthanized and samples processed at 18 h. ELISAs were performed for MCP-1 in BALF (A) and serum (B); KC in BALF (C) and serum (D); IL-6 in BALF (E) and serum (F); and TNF-α in BALF (G). Data represent mean ± SEM for n = 3 or 4 mice per condition from one experiment and were analyzed using one-way ANOVA and Dunnett's multiple comparisons test. *: $p \leq 0.05$.

2.3.7 Intranasally-delivered IDR-1002 reduces *P. aeruginosa* in the lungs and pro-inflammatory cytokines in the lungs and serum in a dose-dependent manner

Next, in pilot experiments, IDR-1002 was delivered IN at low concentrations (1-4 mg/kg) or at various time points (-24 h, -4 h, -2 h, +2 h) relative to infection with *P. aeruginosa* PA103 at 4 to 8 x 10^5 CFU/mouse. Based on these experiments, it was decided to use IDR-1002 (in endotoxin-free water) delivered IN at -24 h relative to infection at 4, 6, or 8 mg/kg. Control mice were given endotoxin-free water. As before, at 0 h mice were given *P. aeruginosa* PA103, monitored at 3 and 18 h post-infection, and then euthanized at 18 h. In this experiment, *P. aeruginosa* PA103 was increased to 8 x 10^5 CFU/mouse to make the infection more consistent. IDR-1002 at 8 mg/kg significantly decreased the CFU burden in the BALF (**Figure 2.16**). While these effects were modest, this was to be expected when using an immunomodulatory treatment. The health scores were similar for all groups at 3 h, although by 18 h some of the IDR-1002 mice were showing improvements, but not consistently. No significant changes in the total leukocyte counts were seen. Differential counts of the leukocytes in the BALF showed >90% neutrophils for all groups and the remainder consisting of a small number of monocytes/macrophages and lymphocytes.

To study a potential anti-inflammatory effect of this peptide, MCP-1, KC, IL-6, and TNF-α levels were measured in the BALF and serum using ELISAs (**Figure 2.17**). Significant decreases in MCP-1 in the BALF and serum and in IL-6 in the BALF were seen in all three groups of mice given IDR-1002. The 8 mg/kg IDR-1002 group also showed a significant decrease in KC in the BALF, and the 6 and 8 mg/kg IDR-1002 mice showed a significant decrease in serum IL-6. KC in the serum and TNF-α in the BALF also trended towards decreases in the mice given IDR-1002. The TNF-α in the serum was below the detectable limit. Thus, overall, IDR-1002 showed a strong anti-inflammatory effect.

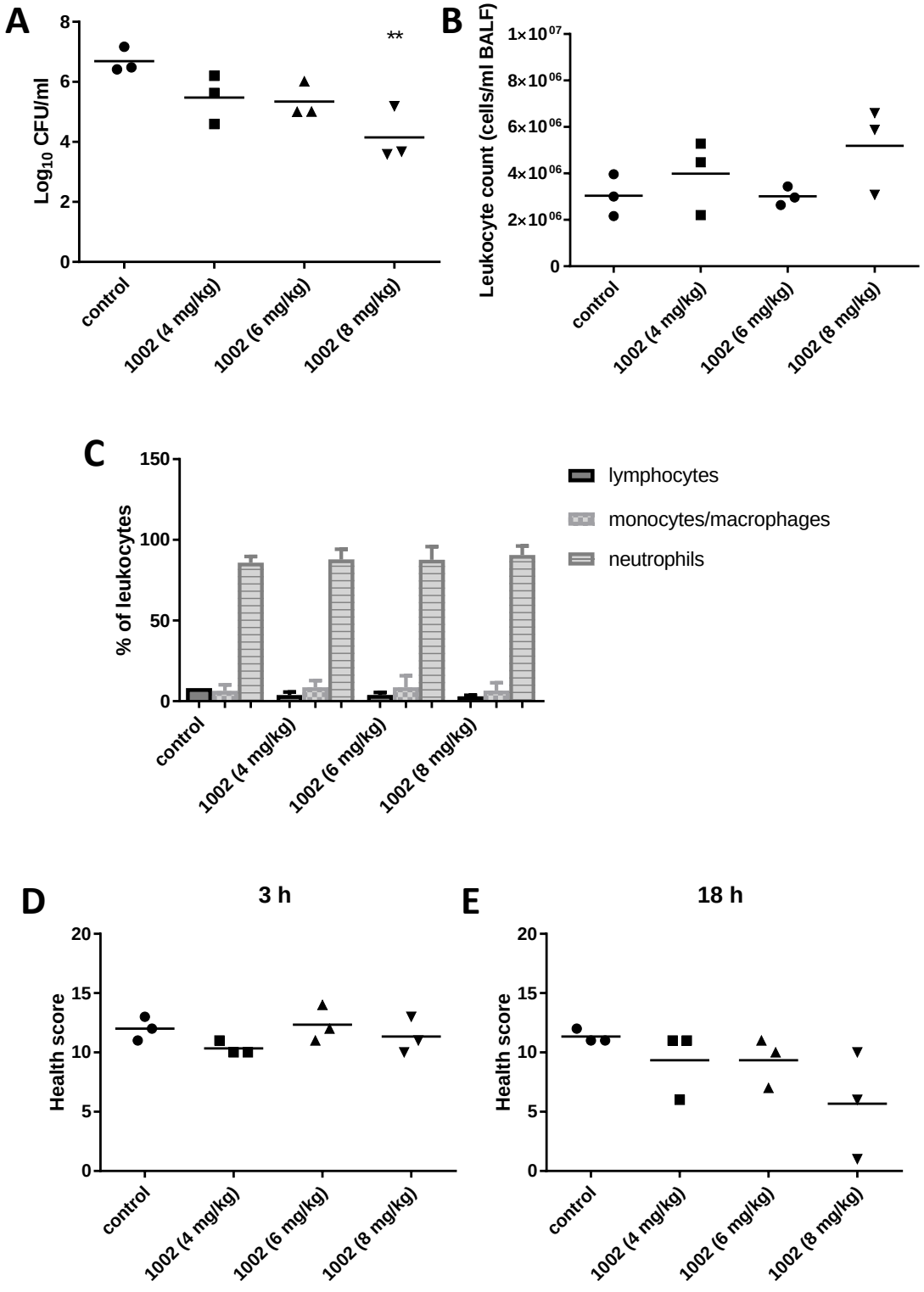

Figure 2.16: Intranasal IDR-1002 reduces *P. aeruginosa* CFUs in the BALF. Mice were given water or IDR-1002 (4, 6, or 8 mg/kg) IN at -24 h, given 8 x 10^5 CFUs of *P. aeruginosa* PA103 IN at 0 h, then euthanized at 18 h. (A) CFU counts from the BALF. (B) Leukocyte counts in the BALF. (C) Distribution of leukocytes in the BALF. (D, E) Health scores at 3 h or 18 h post-infection. Data represent n = 3 mice per condition from one experiment and were analyzed using one-way ANOVA and Dunnett's multiple comparisons test. **: $p \leq 0.01$.

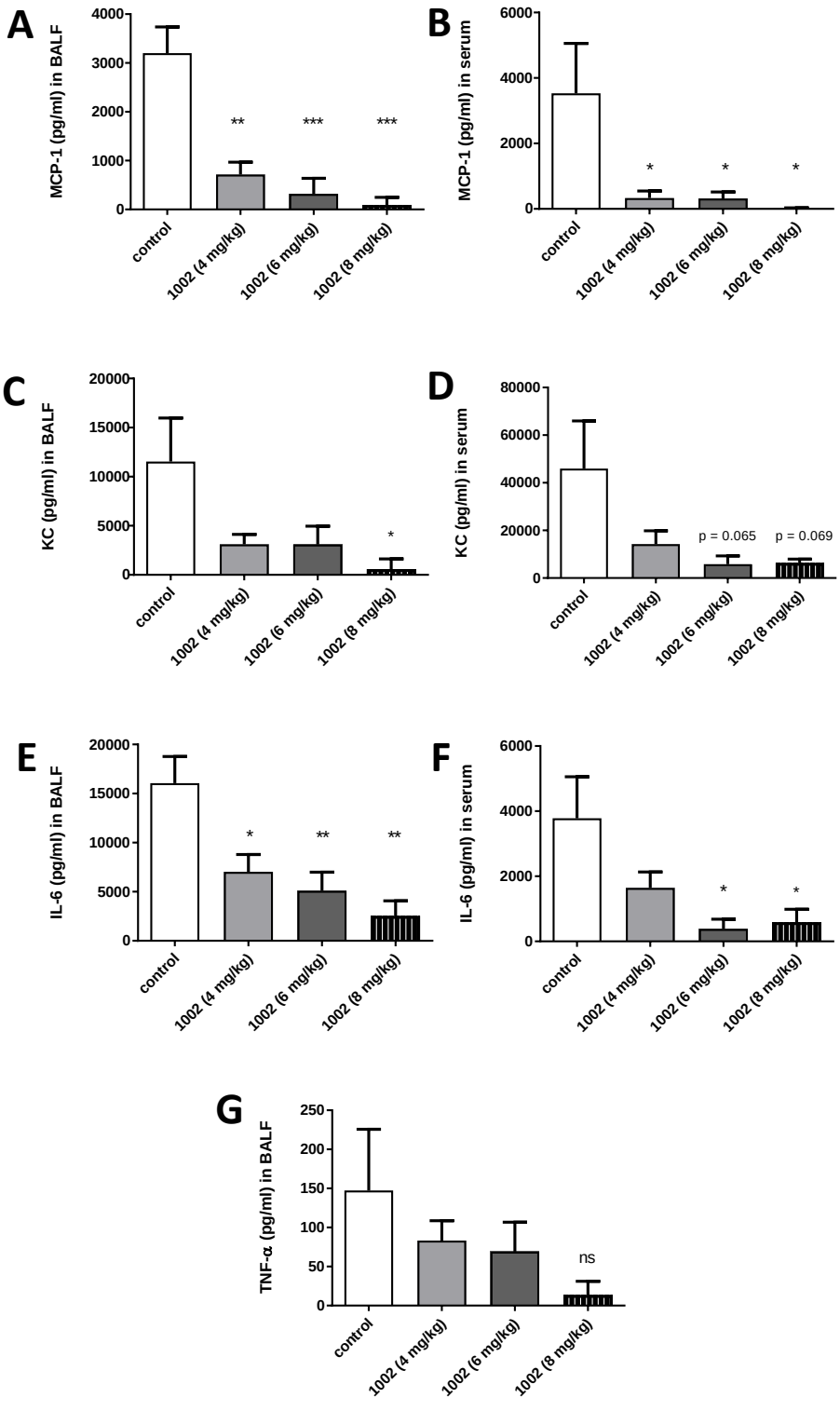

Figure 2.17: IDR-1002 reduces cytokines and chemokines in the BALF and serum. Mice were given water or IDR-1002 (4, 6, or 8 mg/kg) IN at -24 h, given 8 x 10^5 CFUs of *P. aeruginosa* PA103 IN at 0 h, then euthanized at 18 h. ELISAs were performed for MCP-1 in BALF (A) and serum (B); KC in BALF (C) and serum (D); IL-6 in BALF (E) and serum (F); and TNF-α in BALF (G). Data represent mean ± SEM for n = 3 mice per condition from one experiment and were analyzed using one-way ANOVA and Dunnett's multiple comparisons test. *: $p \leq 0.05$, **: $p \leq 0.01$, ***: $p \leq 0.001$.

2.3.8 *P. aeruginosa* strain LESB58 mixed with alginate produces a sustained infection in mice

While IDR-1002 showed encouraging results prophylactically against *P. aeruginosa* PA103 infection, the model was not conducive for testing IDR-1002 therapeutically because the mice became sick rapidly (within two hours) and visible signs of infection typically increased over the course of the experiment, making it difficult to humanely anesthetize the mice and deliver IDR-1002 IN even at the early stages of infection. Decreasing the number of bacteria delivered in order to extend the model to multiple days was also ineffective, as the mice simply cleared the bacteria and appeared fully recovered a few hours after infection. Therefore, a second lung model was developed based on the work of Hoffmann *et al.* (230), who used alginate isolated from a clinical strain of *P. aeruginosa*, then mixed the alginate with the same strain and delivered it IT. In my investigation, I used seaweed alginate to provide consistency, as alginate from *P. aeruginosa* can vary in structure. It was mixed with the clinical isolate strain *P. aeruginosa* LESB58, as initial experiments using PA103 did not produce a sustained infection. Delivery was via the IN route, which is faster and less invasive than IT. Each mouse received 7 x 10^6 CFU delivered in a 20 µl volume at 0 h. The mice were monitored twice daily and euthanized on day 2 at approximately 42 h post-infection. The lungs were homogenized and plated for CFUs. As expected, the mice given only alginate did not have *P. aeruginosa*, while the mice given alginate mixed with *P. aeruginosa* LESB58 had CFUs recovered from their lungs (**Figure 2.18**). Before homogenization, the lungs of alginate + LESB58 mice also appeared red around the opening of the trachea into the lungs, which was absent from the mice given only alginate. The alginate + LESB58 mice showed a slight initial worsening of health scores (increased numbers) but recovered by 24 h, although they lost 6-7% of their initial weight by 18 h after infection and this weight decrease was maintained throughout the course of the experiment. The lung homogenate and serum were used for ELISAs (**Figure 2.19**). Despite being two days after the initial infection, the alginate + LESB58 mice had significant increases in IL-6, MCP-1, and TNF-α in the lungs and in IL-6 in the serum. TNF-α in the serum was below the detectable limit.

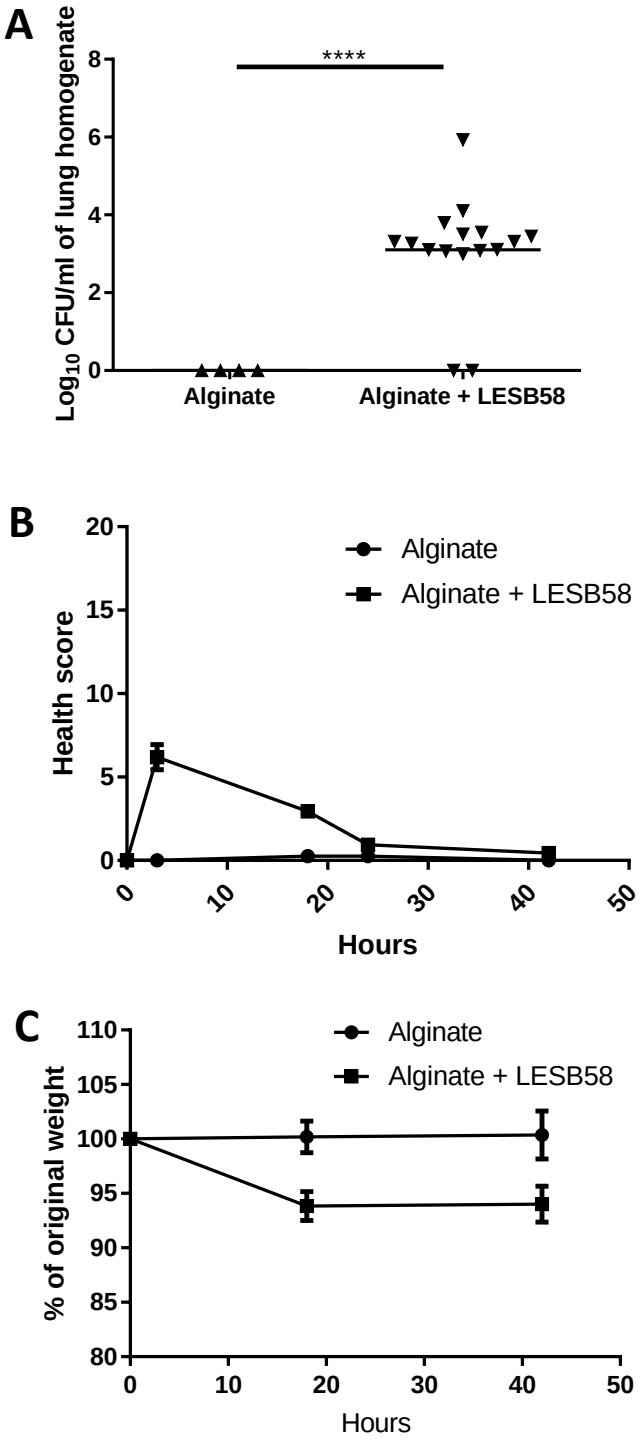

Figure 2.18: *P. aeruginosa* LESB58 is present two days post-infection when delivered with alginate. Mice were given alginate or alginate mixed with *P. aeruginosa* LESB58 (7 x 10^6 CFU/mouse) IN at 0 h, then euthanized and samples processed at 42 h. (A) CFU counts from the lung homogenate. (B) Health scores over the course of the experiment. (C) Percentage of original weight for mice over the course of the experiment. Data represent n = 4 or 16 mice per condition from the combination of two experiments and were analyzed using unpaired an t-test with Welch's correction. ****: $p \leq 0.0001$.

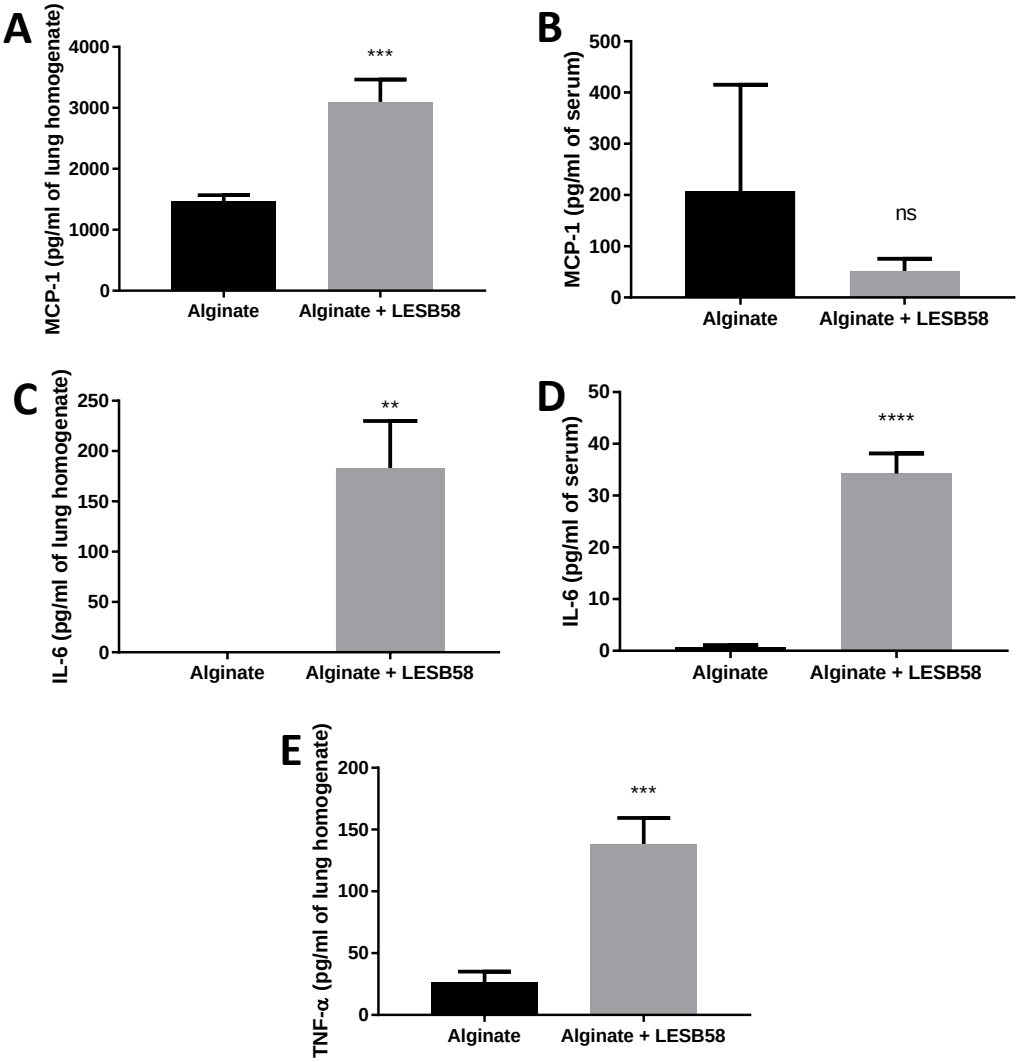

Figure 2.19: *P. aeruginosa* LESB58 produces increases in cytokines and chemokines that are present two days post-infection. Mice were given alginate or alginate mixed with *P. aeruginosa* LESB58 (7 x 10^6 CFU/mouse) IN at 0 h, then euthanized and samples processed at 42 h. ELISAs were performed for MCP-1 in lung homogenate (A) and serum (B); IL-6 in lung homogenate (C) and serum (D); and TNF-α in lung homogenate (E). Data represent mean ± SEM for n = 4 or 16 mice per condition from the combination of two experiments and were analyzed using unpaired t-test with Welch's correction. **: $p \leq 0.01$, ***: $p \leq 0.001$, ****: $p \leq 0.0001$.

2.3.9 IDR-1002 reduces lesion sizes and lung damage in the alginate model but does not reduce *P. aeruginosa* burden

To test the ability of IDR-1002 to be used as a treatment for an established *P. aeruginosa* lung infection, mice were given 7 x 10^6 CFUs of *P. aeruginosa* LESB58 in alginate IN at 0 h, then at 18 h post-infection mice were given IDR-1002 (resuspended in endotoxin-free water) at 12 mg/kg IN. Control mice received an equivalent volume of endotoxin-free water IN. Mice were then euthanized

at 42 h and the lungs homogenized and plated for CFUs. The number of recovered CFUs was indistinguishable between the two groups (**Figure 2.20**). Mice actually showed slight worsening of health scores after being treated with IDR-1002 compared to controls given endotoxin-free water, although the mice given IDR-1002 recovered by 42 h. The IDR-1002 mice also exhibited an 11% decrease in weight by 42 h, while the control mice only had a 5.5% decrease.

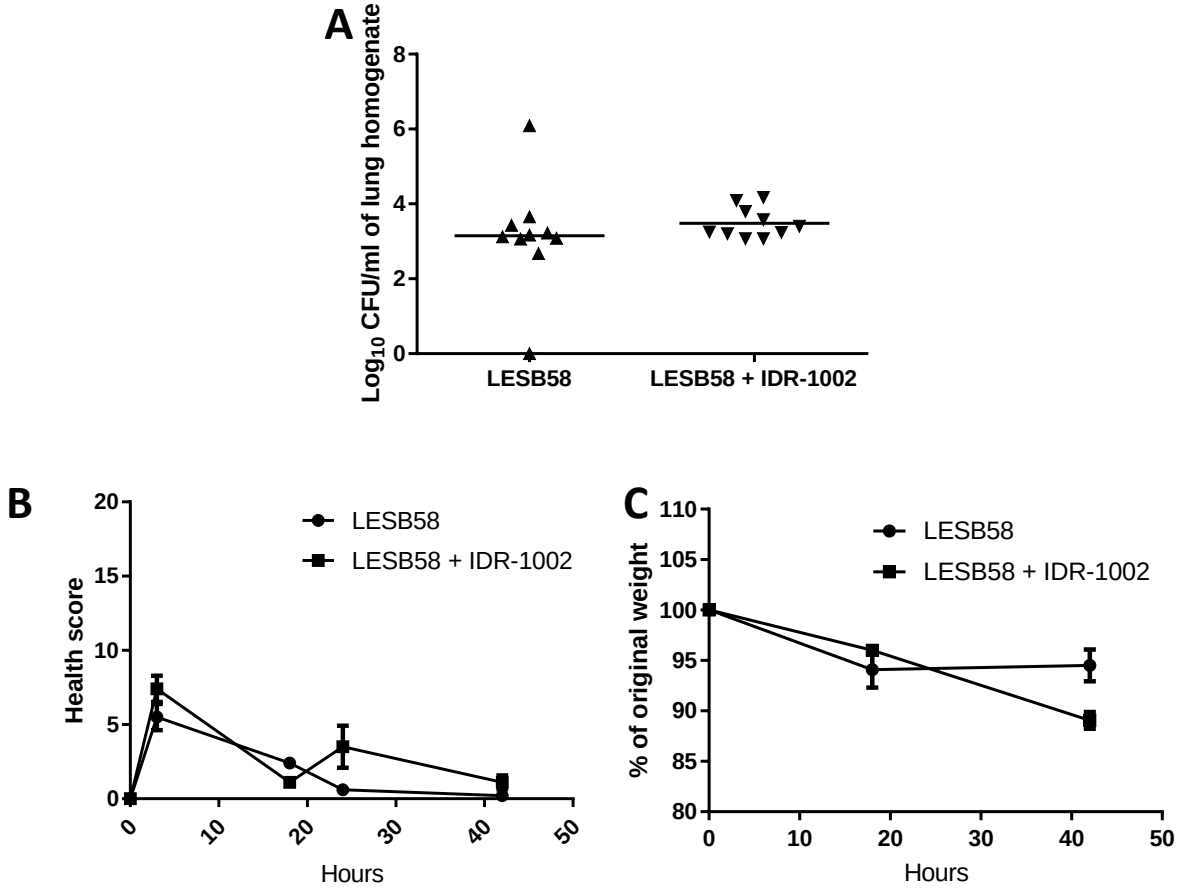

Figure 2.20: IDR-1002 does not decrease *P. aeruginosa* CFUs in the alginate model. Mice were given alginate mixed with *P. aeruginosa* LESB58 (7×10^6 CFU/mouse) IN at 0 h, then IDR-1002 (12 mg/kg) or control IN at 18 h, then euthanized and samples processed at 42 h. (A) CFU counts from the lung homogenate. (B) Health scores over the course of the experiment. (C) Percentage of original weight for mice over the course of the experiment. Data represent n = 10 mice per condition from the combination of two experiments.

The lung homogenate and serum were also used in ELISAs (**Figure 2.21**). In the IDR-1002 mice, IL-6 in the lung homogenate was significantly decreased, while the MCP-1 and TNF-α also trended towards showing decreases.

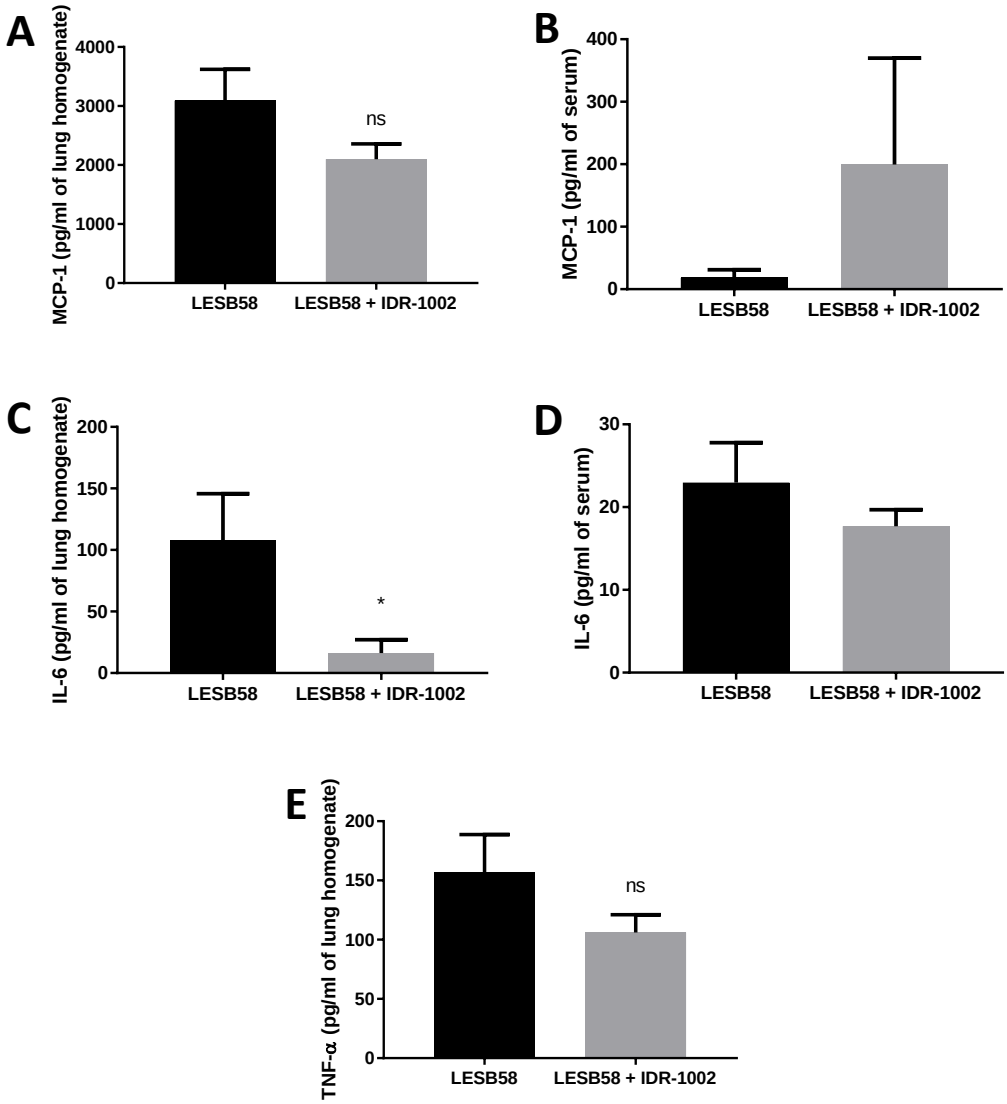

Figure 2.21: IDR-1002 decreases cytokines and chemokines in the alginate model. Mice were given alginate mixed with *P. aeruginosa* LESB58 (7×10^6 CFU/mouse) IN at 0 h, then IDR-1002 (12 mg/kg) or control IN at 18 h, then euthanized and samples processed at 42 h. ELISAs were performed for MCP-1 in lung homogenate (A) and serum (B); IL-6 in lung homogenate (C) and serum (D); and TNF-α in lung homogenate (E). Data represent mean ± SEM for n = 10 mice per condition from the combination of two experiments and were analyzed using unpaired t-test. *: $p \leq 0.05$.

Control mice showed areas of redness near the opening to the trachea (**Figure 2.22**). However, the IDR-1002 treated mice either did not show these lesions or they were greatly reduced. Lung histology revealed that the control mice had more leukocyte infiltration than the IDR-1002 mice, as observed after H&E staining. However, no major differences were seen between control mice and IDR-1002 mice in the PAS or Alcian blue stained samples.

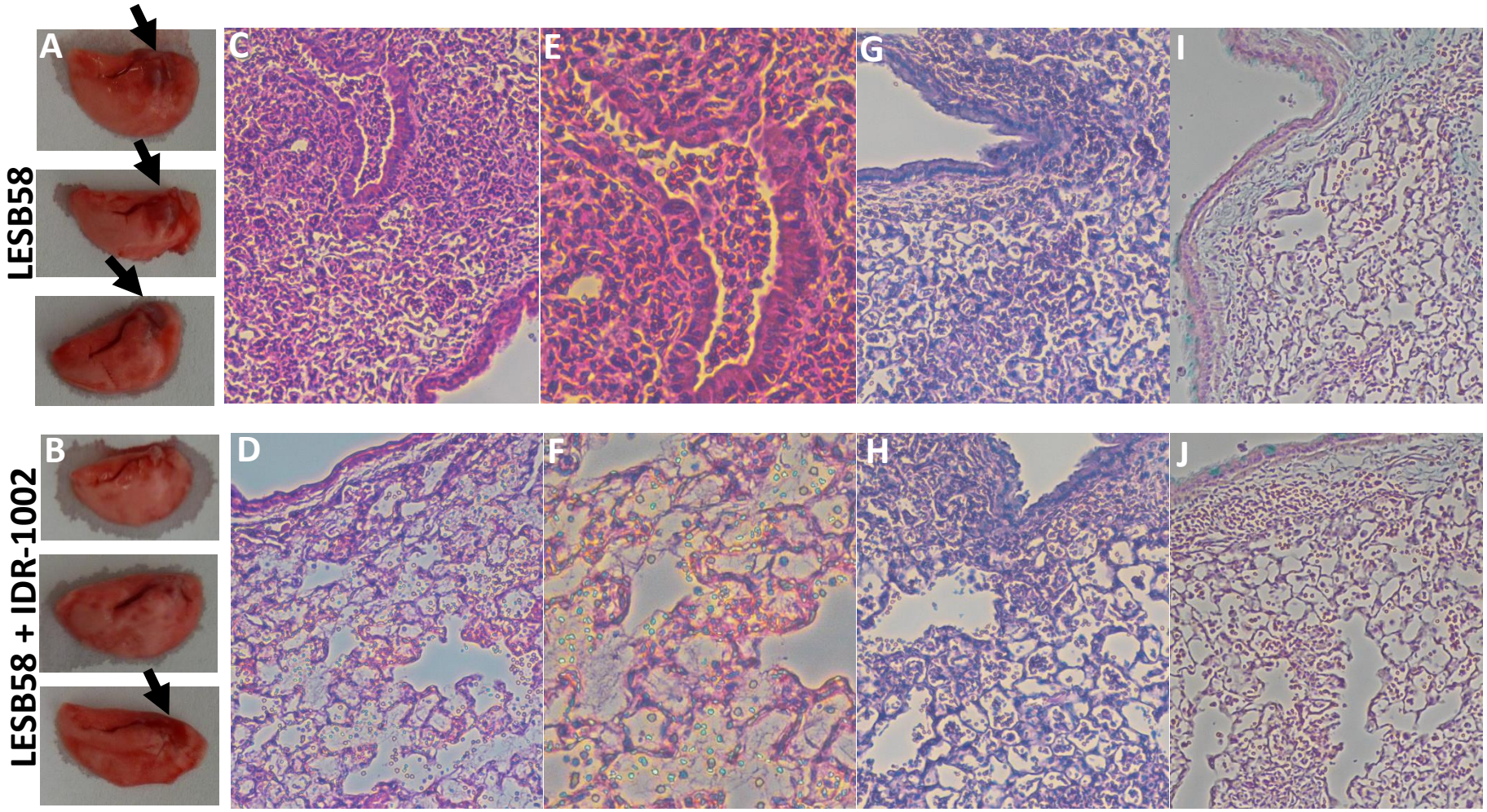

Figure 2.22: IDR-1002 mice demonstrate improved lung appearance in the alginate model. Mice were given alginate mixed with *P. aeruginosa* LESB58 (7 x 10^6 CFU/mouse) IN at 0 h, then IDR-1002 (12 mg/kg) or control IN at 18 h, then euthanized at 42 h. Control mice (A) demonstrated lesions (black arrows), whereas in the IDR-1002 mice (B) the lesions were reduced or eliminated. H&E staining in the control mice (C) showed damage, while in IDR-1002 mice (D) it was reduced. This was also seen with H&E staining in control mice (E) or IDR-1002 mice (F) at 20x. PAS staining in the control mice (G) and IDR-1002 mice (H) and Alcian blue staining in the control mice (I) and IDR-1002 mice (J) appeared similar between the two groups.

2.4 Discussion

In most in vitro and in vivo models of *P. aeruginosa* lung infection, IDR-1002 demonstrated an ability to reduce *P. aeruginosa* burden while also decreasing inflammatory mediators such as TNF-α or IL-6 that are associated with microbial infections. Many *P. aeruginosa* lung infections, such as the chronic infections seen in CF, are highly inflammatory, and so the ability to target both the *P. aeruginosa* and the associated inflammation would be highly beneficial. Importantly, IDR-1002 did not demonstrate any toxicity in vitro, whereas the natural human HDP LL-37 caused toxicity at higher concentrations. In RAW cells, IDR-1002 did not induce the production of TNF-α or IL-6, while in HBE cells increases in IL-6 were slight. IDR-1002 also did not show any toxicity in vivo in the acute *P. aeruginosa* model, and while the mice in the alginate model were slow to recover and had worse health scores after IDR-1002 delivery, their health scores had returned to baseline within a few hours. This initial worsening of health scores might be due to the effect of IDR-1002 on *P. aeruginosa* rather than the peptide itself acting on the mouse, as it had not previously shown toxicity on its own.

IDR-1002 also did not increase MCP-1 in RAW cells. This is in contrast to previous results in human PBMCs and in mouse peritoneal lavage cells, where IDR-1002 strongly induced MCP-1 (192, 200). However, in agreement with my results, in mouse bone marrow-derived macrophages (BMDMs) MCP-1 mRNA was not significantly upregulated at four hours after IDR-1002 exposure (192). PBMCs contain T cells, B cells, and monocytes, with small numbers of DCs and natural killer (NK) cells, while peritoneal lavage mostly contains B cells, T cells, and naïve macrophages (238). It is possible that the induction of MCP-1 in PBMCs and peritoneal lavage cells is due to its expression by a small population of cells, such as γδ T cells (239), or that it requires the interactions of particular combinations of cell types. Another factor might be the cellular differentiation state, as RAW cells and BMDMs are differentiated macrophages, whereas PBMCs contain monocytes and peritoneal lavage often contains naïve macrophages. IDR-1002 did however increase the levels of a different

chemokine, IL-8, in HBE cells, but these cells do not express MCP-1 and thus its expression could not be examined. Further research into the induction of MCP-1 by IDR-1002 in specific cell populations could provide insights into the mechanisms of this response.

In RAW cells, *P. aeruginosa* LPS increased the expression of IL-6, TNF-α, and MCP-1, but in the presence of IDR-1002 the levels of these mediators were significantly reduced, even when IDR-1002 was added up to 24 h prior to, or 2 h after, the addition of LPS. However, IDR-1002 did not alter the production of IL-6 or MCP-1 induced in RAW cells exposed to HKPA103, and slightly increased the TNF-α at some concentrations. Since HKPA103 also has TLR2 agonists (240), the TLR2 ligand LTA was used in combination with IDR-1002 and the peptide reduced the LTA-induced cytokines and chemokine. RAW cells lack TLR5 and PA103 lacks flagellum (23, 241), therefore, flagellin was not examined. The combination of multiple agonists found in HKPA103 may be responsible for the lack of response (240). Another TLR2 agonist, such as Pam3CSK4, may also be useful, although this agonist was tested and showed weaker induction than LTA or HKPA103 for the cytokine outputs. The reason for the lack of response to IDR-1002 in the presence of HKPA103 should be investigated further.

On the other hand, LL-37 reduced the HKPA103-induced IL-6 and MCP-1. LL-37 also reduced TNF-α at higher doses, but at lower concentrations it trended towards increasing TNF-α in the presence of HKPA103. Low doses of LL-37 have been shown to cause an increase in pro-inflammatory cytokines in the presence of TLR agonists in keratinocytes and bronchial epithelial cells (242). To the best of my knowledge, this thesis demonstrates the first report on the effects of LL-37 on cytokines and a chemokine induced by heat-killed bacteria in macrophages. A previous report using heat-killed *Porphyromonas gingivalis* in human gingival fibroblasts showed the agonist-induced IL-6 and IL-8 were reduced in the presence of LL-37 (243).

In the presence of live bacteria in RAW cells, LL-37 did not decrease their toxic effects, and actually produced a slight increase in *P. aeruginosa* PA103 toxicity when added one hour prior to

bacteria, whereas IDR-1002 caused a significant reduction in cytotoxicity. In HBE cells, IDR-1002 blocked the cytotoxic effects of PA103, instead showing cytotoxicity levels near those of the control or IDR-1002. The combination of LL-37 and PA103 in HBEs induced a synergistic effect in cytotoxicity rather than reducing the toxicity or simply having an additive effect. The combination also significantly increased IL-6 and IL-8 expression. The synergism of LL-37 and *P. aeruginosa* PAO1 in cell death in both HBE cells and primary airway epithelial cells was previously reported and found to be caused by the induction of apoptosis (244). The ability of IDR-1002 to eliminate PA103-induced cytotoxicity might have been due in part to direct antimicrobial killing based on published MIC values (204) or to the lack of effect of this peptide on apoptotic cell death.

IDR-1002 was also effective in the *P. aeruginosa* acute lung model, with reductions in both the CFUs and the levels of IL-6, TNF-α, KC, and MCP-1 in the BALF and serum. IDR-1002 was effective despite being delivered 24 h prior to infection, which was purposefully done to exclude direct anti-bacterial effects as a possible reason for its anti-infective activity. Prophylactic treatment for *P. aeruginosa* lung infections would be beneficial in infants and children with CF, as they are likely to develop *P. aeruginosa* lung infections during childhood or adolescence (48). Interestingly, no changes in total leukocyte infiltration into the lungs or in the numbers of neutrophils, monocytes/macrophages, and lymphocytes were seen for the mice given IDR-1002 compared to the control mice. Notably, in an IP *S. aureus* model, the protective effects of IDR-1002 were attributed to leukocyte recruitment to the site of injection, and elimination of monocytes and macrophages abolished the protection by IDR-1002 (192). However, this leukocyte recruitment peaked at 2-4 h post-IDR-1002 injection, and was almost returned to baseline by 24 h (192). Since samples in the acute lung model were collected approximately 42 h after IDR-1002 was administered, it is likely that any changes in leukocyte recruitment due to IDR-1002 occurred earlier or were masked by the strong recruitment in response to *P. aeruginosa*.

The alginate model resulted in a sustained infection over two days, with mice displaying a slight initial worsening in health scores but completely recovering by 24 h other than weight loss. Importantly, significant increases were still seen in inflammatory markers in both the lungs and the serum of infected mice after two days when compared to the mice given only alginate, which helps solidify the model as a prototype for testing peptides in chronic *P. aeruginosa* lung infections such as those seen in CF. When IDR-1002 was used, no changes were seen in the CFU burden. However, the peptide-treated mice had a significant reduction in IL-6 in the lung homogenate, and the macroscopically visible lesions were either eliminated or greatly reduced. Histology revealed that IDR-1002 reduced leukocyte infiltration compared to the control mice. This is in contrast to results seen in the acute model when IDR-1002 was delivered IP and was completely unproductive, with no changes in the CFU burden or lung appearance and no reduction in cytokines or chemokines in the BALF or serum. In the alginate model, decreases in lung cytokine concentrations and the differences in the lung pathology indicated that, despite the lack of change in the CFU counts, IDR-1002 still seemed to be promoting an immune response against the infection and was not completely ineffective. It is possible that mixing bacteria with alginate reduced the access of phagocytic cells to these bacteria, and given that phagocytes appear to be highly influential in protection by IDR peptides (190, 192), this might have impeded the immune response induced by IDR-1002.

In conclusion, this chapter focused on the potential of IDR-1002 as a treatment of *P. aeruginosa* lung infections. IDR-1002 reduced pro-inflammatory cytokines in vitro and in both in vivo models. As excessive inflammation is a life-threatening feature in chronic *P. aeruginosa* lung infections, the results are encouraging for using IDR-1002 against *P. aeruginosa* infections. Critically, IDR-1002 demonstrated both effectiveness and safety, two features that were limited in previous peptide-based drugs against *P. aeruginosa* in vivo lung infections (217-220). Overall, IDR-1002 shows promise as a new agent to combat *P. aeruginosa* lung infections.

Chapter 3: Optimizing IDR-1018 formulations to prevent peptide aggregation and maintain immunomodulatory activity

3.1 Introduction

HDPs are small peptides that have shown numerous immunomodulatory effects and successes against infective diseases in vitro and in vivo in animal models, but issues of cost and toxicity have limited their translation to human medicine.

IDR peptides are examples of synthetic HDPs. To date in our laboratory, 12 amino acid long peptides have been explored to decrease their price of synthesis relative to that for longer HDPs, and their sequences have been modified from the bovine HDP bactenecin to enable improved immunomodulatory functions with reduced cytotoxicity. IDR-1018 is the lead peptide candidate and has shown success in in vivo models for tuberculosis infection, cerebral malaria, neonatal hypoxia/endotoxin challenge, invasive *S. aureus* infections, and *S. aureus*-infected wounds and implants (200, 205-208). However, it was ineffective in other conditions such as a rheumatoid arthritis model and in diabetic wounds (205, 212). While increasing our understanding of the mechanisms through which IDR-1018 acts could elucidate why it works in some models but not others, another possible reason for the disparity in results is due to its aggregation properties. IDR-1018 has been shown to aggregate in numerous solutions and seems to follow the Hofmeister series, a classification of the effects of various ions on protein solubility, in terms of precipitating in solution (Dr. Evan Haney, unpublished results). This aggregation makes it difficult to deliver IDR-1018 in vivo and could lead to toxicity if the peptide cannot be cleared effectively. Recent studies have suggested that aggregation is in fact a widespread issue with cationic amphipathic peptides. For example, a variety of HDPs including LL-37, α-defensins, and dermaseptin aggregate or precipitate at critical concentrations in various solutions (245-247), which could lead to inconsistent data and limit their potential as therapeutics. Protein aggregation contributes to a number of diseases (248), and it is

thought that peptide aggregates are inherently toxic (249). A tendency to aggregate might be a class effect of cationic amphipathic peptides, and a variety of strategies have been proposed for limiting peptide aggregation (250).

One method to combat aggregation is through formulation and altering the drug delivery system, such as by combining the drug with polymers. Polymers have been used in drug delivery systems for decades, with a common example being cellulose derivatives (216). Two of these, carboxymethyl cellulose (CMC) and hydroxypropyl methyl cellulose (HPMC), are already frequently used as food additives and in the pharmaceutical industry. Other polymers have emerged more recently as potential drug formulations. One is hyaluronic acid (HA), a glycosaminoglycan found in numerous human tissues that is also a major component of the extracellular matrix (ECM). It has gained prominence in recent years for use in cosmetic formulations, but is also being tested widely in drug delivery, including for peptides (251). Other polymers emerging for formulation usage are hyperbranched polyglycerols (HPGs), which have shown promise for drug delivery due to their lack of toxicity and long half-lives in vivo (252, 253). All of these polymers possess negatively charged functional groups at physiological pH, making it easy for them to bind and interact with cationic peptides and thus limiting HDP aggregation.

In addition to polymers, resuspending IDR-1018 in other solvents, either alone or in combination with a polymer, could reduce aggregation and improve delivery. PBS, Tris-buffered saline (TBS), and HEPES are common buffers in cell biology. Water, while not appropriate for some methods of delivery such as IV or IP, is commonly used for the resuspension of IDR peptides in vitro and can also be used for IN delivery in vivo. Finally, solvents could also be optimized to limit aggregation of the solutes through the addition of other substances. For example, trehalose is a disaccharide made in bacteria, fungi, plants, and invertebrate animals that has been shown to increase protein stability and limit protein aggregation (254). Trehalose limits the formation of aggregates by amyloid-β, the peptide found in Alzheimer's disease, which has also been shown to have

immunomodulatory and antimicrobial properties (254-256). The use of trehalose has been limited due to high manufacturing costs, but new methods have made it relatively inexpensive and expanded its applications (254).

The goal for this project was to find a new drug delivery system for IDR-1018 that limited aggregation while maintaining or even improving its immunomodulatory actions both in vitro and in vivo in the acute *P. aeruginosa* lung infection model. Additionally, the formulation needed to be nontoxic and safe for delivery in vivo. A screening method in PBMCs and HBE cells stimulated with LPS or poly I:C, respectively, was chosen in order to evaluate the formulations (195). Using IDR-1018 with HPG improved the aggregation and maintained immunomodulatory activity in vitro. In the acute *P. aeruginosa* lung infection model, the formulated peptide was not as effective at reducing CFUs in the BALF as unformulated IDR-1018, but it still showed a trend towards reductions in the release of inflammatory cytokines and chemokines much like the unformulated peptide. These results provide new insight into IDR formulation and a framework for future delivery systems for HDPs and IDRs.

3.2 Materials and methods

3.2.1 Mice and ethics statement

C57Bl/6J mice were ordered from Jackson Laboratory. Female mice were used between 6-8 weeks of age. All experiments were approved by the UBC Animal Care Committee.

3.2.2 Reagents

IDR-1018 (VRLIVAVRIWRR-NH_2) was synthesized by F-moc chemistry (CPC Scientific, Sunnyvale, California, USA). IDR-1018 was formulated with CMC, HPMC, HPG, or HA and resuspended in PBS, TBS, HEPES, trehalose solution, or endotoxin-free water by the Centre for Drug Research and Development (Vancouver, British Columbia) and kept at 4°C for a maximum of two weeks. LPS from *P. aeruginosa* PAO1 strain H103 was isolated in the laboratory by the Darveau-

Hancock method as previously described (237). Briefly, *P. aeruginosa* was grown to an OD_{600} reading of 0.6-0.8, then the bacteria were centrifuged and lyophilized (237). The dried bacterial cells were then resuspended and subjected to a series of purification steps to remove contaminating material, then the LPS concentration was quantified by determining the concentration of the LPS component 2-keto-3-deoxyoctonate (237). Poly I:C was purchased from InvivoGen (San Diego, California, USA).

3.2.3 PBMC isolation

PBMCs were isolated using a standard density gradient centrifugation method. Human venous blood was collected from healthy volunteers into heparin-containing vacutainer tubes (BD Biosciences, San Jose, California, USA), in accordance with University of British Columbia ethical guidelines and protocol approval. Human blood was diluted at a 1:1 ratio with PBS (Gibco 10010) and gently layered onto LymphoPrep (STEMCELL Technologies, Vancouver, British Columbia, Canada) at a ratio of two parts blood and PBS mixture to one part LymphoPrep. The tubes were centrifuged, then the buffy layer was transferred to a fresh tube and washed two times with PBS before being resuspended in RPMI 1640 (GE Healthcare HyClone SH30255.FS) supplemented with 10% (v/v) FBS. Cells were placed in 96-well plates (2×10^6 cells/ml, 50 µl per well) and rested for 1-2 h before the addition of stimuli in 50 µl, giving a final volume of 100 µl. Supernatants were collected 24 h after treatment and used for LDH assays and ELISAs.

3.2.4 HBE cell culture

HBE cells were grown in MEM with Earle's salts (Gibco 11090) with the addition of 10% (v/v) heat-inactivated FBS and 2 mM L-glutamine (Gibco 25030). Cells were maintained at 37°C with 5% carbon dioxide and passaged by removing media, washing with PBS (Gibco 10010), and adding 0.05% trypsin (Gibco 2520) to detach the cells. Cells were centrifuged, the supernatant was removed, and the cells were resuspended and transferred to new flasks.

For experiments, HBE cells were passaged into 96-well plates (2.5×10^5 cells/ml, 0.2 ml per well) and allowed to grow for approximately two days to achieve greater than 80% confluency in a

monolayer. At approximately 2 h before experiments, the medium was removed, cells were washed with fresh MEM supplemented with L-glutamine and 1% FBS, and additional 1% FBS MEM was added. The cells were rested for 2 h, then used for experiments. Culture supernatants were collected 24 h after treatment and used for LDH assays and ELISAs.

3.2.5 ELISAs

Samples were stored at -20°C until use in ELISAs. The levels of cytokines and chemokines were measured using eBioscience (San Diego, California, USA) antibodies for murine TNF-α and IL-6 and for human IL-1β, IL-6, and MCP-1. Murine MCP-1 antibodies were from eBioscience or R&D Systems (Minneapolis, Minnesota, USA). Murine KC (CXCL1) antibodies were from Fitzgerald (Acton, Massachusetts, USA) or R&D Systems. Human IL-8 antibodies were from Invitrogen (Waltham, Massachusetts, USA). Standards were purchased from the same sources. The ELISAs were performed by following the manufacturer protocols with optimization of antibody and sample dilutions, washes, and incubation times. They were developed using TMB (eBioscience) and the reactions were stopped with 2 N sulfuric acid. The plates were read on a Power Wave X340 plate-reader (Bio-Tek Instruments, Winooski, VT) and data were fitted to a 4-parameter standard curve using KC4 software (Bio-Tek).

3.2.6 LDH

Supernatants collected from cell cultures were combined at a 1:1 (v/v) ratio with complete LDH assay reagent (Roche Diagnostics, Basel, Switzerland). After incubating for 15-25 minutes in the dark, the plates were read on a Power Wave X340 plate-reader (Bio-Tek Instruments, Winooski, VT). Results were normalized to the control sample (0% toxicity) and to a sample in which 2% (v/v) Triton X-100 had been added to cause complete lysis of the cells (100% toxicity).

3.2.7 Preparation of bacteria and acute *Pseudomonas* lung infection

Bacterial strain *P. aeruginosa* PA103 was streaked onto LB plates from a frozen stock and grown overnight at 37°C. The following day individual CFUs were used to make overnight cultures

in LB and grown overnight at 37°C with shaking. Overnight cultures were diluted 1:50 and grown to an OD_{600} reading of approximately 0.5. Bacteria were washed with endotoxin-free 0.9% sodium chloride solution (saline), centrifuged, supernatant discarded, and the pellet resuspended in endotoxin-free saline to an OD_{600} of 0.5. Bacteria were then diluted to the appropriate concentration based on previous experiments relating OD_{600} reading to CFU/ml, and serial dilutions were plated on LB to check the final concentration.

Mice were anesthetized with 2-5% isoflurane and placed on an intubation stand (BrainTree Scientific, Massachusetts, USA). IDR-1018, *P. aeruginosa*, or appropriate controls were instilled dropwise using a micropipette into the left nostril of each mouse. *P. aeruginosa* was in a 20 µl volume, while the peptide volume was approximately 10-30 µl depending on the weight of the mouse. Isoflurane was periodically applied to keep the mouse at a steady respiratory rate. After instillation, mice were kept on the stand under isoflurane for 2-3 minutes to ensure absorption of the liquid. Once they were fully recovered, they were returned to their cages.

For sample collection, mice were euthanized with 120 mg/kg of IP injected sodium pentobarbital. Blood was collected from the inferior vena cava and allowed to clot, then centrifuged and the serum was collected. For bronchoalveolar lavage fluid (BALF) collection, the chest cavity and trachea were exposed and an incision was made in the trachea. A cannulated needle was then inserted and used to slowly fill the lungs with sterile PBS (600 µl), which was then slowly withdrawn through the cannulated needle and saved. This procedure was repeated twice for a total of three washes. The first BALF wash was used for CFU enumeration by spread-plating undiluted BALF or ten-fold dilutions made in PBS onto LB agar plates in duplicate. Plates were incubated overnight at 37°C and CFUs were enumerated the following day. The remaining first BALF wash was centrifuged and the supernatant saved for ELISAs. The pellet from the first BALF wash was combined with the pellet from BALF washes 2 and 3 and resuspended in PBS, then leukocytes were counted on a hemocytometer using Turk's stain.

3.2.8 Statistical analysis

Data were analyzed using Microsoft Excel 2013 and GraphPad Prism version 7. GraphPad Prism was used to perform a one-way ANOVA with Tukey's or Dunnett's multiple comparisons tests when comparing the means of all columns or when comparing to only to a control column, respectively. A value of $p \leq 0.05$ was considered statistically significant.

3.3 Results

3.3.1 Unformulated IDR-1018 aggregates at higher concentrations, which limits effectiveness in the acute *P. aeruginosa* lung infection model

To test the effects of unformulated IDR-1018 against *P. aeruginosa*, mice were given peptide resuspended in water or water alone (all endotoxin-free), one day prior to infection. Mice given 4 or 8 mg/kg of IDR-1018 (at concentrations of 8 or 16 mg/ml, respectively) easily inhaled the peptide, but the 12 mg/kg concentration (peptide at 24 mg/ml) led to the peptide forming a gel-like substance on the nostril that could not be completely inhaled. At 0 h, the mice were infected with 8×10^5 CFU/mouse IN of *P. aeruginosa* PA103, then BALF and serum were collected at 18 h. The CFU counts in the BALF showed that the group receiving 8 mg/kg IDR-1018 had a significant reduction in *P. aeruginosa* CFUs and also had improved health scores at 3 and 18 h (**Figure 3.1**). As expected, the 12 mg/kg group had a CFU burden similar to that of the controls due to the aggregation of the peptide at this concentration interfering with its administration. The 4 mg/kg group had one mouse without bacteria but the other mice had a high CFU burden. No significant changes were seen in total leukocyte infiltration into the lungs or in percentage of weight change over the course of two independent experiments.

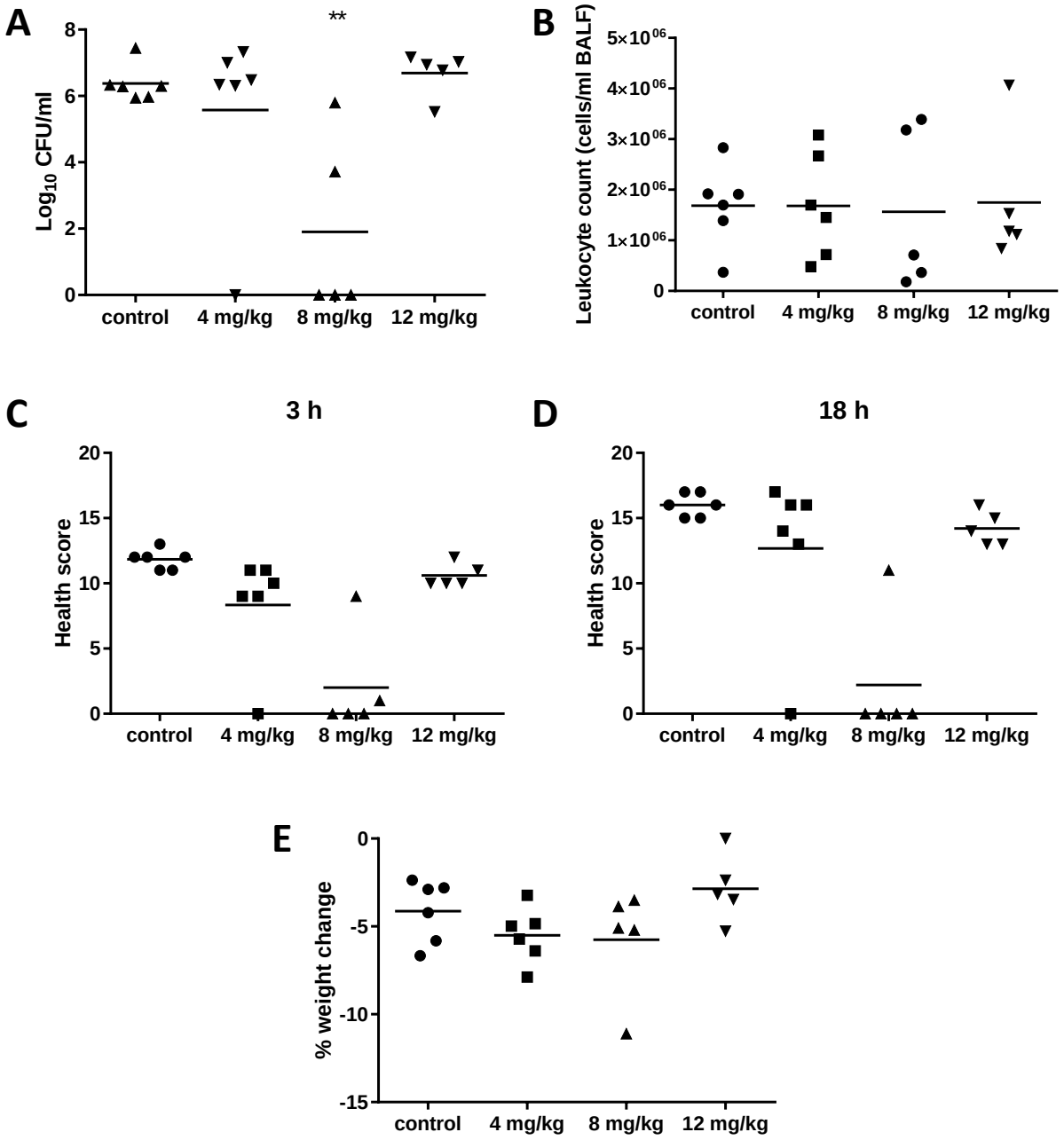

Figure 3.1: IDR-1018 aggregates at higher concentrations and this limits its effectiveness in an in vivo *P. aeruginosa* acute lung model. Mice were given water or IDR-1018 (4, 8, or 12 mg/kg) IN at -24 h, given approximately 8 x 10^5 CFUs of *P. aeruginosa* PA103 IN at 0 h, then euthanized and samples processed at 18 h. (A) CFU counts from the BALF. (B) Leukocyte counts in the BALF. (C, D) Health scores at 3 h or 18 h post-infection. (E) Percentage of weight change from -24 h to 18 h. Data represent n = 5 or 6 mice per condition from two independent experiment and were analyzed using one-way ANOVA and Dunnett's multiple comparisons test. **: $p \leq 0.01$ compared to control.

An examination of pro-inflammatory cytokines and chemokines in the BALF and serum revealed decreases in MCP-1, IL-6, and TNF-α in the BALF and serum in the mice that received 8

mg/kg, although the decreases were not significant (**Figure 3.2**). The control mice and the mice given 4 or 12 mg/kg of IDR-1018 had similar concentrations to each other for every output.

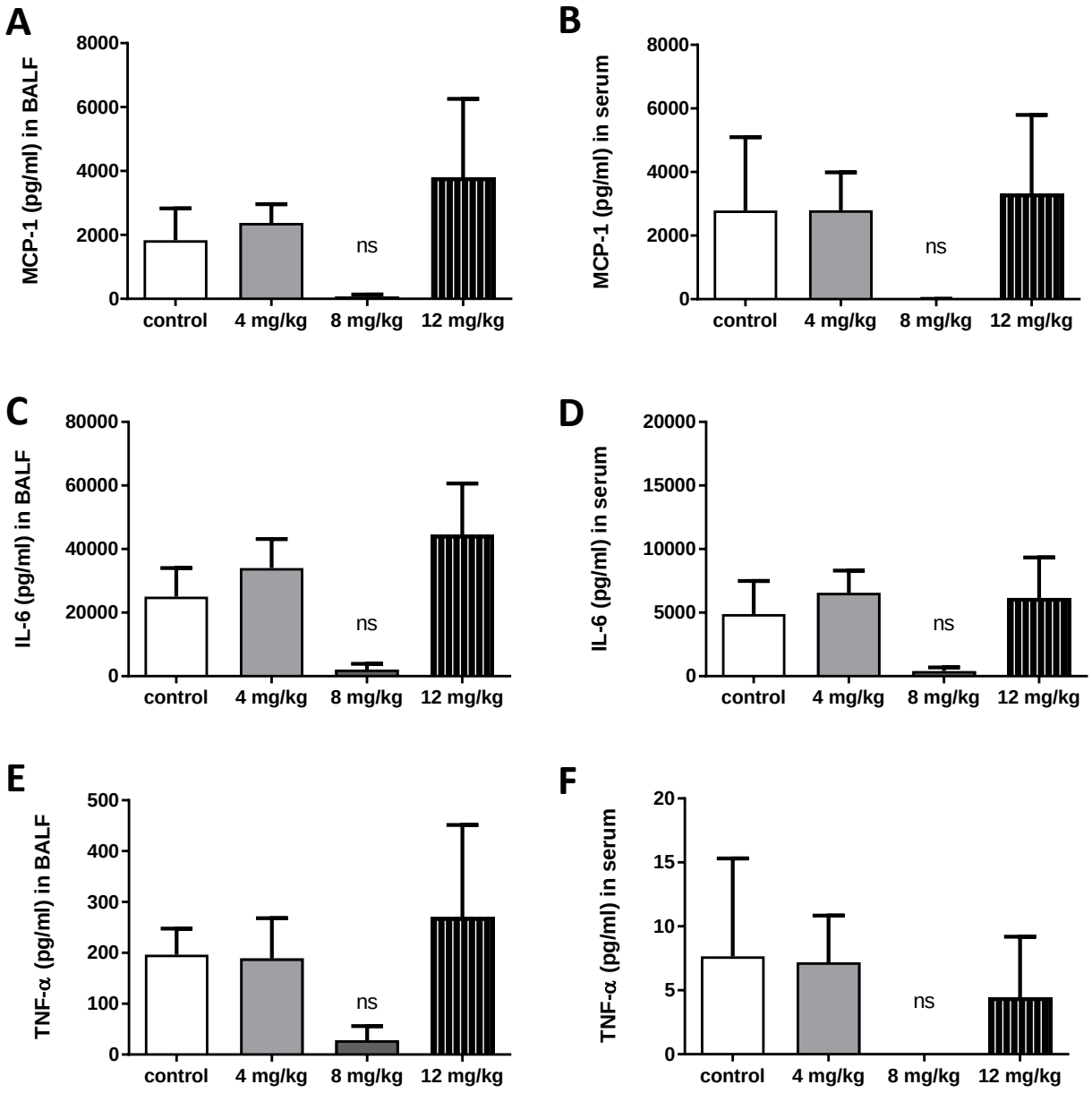

Figure 3.2: Concentrations of cytokines and chemokines in BALF and serum of *P. aeruginosa* infected mice given IDR-1018. Mice were given water or IDR-1018 (4, 8, or 12 mg/kg) IN, at -24 h, given 8 x 10^5 CFUs of *P. aeruginosa* PA103 IN at 0 h, then euthanized and samples processed at 18 h. ELISAs were performed for MCP-1 in BALF (A) and serum (B); IL-6 in BALF (C) and serum (D); and TNF-α in BALF (E) and serum (F). Data represent mean ± SEM for n = 5 or 6 mice per condition from two independent experiments and were analyzed using one-way ANOVA and Dunnett's multiple comparisons test. No groups were significant compared to the control group.

3.3.2 Hyperbranched polyglycerol reduces IDR-1018 aggregation while maintaining immunomodulatory effects in vitro

To identify an IDR-1018 formulation that prevented aggregation, four polymers, CMC, HPMC, HPG, and HA, were resuspended in PBS and mixed with IDR-1018 at ratios (w/w) of 6, 3, 1, or 0.5 of polymer to IDR-1018 to give final concentrations of IDR-1018 of 100, 30, or 10 µg/ml. These were added to PBMCs or HBE cells, along with unformulated IDR-1018 resuspended in water or PBS. Polymers without peptide, equivalent to the concentration of the polymer in the 100 µg/ml formulations, were also included as controls. The peptides were then tested on the cells alone or in combination with TLR agonists, namely either *P. aeruginosa* LPS added to the PBMCs or poly I:C for the HBE cells. Supernatants were collected after 24 h and used for LDH cytotoxicity assays and ELISAs.

In HBE cells, only low levels of toxicity were seen under all conditions. In PBMCs, both CMC and HPMC showed some cytotoxicity (**Figure 3.3**), particularly at 100 µg/ml of IDR-1018. However, this cytotoxicity was also seen when only the polymer was used and no IDR-1018 was included. HPG showed some toxicity at the highest ratio of polymer, while no notable toxicity was seen in the HA formulations. There were also some negative values seen for the percentage of cytotoxicity. These are due to some treatments causing reduced background release of LDH compared to the untreated control, a phenomenon that has been linked to the effects of IDR-1018 on glycolysis (257).

Interestingly, IDR-1018 in PBS at 100 µg/ml also showed some toxicity, which was not seen in the IDR-1018 resuspended in water. This also correlated with the formation of visible sheet-like aggregates found near the surface of the liquid in the wells containing IDR-1018 in PBS. In the wells with IDR-1018 in water, the aggregates were more punctate and located near the cells. Additionally, while the HA formulations did not cause toxicity they were greatly aggregated, and ratios over 1 could not be tested due to aggregation. The formulations with HPMC and CMC showed some aggregation,

while the HPG formulations showed somewhat reduced aggregation. Therefore, it was decided to focus on HPMC, CMC, and HPG for testing immunomodulatory activity.

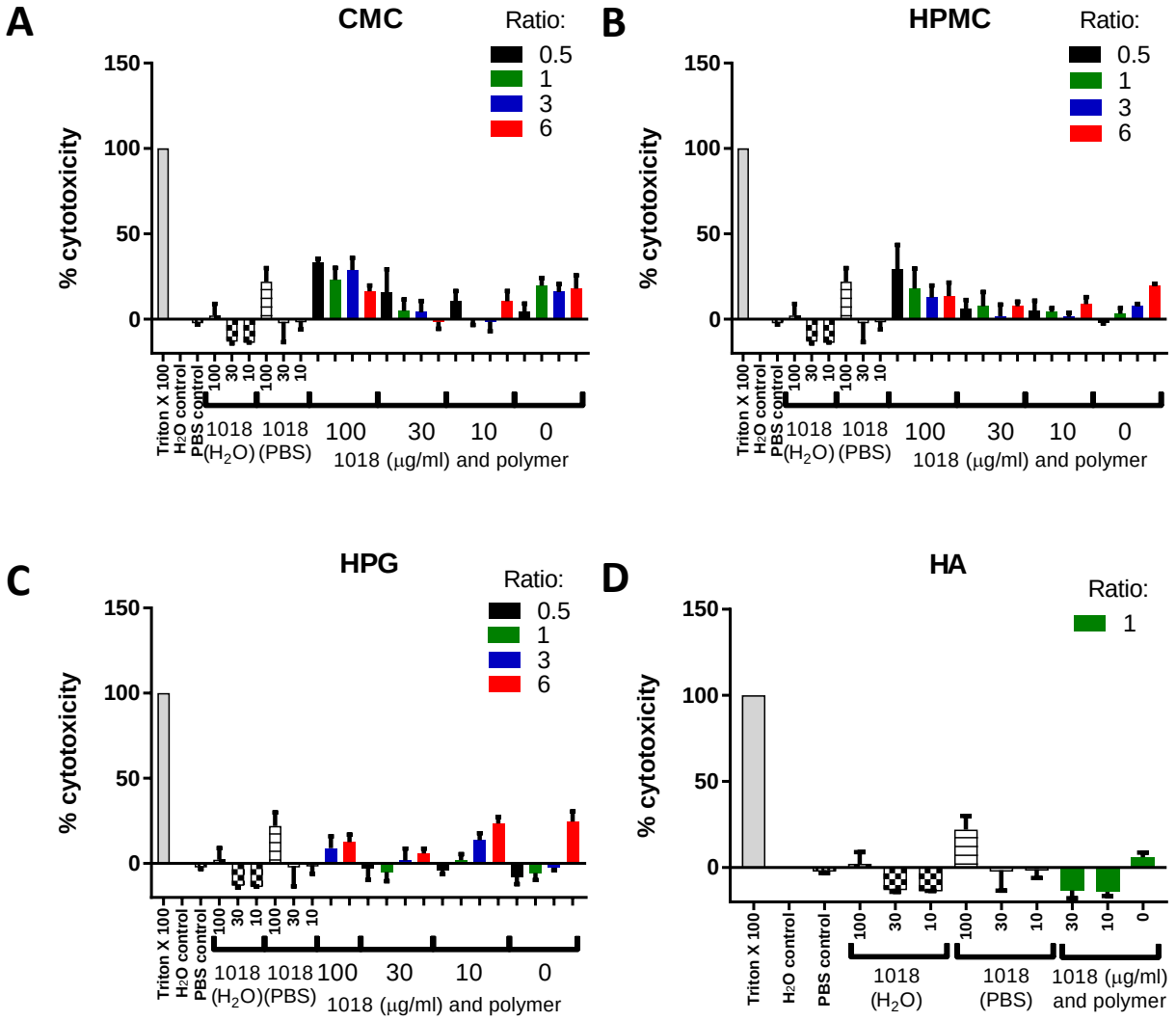

Figure 3.3: CMC and HPMC show cytotoxicity, while HPG and HA show limited toxicity. PBMCs were given IDR-1018 mixed with CMC (A), HPMC (B), HPG (C), or HA (D). The polymers were at a ratio of 6, 3, 1, or 0.5 to 100, 30, or 10 µg/ml of IDR-1018. Unformulated IDR-1018 in PBS or water or controls given water or PBS without peptide were also included (displayed in all graphs for comparison). The polymers at their maximum concentration were also included without IDR-1018. Data represent mean ± SEM from three independent donors.

In PBMCs exposed to *P. aeruginosa* LPS (**Figure 3.4**), IDR-1018 in water decreased LPS-induced IL-1β production in a dose-dependent manner, as expected given its anti-inflammatory effects. IDR-1018 in PBS caused a reduction in IL-1β production but this was not very dose-dependent and was similar at 10, 30 and 100 µg/ml of IDR-1018. The CMC and HPMC samples with peptide

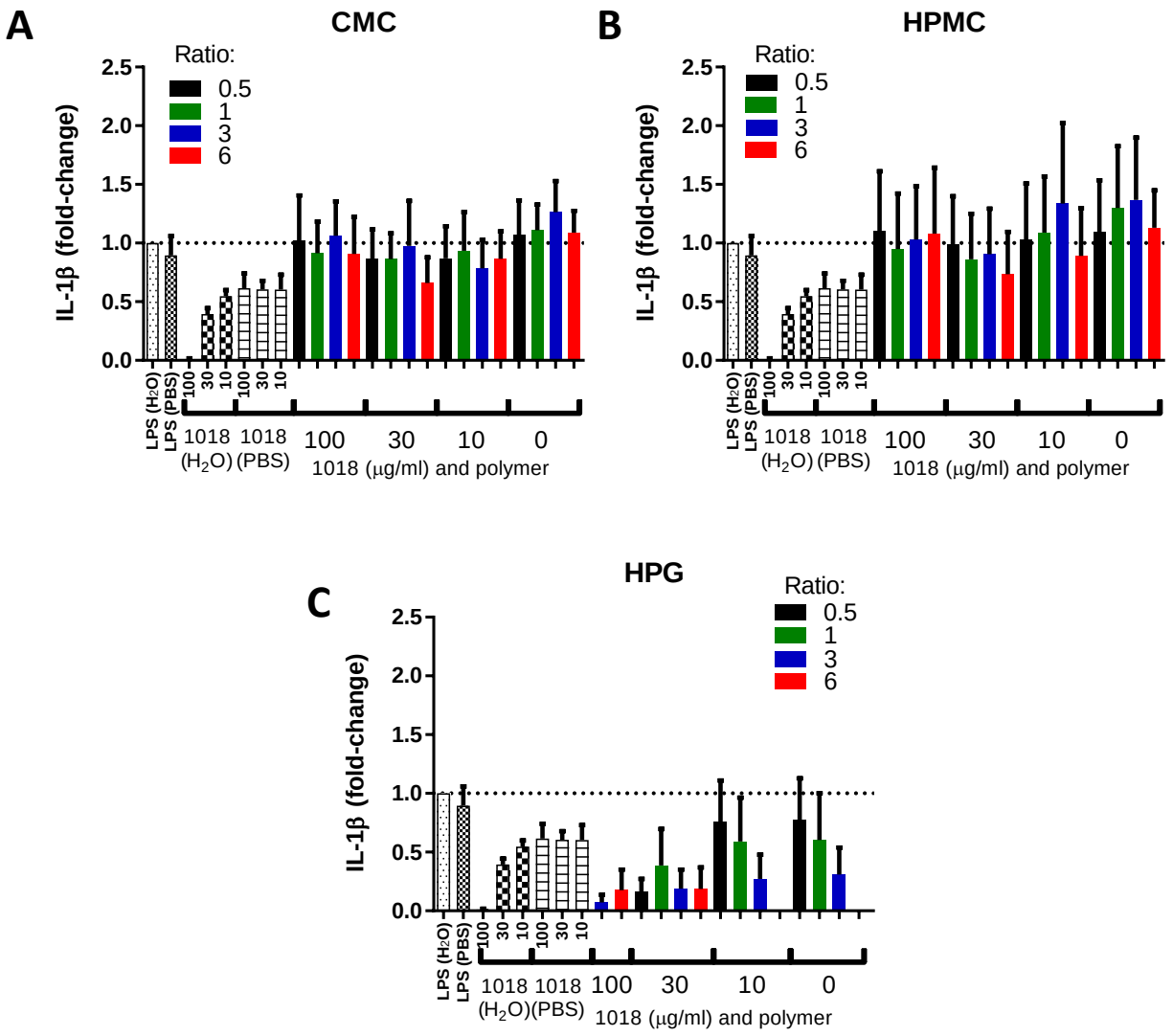

Figure 3.4: Reduction of LPS-induced IL-1β in PBMCs after IDR-1018 treatment. PBMCs were given IDR-1018 mixed with CMC (A), HPMC (B), or HPG (C). The polymers were at a ratio of 6, 3, 1, or 0.5 to 100, 30, or 10 μg/ml of IDR-1018. Unformulated IDR-1018 in PBS or water or controls given water or PBS without peptide were also included (displayed in all graphs for comparison). The polymers at their maximum concentration were also included without IDR-1018. *P. aeruginosa* LPS (10 ng/ml) was added at the same time. Supernatants were collected after 24 h and used in IL-1β ELISAs. Data represent mean ± SEM, expressed relative to control given LPS and water, from three independent donors.

had no effect on IL-1β production. HPG samples with IDR-1018 showed reductions in IL-1β similar to those of unformulated IDR-1018. Interestingly, HPG samples without IDR-1018 (displayed as 0 μg/ml) also showed a reduction in IL-1β. Both unformulated and formulated IDR-1018 or the polymers themselves did not induce IL-1β expression in PBMCs. The formulations were also

evaluated for their effects on MCP-1 production in PBMCs (**Figure 3.5**). Unformulated IDR-1018 in water or PBS increased MCP-1 production, and similar responses were seen in IDR-1018 formulated with CMC, HPMC, or HPG.

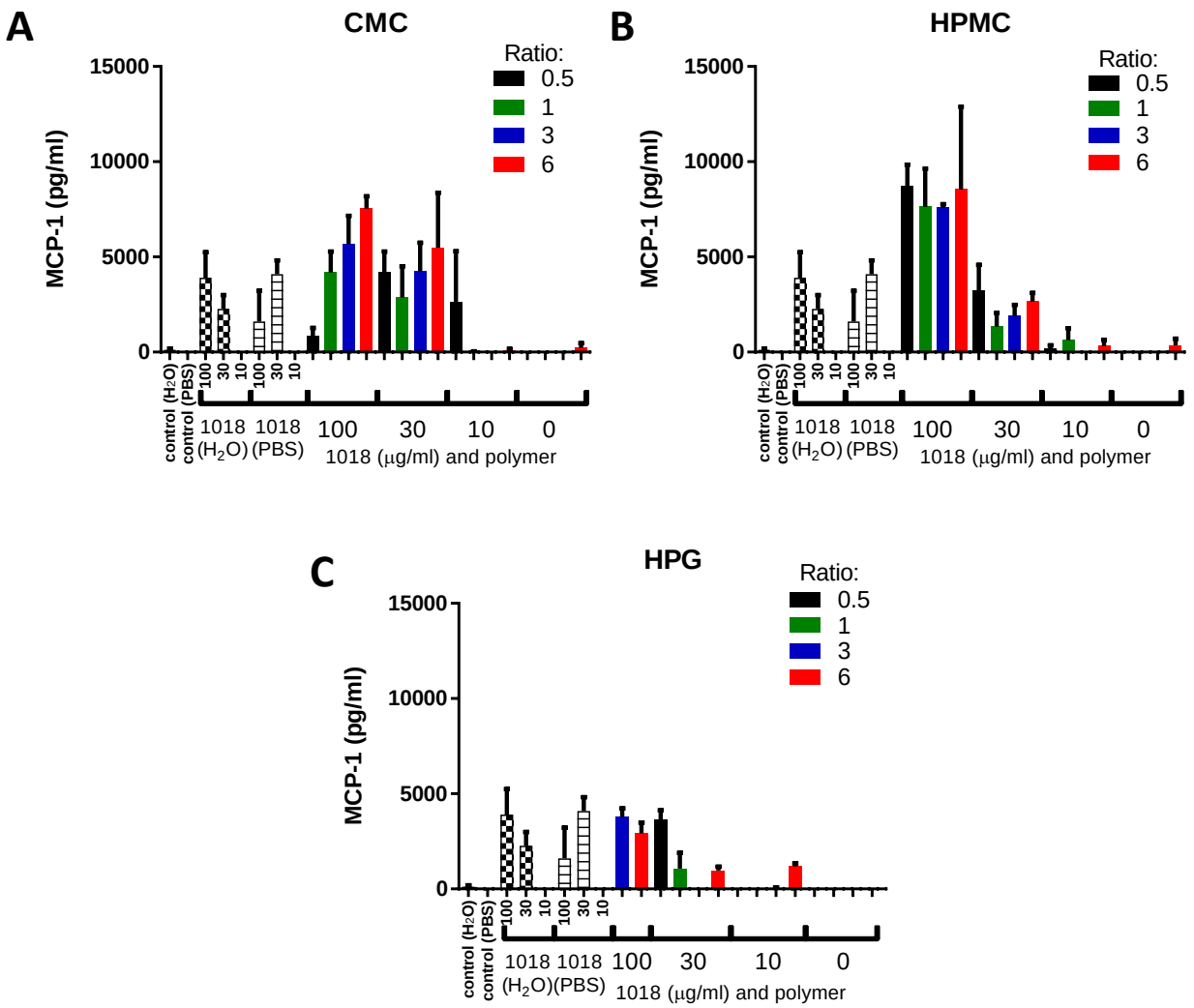

Figure 3.5: Effects of IDR peptide formulations on MCP-1 production in PBMCs. PBMCs were given IDR-1018 mixed with CMC (A), HPMC (B), or HPG (C). Polymers were at a ratio of 6, 3, 1, or 0.5 to 100, 30, or 10 µg/ml of IDR-1018. Unformulated IDR-1018 in PBS or water or controls given water or PBS without peptide were included (displayed in all graphs for comparison). Polymers at their maximum concentration were also included without IDR-1018. Supernatants were collected after 24 h and used in MCP-1 ELISAs. Data represent mean ± SEM from three independent donors.

In HBE cells, IDR-1018 in water slightly increased IL-6 (**Figure 3.6**) and IL-8 (**Figure 3.7**) production, but this was not seen with IDR-1018 in PBS. Treatment with IDR-1018 with CMC or

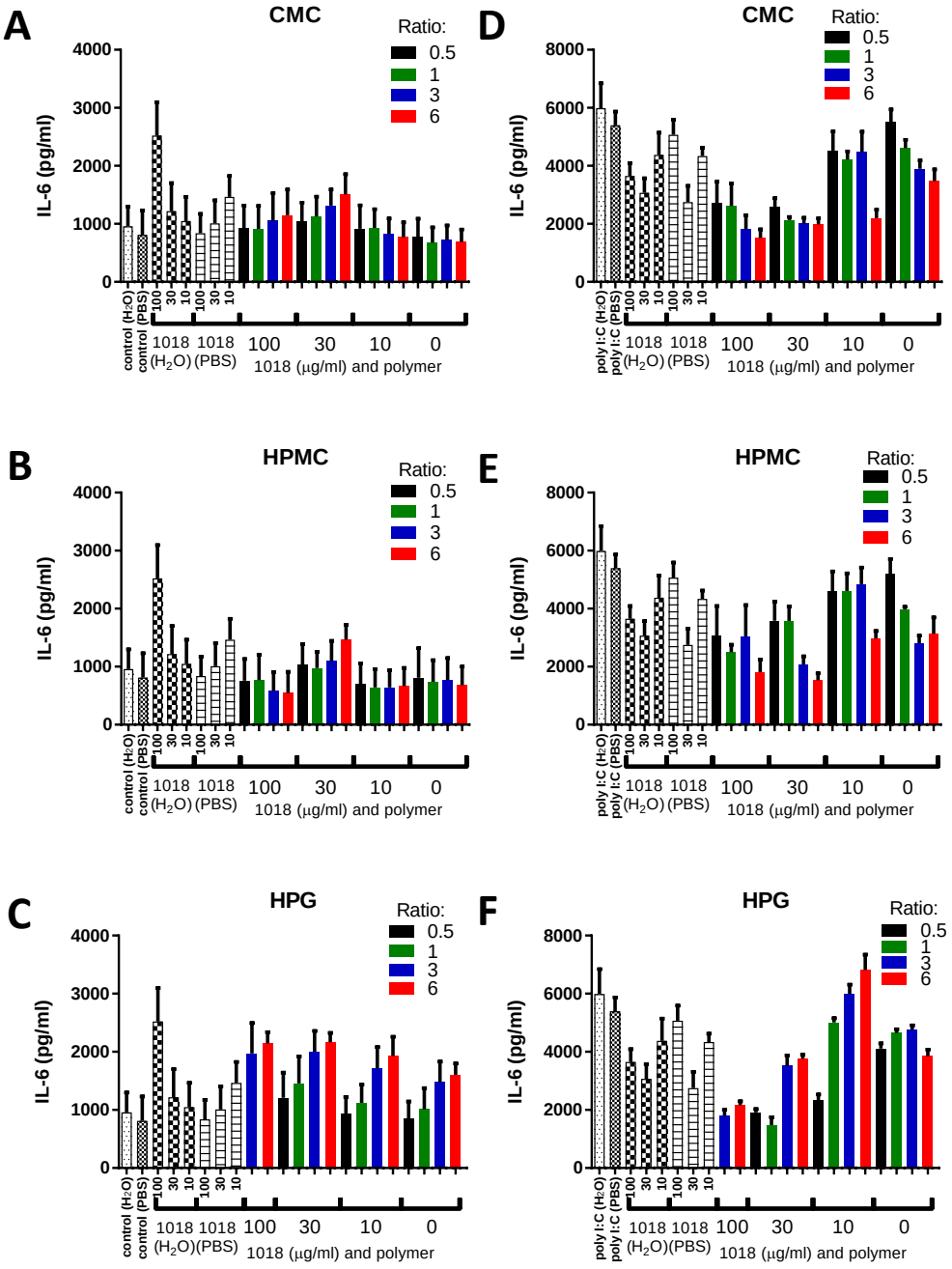

Figure 3.6: Effects of IDR peptide formulations on IL-6 production in HBE cells with or without poly I:C. HBE cells were given IDR-1018 mixed with CMC (A, D), HPMC (B, E), or HPG (C, F). Polymers were at a ratio of 6, 3, 1, or 0.5 to 100, 30, or 10 μg/ml of IDR-1018. Unformulated IDR-1018 in PBS or water or controls given water or PBS without peptide were included (displayed in all graphs for comparison). Polymers at their maximum concentration were also included without IDR-1018. Samples also received control (A-C) or poly I:C (D-F). Supernatants were collected after 24 h and used in IL-6 ELISAs. Data represent mean ± SEM from three independent experiments.

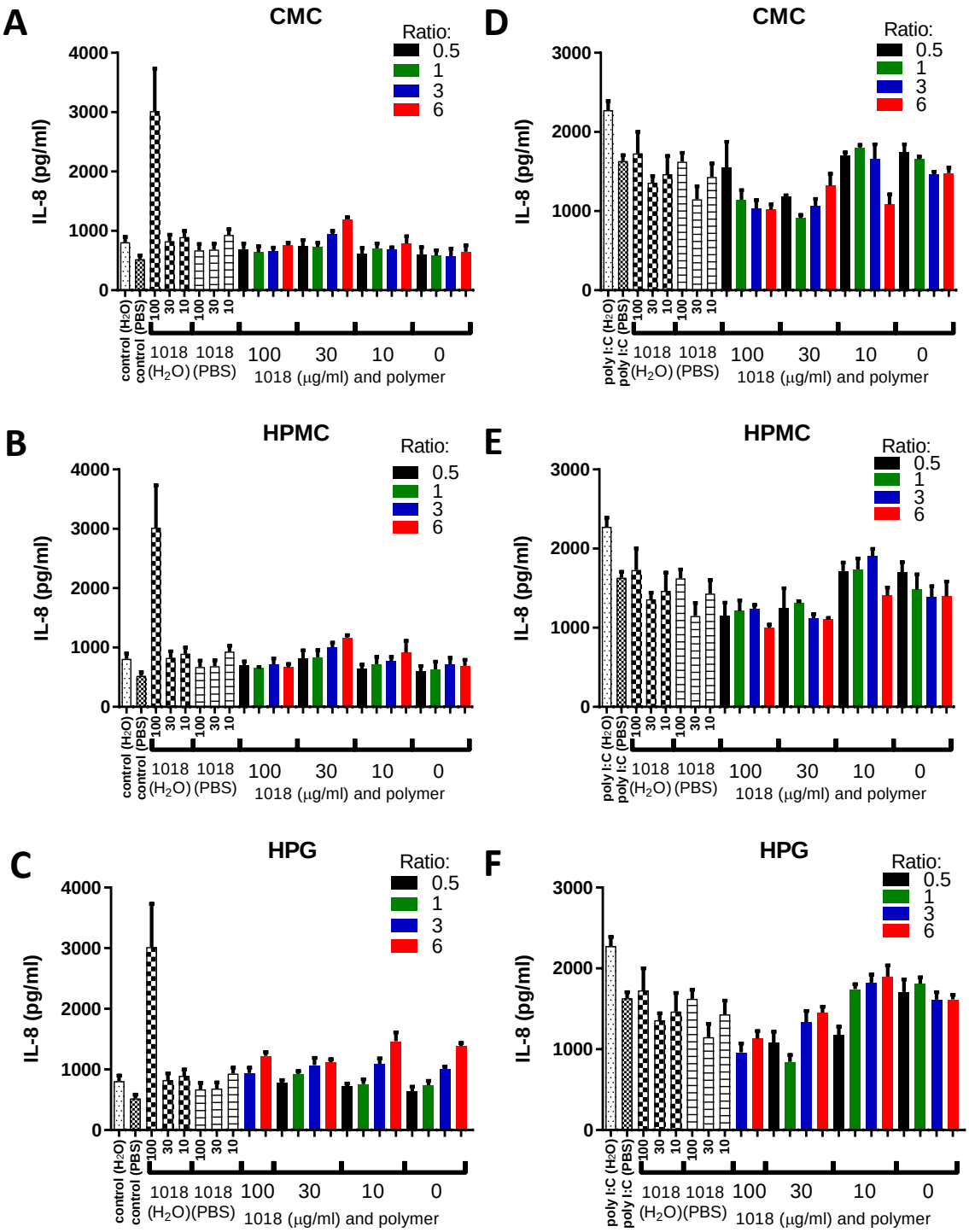

Figure 3.7: Effects of IDR peptide formulations on IL-8 production in HBE cells with or without poly I:C. HBE cells were given IDR-1018 mixed with CMC (A, D), HPMC (B, E), or HPG (C, F). Polymers were at a ratio of 6, 3, 1, or 0.5 to 100, 30, or 10 μg/ml of IDR-1018. Unformulated IDR-1018 in PBS or water or controls given water or PBS without peptide were also included (displayed in all graphs for comparison). Polymers at their maximum concentration were also included without IDR-1018. Samples also received control (A-C) or poly I:C (D-F). Supernatants were collected after 24 h and used in IL-8 ELISAs. Data represent mean ± SEM from three independent experiments.

HPMC or with the polymers alone did not have any major effects on IL-6 or IL-8 expression, while IDR-1018 formulated with HPG and HPG without peptide seemed to increase IL-6 and IL-8, with concentrations increasing as the HPG increased from the 0.5 to the 6 ratio. When poly I:C was used, IDR-1018 slightly reduced the IL-6 induced by poly I:C but did not significantly affect IL-8 production. CMC, HPMC, and HPG formulated IDR-1018 also produced similar responses, with HPG and IDR-1018 treatments showing the best results.

3.3.3 Effects of HPG carboxylation and solvent on IDR-1018 toxicity and immunomodulatory activity in vitro

Based on the results using the four polymers, it was decided to pursue the HPG formulation and examine two factors: 1) the effect of carboxylating the HPG, and 2) the solvent used for suspending the formulation. HPG with no carboxylation (HPG0), 115 carboxylate groups (HPG115), or 224 carboxylate groups (HPG224, which was used in the previous round of screening) resuspended in water, TBS, HEPES, or trehalose solution was mixed with IDR-1018 at ratios (w/w) of 6 or 3 of polymer to IDR-1018 to give final concentrations of IDR-1018 of 100 or 30 µg/ml. PBMCs and HBE cells were given the formulations and TLR agonists as done for the initial screen with the four polymers.

For all four solvents, the HPG0 samples caused toxicity in PBMCs (**Figure 3.8**). HPG0-1018 caused nearly 100% cell death at 100 µg/ml, and this was reduced only slightly at 30 µg/ml. Even without IDR-1018, the HPG0 still caused toxicity. The 6:1 ratio was worse than the 3:1 ratio. With HPG115, the toxicity was reduced but still greater than 20% at 100 µg/ml of IDR-1018 for both ratios. As seen previously, HPG224 samples showed only limited toxicity.

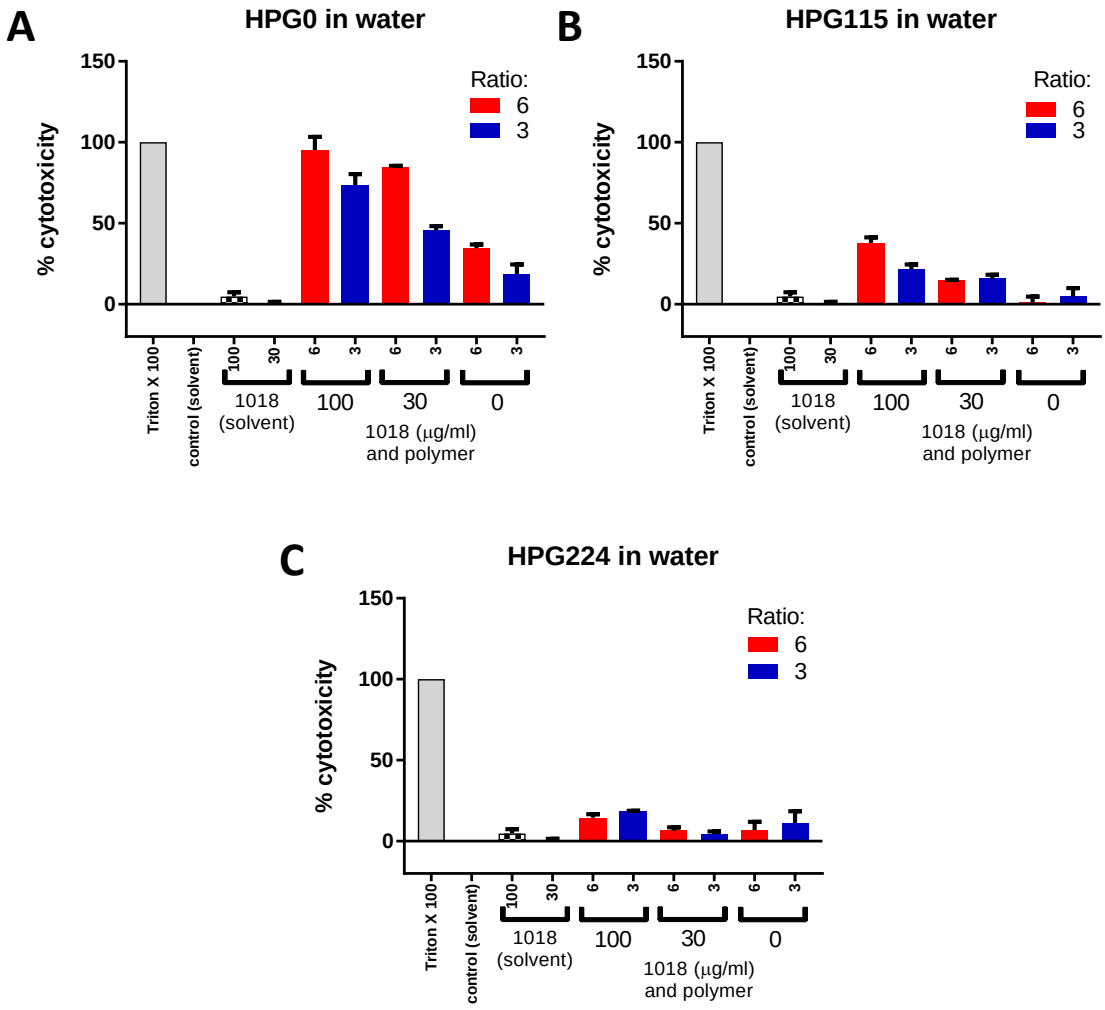

Figure 3.8: Increasing HPG carboxylation decreases toxicity. PBMCs were given IDR-1018 mixed with HPG0 (A), HPG115 (B), or HPG224 (C) resuspended in water. The polymers were at a ratio of 6 or 3 to 100 or 30 µg/ml of IDR-1018. Unformulated IDR-1018 or unformulated HPG were also included for each solution. Supernatants were collected after 24 h and used in LDH cytotoxicity assays. Data represent mean ± SEM from three independent donors.

The effects of the solvent used for the formulation was also examined. As seen with HPG224 in PBMCs (**Figure 3.9**), using TBS or trehalose with the formulated peptide at 100 µg/ml resulted in some toxicity, which was less than 20% for the samples in water or HEPES. Similar results were seen with HPG0 and HPG115 samples, but with greater toxicity overall due to the HPG carboxylation. The solutions with unformulated IDR-1018 produced very little toxicity. In HBE cells, although the toxicity levels were lower overall compared to PBMCs, the same patterns with carboxylation and the solvents were seen.

In both PBMCs and HBE cells, HPG224/1018 showed less aggregation compared to HPG0/1018 and HPG115/1018; this also seemed to be independent of the solution used. Samples using trehalose also appeared to have less aggregation for HPG115/1018 and HPG224/1018. For unformulated IDR-1018, aggregation was seen in TBS and HEPES, while the samples in water and trehalose had some aggregation, with trehalose performing the best.

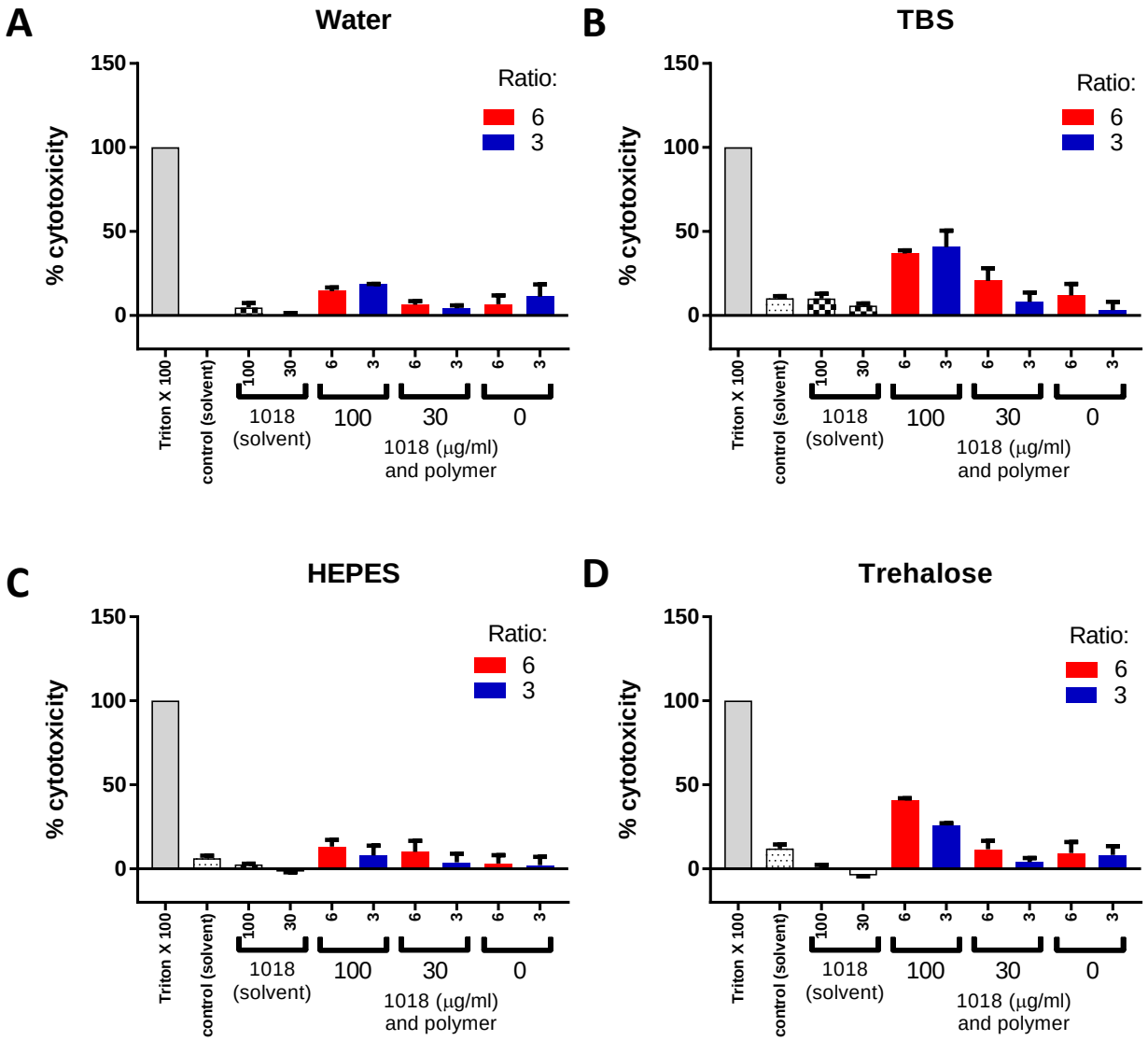

Figure 3.9: HPG formulations in TBS and trehalose show some toxicity, whereas HPG formulations in water and HEPES are nontoxic. PBMCs were given HPG224/1018 suspended in (A) water (A)(same as Fig. 3.8C), TBS (B), HEPES (C), or trehalose (D). The polymers were at a ratio of 6 or 3 to 100 or 30 µg/ml of IDR-1018. Unformulated IDR-1018 or unformulated HPG were also included for each solution. Supernatants were collected after 24 h and used in LDH cytotoxicity assays. Data represent mean ± SEM from three independent donors.

Since the HPG0 and HPG115 samples showed toxicity and did not reduce aggregation, it was decided to focus on the HPG224 samples for examining immunomodulatory effects. In PBMCs without LPS, some IL-1β production was seen with formulated peptide, particularly at the 6:1 ratio, but it varied by blood donor. The cytokine production induced by the formulated peptide at a 6:1 ratio ranged from 3 pg/ml to 912 pg/ml of IL-1β depending on the blood donor for water (mean ± SEM of 375.4 ± 210.3), TBS (mean ± SEM of 185.1 ± 162.0), and HEPES (mean ± SEM of 426.6 ± 248.2). Trehalose showed higher production with 1292 pg/ml to 2804 pg/ml of IL-1β (mean ± SEM of 2060 ± 436.5). In comparison, 10 ng/ml of LPS typically induced around 1000-2000 pg/ml of IL-1β in PBMCs. For other ratios without LPS, the IL-1β production was lower (all with a mean less than 300 pg/ml even for trehalose samples) or even at the background level.

In the presence of LPS (**Figure 3.10**), unformulated IDR-1018 decreased IL-1β at 100 μg/ml with all solutions, compared to cells given LPS and media, but 30 μg/ml of IDR-1018 did not seem to affect IL-1β. However, for the formulated peptide, the 100 μg/ml samples showed no reduction in IL-1β, although the 30 μg/ml and some of the HPG control samples had generally less IL-1β. In PBMCs without LPS, both unformulated and formulated IDR-1018 increased MCP-1 at 100 μg/ml in water (**Figure 3.11**), and similar results were observed with the other solutions.

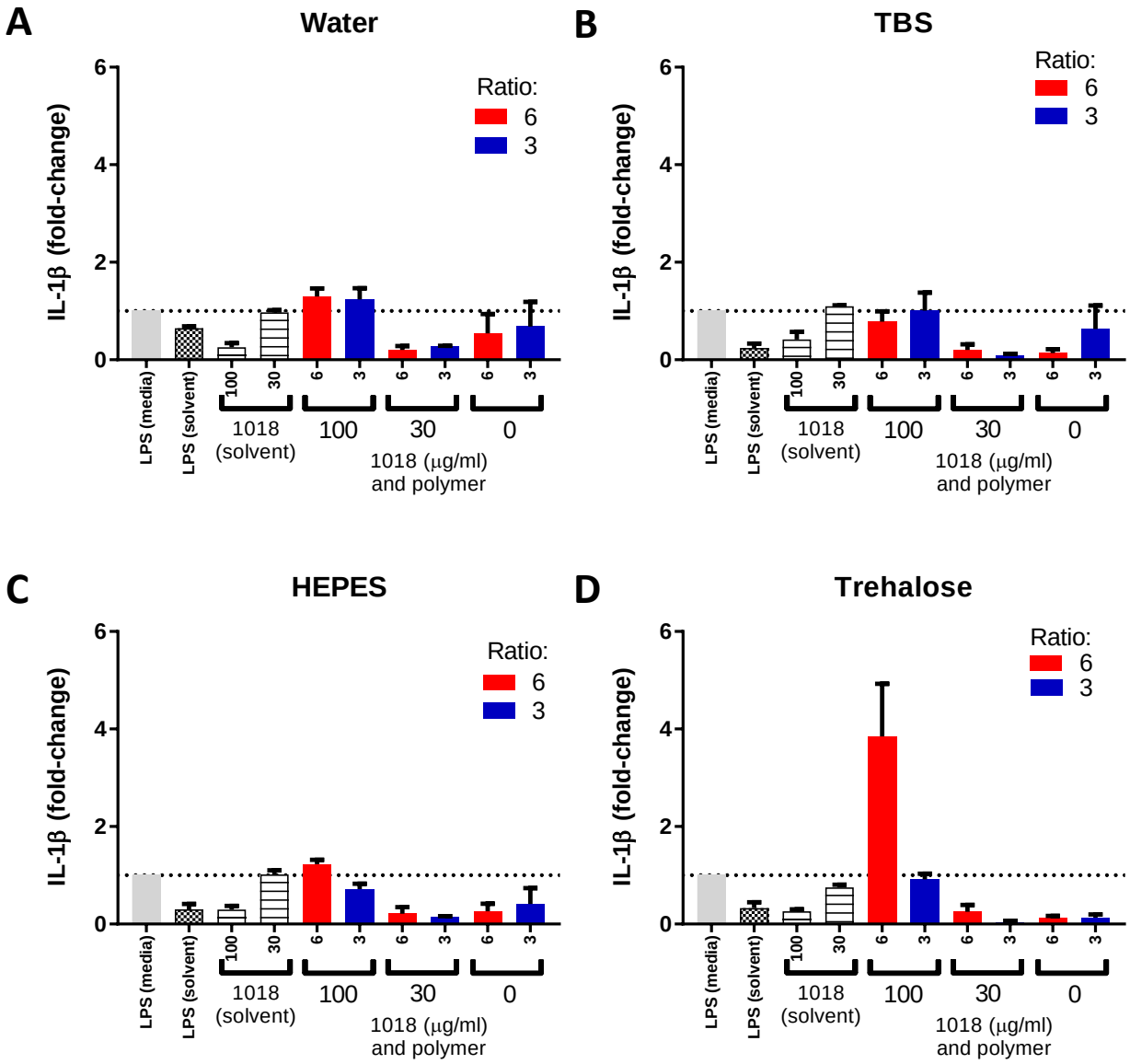

Figure 3.10: HPG224/1018 effects on IL-1β production in cells exposed to LPS. PBMCs were given HPG224/1018 suspended in water (A), TBS (B), HEPES (C), or trehalose (D). The polymers were at a ratio of 6 or 3 to 100 or 30 μg/ml of IDR-1018. Unformulated IDR-1018 or unformulated HPG were also included for each solution. Supernatants were collected after 24 h and used for ELISAs for IL-1β. Data represent mean ± SEM, expressed relative to control given LPS and media, from three independent donors.

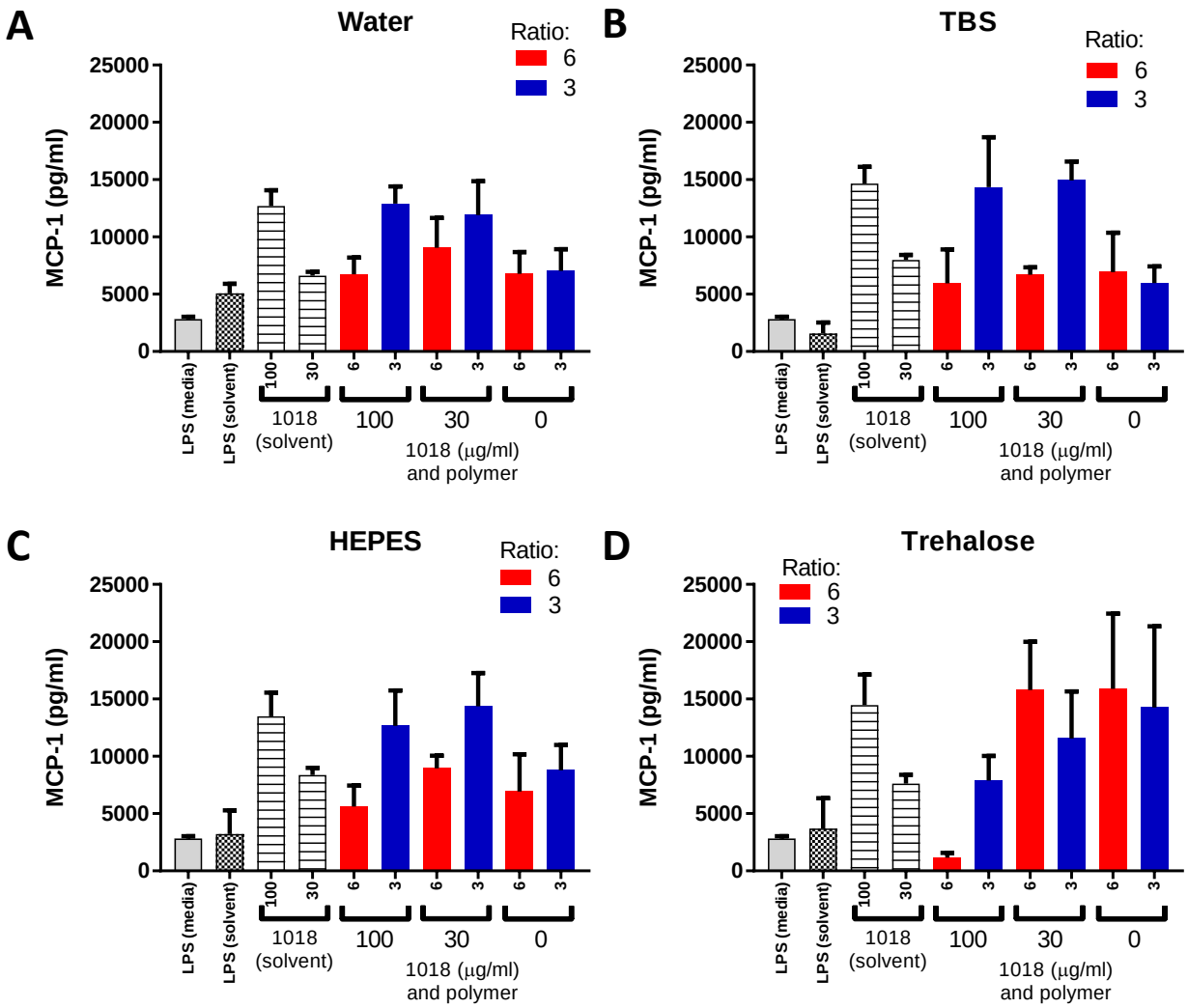

Figure 3.11: HPG224/1018 increases MCP-1 in PBMCs to the same extent as unformulated IDR-1018. PBMCs were given HPG224/1018 suspended in water (A), TBS (B), HEPES (C), or trehalose (D). The polymers were at a ratio of 6 or 3 to 100 or 30 μg/ml of IDR-1018. Unformulated IDR-1018 or unformulated HPG were also included for each solution. Supernatants were collected after 24 h and used for an ELISA for MCP-1. Data represent mean ± SEM from two (trehalose) or three (water, TBS, HEPES) independent donors.

In HBE cells, unformulated IDR-1018 slightly to moderately increased IL-6 (**Figure 3.12**) and IL-8 (**Figure 3.13**) at 100 μg/ml in all four solutions. The effects of HPG224 seemed to be mostly independent of the presence of IDR-1018 but overall produced only slight increases in IL-6 or IL-8. In the presence of poly I:C, unformulated IDR-1018 produced only moderate effects on both IL-6 and IL-8, with the largest decreases in IL-6 seen in IDR-1018 in HEPES and trehalose. Formulated IDR-1018 mostly decreased IL-6 and IL-8 induced by poly I:C as the concentration of IDR-1018 increased.

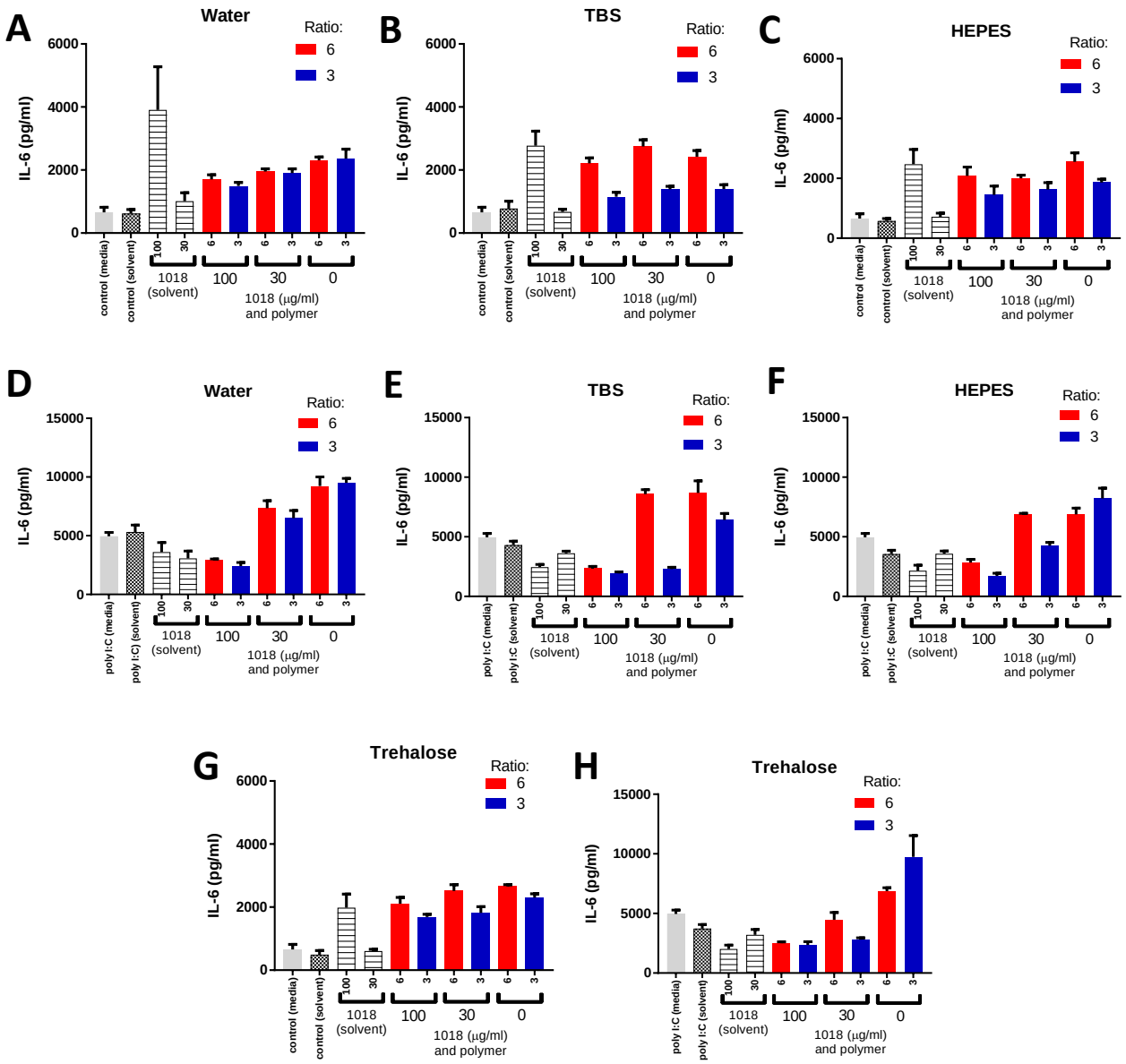

Figure 3.12: HPG224/1018 and solution effects on IL-6 production with or without poly I:C. HBE cells were given HPG224/1018 suspended in water, TBS, HEPES, or trehalose. The polymers were at a ratio of 6 or 3 to 100 or 30 μg/ml of IDR-1018. Unformulated IDR-1018 or unformulated HPG were also included for each solution. Supernatants were collected after 24 h and used for ELISAs for IL-6. A-C and G are without poly I:C and D-F and H are with poly I:C. Data represent mean ± SEM from three independent experiments.

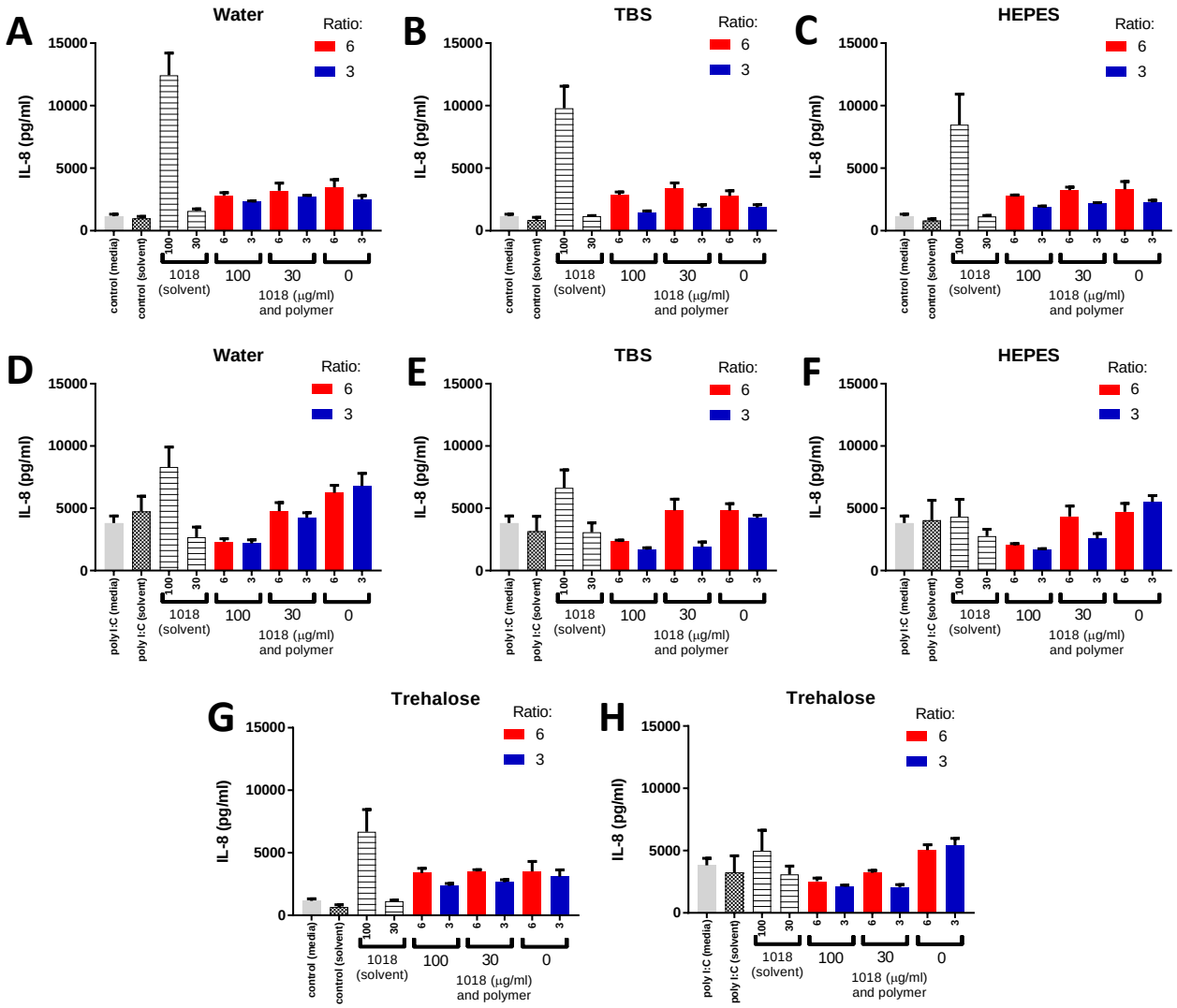

Figure 3.13: HPG224/1018 and solution effects on IL-8 production with or without poly I:C. HBE cells were given HPG224/1018 suspended in water, TBS, HEPES, or trehalose. The polymers were at a ratio of 6 or 3 to 100 or 30 μg/ml of IDR-1018. Unformulated IDR-1018 or unformulated HPG were also included for each solution. Supernatants were collected after 24 h and used for ELISAs for IL-8. A-C and G are without poly I:C and D-F and H are with poly I:C. Data represent mean ± SEM from three independent experiments.

Overall, the screening results in PBMCs and HBEs revealed that HPG appeared to have the best outcomes in terms of aggregation prevention while maintaining or improving immunomodulatory effects. They also showed that HPG224 was vastly superior to HPG115 and HPG0 in terms of limiting cytotoxicity. The 6:1 ratio for all four solutions showed some IL-1β production in PBMCs while not demonstrating a noticeable improvement over the 3:1 ratio for immunomodulatory effects in PBMCs

or HBEs. For the solvents tested, water seemed to be the best for formulated peptide in terms of immunomodulatory activities with limited toxicity.

Based on these results, it was decided to test, in vivo, IDR-1018 formulated with HPG224 at a ratio (w/w) of 3 parts HPG224 to 1 part IDR-1018 in water, since IN delivery does not necessitate using a buffered solution as required for other routes of administration such as IV. However, increasing the concentration of IDR-1018 to the levels needed for in vivo delivery caused the formulation to become insoluble. Therefore, HPG224 was replaced with HPG270. In PBMCs and HBE cells, HPG270/1018 was non-toxic. In PBMCs with LPS, both the formulated peptide and the HPG270 by itself seemed to decrease IL-1β (**Figure 3.14**) more than unformulated IDR-1018. In HBE cells with poly I:C, HPG270/1018 seemed to decrease both IL-6 and IL-8.

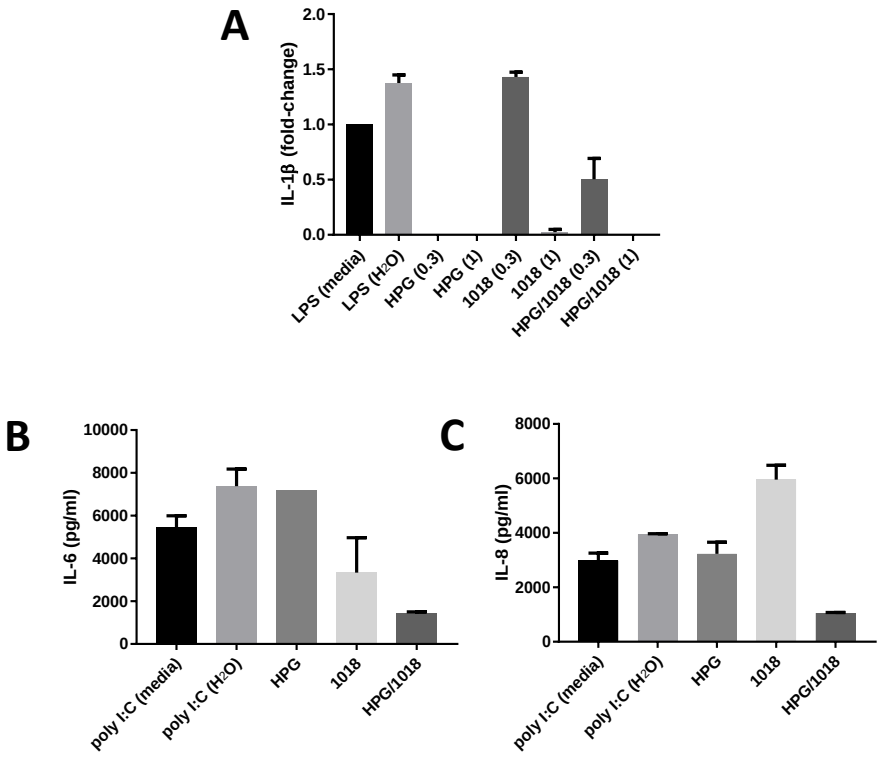

Figure 3.14: Effects of HPG270/1018 in PBMCs and HBE cells. Cells were given HPG270/1018 in water at a ratio of 3 parts HPG to 100 (PBMCs and HBE cells) or 30 (PBMCs only) µg/ml of IDR-1018. Unformulated IDR-1018 or HPG was also included. PBMCs were also given LPS (10 ng/ml) and HBE cells given poly I:C (100 ng/ml). Supernatants were collected after 24 h and used for ELISAs for IL-1β (PBMCs; A) or IL-6 and IL-8 (HBE cells; B and C). Data represent mean ± SEM from two independent donors for PBMCs, expressed relative to LPS, and two independent experiments for HBE cells.

3.3.4 IDR-1018 formulated with HPG appears to reduce pro-inflammatory cytokines in the acute *P. aeruginosa* lung infection model but does not reduce *P. aeruginosa* burden in the lungs

The efficacy of HPG270/1018 against a *P. aeruginosa* lung infection was then assessed. HPG270/1018 or unformulated IDR-1018 at 4 mg/kg was delivered IN to mice one day prior to infection. Control mice received either water or HPG270. At 0 h, the mice were infected with 8 x 10^5 CFU/mouse IN of *P. aeruginosa* PA103, then BALF and serum were collected at 18 h. The mice given unformulated IDR-1018 showed a significant reduction in CFU burden in the BALF compared to the controls, whereas the HPG270/1018 mice had CFUs similar to those of control mice (**Figure 3.15**).

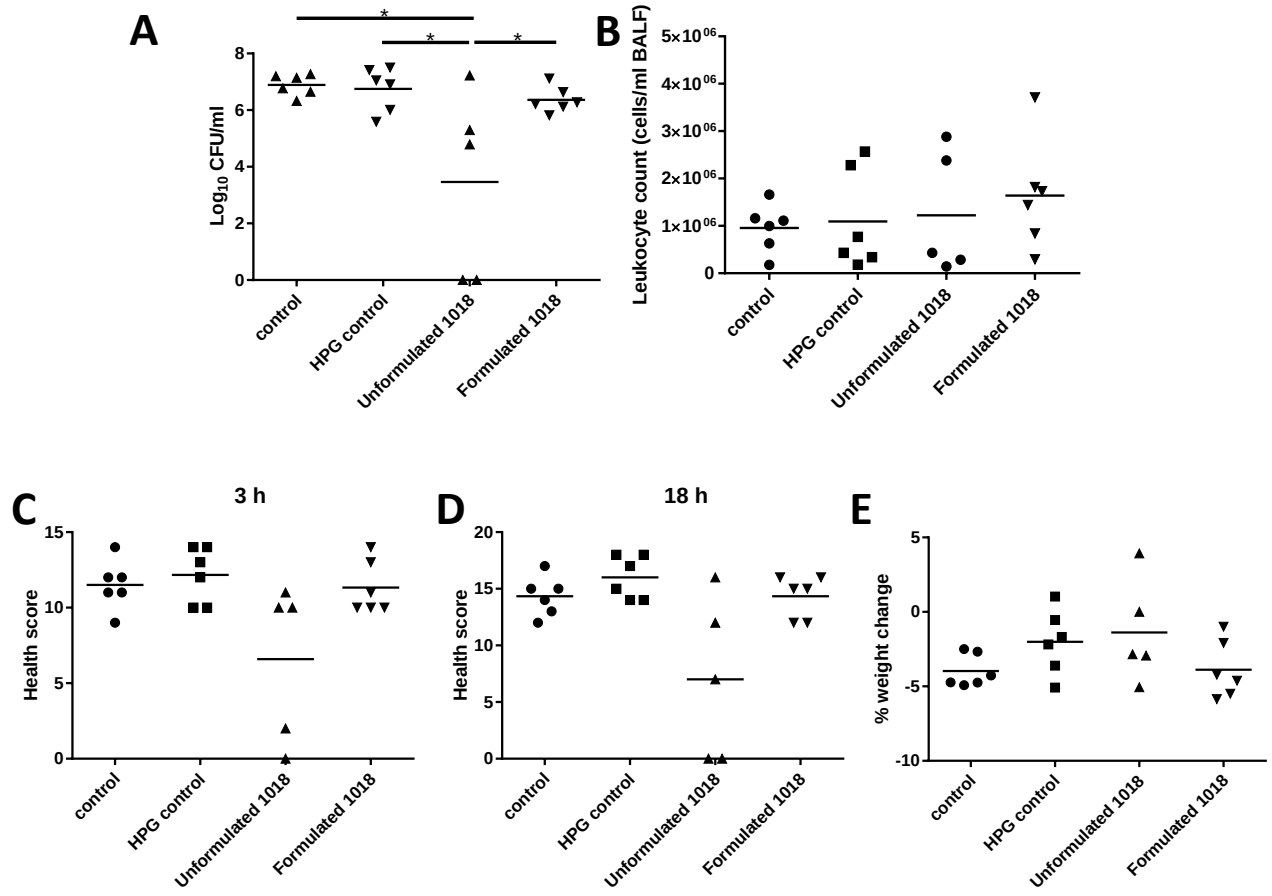

Figure 3.15: HPG270/1018 does not decrease CFUs in an acute *P. aeruginosa* lung infection. Mice were given water, HPG control, unformulated IDR-1018 (4 mg/kg), or HPG270/1018 (4 mg/kg) IN, at -24 h, given 8 x 10^5 CFUs of *P. aeruginosa* PA103 IN at 0 h, then euthanized and samples processed at 18 h. (A) CFU counts in the BALF. (B) Leukocyte counts in the BALF. (C, D) Health scores at 3 h or 18 h post-infection. (E) Percentage of weight change from -24 h to 18 h. Data represent n = 5 or 6 mice per condition from two independent experiment and were analyzed using one-way ANOVA and Tukey's multiple comparisons test. *: $p \leq 0.05$.

The unformulated IDR-1018 mice also showed slightly improved health scores, whereas the HPG270/1018 mice scored similar to the controls. No differences were seen in total leukocyte infiltration into the lungs or in percentage of weight change.

The unformulated IDR-1018 mice had significant reductions in IL-6 in the BALF when compared to the control or HPG control mice and in TNF-α in the BALF when compared to the HPG control mice (**Figure 3.16**). MCP-1 in the BALF and MCP-1, IL-6, and TNF-α in the serum also trended towards a reduction in the unformulated IDR-1018 mice. Intriguingly, the HPG270-1018 mice also trended towards decreases in IL-6 and MCP-1 in the BALF and TNF-α, IL-6, and MCP-1 in the serum. However, the TNF-α in the BALF remained elevated in the HPG270/1018 mice.

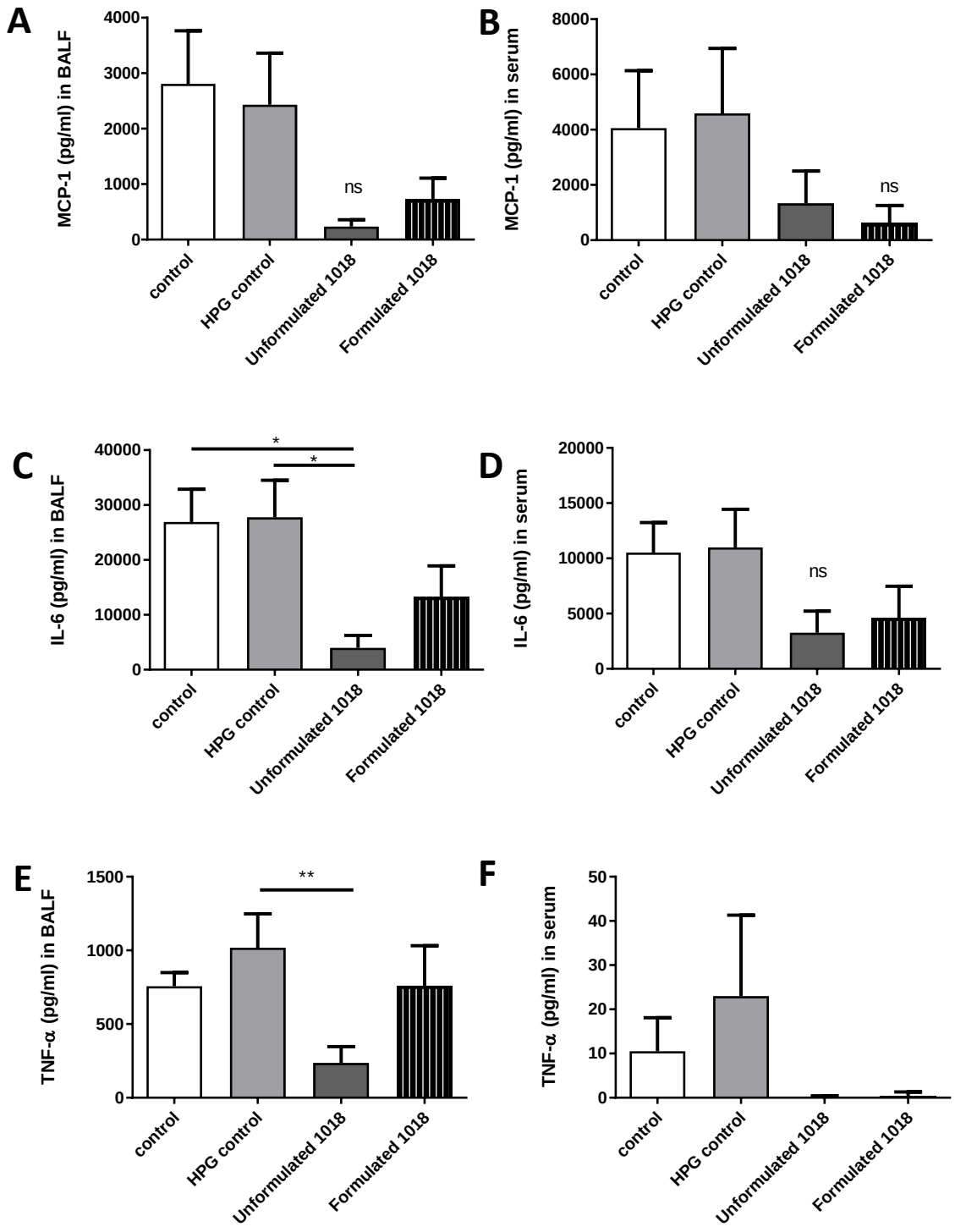

Figure 3.16: Unformulated IDR-1018 reduces cytokines and chemokines in the BALF and serum, whereas HPG270/1018 has limited effects. Mice were given water, HPG control, unformulated IDR-1018 (4 mg/kg), or HPG270/1018 (4 mg/kg) IN at -24 h, given 8 x 10^5 CFUs of *P. aeruginosa* PA103 IN at 0 h, then euthanized and samples processed at 18 h. ELISAs were performed for MCP-1 in BALF (A) and serum (B); IL-6 in BALF (C) and serum (D); and TNF-α in BALF (E) and serum (F). Data represent n = 5 or 6 mice per condition from two independent experiment and were analyzed using one-way ANOVA and Tukey's multiple comparisons test. *: $p \leq 0.05$, **: $p \leq 0.01$.

3.4 Discussion

IDR-1018 is a lead peptide candidate for the treatment of infections and inflammation, but its tendency to aggregate limits its transition to human clinical trials. In this chapter, IDR-1018 formulations were evaluated for their toxicity as well as their immunomodulatory and anti-infective effects.

Of the four polymers tested, HPG showed the most encouraging results in maintaining immunomodulatory activity in vitro while showing limited cellular toxicity and peptide aggregation. The lack of efficacy for 1018 formulated with HPMC and CMC was not altogether unexpected, since artificial tear fluid made with CMC was shown previously to limit the activity of LL-37 and hBD-2 against *P. aeruginosa* (258). This is likely due to the cationic peptide binding to negatively charged functional groups on the polymers and limiting its availability for activity against the bacteria. Conversely, a peptide-containing cream for use against methicillin-resistant *S. aureus* was formulated with HPMC and retained its antimicrobial activity without demonstrating toxicity, although this study assessed direct antimicrobial killing rather than immunomodulatory activity (259). It is possible that adjusting the negative charges on these polymers may improve their anti-aggregation properties while allowing them to maintain peptide activity. Additionally, these formulations were made using PBS as a solvent, and they should ideally be reevaluated in other solvents.

With HPG, decreasing the number of available carboxylate groups increased the toxicity. While HPG270 was the best in terms of reducing aggregation and still demonstrated immunomodulatory activity in vitro, in the acute *P. aeruginosa* lung infection model it was not successful at reducing CFUs. However, the HPG270/1018 mice trended towards decreases in most cytokine and chemokine outputs, similarly to the unformulated peptide, indicating HPG270/1018 was likely having some effect. It is probable that the reduced activity was due to an excessive number of negative charges that neutralized the peptide's activity, which is dependent on the positive charge of the peptide. Nevertheless, since the less-negatively charged HPG224 formulation aggregated at higher

concentrations needed for in vivo delivery, it may be difficult to find a balance between efficacy, aggregation reduction, and toxicity using HPG with IDR-1018. However, HPG has successfully been used for improving the delivery of chemotherapeutic drugs in cancer models in vivo (260). HPG was also used to formulate the HDP aurein 2.2 and it showed improved cytotoxic effects, although it was not evaluated in vivo or for immunomodulatory effects (261). Therefore, it is possible that minor adjustments to the HPG/1018 formulation may result in a more functional peptide. The results also indicated that the trehalose solution reduced aggregation without causing toxicity with unformulated IDR-1018. This may be another route to pursue for 1018 formulation studies. Critically, this chapter demonstrated differences between in vitro and in vivo performance of peptide formulations. This has major implications for future studies of formulations and indicates that it will be critical to test formulations in animals to determine their effectiveness.

In this chapter, I tested polymers and solvents for reducing IDR-1018 aggregation to improve its use as a treatment for *P. aeruginosa* lung infections. IDR-1018 formulated with HPG showed reduced aggregation and maintained in vitro activity, and also retained some in vivo activity as shown by reductions in inflammatory cytokines and chemokines. The research in this chapter provides an important initial screening of IDR-1018 formulations for improving IDR-1018 as well as other IDR peptides and suggests a path for future formulation studies.

Chapter 4: Effects of *P. aeruginosa* lung infection on the host response in the lungs and blood and the role of IDR-1002

4.1 Introduction

In Chapter 2, I showed that IDR-1002 was effective against *P. aeruginosa* lung infections. In this chapter, the aim was to further explore the mechanisms underlying IDR-1002 activities in the acute lung infection model. Previous work on IDR-1002 in the *S. aureus* IP model demonstrated that it helped recruit leukocytes to the infection site, with an increase seen in both neutrophils and the neutrophil chemokine KC (192). Increased numbers of monocytes were also observed, although no changes in MCP-1 expression were seen (192). Eliminating macrophages with liposomal clodronate eliminated the protective effect of IDR-1002 (192). This indicates that a key factor in IDR-1002-mediated protection in the *S. aureus* IP model was the recruitment of macrophages, although there are some reports indicating that clodronate also depletes DCs (262, 263). Similar results were achieved for IDR-1 against *S. aureus* infection, with macrophages and monocytes required for protection, while it was additionally shown that depleting neutrophils, T cells, or B cells had no effect (190). In vitro studies with human monocytes showed that IDR-1002 can promote cell adhesion to fibronectin in the presence of chemokines due to increased activation of β-integrins and the PI3K-Akt pathway, and IDR-1002 also increased the expression of the chemokine receptor CCR5 (213, 214). Therefore, while some aspects of IDR-1002 mechanisms have been uncovered and point to its involvement in leukocyte recruitment, IDR-1002 has not been thoroughly examined in the context of infections, especially in the *P. aeruginosa* lung model. Additionally, it was desired to take a more comprehensive approach to the evaluation of its mechanisms of action. Therefore, RNA-Seq was utilized. RNA-Seq is a powerful method for evaluating the transcriptome of an organism. It uses sequencing by synthesis and does not require the use of probes as with microarray technology, thereby allowing for the more efficient discovery of new or modified transcripts, without substantial and variable backgrounds as seen for

hybridization methods such as microarrays (264). RNA-Seq also has a much broader range of signal detection than microarrays.

In addition, while the host response to murine *P. aeruginosa* lung infections has been evaluated using microarrays (265, 266), to the best of my knowledge only one RNA-Seq study, published during the writing of this thesis, has been performed on mice with a *P. aeruginosa* lung infection and it examined only the response in the lungs (267). Therefore, performing RNA-Seq on both the lungs and blood from infected mice should provide new insights into the effects of *P. aeruginosa* infections and possibly lead to new drug targets.

The RNA-Seq results showed that *P. aeruginosa* caused profound inflammatory responses in both the lungs and the blood, including the induction of pathways not always associated with *P. aeruginosa* infections, such as type I interferon signaling. While the mice given IDR-1002 alone showed few changes in gene expression compared to the controls, differences among the other groups in lymphocyte activation and metabolism provide new leads for understanding IDR mechanisms of action. Critically, in these experiments IDR-1002 led to reductions in the CFU burden and in inflammatory cytokines and chemokines. Overall, *P. aeruginosa* caused inflammation, and this was reduced by the addition of IDR-1002. Furthermore, the RNA-Seq results provided insight into IDR-1002 activity and the effects of *P. aeruginosa* infection, and these results can be used as the basis for additional study into both peptide and *P. aeruginosa* effects on the host immune response.

4.2 Materials and methods

4.2.1 Mice and ethics statement

C57Bl/6J mice were ordered from Jackson Laboratory or were bred at the Modified Barrier Facility (University of British Columbia). Female mice were used between 6-8 weeks of age. All experiments were approved by the UBC Animal Care Committee.

4.2.2 Reagents

IDR-1002 (VQRWLIVWRIRK-NH_2) was synthesized by F-moc chemistry (Kinexus, Vancouver, British Columbia, Canada). Peptide was stored as desiccated powder at -20°C, then resuspended in endotoxin-free water for experiments and stored at -20°C. Neutrophil specific fluorescent imaging agent was from Kerafast (Boston, Massachusetts, USA).

4.2.3 Preparation of bacteria and acute *Pseudomonas* lung infection

Bacterial strain *P. aeruginosa* PA103 was streaked onto LB plates from a frozen stock and grown overnight at 37°C. The following day individual CFUs were used to make overnight cultures in LB and grown overnight at 37°C with shaking. Overnight cultures were diluted 1:50 and grown to an OD_{600} reading of approximately 0.5. Bacteria were washed with endotoxin-free 0.9% sodium chloride solution (saline), centrifuged, supernatant discarded, and the pellet resuspended in endotoxin-free saline to an OD_{600} of 0.5. Bacteria were then diluted to the appropriate concentration based on previous experiments relating OD_{600} reading to CFU/ml, and serial dilutions were plated on LB to check the final concentration.

Mice were anesthetized with 2-5% isoflurane and placed on an intubation stand (BrainTree Scientific, Massachusetts, USA). IDR-1002, *P. aeruginosa*, or appropriate controls were instilled dropwise using a micropipette into the left nostril of each mouse. *P. aeruginosa* was in a 20 µl volume, while the peptide volume was approximately 10-20 µl depending on the weight of the mouse. Isoflurane was periodically applied to keep the mouse at a steady respiratory rate. After instillation, mice were kept on the stand under isoflurane for 2-3 minutes to ensure absorption of the liquid. Once they were fully recovered, they were returned to their cages.

For sample collection, mice were euthanized with 120 mg/kg of intraperitoneally injected sodium pentobarbital. Blood was collected from the inferior vena cava and 100 µl was placed in RNAprotect animal blood tubes (Qiagen, Hilden, Germany) for RNA isolation according to the manufacturer's protocol. The remaining blood was allowed to clot, then centrifuged and the serum

was collected for ELISAs. For bronchoalveolar lavage fluid (BALF) collection, the chest cavity and trachea were exposed and an incision was made in the trachea. A cannulated needle was then inserted and used to slowly fill the lungs with sterile PBS (600 µl), which was then slowly withdrawn through the cannulated needle and saved. This procedure was repeated twice for a total of three washes. After the lavage, the smallest lobe of the lung was placed in RNAlater (Qiagen) and saved for RNA-Seq according to the manufacturer's protocol.

The first BALF wash was used for CFU enumeration by spread-plating undiluted BALF or ten-fold dilutions made in PBS onto LB agar plates in duplicate. Plates were incubated overnight at 37°C and CFUs were enumerated the following day. The remaining first BALF wash was centrifuged and the supernatant saved for ELISAs. The pellet from the first BALF wash was combined with the pellet from BALF washes 2 and 3 and resuspended in PBS, then leukocytes were counted on a hemocytometer using Turk's stain.

The leukocytes were also used in a StatSpin Cytofuge 2 (Beckman-Coulter) and the resulting slides were air-dried overnight, stained with the Diff-Quik Staining Kit (VWR, Radnor, PA) according to the manufacturer's protocol, and then 200 cells/slide were counted.

4.2.4 ELISAs

Samples were stored at -20°C until use in ELISAs. The levels of cytokines and chemokines were measured using eBioscience (San Diego, California, USA) antibodies for murine TNF-α and IL-6. Murine MCP-1 antibodies were from eBioscience or R&D Systems (Minneapolis, Minnesota, USA). Murine KC (CXCL1) antibodies were from Fitzgerald (Acton, Massachusetts, USA) or R&D Systems. Standards were purchased from the same sources. The ELISAs were performed by following the manufacturer protocols with optimization of antibody and sample dilutions, washes, and incubation times. They were developed using TMB (eBioscience) and the reactions were stopped with 2 N sulfuric acid. The plates were read on a Power Wave X340 plate-reader (Bio-Tek Instruments, Winooski, VT) and data were fitted to a 4-parameter standard curve using KC4 software (Bio-Tek).

4.2.5 RNA isolation and RNA-Seq

Total RNA was isolated from the lungs and blood from one experiment (n = 5 per condition) using the RNAeasy Plus Mini kit (Qiagen). The quality of the RNA was analyzed using an RNA 6000 Nano Chip (Agilent Technologies, Santa Clara, California, USA) on an Agilent 2100 Bioanalyzer, with all samples showing excellent quality. A polyA enrichment with d(T) beads (New England Biolabs, Ipswich, Massachusetts, USA) was then used to isolate the mRNA, and a KAPA Stranded Total RNA-Seq kit (Kapa Biosystems, Wilmington, Massachusetts, USA) was used to create the cDNA libraries. In brief, first strand cDNA was synthesized, following by second strand synthesis and blunt-end formation. After 3' adenylation, adapters (Bioo Scientific, Austin, Texas, USA) for multiplexing were ligated, followed by amplification and then purification using Agencourt Ampure XP beads (Beckman Coulter). The quality of the library was checked using a High Sensitivity DNA chip (Agilent, Santa Clara, California, USA) on an Agilent 2100 Bioanalyzer and all samples were shown to have RNA integrity number (RIN) values of greater than 8. The samples were used for RNA-Seq on an Illumina (San Diego, California, USA) GAIIx (lungs) or HiSeq 2500 (blood).

After demultiplexing, the resulting FASTQ files were aligned to the Ensembl murine reference genome GRCm38.p5 (build 86) using STAR aligner (version 2.5.2B) (268). Counts were generated using HTSeq (version 0.6.1p1) (269). DESeq2 (version 1.14.1) in R (3.3.2) was used for finding differentially expressed (DE) genes, with cutoffs for DE genes set as a fold-change of ± 1.5, equivalent to a log with base 2 fold change (log2 FC) of ± 0.58, and an adjusted p-value (false discovery rate) of < 0.05 (270, 271). One mouse in the PA103 group was inadequately infected and was removed from the analysis for lungs and blood. All remaining lung samples had excellent quality and number of read counts. For the blood, samples with < 800,000 read counts were excluded, leaving n = 3 per condition except for the PA103 group which had n = 4. The DE genes were used in NetworkAnalyst for network visualization using the Imex database and in PANTHER for overrepresentation analysis (ORA) using

gene ontology (GO) biological processes (PANTHER overrepresentation test release 20160715 and GO Ontology database release 2017-2-28) (272-274). Venn diagrams were created using Venny (275).

4.2.6 Statistical analysis

Data from the lung model were analyzed using Microsoft Excel 2013 and GraphPad Prism version 7. GraphPad Prism was used to perform an unpaired two-tailed t-test or one-way ANOVA with Tukey's multiple comparisons tests. A value of $p \leq 0.05$ was considered statistically significant.

4.3 Results

4.3.1 IDR-1002 reduces *P. aeruginosa* burden and inflammation in the lungs and does not itself produce inflammatory cytokines

To examine the effects of IDR-1002, *P. aeruginosa*, or their combination, the acute *P. aeruginosa* lung model was used. As with previous acute *P. aeruginosa* lung model experiments, female C57Bl/6J mice 6-8 weeks of age were given 8 mg/kg IDR-1002 or the vehicle (endotoxin-free water) IN 24 h prior to infection with approximately 8 x 10^5 CFU/mouse of *P. aeruginosa* PA103 or the vehicle (endotoxin-free saline) and then euthanized at 18 h post-infection. The groups of mice are hereafter referred to as control (received only vehicles), IDR-1002 (received IDR-1002 and saline), PA103 (received water and PA103), and treatment (received IDR-1002 and PA103). As seen in Chapter 2, the addition of IDR-1002 significantly decreased the CFU burden in the lungs (**Figure 4.1**). The addition of PA103 significantly increased leukocyte infiltration into the lungs compared to either control or IDR-1002 mice, whereas the treatment mice showed a leukocyte count that was in between the PA103 and the control or IDR-1002 mice. The addition of IDR-1002 did not change the total leukocyte count compared to the control mice. However, when the distribution of leukocytes in the lungs was examined, the IDR-1002 mice seemed to show a slight increase in neutrophils compared to the controls. This was investigated further by using a probe for fluorescent tracking of neutrophils in vivo (276). However, no differences were observed in IDR-1002 mice for neutrophils either 4 or 24 h

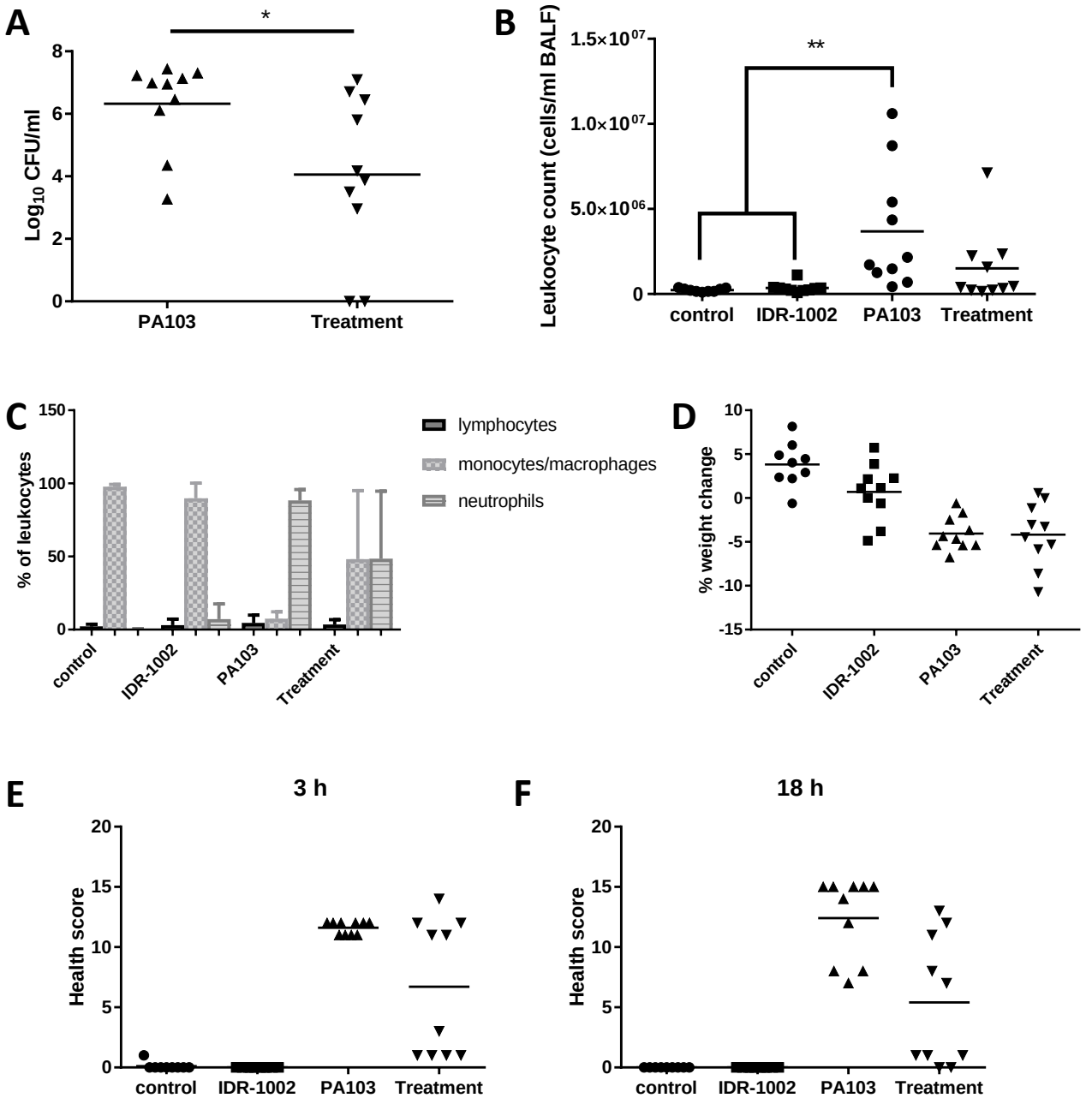

Figure 4.1: IDR-1002 reduces CFU burden and improves health scores in mice infected with *P. aeruginosa* PA103. Mice were given water or IDR-1002 (8 mg/kg) IN at -24 h, given saline or 8 x 10^5 CFUs of *P. aeruginosa* PA103 IN at 0 h, then euthanized and samples processed at 18 h. (A) CFU counts from the BALF. (B) Leukocyte counts in the BALF. (C) Distribution of leukocytes in the BALF. (D) Percentage of weight loss. (E, F) Health scores at 3 h or 18 h post-infection. Data represent n = 9 or 10 per condition from the combination of two experiments and were analyzed using an unpaired two-tailed t-test for the CFUs and a one-way ANOVA and Tukey's multiple comparisons test for the leukocytes. *: $p \leq 0.05$, **: $p \leq 0.01$.

after IN administration of peptide compared to endotoxin-free water controls; however, it should be noted that imaging of the fluorescence is hindered in mice with black fur. As expected, the PA103 mice showed a strong increase in neutrophils compared to the uninfected mice, while the treatment mice showed a mixture of neutrophils and monocytes/macrophages that leaned towards neutrophils in sick mice and showed more monocytes/macrophages in mice that had few signs of infection. The health scores also showed an improvement in the treatment group at both 3 and 18 h post-infection compared to the PA103 mice.

The expression of cytokines and chemokines in the BALF and serum was also examined (**Figure 4.2**). MCP-1, KC, and IL-6 showed significant increases in the BALF and serum of the PA103 mice compared to either control or IDR-1002 mice, while the treatment mice had significant decreases in most of these outputs compared to the PA103 mice. TNF-α also showed similar trends. Notably, there were no significant increases for IDR-1002 compared to control mice for any of the cytokines or chemokines.

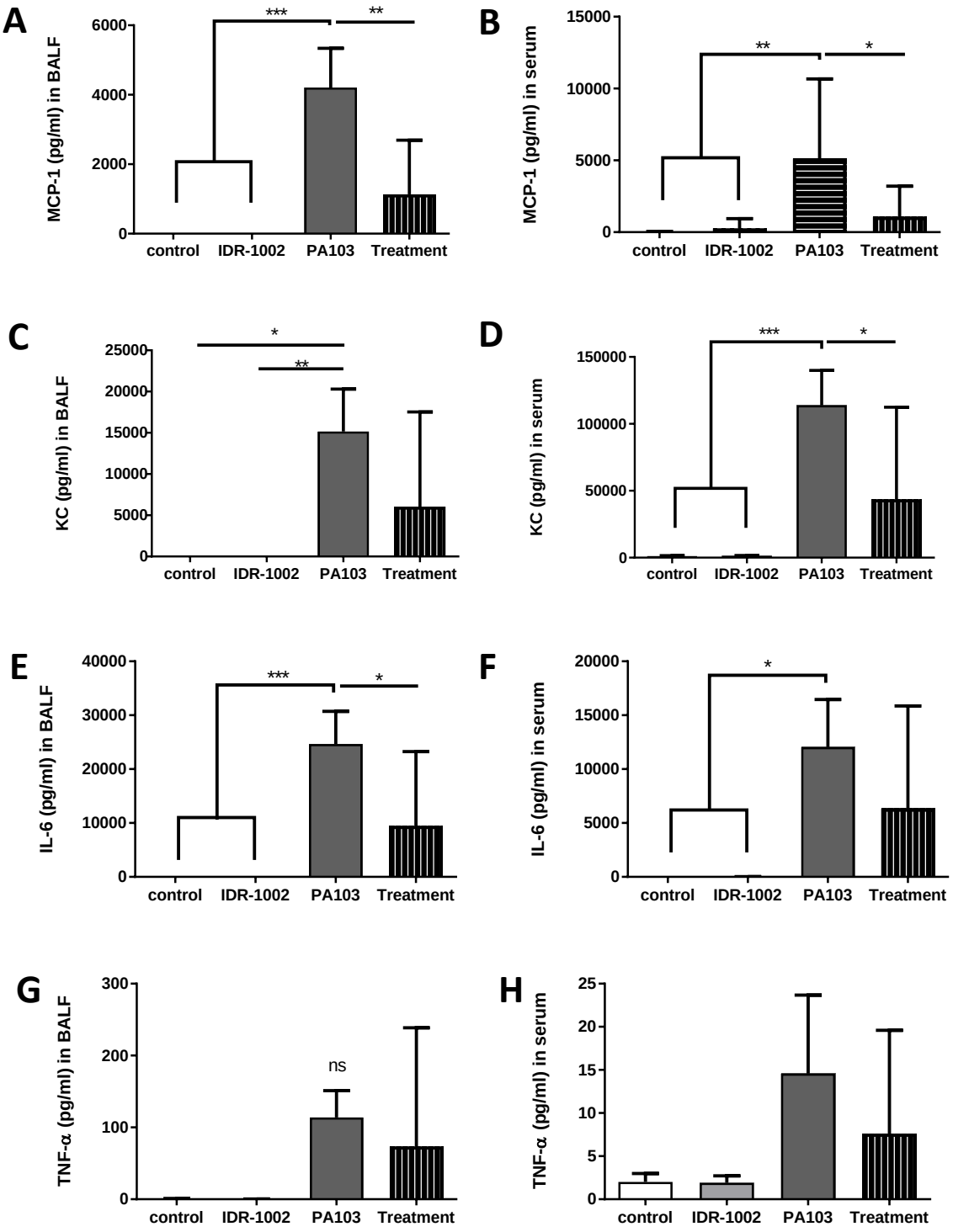

Figure 4.2: IDR-1002 reduces cytokines and chemokines in the BALF and serum that were induced by *P. aeruginosa* PA103. Mice were given water or IDR-1002 (8 mg/kg) IN at -24 h, given saline or 8 x 10^5 CFUs of *P. aeruginosa* PA103 IN at 0 h, then euthanized and samples processed at 18 h. ELISAs were performed for MCP-1 in BALF (A) and serum (B); KC in BALF (C) and serum (D); IL-6 in BALF (E) and serum (F); and TNF-α in BALF (G) and serum (H). Data represent n = 9 or 10 per condition from the combination of two experiments and were analyzed using one-way ANOVA and Tukey's multiple comparisons test. *: $p \leq 0.05$, **: $p \leq 0.01$, ***: $p \leq 0.001$.

4.3.2 *P. aeruginosa* lung infection induces widespread inflammation in the lungs and blood

The lungs and whole blood from one of two experiments, consisting of 4-5 mice per condition, were used to isolate RNA and run RNA-Seq to characterize the DE genes of the transcriptome during infection and treatment. Principal component analysis (PCA) of the results (**Figure 4.3**) indicated that most of the variance was between infected mice (PA103 or treatment) and uninfected mice (control or IDR-1002). The IDR-1002 and control mice clustered together. The clustering of the treatment mice correlated with their CFU burdens, with mice having no or reduced CFUs clustering towards the untreated mice, while two treatment mice that had higher CFU counts were interspersed among the PA103 mice.

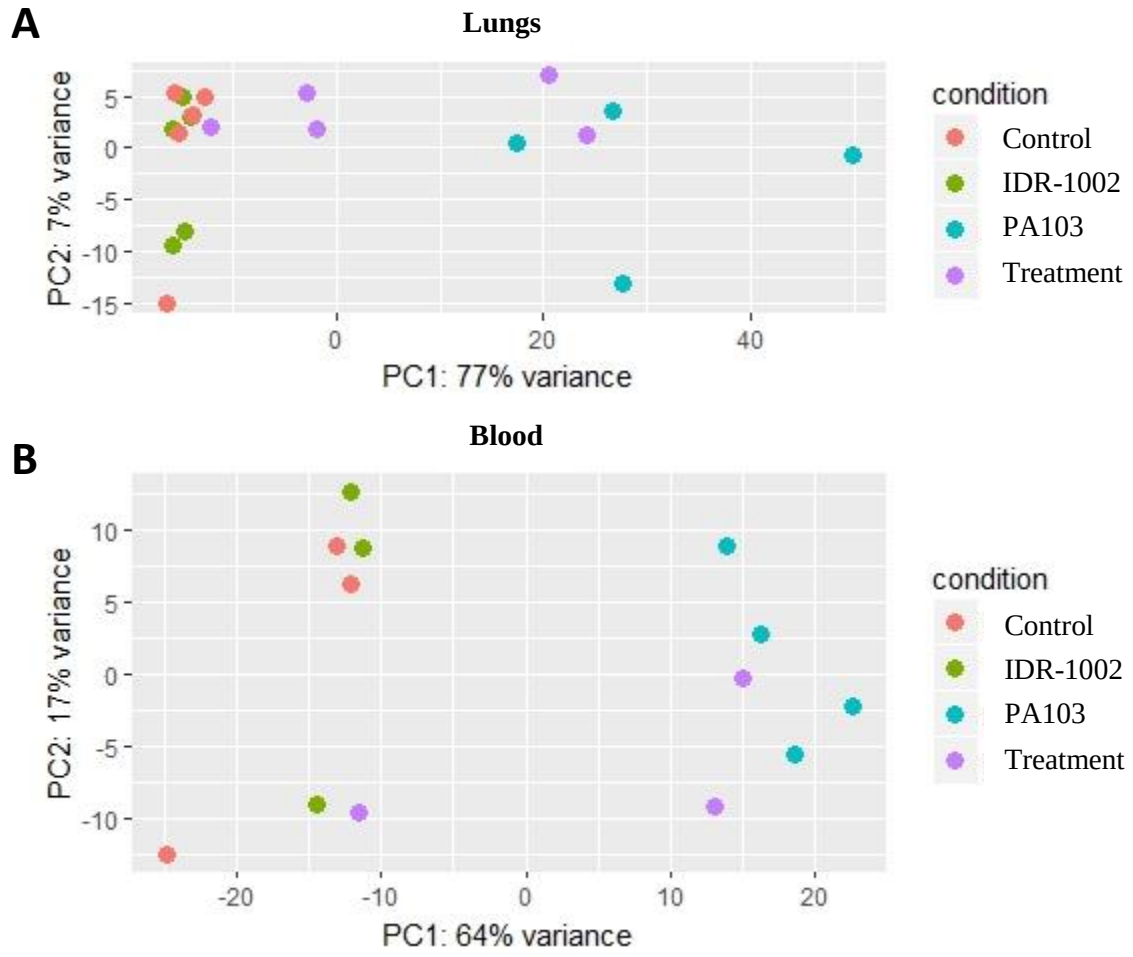

Figure 4.3: PCA plots show clustering of the transcriptome of infected versus uninfected mice. A) Results from the lungs. B) Results from the blood. Red is the uninfected control mice, green is uninfected mice given IDR-1002, blue is PA103-infected mice, and purple is IDR-1002 treatment of PA103-infected mice.

Next, the total number of DE genes for several comparisons was determined (**Table 4.1**). As expected, PA103 infection led to the differential expression of many genes, with nearly five thousand DE genes in the lungs and 1327 in the blood when compared to the control samples.

Table 4.1: Number of DE genes for different comparisons in the lungs and blood.

Comparison	Lungs	Blood
IDR-1002 vs. Control	2	0
PA103 vs. Control	4739	1327
Treatment vs. Control	813	294
Treatment vs. IDR-1002	638	271
Treatment vs. PA103	2111	1

In the lungs, there were 2360 upregulated DE genes and 2379 downregulated DE genes with PA103 infection compared to the control mice. For upregulated DE genes in the lungs, the PA103 DE genes had multiple genes encoding inflammatory response proteins, including CRAMP and acute phase serum amyloid A proteins, and numerous chemokines. There were also genes for several matrix metalloproteinases (MMPs) upregulated (MMP-3, -8, -9, -12, -14, and -25). The genes for the cytokines and chemokines examined in the ELISAs, IL-6, TNF-α, MCP-1, and KC, were all upregulated in the PA103 mice similar to the results seen at the protein level, with the genes showing greater than 32-fold changes compared to the control mice. The downregulated DE genes in the lungs were more varied in function but notably included several genes encoding subunits of various types of collagen, which is a major component of ECM organization (277).

While the top DE genes according to fold-change can provide some interesting targets to evaluate, it is important to take a systemic approach to the data. Therefore, ORA examining GO biological processes was performed on the upregulated or downregulated DE genes for PA103 vs. control in the lungs. There were dozens of pathways for the upregulated DE genes in the lungs for PA103 vs. control (**Table 4.2**), including many pathways associated with inflammation and infection such as the acute-phase response and acute inflammatory response, NF-κB and TLR signaling and

their regulation, responses to bacteria and their components, response and regulation of cytokines, and leukocyte chemotaxis, particularly for neutrophils and lymphocytes. In addition, there were pathways associated with a type I interferon or viral response. There were considerably fewer pathways for the downregulated DE genes (**Table 4.3**) but these included ones for ECM organization, cilium organization and assembly, and some involving metabolic processes for sulfur compounds, cellular lipids, and monocarboxylic acids. There were also some pathways associated with the nervous system, particularly axon guidance. Since the lungs contain airway neurons and guidance molecules (278, 279), these pathways likewise indicate the loss of structural integrity and cell growth during the *P. aeruginosa* infection. Importantly, the downregulated pathways did not show any involving the immune system or an inflammatory response to a bacterial infection.

Table 4.2: Selected overrepresented pathways for upregulated DE genes in the lungs for PA103 vs. control mice.

GO biological process (accession number)	Genes in pathway	Seen	Expect	Fold-Enrich-ment	P-value
Response to interferon-beta (GO:0035456)	45	29	4.54	6.39	1.11E-10
Response to interferon-alpha (GO:0035455)	19	11	1.92	5.74	4.39E-02
Chemokine-mediated signaling pathway (GO:0070098)	45	25	4.54	5.51	1.60E-07
Pattern recognition receptor signaling pathway (GO:0002221)	55	30	5.54	5.41	2.60E-09
Toll-like receptor signaling pathway (GO:0002224)	46	25	4.64	5.39	2.51E-07
Lymphocyte chemotaxis (GO:0048247)	39	21	3.93	5.34	1.07E-05
Innate immune response-activating signal transduction (GO:0002758)	58	31	5.85	5.3	1.78E-09
Neutrophil chemotaxis (GO:0030593)	60	32	6.05	5.29	7.80E-10
Activation of innate immune response (GO:0002218)	65	34	6.55	5.19	2.31E-10
I-kappaB kinase/NF-kappaB signaling (GO:0007249)	46	23	4.64	4.96	7.27E-06
Acute-phase response (GO:0006953)	33	16	3.33	4.81	3.70E-03
Regulation of neutrophil chemotaxis (GO:0090022)	33	16	3.33	4.81	3.70E-03
Regulation of toll-like receptor signaling pathway (GO:0034121)	49	23	4.94	4.66	2.34E-05

GO biological process (accession number)	Genes in pathway	Seen	Expect	Fold-Enrich-ment	P-value
Response to interferon-gamma (GO:0034341)	75	35	7.56	4.63	2.42E-09
Leukocyte chemotaxis (GO:0030595)	114	53	11.49	4.61	2.63E-15
Regulation of type I interferon production (GO:0032479)	61	27	6.15	4.39	3.62E-06
Regulation of interleukin-12 production (GO:0032655)	50	22	5.04	4.37	1.57E-04
Leukocyte cell-cell adhesion (GO:0007159)	41	18	4.13	4.36	3.03E-03
Response to interleukin-1 (GO:0070555)	82	36	8.27	4.36	6.32E-09
Regulation of interleukin-1 production (GO:0032652)	57	25	5.75	4.35	1.88E-05
Cell chemotaxis (GO:0060326)	167	73	16.83	4.34	1.82E-20
Regulation of interferon-beta production (GO:0032648)	45	19	4.54	4.19	2.61E-03
Response to molecule of bacterial origin (GO:0002237)	249	105	25.1	4.18	2.66E-29
Regulation of viral genome replication (GO:0045069)	69	29	6.96	4.17	2.70E-06
Regulation of interleukin-1 beta production (GO:0032651)	43	18	4.33	4.15	5.93E-03
Response to lipopolysaccharide (GO:0032496)	232	97	23.39	4.15	1.38E-26
Regulation of NF-kappaB import into nucleus (GO:0042345)	39	16	3.93	4.07	3.07E-02
Maturation of SSU-rRNA (GO:0030490)	49	20	4.94	4.05	2.18E-03
Regulation of cytokine biosynthetic process (GO:0042035)	99	40	9.98	4.01	4.53E-09
Regulation of innate immune response (GO:0045088)	208	84	20.97	4.01	1.05E-21
Cytokine secretion (GO:0050663)	40	16	4.03	3.97	4.19E-02
Response to virus (GO:0009615)	178	71	17.94	3.96	1.14E-17
Acute inflammatory response (GO:0002526)	63	25	6.35	3.94	1.30E-04

Table 4.3: Selected overrepresented pathways for downregulated DE genes in the lungs for PA103 vs. control mice.

GO biological process (accession number)	Genes in pathway	Seen	Expect	Fold-Enrich-ment	P-value
Regulation of smoothened signaling pathway (GO:0008589)	72	24	7.23	3.32	5.10E-03

GO biological process (accession number)	Genes in pathway	Seen	Expect	Fold-Enrich-ment	P-value
Smoothened signaling pathway (GO:0007224)	76	25	7.63	3.28	3.82E-03
Axon guidance (GO:0007411)	173	41	17.37	2.36	6.91E-03
Neuron projection guidance (GO:0097485)	175	41	17.57	2.33	9.15E-03
Extracellular matrix organization (GO:0030198)	173	40	17.37	2.3	1.68E-02
Cilium organization (GO:0044782)	246	56	24.7	2.27	2.89E-04
Cilium assembly (GO:0060271)	225	50	22.59	2.21	3.03E-03
Sulfur compound metabolic process (GO:0006790)	253	52	25.4	2.05	1.68E-02
Axon development (GO:0061564)	325	64	32.63	1.96	5.01E-03
Axonogenesis (GO:0007409)	302	59	30.32	1.95	1.71E-02
Cell projection assembly (GO:0030031)	316	60	31.72	1.89	3.33E-02
Cell morphogenesis involved in neuron differentiation (GO:0048667)	369	69	37.05	1.86	1.11E-02
Neuron projection morphogenesis (GO:0048812)	400	74	40.16	1.84	6.84E-03
Cell projection morphogenesis (GO:0048858)	411	75	41.26	1.82	9.44E-03
Monocarboxylic acid metabolic process (GO:0032787)	440	80	44.17	1.81	4.84E-03
Cell part morphogenesis (GO:0032990)	435	76	43.67	1.74	3.70E-02
Cell morphogenesis involved in differentiation (GO:0000904)	486	83	48.79	1.7	3.18E-02
Cell projection organization (GO:0030030)	951	161	95.47	1.69	1.83E-06
Oxoacid metabolic process (GO:0043436)	765	129	76.8	1.68	1.48E-04
Sensory organ development (GO:0007423)	540	91	54.21	1.68	1.88E-02
Organic acid metabolic process (GO:0006082)	777	130	78.01	1.67	2.01E-04
Cell morphogenesis (GO:0000902)	620	103	62.24	1.65	7.72E-03
Oxidation-reduction process (GO:0055114)	832	137	83.53	1.64	2.11E-04
Cellular lipid metabolic process (GO:0044255)	759	123	76.2	1.61	2.45E-03
Carboxylic acid metabolic process (GO:0019752)	710	115	71.28	1.61	6.07E-03
Animal organ morphogenesis (GO:0009887)	922	145	92.56	1.57	1.19E-03
Small molecule metabolic process (GO:0044281)	1422	223	142.76	1.56	5.48E-07
Lipid metabolic process (GO:0006629)	986	149	98.99	1.51	7.49E-03
Regulation of nervous system development (GO:0051960)	891	134	89.45	1.5	3.35E-02

To gain further insights into the genes and interactions involved in some of these pathways, NetworkAnalyst was used to create and visualize protein-protein interaction networks (272). Since the genes for multiple chemokines were upregulated, as well as pathways associated with chemotaxis, a zero-order network showing the interactions of DE genes associated with leukocyte migration was created (**Figure 4.4**). Almost all of the genes in the network were increased (red-colored nodes) in the PA103 mice compared to the control mice, and numerous chemokines from both the CXC and CC families were seen. *P. aeruginosa* lung infections are known to lead to an influx of leukocytes, particularly neutrophils (44, 58), and an increase in neutrophils was seen in the leukocyte differential counts in the BALF. Therefore, the induction of numerous chemokine genes is in agreement with these observations.

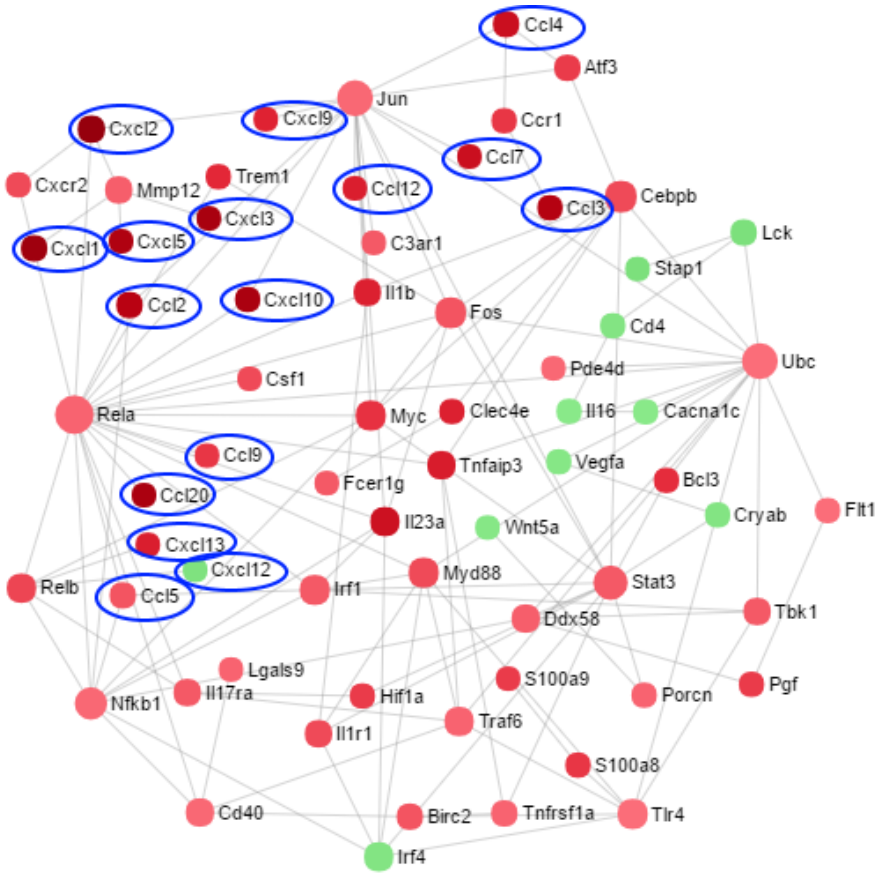

Figure 4.4: Zero-order protein-protein interaction network of DE genes in the lungs for PA103 vs. control mice that are associated with leukocyte migration and their interacting partners. Red nodes were upregulated in the PA103 group and green nodes were downregulated in the PA103 group. A darker color indicates a stronger fold-change. Chemokines are highlighted with blue circles.

For the pathways seen in the ORA of downregulated DE genes in the lungs, genes involved in ECM organization were also used to create a network (**Figure 4.5**). The upregulated DE genes included *Mmp9*, which encodes a matrix metalloproteinase that is upregulated and released during numerous lung injury models and which decreases ECM integrity (280). In contrast, the downregulated DE genes included several for chains of types of collagen, the major fibrous component of the ECM (277).

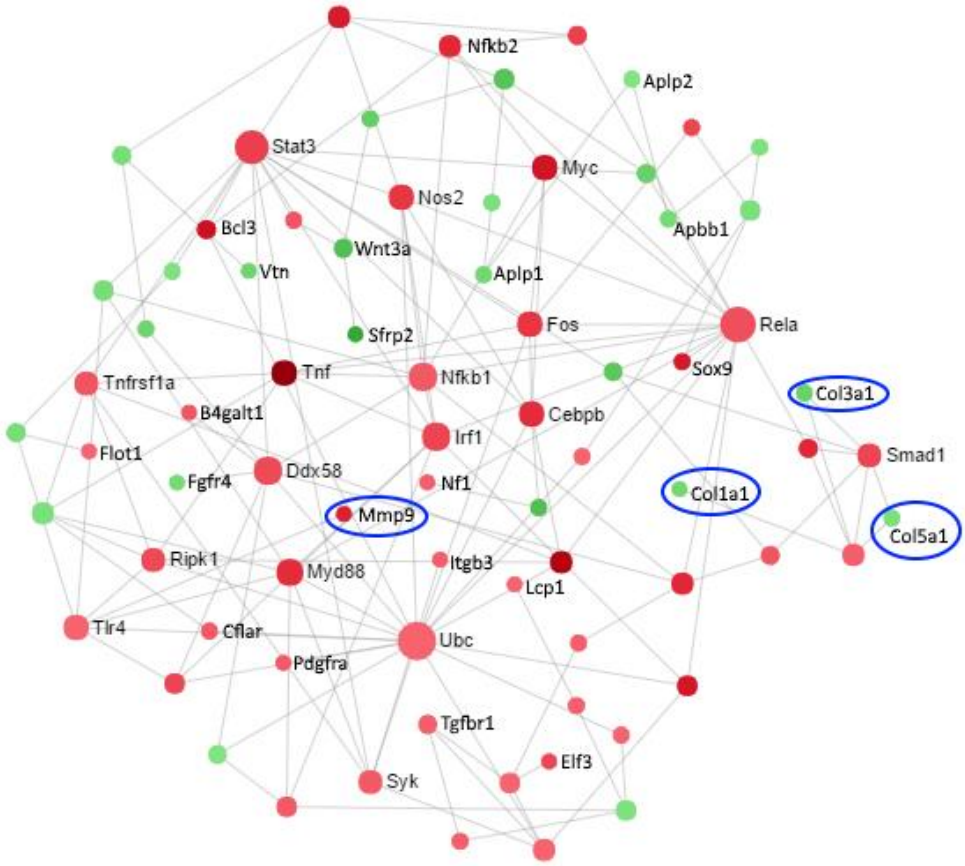

Figure 4.5: Zero-order protein-protein interaction network of DE genes in the lungs for PA103 vs. control mice that are associated with ECM organization and their interacting partners. Red nodes were upregulated in the PA103 group and green nodes were downregulated in the PA103 group. A darker color indicates a stronger fold-change. The gene for matrix metalloproteinase MMP-9 and components of collagen are highlighted with blue circles.

Other interesting pathways that appeared in the ORA for the upregulated DE genes involved those reflecting responses to viruses, including type I interferon pathways. A zero-order interaction network was created to examine these more closely (**Figure 4.6**). Multiple genes were upregulated,

and while some of these have also been associated with bacterial infections, others have been more typically linked to viral infections, including *Irf1*, *Irf5*, *Tlr7*, and *Ddx58*, the gene encoding RIG-I.

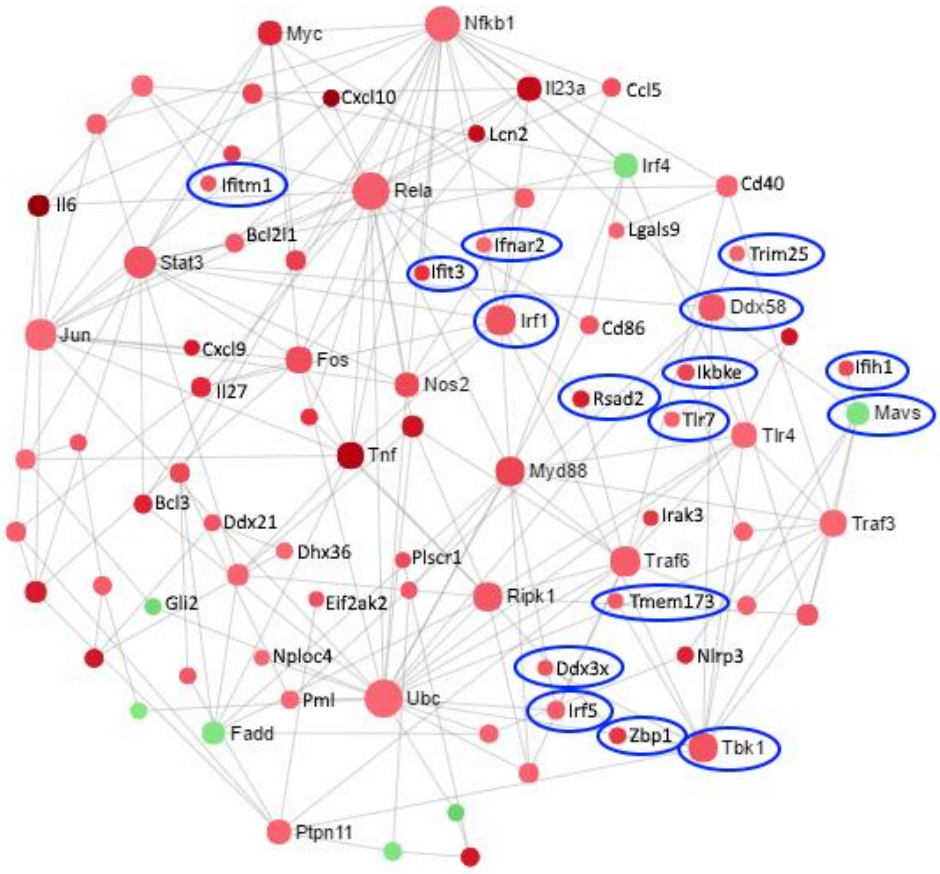

Figure 4.6: Zero-order protein-protein interaction network of DE genes in the lungs for PA103 vs. control mice that are associated with a response to viruses and their interacting partners. Red nodes were upregulated in the PA103 group and green nodes were downregulated in the PA103 group. A darker color indicates a stronger fold-change. Proteins that are closely associated with an immune response to viruses are highlighted with blue circles.

In the blood, there were 686 upregulated and 641 downregulated DE genes in the PA103 mice compared to the control mice. As with the lungs, many of the top upregulated DE genes in the blood were associated with infection and inflammation, such as the genes for CRAMP and lactotransferrin, an antimicrobial and iron-sequestering protein, and several chemokines. There were also genes associated with neutrophil-induced inflammation, such as *Lcn2*, *Cd177*, and *Ngp*. While IL-6, MCP-1, and KC were significantly upregulated in the serum and TNF-α showed a trend towards

upregulation, only the genes for MCP-1 and TNF-α were significantly upregulated in the blood, probably reflecting differences in kinetics for these cytokines and chemokines. For the downregulated DE genes, there were several involved with immunoglobulins or their receptors, or other aspects of a B cell response.

As determined by ORA, the pathways for upregulated DE genes (**Table 4.4**) included many that are related to infection as seen for the lungs, such as the acute inflammatory response and other inflammation-related pathways, leukocyte chemotaxis including pathways for neutrophil and lymphocyte chemotaxis, regulation of and response to cytokines, and responses to bacteria and their components**.** Although lymphocyte chemotaxis was the only lymphocyte pathway upregulated, there were multiple pathways involving lymphocyte activation, proliferation, and differentiation in the pathways overrepresented in the downregulated DE genes (**Table 4.5**), which seemed to be related to B cell processes rather than T cells. In addition, the pathways for the downregulated DE genes included ones related to protein ubiquitination.

Table 4.4: Selected overrepresented pathways for upregulated DE genes in the blood for PA103 vs. control mice.

GO biological process (accession number)	Genes in pathway	Seen	Expect	Fold-Enrich-ment	P-value
Leukocyte migration involved in inflammatory response (GO:0002523)	17	7	0.52	13.5	9.94E-03
Lipopolysaccharide-mediated signaling pathway (GO:0031663)	29	9	0.88	10.17	3.18E-03
Neutrophil chemotaxis (GO:0030593)	60	18	1.83	9.83	9.83E-09
Leukocyte chemotaxis (GO:0030595)	114	27	3.48	7.76	7.18E-12
ADP metabolic process (GO:0046031)	43	10	1.31	7.62	9.68E-03
Regulation of plasma lipoprotein particle levels (GO:0097006)	43	10	1.31	7.62	9.68E-03
Regulation of mononuclear cell migration (GO:0071675)	39	9	1.19	7.56	3.50E-02
Lymphocyte chemotaxis (GO:0048247)	39	9	1.19	7.56	3.50E-02
Modification by host of symbiont morphology or physiology (GO:0051851)	53	12	1.62	7.42	1.12E-03
Regulation of phagocytosis (GO:0050764)	84	19	2.56	7.41	2.80E-07

GO biological process (accession number)	Genes in pathway	Seen	Expect	Fold-Enrich-ment	P-value
Chemokine-mediated signaling pathway (GO:0070098)	45	10	1.37	7.28	1.44E-02
Modification of morphology or physiology of other organism (GO:0035821)	77	17	2.35	7.24	4.29E-06
Myeloid leukocyte migration (GO:0097529)	96	21	2.93	7.17	4.84E-08
Defense response to Gram-negative bacterium (GO:0050829)	46	10	1.4	7.13	1.75E-02
Interaction with symbiont (GO:0051702)	56	12	1.71	7.02	2.00E-03
Regulation of acute inflammatory response (GO:0002673)	57	12	1.74	6.9	2.41E-03
Purine ribonucleoside diphosphate metabolic process (GO:0009179)	48	10	1.46	6.83	2.54E-02
Regulation of myeloid leukocyte mediated immunity (GO:0002886)	48	10	1.46	6.83	2.54E-02
Regulation of toll-like receptor signaling pathway (GO:0034121)	49	10	1.49	6.69	3.04E-02
Myeloid leukocyte activation (GO:0002274)	99	20	3.02	6.62	6.10E-07
Cell chemotaxis (GO:0060326)	167	33	5.09	6.48	8.16E-13
Translational initiation (GO:0006413)	61	12	1.86	6.45	4.88E-03
Response to interleukin-1 (GO:0070555)	82	16	2.5	6.4	7.62E-05
Acute inflammatory response (GO:0002526)	63	12	1.92	6.24	6.80E-03
Innate immune response-activating signal transduction (GO:0002758)	58	11	1.77	6.22	2.01E-02
Regulation of tumor necrosis factor superfamily cytokine production (GO:1903555)	122	23	3.72	6.18	9.12E-08
Regulation of interleukin-6 production (GO:0032675)	119	22	3.63	6.06	3.67E-07
Activation of innate immune response (GO:0002218)	65	12	1.98	6.05	9.36E-03
Regulation of tumor necrosis factor production (GO:0032680)	120	22	3.66	6.01	4.29E-07
Response to molecule of bacterial origin (GO:0002237)	249	43	7.6	5.66	2.34E-15

Table 4.5: Selected overrepresented pathways for downregulated DE genes in the blood for PA103 vs. control mice.

GO biological process (accession number)	Genes in pathway	Seen	Expect	Fold-Enrich-ment	P-value
Regulation of B cell proliferation (GO:0030888)	63	14	1.76	7.97	4.24E-05
B cell activation (GO:0042113)	155	25	4.32	5.79	4.51E-08

GO biological process (accession number)	Genes in pathway	Seen	Expect	Fold-Enrich-ment	P-value
B cell differentiation (GO:0030183)	106	16	2.95	5.42	7.11E-04
Cofactor biosynthetic process (GO:0051188)	129	16	3.59	4.45	9.18E-03
Protein polyubiquitination (GO:0000209)	167	20	4.65	4.3	7.58E-04
Myeloid cell differentiation (GO:0030099)	213	24	5.94	4.04	1.26E-04
Regulation of mononuclear cell proliferation (GO:0032944)	209	22	5.82	3.78	1.56E-03
Regulation of lymphocyte proliferation (GO:0050670)	207	21	5.77	3.64	5.28E-03
Regulation of leukocyte proliferation (GO:0070663)	217	22	6.05	3.64	2.91E-03
Protein ubiquitination (GO:0016567)	414	41	11.54	3.55	5.56E-08
Lymphocyte activation (GO:0046649)	381	37	10.62	3.49	1.03E-06
Lymphocyte differentiation (GO:0030098)	249	24	6.94	3.46	2.12E-03
Protein modification by small protein conjugation (GO:0032446)	453	43	12.62	3.41	6.43E-08
Regulation of B cell activation (GO:0050864)	245	23	6.83	3.37	5.85E-03
Immune system development (GO:0002520)	691	63	19.25	3.27	4.24E-12
Hematopoietic or lymphoid organ development (GO:0048534)	660	60	18.39	3.26	2.51E-11
Protein modification by small protein conjugation or removal (GO:0070647)	572	48	15.94	3.01	2.55E-07
Regulation of chromosome organization (GO:0033044)	290	24	8.08	2.97	2.88E-02
Modification-dependent protein catabolic process (GO:0019941)	403	31	11.23	2.76	5.25E-03
Ubiquitin-dependent protein catabolic process (GO:0006511)	396	29	11.03	2.63	3.07E-02
Covalent chromatin modification (GO:0016569)	428	30	11.93	2.52	4.87E-02
Regulation of lymphocyte activation (GO:0051249)	503	35	14.02	2.5	9.73E-03
Immune effector process (GO:0002252)	507	35	14.13	2.48	1.16E-02
Proteolysis involved in cellular protein catabolic process (GO:0051603)	469	32	13.07	2.45	4.12E-02
Macromolecule catabolic process (GO:0009057)	716	46	19.95	2.31	1.94E-03
Protein modification process (GO:0036211)	2157	131	60.1	2.18	1.41E-13
Macromolecule modification (GO:0043412)	2390	141	66.6	2.12	6.64E-14
Heterocycle biosynthetic process (GO:0018130)	2200	121	61.3	1.97	3.37E-09
Aromatic compound biosynthetic process (GO:0019438)	2207	120	61.5	1.95	9.25E-09
RNA biosynthetic process (GO:0032774)	1897	102	52.86	1.93	1.21E-06

A zero-order interaction network for the blood (**Figure 4.7**) showed a mixture of up- and downregulated genes. Prominent hubs for upregulated genes included *Rela*, a subunit of the transcription factor NF-κB; *MyD88*; and *Cebpa* and *Cebpb*, two members of the CCAAT/enhancer binding proteins (C/EBP) transcription factor family that are involved in lung inflammation (281). The downregulated gene *Sp3*, which encodes a proteinase inhibitor, was also a hub.

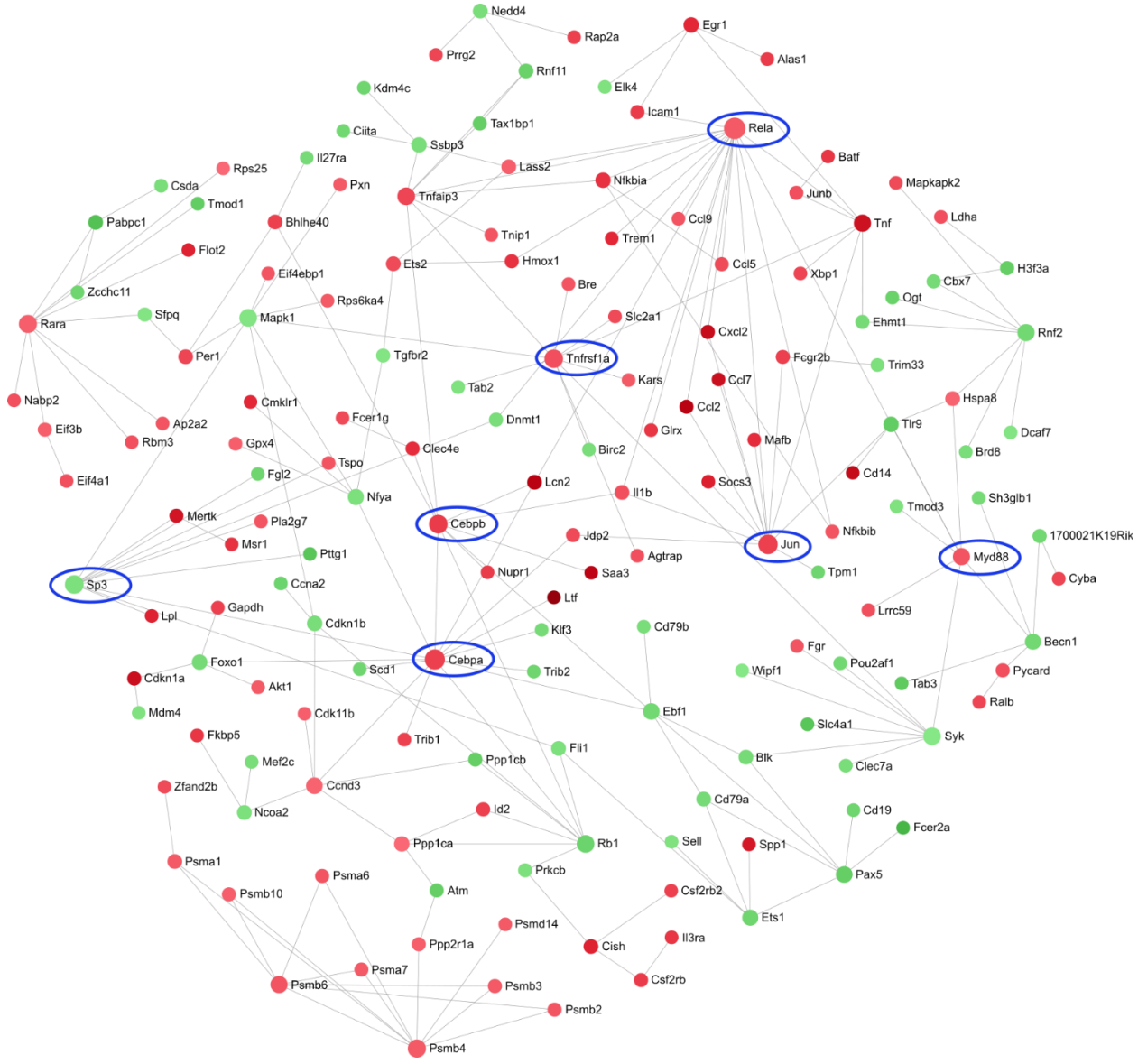

Figure 4.7: Zero-order protein-protein interaction network of DE genes in the blood for PA103 vs. control mice. Red nodes were upregulated in the PA103 group and green nodes were downregulated in the PA103 group. A darker color indicates a stronger fold-change. Several key genes involved in the immune response to an infection are highlighted with blue circles.

4.3.3 Administration of IDR-1002 reduces inflammation responses induced by *P. aeruginosa* in the lungs and blood

The use of IDR-1002 in uninfected mice led to only two DE genes in the lungs, *Csf3* and *Saa2*, the genes encoding G-CSF and serum amyloid A2, which were upregulated and downregulated, respectively, compared to the control mice.

While the response in uninfected mice was limited, the administration of IDR-1002 in combination with PA103 infection had a large impact on the transcriptome. The comparison between the treatment and PA103 groups showed 2111 DE genes in the lungs, with 1110 upregulated and 1001 downregulated DE genes. The genes for the four proteins examined in ELISAs, namely MCP-1, KC, IL-6, and TNF-α, showed a trend towards downregulation in the treatment mice but were not significantly DE. However, the treatment mice had the genes for several chemokines downregulated compared to the PA103 mice, including *Ccl4*, *Cxcl10*, *Ccl11*, and *Cxcl13*, along with other genes associated with an inflammatory response, while the upregulated genes were more diverse. This was also reflected in the pathways from the ORA (**Tables 4.6 and 4.7**), with only a limited number of upregulated pathways and most of these related to broad biological processes. Of the more specific pathways, there were ones related to regulation of epithelial cell proliferation and cell projection organization as well as metabolism, including sulfur compound and oxoacid metabolic processes. In contrast, there were numerous downregulated pathways including responses to LPS; viral and type I interferon responses and their regulation; apoptotic processes and their regulation; regulation of protein polyubiquitination; and regulation of and response to numerous cytokines.

Table 4.6: Selected overrepresented pathways for upregulated DE genes in the lungs for treatment vs. PA103 mice.

GO biological process (accession number)	Genes in pathway	Seen	Expect	Fold-Enrich-ment	P-value
Regulation of smoothened signaling pathway (GO:0008589)	72	15	3.43	4.37	2.53E-02

GO biological process (accession number)	Genes in pathway	Seen	Expect	Fold-Enrich-ment	P-value
Neuron migration (GO:0001764)	134	21	6.38	3.29	2.70E-02
Sulfur compound metabolic process (GO:0006790)	253	31	12.05	2.57	2.47E-02
Regulation of epithelial cell proliferation (GO:0050678)	319	37	15.19	2.44	1.01E-02
Regulation of cell projection organization (GO:0031344)	638	61	30.38	2.01	3.40E-03
Small molecule metabolic process (GO:0044281)	1422	125	67.72	1.85	4.54E-07
Oxoacid metabolic process (GO:0043436)	765	67	36.43	1.84	1.84E-02
Organic acid metabolic process (GO:0006082)	777	68	37	1.84	1.58E-02
Animal organ morphogenesis (GO:0009887)	922	76	43.91	1.73	3.37E-02
Cell projection organization (GO:0030030)	951	78	45.29	1.72	3.00E-02
Nervous system development (GO:0007399)	2052	162	97.72	1.66	1.54E-06
Neurogenesis (GO:0022008)	1551	120	73.86	1.62	1.36E-03
Generation of neurons (GO:0048699)	1450	108	69.05	1.56	3.23E-02
Single-organism metabolic process (GO:0044710)	2762	201	131.53	1.53	6.18E-06

Table 4.7: Selected overrepresented pathways for downregulated DE genes in the lungs for treatment vs. PA103 mice.

GO biological process (accession number)	Genes in pathway	Seen	Expect	Fold-Enrich-ment	P-value
Regulation of protein polyubiquitination (GO:1902914)	14	8	0.61	13.02	2.29E-03
Regulation of interferon-alpha production (GO:0032647)	19	9	0.83	10.79	1.98E-03
Response to interferon-alpha (GO:0035455)	19	8	0.83	9.59	2.18E-02
Toll-like receptor signaling pathway (GO:0002224)	46	18	2.02	8.91	5.12E-08
Pattern recognition receptor signaling pathway (GO:0002221)	55	21	2.41	8.7	1.46E-09
NIK/NF-kappaB signaling (GO:0038061)	21	8	0.92	8.68	4.49E-02
Innate immune response-activating signal transduction (GO:0002758)	58	22	2.55	8.64	4.44E-10
Activation of innate immune response (GO:0002218)	65	24	2.85	8.41	5.73E-11
I-kappaB kinase/NF-kappaB signaling (GO:0007249)	46	15	2.02	7.43	3.25E-05
Regulation of interferon-beta production (GO:0032648)	45	14	1.98	7.09	1.89E-04

GO biological process (accession number)	Genes in pathway	Seen	Expect	Fold-Enrich-ment	P-value
Response to interferon-beta (GO:0035456)	45	14	1.98	7.09	1.89E-04
Regulation of type I interferon production (GO:0032479)	61	18	2.68	6.72	4.48E-06
Regulation of viral genome replication (GO:0045069)	69	20	3.03	6.6	6.83E-07
Regulation of NF-kappaB import into nucleus (GO:0042345)	39	11	1.71	6.42	1.50E-02
Regulation of toll-like receptor signaling pathway (GO:0034121)	49	13	2.15	6.04	3.53E-03
Regulation of interleukin-1 production (GO:0032652)	57	14	2.5	5.59	3.20E-03
Regulation of defense response to virus (GO:0050688)	59	14	2.59	5.4	4.78E-03
Response to molecule of bacterial origin (GO:0002237)	249	59	10.93	5.4	7.35E-21
Intrinsic apoptotic signaling pathway in response to DNA damage (GO:0008630)	69	16	3.03	5.28	1.04E-03
Regulation of response to biotic stimulus (GO:0002831)	119	27	5.22	5.17	9.36E-08
Regulation of interleukin-2 production (GO:0032663)	53	12	2.33	5.16	4.78E-02
Regulation of innate immune response (GO:0045088)	208	47	9.13	5.15	2.78E-15
Response to lipopolysaccharide (GO:0032496)	232	52	10.19	5.11	4.91E-17
Cellular response to interleukin-1 (GO:0071347)	68	15	2.99	5.02	4.72E-03
Response to virus (GO:0009615)	178	39	7.81	4.99	8.01E-12
Regulation of lymphocyte apoptotic process (GO:0070228)	65	14	2.85	4.91	1.46E-02
Defense response to virus (GO:0051607)	136	29	5.97	4.86	7.07E-08
Regulation of tumor necrosis factor superfamily cytokine production (GO:1903555)	122	26	5.36	4.85	8.42E-07

A zero-order interaction network (**Figure 4.8**) also demonstrated that a large number of the downregulated genes were associated with the inflammatory response in the treatment mice, including *Myd88*, *Traf6*, and *Rela*. This indicates that IDR-1002 treatment reduced inflammation.

Figure 4.8: Zero-order protein-protein interaction network of DE genes in the lungs for treatment vs. PA103 mice. Red nodes were upregulated in the treatment group and green nodes were downregulated in the treatment group. A darker color indicates a stronger fold-change. Several key genes involved in the immune response to an infection are highlighted with blue circles.

The number of DE genes for the treatment mice compared to either control (813 DE genes) or IDR-1002 (638 DE genes) mice was much smaller than for the PA103 vs. control comparison, with the comparison of treatment mice to control mice producing 512 upregulated and 301 downregulated DE genes, while treatment vs. IDR-1002 had 475 upregulated and 163 downregulated DE genes. This indicated that the treated mice were more like the uninfected mice. While the genes for the four cytokines and chemokines examined in the ELISAs were upregulated in the treatment mice compared to the control mice and the treatment vs. control comparison still indicated genes and pathways associated with an immune response were upregulated, there were far fewer DE genes associated with the inflammatory response than the number observed for PA103 vs. control. For the overrepresented pathways for downregulated DE genes when comparing treatment vs. control, many of the pathways were associated with lymphocyte activation and differentiation as well as MHC class II antigen processing, although some pathways involving lymphocytes and the adaptive response were also seen in the upregulated pathways. The comparison of treatment to IDR-1002 showed similar results to those for treatment vs. control.

To better understand the role of IDR-1002 in restoring a baseline condition, the DE genes found in PA103 vs. control were compared to the DE genes found in treatment vs. control (**Figure 4.9**). There was considerable overlap between the two comparisons, but there were still 45 DE genes found exclusively in the treatment vs. control comparison. These included 22 downregulated genes and 23 upregulated genes. Many of these genes were associated with an immune response, including the downregulated genes *Bpifa1* and *Nkg7* and the upregulated genes *Cd300a* and *Ccr2*. In particular, some of these genes were associated with lymphocyte activities and maturation, including downregulated genes *Cd3d*, *Cd8a*, *Il21r*, *Blnk*, *Lat*, *Igf1*, *H2-Ab1*, *H2-Aa*, and the upregulated gene *Vsir*. Using only the downregulated genes exclusive to the treatment vs. control comparison for ORA did not reveal any pathways, but the upregulated genes resulted in two pathways, the negative

regulation of eosinophil activation and the negative regulation of immune effector process. There were no DE genes that were upregulated in one comparison and downregulated in the other.

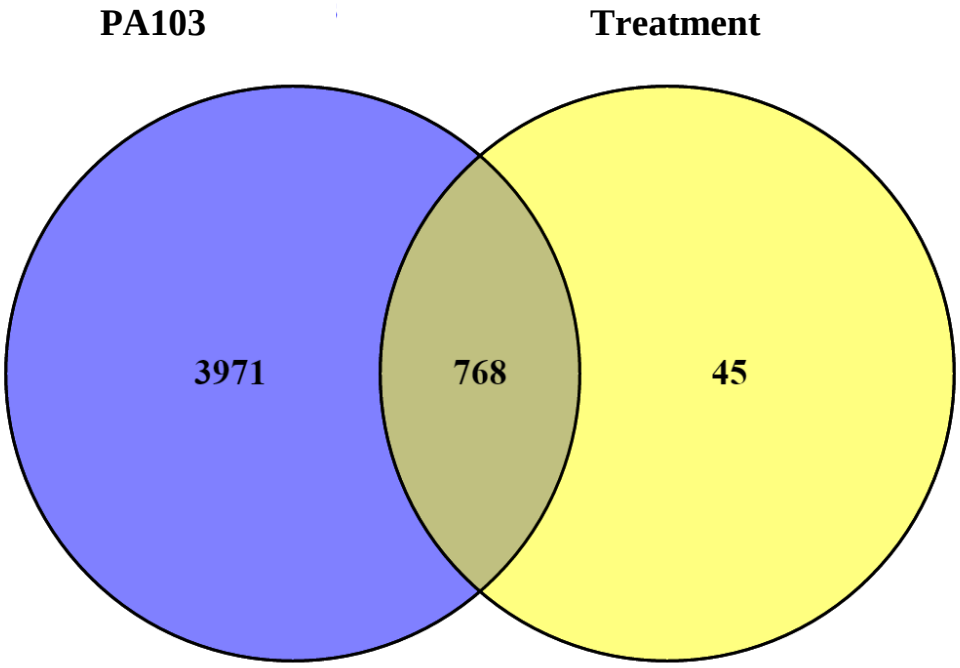

Figure 4.9: Venn diagram comparing the DE genes found in PA103 vs. control to those in treatment vs. control in the lungs.

Once again considering all of the DE genes and pathways found in PA103 vs. control compared to the ones found in treatment vs. control, as mentioned previously there was still a strong immune response seen in the treatment vs. control upregulated pathways but it was greatly reduced when compared to the number of DE genes and pathways upregulated for PA103 vs. control. Despite the reduced number of pathways, there were some pathways that were exclusive to the treatment vs. control comparison (**Tables 4.8 and 4.9**), with ones for upregulated DE genes including response to peptidoglycan; necroptotic process; the regulation of leukocyte degranulation, mast cell activation, mononuclear cell migration, vascular endothelial growth factor production, or endocytosis; and calcium ion homeostasis and its regulation. For the downregulated DE genes, the overrepresented pathways found only in treatment vs. control included some related to antigen processing for MHC class II presentation. Interestingly, while there were some upregulated pathways involving the

regulation of lymphocytes in PA103 vs. control, the processes themselves such as T cell selection, T cell differentiation, T cell activation, and B cell activation were all found exclusively in the downregulated pathways for treatment vs. control, while regulation of T-helper cell differentiation was seen only in the upregulated pathways for treatment vs. control.

Table 4.8: Selected overrepresented pathways for upregulated DE genes in the lungs seen in treatment vs. control but not in PA103 vs. control mice.

GO biological process (accession number)	Genes in pathway	Seen	Expect	Fold-Enrich-ment	P-value
Response to peptidoglycan (GO:0032494)	10	5	0.22	22.41	3.01E-02
Necroptotic process (GO:0070266)	18	6	0.4	14.94	3.23E-02
Regulation of vascular endothelial growth factor production (GO:0010574)	30	8	0.67	11.95	4.22E-03
Regulation of T-helper cell differentiation (GO:0045622)	28	7	0.62	11.21	3.31E-02
Regulation of leukocyte degranulation (GO:0043300)	42	9	0.94	9.6	5.01E-03
Regulation of mononuclear cell migration (GO:0071675)	39	8	0.87	9.19	2.89E-02
Regulation of mast cell activation (GO:0033003)	44	9	0.98	9.17	7.32E-03
Regulation of endocytosis (GO:0030100)	219	22	4.89	4.5	7.34E-05
Regulation of cytosolic calcium ion concentration (GO:0051480)	243	19	5.42	3.5	2.94E-02
Calcium ion homeostasis (GO:0055074)	363	24	8.1	2.96	2.84E-02

Table 4.9: Selected overrepresented pathways for downregulated DE genes in the lungs seen in treatment vs. control but not in PA103 vs. control mice.

GO biological process (accession number)	Genes in pathway	Seen	Expect	Fold-Enrich-ment	P-value
Antigen processing and presentation of exogenous peptide antigen via MHC class II (GO:0019886)	14	5	0.19	27.02	1.20E-02
Antigen processing and presentation of peptide or polysaccharide antigen via MHC class II (GO:0002504)	16	5	0.21	23.65	2.29E-02
Antigen processing and presentation of peptide antigen via MHC class II (GO:0002495)	16	5	0.21	23.65	2.29E-02

GO biological process (accession number)	Genes in pathway	Seen	Expect	Fold-Enrich-ment	P-value
Antigen processing and presentation of exogenous antigen (GO:0019884)	27	6	0.36	16.82	1.62E-02
T cell selection (GO:0045058)	43	7	0.57	12.32	1.75E-02
B cell activation (GO:0042113)	155	16	2.05	7.81	3.93E-06
T cell differentiation (GO:0030217)	153	14	2.02	6.92	2.13E-04
Lymphocyte activation (GO:0046649)	381	34	5.04	6.75	3.56E-14
Lymphocyte differentiation (GO:0030098)	249	22	3.29	6.69	4.14E-08
Antigen receptor-mediated signaling pathway (GO:0050851)	205	15	2.71	5.54	1.19E-03
T cell activation (GO:0042110)	254	18	3.36	5.36	1.09E-04

A first-order network for lymphocyte activation-associated DE genes for treatment vs. control results was made (**Figure 4.10**) and demonstrated the presence of many DE genes related to lymphocyte activation found in this comparison.

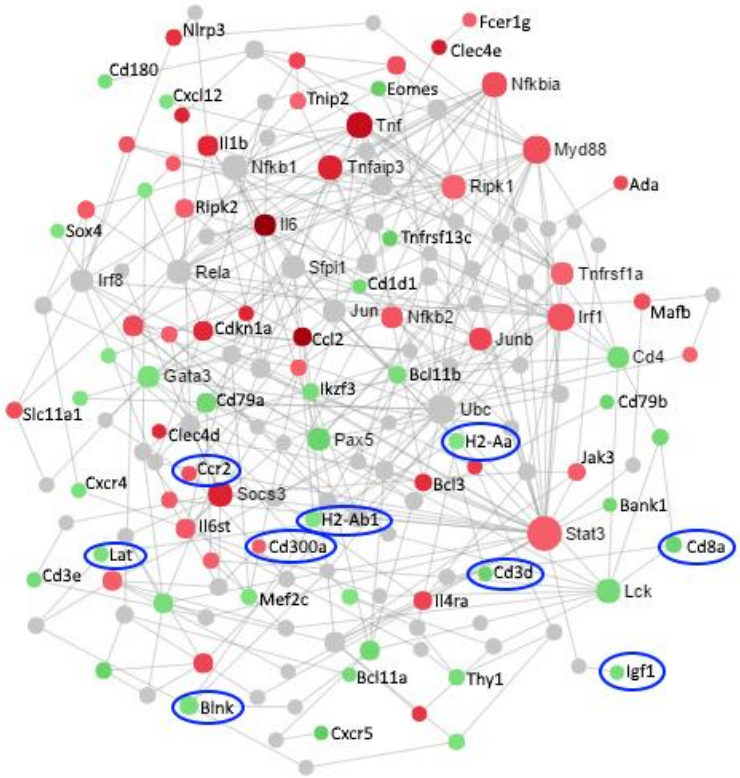

Figure 4.10: First-order protein-protein interaction network of DE genes in the lungs for treatment vs. control mice that are associated with lymphocyte activation and their interacting partners. Red nodes were upregulated in the treatment group, green nodes were downregulated in the treatment group, and grey nodes are not DE. A darker color indicates a stronger fold-change. Genes involved in lymphocyte activation that were DE in treatment vs. control but were not DE for PA103 vs. control are highlighted with blue circles.

In the blood, no DE genes were detected for IDR-1002 mice compared to control mice. There was also only one DE gene related to treatment vs. PA103 in the blood, *Ighd*, a gene encoding the heavy constant region of IgD, which was upregulated in the treatment group. For treatment vs. control mice, there were 248 upregulated and 46 downregulated genes, and the comparison between treatment vs. IDR-1002 mice showed similar numbers, with 221 upregulated and 50 downregulated genes.

Assessing the pathways overrepresented in the upregulated DE genes in the blood of treatment vs. control mice indicated pathways associated with an immune response to infection, including regulation of mast cell activation and degranulation, neutrophil chemotaxis, regulation of cytokine production, and inflammatory response, whereas only four downregulated pathways were seen and all were associated with general biological processes. The treatment vs. IDR-1002 showed similar results, although amongst the genes encoding proteins that were analyzed in ELISAs, *Ccl2* (MCP-1) was increased in treatment vs. IDR-1002, but was not DE in treatment vs. control mice. The genes for TNF-α, IL-6, and KC were not DE in either comparison.

The DE genes found in PA103 vs. control compared to the DE genes found in treatment vs. control in the blood (**Figure 4.11**) demonstrated considerable overlap, but there were 20 DE genes (3 downregulated, 17 upregulated) found exclusively in the treatment vs. control comparison. Although there were no pathways found in ORA for these twenty genes, there were some upregulated genes associated with immune responses, including *Igsf6*, *Slfn4*, *Mefv*, and *Iftim1*.

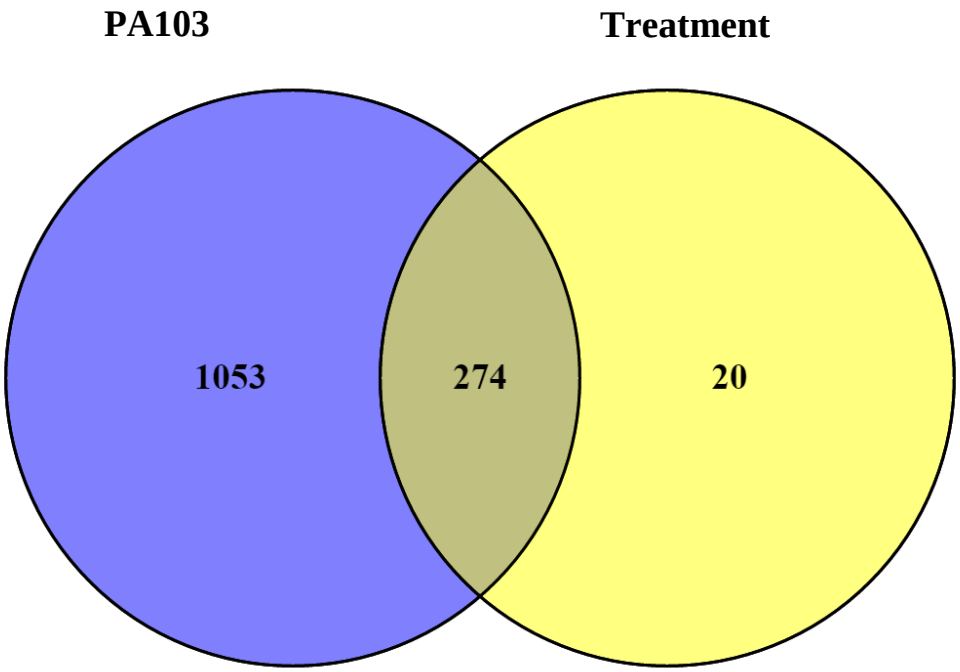

Figure 4.11: Venn diagram comparing the DE genes found in PA103 vs. control to those in treatment vs. control in the blood.

For PA103 vs. control compared to treatment vs. control in the blood, there were many upregulated pathways in common that are associated with an immune response to infection as described above, although PA103 vs. control had many more upregulated and downregulated pathways compared to treatment vs. control. However, there were still certain overrepresented pathways seen for treatment vs. control upregulated DE genes that were not present in PA103 vs. control (**Table 4.10**). These included response to peptidoglycan, regulation of mast cell activation and degranulation, and regulation of peptidase activity.

Table 4.10: Selected overrepresented pathways for upregulated DE genes in the blood seen in treatment vs. control but not in PA103 vs. control.

GO biological process (accession number)	Genes in pathway	Seen	Expect	Fold-Enrich-ment	P-value
Response to peptidoglycan (GO:0032494)	10	4	0.11	36.3	4.41E-02
Regulation of mast cell activation involved in immune response (GO:0033006)	32	7	0.35	19.85	7.33E-04

GO biological process (accession number)	Genes in pathway	Seen	Expect	Fold-Enrich-ment	P-value
Regulation of mast cell degranulation (GO:0043304)	32	7	0.35	19.85	7.33E-04
Regulation of mast cell activation (GO:0033003)	44	9	0.48	18.56	1.85E-05
Regulation of leukocyte degranulation (GO:0043300)	42	7	0.46	15.12	4.48E-03
Regulation of endopeptidase activity (GO:0052548)	249	14	2.74	5.1	7.75E-03
Regulation of peptidase activity (GO:0052547)	348	18	3.84	4.69	7.30E-04

4.4 Discussion

Infection with *P. aeruginosa* PA103 led to almost 5000 DE genes in the lungs and almost 1500 DE genes in the blood compared to the control group. These numbers were greatly reduced in the treatment vs. control comparisons for either the lungs or the blood, indicating more similarity with the controls. This was in agreement with the CFU burdens and the ELISA results for cytokine and chemokine expression, which showed decreases in the treatment mice compared to the PA103 mice, but with levels that were still above those seen in the control or IDR-1002 mice. The use of IDR-1002 with PA103 infection produced a range of results with regards to individual mice, with some mice showing either a complete or partial elimination in CFUs and signs of inflammation, while a few showed results similar to those of the untreated PA103 mice. This was also seen in the PCA plots for the RNA-Seq results, with some treatment mice clustering with untreated controls, and others being closer to the PA103 mice. It is possible that this diversity might reflect minor differences in bacterial infectious doses or the heterogeneity implicit in biological systems in response to both bacteria and peptide. Indeed such variation in response to IDR-1002 has been observed with IDRs in other in vivo models, such as IDR-1018 in a malaria model and IDR-1002 in IP-administered *E. coli* and *S. aureus* models (192, 200). Increasing the IDR-1002 dose or formulating it to improve delivery could improve its effectiveness in individual mice. Regardless of this heterogeneity, there were still 2111 DE genes

in the lungs when comparing the treated and the PA103 mice, with the treated mice showing upregulated DE genes for processes involved in morphogenesis and some metabolic pathways, while the pathways for downregulated DE genes included numerous immune pathways such as activation of the innate immune response and the response to LPS. In other words, the treatment vs. PA103 comparison showed almost the opposite results to PA103 vs. control, indicating that the treatment with IDR-1002 reduced the overwhelming inflammatory response induced by PA103, as seen with both the ELISA and the RNA-Seq results.

There were only two DE genes in IDR-1002 vs. control for the lungs and none for the blood. Since the samples were collected 42 h after IDR-1002 administration it was unsurprising that few changes were seen at the transcriptional level. Regardless, the results from the comparison of the DE genes for treatment vs. control compared to PA103 vs. control offered some interesting differences that could be explored further for unraveling the mechanisms behind the anti-inflammatory activities of IDR-1002. PA103 vs. control had twice as many DE genes as treatment vs. control in the lungs and four times as many DE genes in the blood, and as expected the majority of the DE genes overlapped. Nevertheless, certain genes were only DE in IDR-1002 treated vs. control mice. In the lungs, several genes associated with MHC class II antigen processing and lymphocyte activation were downregulated in the lungs in the treated mice compared to the control and these were not DE in PA103 vs. control. It is possible that this relates to the composition of cells in the samples, and it was observed that some of these pathways were also downregulated in the whole blood samples for PA103 vs. control. The differential cell count in the BALF showed that lymphocyte numbers were similar between the PA103 and treatment groups, whereas the PA103 mice had a large proportion of neutrophils compared to monocytes/macrophages and the treated mice had a mixture of neutrophils and monocytes/macrophages that varied with the CFU burden. Examining cell populations in the lungs with flow cytometry would provide insight into both the cell types involved and their activation states. Another possibility is that IDR-1002 administration altered the immune response and these changes

were then potentiated by the additional stimulus of PA103 infection, whereas in the mice given only IDR-1002 the mice did not receive an additional signal to the immune system, which then returned essentially to baseline levels. For example, the anti-inflammatory cytokine IL-10 decreases signaling through MHC class II, and IDR-1002 has been shown to increase IL-10 secretion by peritoneal mouse macrophages stimulated ex vivo, although the overexpression of IL-10 in *P. aeruginosa* lung infections can have both beneficial and deleterious effects, which could also partly explain the differences in responses in the treatment mice (192, 282, 283). Performing RNA-Seq on samples collected within a few hours of IDR-1002 administration might provide additional insight into the mechanisms of IDR-1002, and the changes seen in the RNA-Seq should be confirmed at both the gene and protein level.

Overall, while the exact mechanism of IDR-1002 reduction of CFUs and inflammation in the acute *P. aeruginosa* lung model is unknown, based on these results and previous experiments with the *S. aureus* IP model and with human neutrophils (192, 201), it is possible that IDR-1002 is leading to early cell recruitment and/or activation, particularly in the upper respiratory tract. This is based on the slight increase of neutrophils seen in the BALF of IDR-1002 mice, even though these counts were done 42 h after IDR-1002 delivery, as well as the increase in the gene for G-CSF in the RNA-Seq data for IDR-1002 mice compared to the control mice. Additionally, preliminary experiments indicate that the concentration of KC is increased in the serum 4 h after IN IDR-1002 and returned to baseline by 24 h after IDR-1002 delivery, while no changes were seen in MCP-1, IL-6, or TNF-α concentrations in the BALF or serum, in KC levels in the BALF, or in total leukocyte recruitment in the BALF. Experiments with IP IDR-1002 indicated that monocytes/macrophages and neutrophils were recruited to the site of injection and peaked at 2-4 h post-injection (192). Human neutrophils also showed increased activation with IDR-1002 treatment (201). These results provide evidence that IDR-1002 in the acute *P. aeruginosa* lung model could also be increasing recruitment and/or activation of monocytes/macrophages and neutrophils, but this could be occurring in the upper respiratory tract

closer to the site of IDR-1002 delivery. While in vivo imaging using a dye specific for neutrophils did not indicate differences with the control, the dye also did not appear to image properly in mice with black fur, as seen with C57Bl/6J mice. Therefore, if IDR-1002 is acting in the acute *P. aeruginosa* through cell activation and/or recruitment in the upper respiratory tract, it will be necessary to use other methods for evaluating this activity. This could include using white mice or fur removal to properly image using the neutrophil-specific dye. For other cell populations, nasal aspirates could be used to evaluate local cells and cytokines or chemokines, but this procedure is prone to reproducibility issues due to washes entering the mouth. Therefore, although not location specific, using antibodies to eliminate certain cells or using adoptive transfer of IDR-1002-treated cells could be useful for further evaluation of IDR-1002 mechanisms of action.

The RNA-Seq results showed that multiple inflammatory pathways upregulated in the lungs and blood in response to *P. aeruginosa*. The large number of chemokine genes upregulated was in agreement with the increased number of leukocytes seen in the BALF with PA103. Consistent with this, *P. aeruginosa* lung infection, even in chronic conditions such as CF, is associated with increased neutrophils in the lungs (44), a feature that was also seen in this acute *P. aeruginosa* model, along with the upregulation of many genes associated with neutrophil activation. The upregulation of numerous MMP genes and the decrease in ECM organization pathways, as observed with the mice infected with PA103, also occurs with the early stages of lung disease such as CF and COPD (284-287). As the diseases progress, the deposition of certain classes of collagen (particularly I and III) leads to fibrosis and decreases patient respiratory capacity (284, 287).

There were also some unexpected pathways seen in PA103 infection, such as ones related to viral infection and the type I interferon response. While the type I interferon response has traditionally been associated with viral and intracellular bacterial infections, recent research has shown that it can also be induced in extracellular bacterial infections, including *P. aeruginosa* (288, 289). IRF3 and TRIF are both critical for the response to *P. aeruginosa* lung infections in mice and are also involved

in type I interferon signaling (290, 291). In the RNA-Seq results for PA103 vs. control, several genes were upregulated that are associated with the type I interferon response, including *Irf1*, *Irf5*, *Irf7*, *TLR7*, and the type I interferon receptor component *Ifnar2*. *Ddx58*, which encodes RIG-I, was also upregulated. RIG-I has been proposed to detect bacterial DNA after it has been transcribed to RNA using RNA polymerase II (288), but the upregulation of *Ddx58* or RIG-I in response to *P. aeruginosa* has not previously been reported. However, the data did not show the differential expression of the genes for IFN-α, IFN-β, TRIF, or IRF3. Nevertheless, it is possible that some of these genes were differentially expressed at an earlier time point.

In conclusion, using IDR-1002 reduced CFUs and inflammation caused by *P. aeruginosa* infection. The RNA-Seq results revealed the differential expression of 4739 genes in the lungs and 1327 genes in the blood in response to *P. aeruginosa* infection, while the treatment of *P. aeruginosa* infections with IDR-1002 revealed a more muted response with only a few hundred DE genes compared to controls. Finally, the combination of IDR-1002 and PA103 compared to PA103 alone indicated 2111 DE genes that were influenced by peptide treatment. These data gave new insights into both *P. aeruginosa* infections and possible mechanisms of IDR-1002 activity. Most importantly, the results in this chapter provided further evidence supporting the use of IDR-1002 as an agent for use against *P. aeruginosa* lung infections.

Chapter 5: Discussion: IDR peptides as novel therapeutics against *P. aeruginosa* lung infections

P. aeruginosa is the most common cause of chronic lung infections in adolescent and adult CF patients, and its colonization is associated with increased illness and death. Although advances have been made in therapies to treat the underlying cause of CF, these treatments are very expensive and are not always covered by public health services, as seen in the United Kingdom with the National Health Service decision in 2016 to not pay for lumacaftor/ivacaftor, the combination drug that targets the most common CFTR mutation, ΔF508, by increasing the production of functional CFTR and CFTR channel potentiation (292). The CFTR mutations targeted by lumacaftor/ivacaftor and ivacaftor alone also account for only a portion of the CFTR mutations causing CF, with more than 1500 mutations identified (293). Therefore, in the immediate future, it will still be necessary to directly target *P. aeruginosa* infections rather than treat the underlying cause. *P. aeruginosa* is also a major cause of pneumonia, particularly in ICU cases, and in COPD. Due to antibiotic resistance, both inherent and acquired, *P. aeruginosa* is difficult to treat, and alternatives to antibiotics are required.

HDPs are naturally occurring peptides that have key roles in fighting microbial infections (171, 294). IDRs are synthetic HDPs that have been designed to have lower toxicity and improved immunomodulatory effects. Although IDRs have shown promise in several infection models, they had not previously been tested against *P. aeruginosa* in vivo. Other synthetic HDPs have shown limited efficacy and/or have issues with toxicity in *P. aeruginosa* in vivo lung infection models (217-220). This thesis examined the potential of IDR peptides against *P. aeruginosa* lung infections, using both an acute model and a model mimicking the alginate-protected state found in chronic *P. aeruginosa* infections, and found that IDR-1002 provided protection against *P. aeruginosa* infection and also suppressed damaging lung inflammation when used after the infection was established. Additionally, the research in this thesis examined the formulation of IDR-1018 in order to decrease aggregation,

providing an important basis for future research into drug delivery systems for IDRs. Finally, this thesis studied the host response to both IDR-1002 and *P. aeruginosa* infections using RNA-Seq and found differences in the inflammatory response in the lungs and whole blood. These RNA-Seq datasets will be valuable for future research questions about the effects of *P. aeruginosa* infection and potential new avenues of treatment.

5.1 IDR-1002 can act as both a prophylactic and therapeutic agent against *P. aeruginosa* lung infections

In Chapter 2, I examined the use of IDR-1002 in countering the effects of *P. aeruginosa* LPS and both live and heat-killed whole bacteria in macrophages and bronchial epithelial cells in vitro. In both types of cells, IDR-1002 did not cause any toxicity, whereas the human HDP LL-37 caused nearly complete cell death at the same molar concentrations. In RAW cells given IDR-1002 along with the LPS, the levels of inflammatory mediators such as IL-6, TNF-α, and MCP-1 were reduced to levels comparable to unstimulated controls. Importantly, this occurred even when IDR-1002 was delivered up to 24 h prior to stimulation or 2 hours post-stimulation. IDR-1002 was also effective at reducing toxicity caused by live *P. aeruginosa* in both macrophages and bronchial epithelial cells. These results were extended to the acute *P. aeruginosa* lung infection model, with IN delivery of IDR-1002 one day prior to infection leading to reductions in CFU counts in the BALF and decreases in IL-6, TNF-α, MCP-1, and KC in the BALF and serum. Notably, the early stages of lung infections in CF have been described as an acute infection, and, furthermore, 80% of CF patients acquire *P. aeruginosa* by their mid-twenties (48). Therefore, the use of an agent such as IDR-1002 could help prevent *P. aeruginosa* infection in this population. However, the research in Chapter 2 focused on a single dose of IDR-1002, whereas prophylactic treatment against *P. aeruginosa* lung infections would require long term administration. An assessment of repeated doses of IDR-1002 should be undertaken to look at effects on toxicity, the immune system, weight, and other parameters such as overall health.

The evaluation of IDR-1002 as a therapeutic also showed encouraging results in the alginate model. The lungs showed less inflammation and there was a significant decrease in IL-6 in the lungs after IDR-1002 delivery compared to mice given only *P. aeruginosa* LESB58. However, the CFU counts were similar to the LESB58 mice. Future experiments should clarify the mechanisms influenced by IDR-1002. It is, however, possible that the protective mechanisms elicited by IDR-1002 in acute infections are ineffective against bacteria encased in alginate. Extending the model for additional days might give the immune system more time to attack the bacteria. Alternatively, IDR-1002 could be paired with an antibiotic. By combining both immunomodulatory and antimicrobial therapies, the risk of the development of antibiotic resistance would be reduced (295).

One area where IDR-1002 did not reduce inflammation was in the response of RAW cells to HKPA103. Heat-killed *P. aeruginosa* is known to contain agonists for TLR2, TLR4, and TLR5 (240). Since IDR-1002 decreased the responses to TLR4 or TLR2 agonists alone, and RAW cells do not express TLR5 (241), it is possible that the lack of response was due to the presence of multiple agonists, or that the HKPA103 was activating an alternative pathway, such as through an NLR. Future experiments should seek to further examine the individual components of HKPA103 and their combinations in the presence of IDR-1002 in order to determine the pathways being activated and the reason for the lack of activity by IDR-1002 in this system.

Overall, the results in Chapter 2 showed that IDR-1002 can reduce inflammation caused by *P. aeruginosa* LPS and live bacteria, and that these results can be translated in vivo in both acute and chronic-like *P. aeruginosa* lung infections. IDR-1002 also reduced bacterial loads in the acute model and bacterial-induced toxicity in vitro. Furthermore, no toxicity from the peptide was seen in vitro or in vivo, something that has hampered previous work on synthetic HDPs in *P. aeruginosa* lung models. These results provide evidence that IDR peptides could be used as a novel treatment against *P. aeruginosa* lung infections.

5.2 Formulating peptide with HPG reduces aggregation

IDR-1018 is one of the lead IDR drug candidates due to its strong ability to induce chemokines in vitro and protect in vivo in multiple animal models, but its tendency to aggregate hinders its delivery in vivo. In Chapter 2, I focused on using an alternatively designed peptide, IDR-1002, against *P. aeruginosa* lung infections. In Chapter 3, I tested new formulations of IDR-1018 that were designed to limit aggregation while retaining or even improving immunomodulatory function. Without formulation, IDR-1018 showed a dose response in reducing CFU burden and IL-6, TNF-α, MCP-1, and KC that was then abrogated at higher doses due to peptide aggregation. Combining IDR-1018 with HPG reduced LPS-induced inflammation in vitro and also trended towards a reduction in inflammatory cytokines in vivo, although the *P. aeruginosa* CFU burden was not reduced.

Despite these mixed results in terms of efficacy, the data in Chapter 3 are an important basis for future peptide formulation studies. Although many peptide-based drugs have been approved, they often require IV delivery due to low bioavailability (296). If the peptide aggregates, as with IDR-1018, then IV delivery is difficult. However, drugs would ideally be delivered orally or intranasally, as these do not require injections and thus improve patient compliance (297). While oral administration is traditional, the use of nasal drug delivery has increased within the past two decades and is a promising route of administration for respiratory infections (298). However, this route of delivery is challenging due to low nasal absorption, especially for substances with high molecular weights, as well as mucociliary clearance (298). The results with HPG270/1018 are therefore encouraging, since HPG has a high molecular weight and yet the cytokine and chemokine results in vivo indicated that some IDR-1018 activity was retained, while also showing reduced aggregation of the peptide. Going forward, making minor changes to the HPG structure, such as modestly decreasing the carboxylation, may improve efficacy. Alternatively, other polymers could be used, with chitosan a possible candidate as it is already being used in numerous applications and has been formulated for nasal drug delivery systems (297-299). Other options include nanoparticles and liposomes (299-302). Ultimately, the

formulation candidate should be tested in both the acute and alginate *P. aeruginosa* lung models to ensure its efficacy under both scenarios. Finally, it is also possible that IDR-1018 aggregation is necessary for its immunomodulatory function, and that other peptides, such as IDR-1002, also aggregate but at levels that would require more powerful microscopy, such as transmission electron or atomic force microscopy, to be visible. Evaluating the role of peptide aggregation in immunomodulatory function is therefore another area that should be examined.

5.3 *P. aeruginosa* causes widespread inflammation in the lungs and blood, which is reduced by IDR-1002

In Chapter 2, I showed that IDR-1002 is effective against *P. aeruginosa* lung infections. In Chapter 4, the goal was to further examine the effects of IDR-1002, *P. aeruginosa*, and the combination of IDR-1002 and *P. aeruginosa* on the host. This was done using RNA-Seq, which had not previously been used on animals given IDR-1002. In addition, the RNA-Seq of samples from an in vivo *P. aeruginosa* lung infection provided the first detailed analysis of the results of infection in both lungs and blood simultaneously by this organism in a model that is arguably relevant to human infections.

The results for *P. aeruginosa* infection indicated the induction of multiple pathways associated with inflammation and infection. There were also DE genes and pathways that have not previously been associated with *P. aeruginosa* infection and these represent potential new targets for treating the inflammation associated with bacterial infection

The samples given IDR-1002 alone had only two DE genes in the lungs and zero in the blood when compared to controls. However, in infected mice that had been given IDR-1002, there were strong reductions in inflammatory genes and pathways, as well as in CFU counts and cytokines and chemokines. Interestingly, the treated mice showed the downregulation of several genes related to lymphocyte activation and MHC class II expression when compared to the control mice, and these

genes were not seen for the PA103 mice compared to the control mice. There were also overrepresented pathways found in the upregulated genes involving regulation of mast cells and in the downregulated genes for MHC class II antigen presentation and several pathways involving lymphocyte activation or differentiation. These results indicate that one area for further study would be the effect of IDR-1002 on specific cell populations, particularly mast cells and lymphocytes. While pathways associated with T and B cells were found in the treatment samples, it would also be of interest to look at other lymphocyte populations such as NK cells and other cells now classified as innate lymphoid cells (303).

The next steps should be confirming RNA-Seq results at both the transcript and protein levels, then moving on to examine the role of pathways or individual genes in *P. aeruginosa* infection and IDR-1002 activities. It would also be of interest to conduct further analysis on the RNA-Seq data to look at markers to determine which cell types were present in the blood and the lungs and how these populations contributed to the DE genes. Additionally, using another method of analysis that does not rely on existing gene ontology information, but rather looks at co-expression data to discover modules and to infer new interactions, would be useful for finding potential new treatments for *P. aeruginosa* infection.

Additional RNA-Seq could also be implemented to examine the response of both the host and the pathogen simultaneously, to look at responses over time for both IDR-1002 and *P. aeruginosa,* to find any changes to the microbiome associated with infection or IDR-1002 treatment, or to look at the effects of polymicrobial lung infection. Finally, while mouse models are a cost-effective and acceptable approach for in vivo evaluation of the IDRs, it would also be useful to evaluate their efficacy in lung infection models that more closely resemble human disease. In particular, lung models in pigs and ferrets are more representative of conditions such as CF because the distribution of submucosal glands and the production of excessive mucus mimic human disease (304). Evaluating

IDR activity in the presence of the thick mucus found in pig or ferret models would help determine if IDRs can be efficacious in human lung infections.

5.4 Concluding remarks

The rise of MDR strains of *P. aeruginosa* necessitates the use of alternatives to antibiotics to treat infections. HDPs are promising anti-infective agents due to their actions on the immune system rather than targeting the bacteria directly. However, the use of HDPs found in nature is often limited by their toxicity. In this thesis, I showed that IDR-1002, a synthetic HDP with a sequence derived from the bovine HDP bactenecin, is a promising prophylactic and therapeutic agent that can decrease both the number of bacteria and the inflammation caused by a *P. aeruginosa* lung infection. In addition, I also showed how different formulations and solvents can affect IDR-1018 aggregation, immunomodulatory properties, and toxicity, and how this translates to in vivo results. Finally, I also looked at the effects of both *P. aeruginosa* and IDR-1002 on the transcriptome of the host and found potential new targets involved in the response to *P. aeruginosa* infection as well as new insights into the mechanisms of action of IDR-1002. In conclusion, these results provide valuable new evidence regarding the potential use of IDRs as agents against *P. aeruginosa* lung infections and will help inform future work on the goal of translating IDRs to human medicine.

References

1. Griffith, S. J., C. Nathan, R. K. Selander, W. Chamberlin, S. Gordon, S. Kabins, and R. A. Weinstein. 1989. The epidemiology of *Pseudomonas aeruginosa* in oncology patients in a general hospital. *J Infect Dis* 160:1030-1036.
2. Erb-Downward, J. R., D. L. Thompson, M. K. Han, C. M. Freeman, L. McCloskey, L. A. Schmidt, V. B. Young, G. B. Toews, J. L. Curtis, B. Sundaram, F. J. Martinez, and G. B. Huffnagle. 2011. Analysis of the lung microbiome in the "healthy" smoker and in COPD. *PLoS One* 6:e16384.
3. CDC. 2013. Antibiotic resistance threats in the United States.
4. Gellatly, S. L., and R. E. Hancock. 2013. *Pseudomonas aeruginosa*: new insights into pathogenesis and host defenses. *Pathog Dis* 67:159-173.
5. Jimenez, P. N., G. Koch, J. A. Thompson, K. B. Xavier, R. H. Cool, and W. J. Quax. 2012. The multiple signaling systems regulating virulence in *Pseudomonas aeruginosa*. *Microbiol Mol Biol Rev* 76:46-65.
6. Bleves, S., V. Viarre, R. Salacha, G. P. Michel, A. Filloux, and R. Voulhoux. 2010. Protein secretion systems in *Pseudomonas aeruginosa*: A wealth of pathogenic weapons. *Int J Med Microbiol* 300:534-543.
7. Meyer, J. M., A. Neely, A. Stintzi, C. Georges, and I. A. Holder. 1996. Pyoverdin is essential for virulence of *Pseudomonas aeruginosa*. *Infect Immun* 64:518-523.
8. Lau, G. W., D. J. Hassett, H. Ran, and F. Kong. 2004. The role of pyocyanin in *Pseudomonas aeruginosa* infection. *Trends Mol Med* 10:599-606.
9. Lau, G. W., H. Ran, F. Kong, D. J. Hassett, and D. Mavrodi. 2004. *Pseudomonas aeruginosa* pyocyanin is critical for lung infection in mice. *Infect Immun* 72:4275-4278.
10. Rada, B., and T. L. Leto. 2013. Pyocyanin effects on respiratory epithelium: relevance in *Pseudomonas aeruginosa* airway infections. *Trends Microbiol* 21:73-81.
11. Brandel, J., N. Humbert, M. Elhabiri, I. J. Schalk, G. L. Mislin, and A. M. Albrecht-Gary. 2012. Pyochelin, a siderophore of *Pseudomonas aeruginosa*: physicochemical characterization of the iron(III), copper(II) and zinc(II) complexes. *Dalton Trans* 41:2820-2834.
12. Michalska, M., and P. Wolf. 2015. *Pseudomonas* Exotoxin A: optimized by evolution for effective killing. *Front Microbiol* 6.
13. Beckert, U., S. Wolter, C. Hartwig, H. Bähre, V. Kaever, D. Ladant, D. W. Frank, and R. Seifert. 2014. ExoY from *Pseudomonas aeruginosa* is a nucleotidyl cyclase with preference for cGMP and cUMP formation. *Biochem Biophys Res Commun* 450:870-874.
14. Galle, M., I. Carpentier, and R. Beyaert. 2012. Structure and function of the Type III secretion system of *Pseudomonas aeruginosa*. *Curr Protein Pept Sci* 13:831-842.
15. Sawa, T. 2014. The molecular mechanism of acute lung injury caused by *Pseudomonas aeruginosa*: from bacterial pathogenesis to host response. *J Intensive Care* 2:10.
16. Finck-Barbancon, V., J. Goranson, L. Zhu, T. Sawa, J. P. Wiener-Kronish, S. M. Fleiszig, C. Wu, L. Mende-Mueller, and D. W. Frank. 1997. ExoU expression by *Pseudomonas aeruginosa* correlates with acute cytotoxicity and epithelial injury. *Mol Microbiol* 25:547-557.
17. Shaver, C. M., and A. R. Hauser. 2004. Relative contributions of *Pseudomonas aeruginosa* ExoU, ExoS, and ExoT to virulence in the lung. *Infect Immun* 72:6969-6977.
18. Kamath, S., V. Kapatral, and A. M. Chakrabarty. 1998. Cellular function of elastase in *Pseudomonas aeruginosa*: role in the cleavage of nucleoside diphosphate kinase and in alginate synthesis. *Mol Microbiol* 30:933-941.
19. Kuang, Z., Y. Hao, B. E. Walling, J. L. Jeffries, D. E. Ohman, and G. W. Lau. 2011. *Pseudomonas aeruginosa* elastase provides an escape from phagocytosis by degrading the pulmonary surfactant protein-A. *PLoS One* 6:e27091.

20. Lau, G. W., D. J. Hassett, and B. E. Britigan. 2005. Modulation of lung epithelial functions by *Pseudomonas aeruginosa*. *Trends Microbiol* 13:389-397.
21. Feldman, M., R. Bryan, S. Rajan, L. Scheffler, S. Brunnert, H. Tang, and A. Prince. 1998. Role of flagella in pathogenesis of *Pseudomonas aeruginosa* pulmonary infection. *Infect Immun* 66:43-51.
22. Kazmierczak, B. I., M. Schniederberend, and R. Jain. 2015. Cross-regulation of *Pseudomonas* motility systems: the intimate relationship between flagella, pili and virulence. *Curr Opin Microbiol* 28:78-82.
23. Montie, T. C., R. C. Craven, and I. A. Holder. 1982. Flagellar preparations from *Pseudomonas aeruginosa*: isolation and characterization. *Infect Immun* 35:281-288.
24. Burrows, L. L. 2012. *Pseudomonas aeruginosa* twitching motility: type IV pili in action. *Annu Rev Microbiol* 66:493-520.
25. Bjarnsholt, T., M. Alhede, S. R. Eickhardt-Sorensen, C. Moser, M. Kuhl, P. O. Jensen, and N. Hoiby. 2013. The in vivo biofilm. *Trends Microbiol* 21:466-474.
26. Donlan, R. M., and J. W. Costerton. 2002. Biofilms: survival mechanisms of clinically relevant microorganisms. *Clin Microbiol Rev* 15:167-193.
27. Fuxman Bass, J. I., D. M. Russo, M. L. Gabelloni, J. R. Geffner, M. Giordano, M. Catalano, A. Zorreguieta, and A. S. Trevani. 2010. Extracellular DNA: a major proinflammatory component of *Pseudomonas aeruginosa* biofilms. *J Immunol* 184:6386-6395.
28. Huse, H. K., T. Kwon, J. E. Zlosnik, D. P. Speert, E. M. Marcotte, and M. Whiteley. 2013. *Pseudomonas aeruginosa* enhances production of a non-alginate exopolysaccharide during long-term colonization of the cystic fibrosis lung. *PLoS One* 8:e82621.
29. Colvin, K. M., Y. Irie, C. S. Tart, R. Urbano, J. C. Whitney, C. Ryder, P. L. Howell, D. J. Wozniak, and M. R. Parsek. 2012. The Pel and Psl polysaccharides provide *Pseudomonas aeruginosa* structural redundancy within the biofilm matrix. *Environ Microbiol* 14.
30. Lee, K. Y., and D. J. Mooney. 2012. Alginate: properties and biomedical applications. *Prog Polym Sci* 37:106-126.
31. Boyd, A., and A. M. Chakrabarty. 1995. *Pseudomonas aeruginosa* biofilms: role of the alginate exopolysaccharide. *J Ind Microbiol* 15:162-168.
32. Lebeaux, D., A. Chauhan, O. Rendueles, and C. Beloin. 2013. From in vitro to in vivo models of bacterial biofilm-related infections. *Pathogens* 2:288-356.
33. de Kievit, T. R. 2009. Quorum sensing in *Pseudomonas aeruginosa* biofilms. *Environ Microbiol* 11:279-288.
34. Balasubramanian, D., L. Schneper, H. Kumari, and K. Mathee. 2013. A dynamic and intricate regulatory network determines *Pseudomonas aeruginosa* virulence. *Nucleic Acids Res* 41:1-20.
35. Livermore, D. M. 2002. Multiple mechanisms of antimicrobial resistance in *Pseudomonas aeruginosa*: our worst nightmare? *Clin Infect Dis* 34:634-640.
36. Breidenstein, E. B., C. de la Fuente-Nunez, and R. E. Hancock. 2011. *Pseudomonas aeruginosa*: all roads lead to resistance. *Trends Microbiol* 19:419-426.
37. Fernandez, L., E. B. Breidenstein, and R. E. Hancock. 2011. Creeping baselines and adaptive resistance to antibiotics. *Drug Resist Updat* 14:1-21.
38. Strateva, T., and D. Yordanov. 2009. *Pseudomonas aeruginosa* - a phenomenon of bacterial resistance. *J Med Microbiol* 58:1133-1148.
39. Gaynes, R., and J. R. Edwards. 2005. Overview of nosocomial infections caused by gram-negative bacilli. *Clin Infect Dis* 41:848-854.
40. Mittal, R., S. Aggarwal, S. Sharma, S. Chhibber, and K. Harjai. 2009. Urinary tract infections caused by *Pseudomonas aeruginosa*: a minireview. *J Infect Public Health* 2:101-111.

41. Mayhall, C. G. 2003. The epidemiology of burn wound infections: then and now. *Clin Infect Dis* 37:543-550.
42. Sadikot, R. T., T. S. Blackwell, J. W. Christman, and A. S. Prince. 2005. Pathogen-host interactions in *Pseudomonas aeruginosa* pneumonia. *Am J Respir Crit Care Med* 171:1209-1223.
43. Murphy, T. F. 2009. *Pseudomonas aeruginosa* in adults with chronic obstructive pulmonary disease. *Curr Opin Pulm Med* 15:138-142.
44. Folkesson, A., L. Jelsbak, L. Yang, H. K. Johansen, O. Ciofu, N. Hoiby, and S. Molin. 2012. Adaptation of *Pseudomonas aeruginosa* to the cystic fibrosis airway: an evolutionary perspective. *Nat Rev Microbiol* 10:841-851.
45. Berkebile, A. R., and P. B. McCray, Jr. 2014. Effects of airway surface liquid pH on host defense in cystic fibrosis. *Int J Biochem Cell Biol* 52:124-129.
46. Hartl, D., A. Gaggar, E. Bruscia, A. Hector, V. Marcos, A. Jung, C. Greene, G. McElvaney, M. Mall, and G. Doring. 2012. Innate immunity in cystic fibrosis lung disease. *J Cyst Fibros* 11:363-382.
47. Ehre, C., C. Ridley, and D. J. Thornton. 2014. Cystic fibrosis: an inherited disease affecting mucin-producing organs. *Int J Biochem Cell Biol* 52:136-145.
48. FitzSimmons, S. C. 1993. The changing epidemiology of cystic fibrosis. *J Pediatr* 122:1-9.
49. Li, Z., M. R. Kosorok, P. M. Farrell, A. Laxova, S. E. West, C. G. Green, J. Collins, M. J. Rock, and M. L. Splaingard. 2005. Longitudinal development of mucoid *Pseudomonas aeruginosa* infection and lung disease progression in children with cystic fibrosis. *JAMA* 293:581-588.
50. Emerson, J., M. Rosenfeld, S. McNamara, B. Ramsey, and R. L. Gibson. 2002. *Pseudomonas aeruginosa* and other predictors of mortality and morbidity in young children with cystic fibrosis. *Pediatr Pulmonol* 34:91-100.
51. Parameswaran, G. I., and S. Sethi. 2012. *Pseudomonas* infection in chronic obstructive pulmonary disease. *Future Microbiol* 7:1129-1132.
52. Organization, W. H. November 2016. Chronic obstructive pulmonary disease (COPD).
53. Rotstein, C., G. Evans, A. Born, R. Grossman, R. B. Light, S. Magder, B. McTaggart, K. Weiss, and G. G. Zhanel. 2008. Clinical practice guidelines for hospital-acquired pneumonia and ventilator-associated pneumonia in adults. *Can J Infect Dis Med Microbiol* 19:19-53.
54. Lynch, J. P., 3rd. 2001. Hospital-acquired pneumonia: risk factors, microbiology, and treatment. *Chest* 119:373S-384S.
55. Widdicombe, J. 2002. Regulation of the depth and composition of airway surface liquid. *J Anat* 201:313-318.
56. Hiemstra, P. S., G. D. Amatngalim, A. M. van der Does, and C. Taube. 2016. Antimicrobial peptides and innate lung defenses: role in infectious and noninfectious lung diseases and therapeutic applications. *Chest* 149:545-551.
57. Williams, B. J., J. Dehnbostel, and T. S. Blackwell. 2010. *Pseudomonas aeruginosa*: host defence in lung diseases. *Respirology* 15:1037-1056.
58. Campodonico, V. L., M. Gadjeva, C. Paradis-Bleau, A. Uluer, and G. B. Pier. 2008. Airway epithelial control of *Pseudomonas aeruginosa* infection in cystic fibrosis. *Trends Mol Med* 14:120-133.
59. Davies, J. C., and D. Bilton. 2009. Bugs, biofilms, and resistance in cystic fibrosis. *Respir Care* 54:628-640.
60. Thorley, A. J., and T. D. Tetley. 2007. Pulmonary epithelium, cigarette smoke, and chronic obstructive pulmonary disease. *Int J Chron Obstruct Pulmon Dis* 2:409-428.

61. Holtzman, M. J., D. E. Byers, J. Alexander-Brett, and X. Wang. 2014. The role of airway epithelial cells and innate immune cells in chronic respiratory disease. *Nat Rev Immunol* 14:686-698.
62. Kawai, T., and S. Akira. 2010. The role of pattern-recognition receptors in innate immunity: update on Toll-like receptors. *Nat Immunol* 11:373-384.
63. Blohmke, C. J., J. Park, A. F. Hirschfeld, R. E. Victor, J. Schneiderman, D. Stefanowicz, M. A. Chilvers, P. R. Durie, M. Corey, J. Zielenski, R. Dorfman, A. J. Sandford, D. Daley, and S. E. Turvey. 2010. TLR5 as an anti-inflammatory target and modifier gene in cystic fibrosis. *J Immunol* 185:7731-7738.
64. Zhang, Z., J. P. Louboutin, D. J. Weiner, J. B. Goldberg, and J. M. Wilson. 2005. Human airway epithelial cells sense *Pseudomonas aeruginosa* infection via recognition of flagellin by Toll-like receptor 5. *Infect Immun* 73:7151-7160.
65. Blohmke, C. J., R. E. Victor, A. F. Hirschfeld, I. M. Elias, D. G. Hancock, C. R. Lane, A. G. Davidson, P. G. Wilcox, K. D. Smith, J. Overhage, R. E. Hancock, and S. E. Turvey. 2008. Innate immunity mediated by TLR5 as a novel antiinflammatory target for cystic fibrosis lung disease. *J Immunol* 180:7764-7773.
66. Power, M. R., Y. Peng, E. Maydanski, J. S. Marshall, and T. J. Lin. 2004. The development of early host response to *Pseudomonas aeruginosa* lung infection is critically dependent on myeloid differentiation factor 88 in mice. *J Biol Chem* 279:49315-49322.
67. Epelman, S., D. Stack, C. Bell, E. Wong, G. G. Neely, S. Krutzik, K. Miyake, P. Kubes, L. D. Zbytnuik, L. L. Ma, X. Xie, D. E. Woods, and C. H. Mody. 2004. Different domains of *Pseudomonas aeruginosa* exoenzyme S activate distinct TLRs. *J Immunol* 173:2031-2040.
68. Travassos, L. H., L. A. Carneiro, S. E. Girardin, I. G. Boneca, R. Lemos, M. T. Bozza, R. C. Domingues, A. J. Coyle, J. Bertin, D. J. Philpott, and M. C. Plotkowski. 2005. Nod1 participates in the innate immune response to *Pseudomonas aeruginosa*. *J Biol Chem* 280:36714-36718.
69. Franchi, L., J. Stoolman, T. D. Kanneganti, A. Verma, R. Ramphal, and G. Nunez. 2007. Critical role for Ipaf in *Pseudomonas aeruginosa*-induced caspase-1 activation. *Eur J Immunol* 37:3030-3039.
70. Zhao, Y., J. Yang, J. Shi, Y. N. Gong, Q. Lu, H. Xu, L. Liu, and F. Shao. 2011. The NLRC4 inflammasome receptors for bacterial flagellin and type III secretion apparatus. *Nature* 477:596-600.
71. Sutterwala, F. S., L. A. Mijares, L. Li, Y. Ogura, B. I. Kazmierczak, and R. A. Flavell. 2007. Immune recognition of *Pseudomonas aeruginosa* mediated by the IPAF/NLRC4 inflammasome. *J Exp Med* 204:3235-3245.
72. Saiman, L., and A. Prince. 1993. *Pseudomonas aeruginosa* pili bind to asialoGM1 which is increased on the surface of cystic fibrosis epithelial cells. *J Clin Invest* 92:1875-1880.
73. Adamo, R., S. Sokol, G. Soong, M. I. Gomez, and A. Prince. 2004. *Pseudomonas aeruginosa* flagella activate airway epithelial cells through asialoGM1 and toll-like receptor 2 as well as toll-like receptor 5. *Am J Respir Cell Mol Biol* 30:627-634.
74. Maurer, S., G. H. Wabnitz, N. A. Kahle, S. Stegmaier, B. Prior, T. Giese, M. M. Gaida, Y. Samstag, and G. M. Hänsch. 2015. Tasting *Pseudomonas aeruginosa* Biofilms: Human Neutrophils Express the Bitter Receptor T2R38 as Sensor for the Quorum Sensing Molecule N-(3-Oxododecanoyl)-l-Homoserine Lactone. *Front Immunol* 6.
75. Heale, J. P., A. J. Pollard, R. W. Stokes, D. Simpson, A. Tsang, B. Massing, and D. P. Speert. 2001. Two distinct receptors mediate nonopsonic phagocytosis of different strains of *Pseudomonas aeruginosa*. *J Infect Dis* 183:1214-1220.
76. Oeckinghaus, A., M. S. Hayden, and S. Ghosh. 2011. Crosstalk in NF-kappaB signaling pathways. *Nat Immunol* 12:695-708.

77. Pahl, H. L. 1999. Activators and target genes of Rel/NF-kappaB transcription factors. *Oncogene* 18:6853-6866.
78. Lavoie, E. G., T. Wangdi, and B. I. Kazmierczak. 2011. Innate immune responses to *Pseudomonas aeruginosa* infection. *Microbes Infect* 13:1133-1145.
79. Kelly, E., C. M. Greene, and N. G. McElvaney. 2008. Targeting neutrophil elastase in cystic fibrosis. *Expert Opin Ther Targets* 12:145-157.
80. Park, P. W., G. B. Pier, M. T. Hinkes, and M. Bernfield. 2001. Exploitation of syndecan-1 shedding by *Pseudomonas aeruginosa* enhances virulence. *Nature* 411:98-102.
81. Schaber, J. A., W. J. Triffo, S. J. Suh, J. W. Oliver, M. C. Hastert, J. A. Griswold, M. Auer, A. N. Hamood, and K. P. Rumbaugh. 2007. *Pseudomonas aeruginosa* forms biofilms in acute infection independent of cell-to-cell signaling. *Infect Immun* 75:3715-3721.
82. Cullen, L., and S. McClean. 2015. Bacterial adaptation during chronic respiratory infections. *Pathogens* 4:66-89.
83. Hancock, R. E., L. M. Mutharia, L. Chan, R. P. Darveau, D. P. Speert, and G. B. Pier. 1983. *Pseudomonas aeruginosa* isolates from patients with cystic fibrosis: a class of serum-sensitive, nontypable strains deficient in lipopolysaccharide O side chains. *Infect Immun* 42:170-177.
84. Sousa, A. M., and M. O. Pereira. 2014. *Pseudomonas aeruginosa* diversification during infection development in cystic fibrosis lungs—a review. *Pathogens* 3:680-703.
85. Birnbaum, J., F. M. Kahan, H. Kropp, and J. S. MacDonald. 1985. Carbapenems, a new class of beta-lactam antibiotics. Discovery and development of imipenem/cilastatin. *Am J Med* 78:3-21.
86. Sader, H. S., M. R. Jacobs, and T. R. Fritsche. 2007. Review of the spectrum and potency of orally administered cephalosporins and amoxicillin/clavulanate. *Diagn Microbiol Infect Dis* 57:5S-12S.
87. Kirkby, S., K. Novak, and K. McCoy. 2011. Aztreonam (for inhalation solution) for the treatment of chronic lung infections in patients with cystic fibrosis: an evidence-based review. *Core Evid* 6:59-66.
88. Zobell, J. T., C. D. Waters, D. C. Young, C. Stockmann, K. Ampofo, C. M. Sherwin, and M. G. Spigarelli. 2013. Optimization of anti-pseudomonal antibiotics for cystic fibrosis pulmonary exacerbations: II. cephalosporins and penicillins. *Pediatr Pulmonol* 48:107-122.
89. Kong, K. F., L. Schneper, and K. Mathee. 2010. Beta-lactam antibiotics: from antibiosis to resistance and bacteriology. *APMIS* 118:1-36.
90. Drawz, S. M., and R. A. Bonomo. 2010. Three decades of β-lactamase inhibitors. *Clin Microbiol Rev* 23:160-201.
91. Page, M. G., and J. Heim. 2009. Prospects for the next anti-*Pseudomonas* drug. *Curr Opin Pharmacol* 9:558-565.
92. Poole, K. 2005. Aminoglycoside resistance in *Pseudomonas aeruginosa*. *Antimicrob Agents Chemother* 49:479-487.
93. Rossolini, G. M., and E. Mantengoli. 2005. Treatment and control of severe infections caused by multiresistant *Pseudomonas aeruginosa*. *Clin Microbiol Infect* 11 Suppl 4:17-32.
94. Cheer, S. M., J. Waugh, and S. Noble. 2003. Inhaled tobramycin (TOBI): a review of its use in the management of *Pseudomonas aeruginosa* infections in patients with cystic fibrosis. *Drugs* 63:2501-2520.
95. Selimoglu, E. 2007. Aminoglycoside-induced ototoxicity. *Curr Pharm Des* 13:119-126.
96. Zhanel, G. G., K. Ennis, L. Vercaigne, A. Walkty, A. S. Gin, J. Embil, H. Smith, and D. J. Hoban. 2002. A critical review of the fluoroquinolones: focus on respiratory infections. *Drugs* 62:13-59.
97. Zhanel, G. G., A. Walkty, L. Vercaigne, J. A. Karlowsky, J. Embil, A. S. Gin, and D. J. Hoban. 1999. The new fluoroquinolones: a critical review. *Can J Infect Dis* 10:207-238.

98. Falagas, M. E., and S. K. Kasiakou. 2005. Colistin: the revival of polymyxins for the management of multidrug-resistant gram-negative bacterial infections. *Clin Infect Dis* 40:1333-1341.
99. Bergen, P. J., J. Li, C. R. Rayner, and R. L. Nation. 2006. Colistin methanesulfonate is an inactive prodrug of colistin against *Pseudomonas aeruginosa*. *Antimicrob Agents Chemother* 50:1953-1958.
100. Langton Hewer, S. C., and A. R. Smyth. 2014. Antibiotic strategies for eradicating *Pseudomonas aeruginosa* in people with cystic fibrosis. *Cochrane Database Syst Rev*:CD004197.
101. Waters, V., and A. Smyth. 2015. Cystic fibrosis microbiology: advances in antimicrobial t herapy. *J Cyst Fibros* 14:551-560.
102. Martinez-Solano, L., M. D. Macia, A. Fajardo, A. Oliver, and J. L. Martinez. 2008. Chronic *Pseudomonas aeruginosa* infection in chronic obstructive pulmonary disease. *Clin Infect Dis* 47:1526-1533.
103. Peleg, A. Y., and D. C. Hooper. 2010. Hospital-acquired infections due to gram-negative bacteria. *N Engl J Med* 362:1804-1813.
104. Aloush, V., S. Navon-Venezia, Y. Seigman-Igra, S. Cabili, and Y. Carmeli. 2006. Multidrug-resistant *Pseudomonas aeruginosa*: risk factors and clinical impact. *Antimicrob Agents Chemother* 50:43-48.
105. Obritsch, M. D., D. N. Fish, R. MacLaren, and R. Jung. 2005. Nosocomial infections due to multidrug-resistant *Pseudomonas aeruginosa*: epidemiology and treatment options. *Pharmacotherapy* 25:1353-1364.
106. Lewis, K. 2013. Platforms for antibiotic discovery. *Nat Rev Drug Discov* 12:371-387.
107. Andriole, V. T. 2005. The quinolones: past, present, and future. *Clin Infect Dis* 41 Suppl 2:S113-119.
108. Ling, L. L., T. Schneider, A. J. Peoples, A. L. Spoering, I. Engels, B. P. Conlon, A. Mueller, T. F. Schaberle, D. E. Hughes, S. Epstein, M. Jones, L. Lazarides, V. A. Steadman, D. R. Cohen, C. R. Felix, K. A. Fetterman, W. P. Millett, A. G. Nitti, A. M. Zullo, C. Chen, and K. Lewis. 2015. A new antibiotic kills pathogens without detectable resistance. *Nature* 517:455-459.
109. Hraiech, S., F. Bregeon, and J. M. Rolain. 2015. Bacteriophage-based therapy in cystic fibrosis-associated *Pseudomonas aeruginosa* infections: rationale and current status. *Drug Des Devel Ther* 9:3653-3663.
110. Alemayehu, D., P. G. Casey, O. McAuliffe, C. M. Guinane, J. G. Martin, F. Shanahan, A. Coffey, R. P. Ross, and C. Hill. 2012. Bacteriophages phiMR299-2 and phiNH-4 can eliminate *Pseudomonas aeruginosa* in the murine lung and on cystic fibrosis lung airway cells. *MBio* 3:e00029-00012.
111. Sharma, G., S. Rao, A. Bansal, S. Dang, S. Gupta, and R. Gabrani. 2014. *Pseudomonas aeruginosa* biofilm: potential therapeutic targets. *Biologicals* 42:1-7.
112. Di Luca, M., G. Maccari, and R. Nifosi. 2014. Treatment of microbial biofilms in the post-antibiotic era: prophylactic and therapeutic use of antimicrobial peptides and their design by bioinformatics tools. *Pathog Dis* 70:257-270.
113. Priebe, G. P., and J. B. Goldberg. 2014. Vaccines for *Pseudomonas aeruginosa*: a long and winding road. *Expert Rev Vaccines* 13:507-519.
114. Johansen, H. K., and P. C. Gotzsche. 2015. Vaccines for preventing infection with *Pseudomonas aeruginosa* in cystic fibrosis. *Cochrane Database Syst Rev*:CD001399.
115. Doring, G., and G. B. Pier. 2008. Vaccines and immunotherapy against *Pseudomonas aeruginosa*. *Vaccine* 26:1011-1024.

116. Doring, G., and F. Dorner. 1997. A multicenter vaccine trial using the *Pseudomonas aeruginosa* flagella vaccine IMMUNO in patients with cystic fibrosis. *Behring Inst Mitt*:338-344.
117. Schwab, I., and F. Nimmerjahn. 2013. Intravenous immunoglobulin therapy: how does IgG modulate the immune system? *Nat Rev Immunol* 13:176-189.
118. Razaghi, A., L. Owens, and K. Heimann. 2016. Review of the recombinant human interferon gamma as an immunotherapeutic: Impacts of production platforms and glycosylation. *J Biotechnol* 240:48-60.
119. Dale, D. C. 2002. Colony-stimulating factors for the management of neutropenia in cancer patients. *Drugs* 62 Suppl 1:1-15.
120. Walsh, T. J., E. J. Anaissie, D. W. Denning, R. Herbrecht, D. P. Kontoyiannis, K. A. Marr, V. A. Morrison, B. H. Segal, W. J. Steinbach, D. A. Stevens, J. A. van Burik, J. R. Wingard, and T. F. Patterson. 2008. Treatment of aspergillosis: clinical practice guidelines of the Infectious Diseases Society of America. *Clin Infect Dis* 46:327-360.
121. Schulte, W., J. Bernhagen, and R. Bucala. 2013. Cytokines in sepsis: potent immunoregulators and potential therapeutic targets--an updated view. *Mediators Inflamm* 2013:165974.
122. Jenssen, H., P. Hamill, and R. E. W. Hancock. 2006. Peptide antimicrobial agents. *Clin Microbiol Rev* 19:491-511.
123. Wuerth, K. C., A. L. Hilchie, K. L. Brown, and R. E. W. Hancock. 2013. Host defence (antimicrobial) peptides and proteins. *www.els.net*. DOI: 10.1002/9780470015902.a0001212.pub3.
124. Wang, G. 2014. Human antimicrobial peptides and proteins. *Pharmaceuticals (Basel)* 7:545-594.
125. Lee, C. C., Y. Sun, S. Qian, and H. W. Huang. 2011. Transmembrane pores formed by human antimicrobial peptide LL-37. *Biophys J* 100:1688-1696.
126. Hancock, R. E. W., and H.-G. Sahl. 2006. Antimicrobial and host-defense peptides as new anti-infective therapeutic strategies. *Nature Biotechnology* 24:1551-1557.
127. Bals, R., X. Wang, M. Zasloff, and J. M. Wilson. 1998. The peptide antibiotic LL-37/hCAP-18 is expressed in epithelia of the human lung where it has broad antimicrobial activity at the airway surface. *Proc Natl Acad Sci U S A* 95:9541-9546.
128. Nguyen, L. T., J. K. Chau, N. A. Perry, L. de Boer, S. A. J. Zaat, and H. J. Vogel. 2010. Serum Stabilities of Short Tryptophan- and Arginine-Rich Antimicrobial Peptide Analogs. *PLoS One* 5.
129. Turner, J., Y. Cho, N. N. Dinh, A. J. Waring, and R. I. Lehrer. 1998. Activities of LL-37, a cathelin-associated antimicrobial peptide of human neutrophils. *Antimicrob Agents Chemother* 42:2206-2214.
130. Abou Alaiwa, M. H., L. R. Reznikov, N. D. Gansemer, K. A. Sheets, A. R. Horswill, D. A. Stoltz, J. Zabner, and M. J. Welsh. 2014. pH modulates the activity and synergism of the airway surface liquid antimicrobials beta-defensin-3 and LL-37. *Proc Natl Acad Sci U S A* 111:18703-18708.
131. Bals, R., X. Wang, Z. Wu, T. Freeman, V. Bafna, M. Zasloff, and J. M. Wilson. 1998. Human beta-defensin 2 is a salt-sensitive peptide antibiotic expressed in human lung. *J Clin Invest* 102:874-880.
132. Garcia, J. R., A. Krause, S. Schulz, F. J. Rodriguez-Jimenez, E. Kluver, K. Adermann, U. Forssmann, A. Frimpong-Boateng, R. Bals, and W. G. Forssmann. 2001. Human beta-defensin 4: a novel inducible peptide with a specific salt-sensitive spectrum of antimicrobial activity. *FASEB J* 15:1819-1821.

133. Goldman, M. J., G. M. Anderson, E. D. Stolzenberg, U. P. Kari, M. Zasloff, and J. M. Wilson. 1997. Human beta-defensin-1 is a salt-sensitive antibiotic in lung that is inactivated in cystic fibrosis. *Cell* 88:553-560.
134. Hilchie, A. L., K. Wuerth, and R. E. Hancock. 2013. Immune modulation by multifaceted cationic host defense (antimicrobial) peptides. *Nat Chem Biol* 9:761-768.
135. Wuerth, K., and R. E. W. Hancock. Submitted. Immunomodulatory activities of cationic host defence peptides and novel therapeutic strategies. In *Antimicrobial Peptides: Discovery, Design and Novel Therapeutic Strategies* G. Wang, ed.
136. Afacan, N. J., A. T. Yeung, O. M. Pena, and R. E. Hancock. 2012. Therapeutic potential of host defense peptides in antibiotic-resistant infections. *Curr Pharm Des* 18:807-819.
137. Bowdish, D. M., D. J. Davidson, and R. E. Hancock. 2005. A re-evaluation of the role of host defence peptides in mammalian immunity. *Curr Protein Pept Sci* 6:35-51.
138. Yeung, A. T. Y., S. L. Gellatly, and R. E. W. Hancock. 2011. Multifunctional cationic host defence peptides and their clinical applications. *Cell. Mol. Life Sci.* 68:2161-2176.
139. Lai, Y., and R. L. Gallo. 2009. AMPed up immunity: how antimicrobial peptides have multiple roles in immune defense. *Trends in Immunol.* 30:131-141.
140. Michels, K., E. Nemeth, T. Ganz, and B. Mehrad. 2015. Hepcidin and host defense against infectious diseases. *PLoS Pathog* 11:e1004998.
141. Krause, A., R. Sillard, B. Kleemeier, E. Kluver, E. Maronde, J. R. Conejo-Garcia, W. G. Forssmann, P. Schulz-Knappe, M. C. Nehls, F. Wattler, S. Wattler, and K. Adermann. 2003. Isolation and biochemical characterization of LEAP-2, a novel blood peptide expressed in the liver. *Protein Sci* 12:143-152.
142. Oudhoff, M. J., J. G. Bolscher, K. Nazmi, H. Kalay, W. van 't Hof, A. V. Amerongen, and E. C. Veerman. 2008. Histatins are the major wound-closure stimulating factors in human saliva as identified in a cell culture assay. *FASEB J* 22:3805-3812.
143. Oudhoff, M. J., M. E. Blaauboer, K. Nazmi, N. Scheres, J. G. Bolscher, and E. C. Veerman. 2010. The role of salivary histatin and the human cathelicidin LL-37 in wound healing and innate immunity. *Biol Chem* 391:541-548.
144. Melino, S., C. Santone, P. Di Nardo, and B. Sarkar. 2014. Histatins: salivary peptides with copper(II)- and zinc(II)-binding motifs: perspectives for biomedical applications. *FEBS J* 281:657-672.
145. Mashaghi, A., A. Marmalidou, M. Tehrani, P. M. Grace, C. Pothoulakis, and R. Dana. 2016. Neuropeptide substance P and the immune response. *Cell Mol Life Sci*.
146. Vollmar, A. M., R. Forster, and R. Schulz. 1997. Effects of atrial natriuretic peptide on phagocytosis and respiratory burst in murine macrophages. *Eur J Pharmacol* 319:279-285.
147. Tsukagoshi, H., Y. Shimizu, T. Kawata, T. Hisada, S. Iwamae, T. Ishizuka, K. Iizuka, K. Dobashi, and M. Mori. 2001. Atrial natriuretic peptide inhibits tumor necrosis factor-alpha production by interferon-gamma-activated macrophages via suppression of p38 mitogen-activated protein kinase and nuclear factor-kappa B activation. *Regul Pept* 99:21-29.
148. Scotland, R. S., M. Cohen, P. Foster, M. Lovell, A. Mathur, A. Ahluwalia, and A. J. Hobbs. 2005. C-type natriuretic peptide inhibits leukocyte recruitment and platelet-leukocyte interactions via suppression of P-selectin expression. *Proc Natl Acad Sci U S A* 102:14452-14457.
149. Potter, L. R., A. R. Yoder, D. R. Flora, L. K. Antos, and D. M. Dickey. 2009. Natriuretic peptides: their structures, receptors, physiologic functions and therapeutic applications. *Handb Exp Pharmacol*:341-366.
150. Eissa, N., and J. E. Ghia. 2015. Immunomodulatory effect of ghrelin in the intestinal mucosa. *Neurogastroenterol Motil* 27:1519-1527.

151. Zanetti, M. 2004. Cathelicidins, multifunctional peptides of the innate immunity. *J. Leukoc. Biol.* 75:39-48.
152. Zanetti, M. 2005. The role of cathelicidins in the innate host defenses of mammals. *Current issues in molecular biology* 7:179-196.
153. Ganz, T. 2003. Defensins: antimicrobial peptides of innate immunity. *Nat Rev Immunol* 3:710-720.
154. Wilmes, M., and H. G. Sahl. 2014. Defensin-based anti-infective strategies. *Int J Med Microbiol* 304:93-99.
155. Fabisiak, A., N. Murawska, and J. Fichna. 2016. LL-37: Cathelicidin-related antimicrobial peptide with pleiotropic activity. *Pharmacol Rep* 68:802-808.
156. Nijnik, A., and R. E. W. Hancock. 2009. The roles of cathelicidin LL-37 in immune defences and novel clinical applications. *Curr Opin Hematol* 16:41-47.
157. Agerberth, B., J. Charo, J. Werr, B. Olsson, F. Idali, L. Lindbom, R. Kiessling, H. Jörnvall, H. Wigzell, and G. H. Gudmundsson. 2000. The human antimicrobial and chemotactic peptides LL-37 and α-defensins are expressed by specific lymphocyte and monocyte populations. *Blood* 96:3086-3093.
158. Sorensen, O. E., P. Follin, A. H. Johnsen, J. Calafat, G. S. Tjabringa, P. S. Hiemstra, and N. Borregaard. 2001. Human cathelicidin, hCAP-18, is processed to the antimicrobial peptide LL-37 by extracellular cleavage with proteinase 3. *Blood* 97:3951-3959.
159. Brown, K. L., G. F. T. Poon, D. Birkenhead, O. M. Pena, R. Falsafi, C. Dahlgren, A. Karlsson, J. Bylund, R. E. W. Hancock, and P. Johnson. 2011. Host defense peptide LL-37 selectively reduces proinflammatory macrophage responses. *J. Immunol.* 186:5497-5505.
160. Amatngalim, G. D., A. Nijnik, P. S. Hiemstra, and R. E. Hancock. 2011. Cathelicidin peptide LL-37 modulates TREM-1 expression and inflammatory responses to microbial compounds. *Inflammation* 34:412-425.
161. Bals, R., D. J. Weiner, R. L. Meegalla, and J. M. Wilson. 1999. Transfer of a cathelicidin peptide antibiotic gene restores bacterial killing in a cystic fibrosis xenograft model. *J Clin Invest* 103:1113-1117.
162. Chen, C. I., S. Schaller-Bals, K. P. Paul, U. Wahn, and R. Bals. 2004. Beta-defensins and LL-37 in bronchoalveolar lavage fluid of patients with cystic fibrosis. *J Cyst Fibros* 3:45-50.
163. Shu, Q., Z. Shi, Z. Zhao, Z. Chen, H. Yao, Q. Chen, A. Hoeft, F. Stuber, and X. Fang. 2006. Protection against *Pseudomonas aeruginosa* pneumonia and sepsis-induced lung injury by overexpression of beta-defensin-2 in rats. *Shock* 26:365-371.
164. Wu, M., S. A. McClellan, R. P. Barrett, and L. D. Hazlett. 2009. Beta-defensin-2 promotes resistance against infection with *P. aeruginosa*. *J Immunol* 182:1609-1616.
165. Wu, M., S. A. McClellan, R. P. Barrett, Y. Zhang, and L. D. Hazlett. 2009. Beta-defensins 2 and 3 together promote resistance to *Pseudomonas aeruginosa* keratitis. *J Immunol* 183:8054-8060.
166. Overhage, J., A. Campisano, M. Bains, E. C. W. Torfs, B. H. A. Rehm, and R. E. W. Hancock. 2008. Human host defense peptide LL-37 prevents bacterial biofilm formation *Infect Immun* 76:4176-4182.
167. Klockgether, J., A. Munder, J. Neugebauer, C. F. Davenport, F. Stanke, K. D. Larbig, S. Heeb, U. Schock, T. M. Pohl, L. Wiehlmann, and B. Tummler. 2010. Genome diversity of *Pseudomonas aeruginosa* PAO1 laboratory strains. *J Bacteriol* 192:1113-1121.
168. Bals, R., D. J. Weiner, A. D. Moscioni, R. L. Meegalla, and J. M. Wilson. 1999. Augmentation of innate host defense by expression of a cathelicidin antimicrobial peptide. *Infect Immun* 67:6084-6089.
169. Beaumont, P. E., B. McHugh, E. Gwyer Findlay, A. Mackellar, K. J. Mackenzie, R. L. Gallo, J. R. Govan, A. J. Simpson, and D. J. Davidson. 2014. Cathelicidin host defence peptide

augments clearance of pulmonary *Pseudomonas aeruginosa* infection by its influence on neutrophil function in vivo. *PLoS One* 9:e99029.

170. Kovach, M. A., M. N. Ballinger, M. W. Newstead, X. Zeng, U. Bhan, F. S. Yu, B. B. Moore, R. L. Gallo, and T. J. Standiford. 2012. Cathelicidin-related antimicrobial peptide is required for effective lung mucosal immunity in Gram-negative bacterial pneumonia. *J Immunol* 189:304-311.
171. Huang, L. C., R. Y. Reins, R. L. Gallo, and A. M. McDermott. 2007. Cathelicidin-deficient (Cnlp -/-) mice show increased susceptibility to *Pseudomonas aeruginosa* keratitis. *Invest Ophthalmol Vis Sci* 48:4498-4508.
172. Cirioni, O., R. Ghiselli, L. Tomasinsig, F. Orlando, C. Silvestri, B. Skerlavaj, A. Riva, M. Rocchi, V. Saba, M. Zanetti, G. Scalise, and A. Giacometti. 2008. Efficacy of LL-37 and granulocyte colony-stimulating factor in a neutropenic murine sepsis due to *Pseudomonas aeruginosa*. *Shock* 30:443-448.
173. Strempel, N., A. Neidig, M. Nusser, R. Geffers, J. Vieillard, O. Lesouhaitier, G. Brenner-Weiss, and J. Overhage. 2013. Human host defense peptide LL-37 stimulates virulence factor production and adaptive resistance in *Pseudomonas aeruginosa*. *PLoS One* 8:e82240.
174. McPhee, J. B., S. Lewenza, and R. E. Hancock. 2003. Cationic antimicrobial peptides activate a two-component regulatory system, PmrA-PmrB, that regulates resistance to polymyxin B and cationic antimicrobial peptides in *Pseudomonas aeruginosa*. *Mol Microbiol* 50:205-217.
175. Fernandez, L., H. Jenssen, M. Bains, I. Wiegand, W. J. Gooderham, and R. E. Hancock. 2012. The two-component system CprRS senses cationic peptides and triggers adaptive resistance in *Pseudomonas aeruginosa* independently of ParRS. *Antimicrob Agents Chemother* 56:6212-6222.
176. Cummins, J., F. J. Reen, C. Baysse, M. J. Mooij, and F. O'Gara. 2009. Subinhibitory concentrations of the cationic antimicrobial peptide colistin induce the pseudomonas quinolone signal in *Pseudomonas aeruginosa*. *Microbiology* 155:2826-2837.
177. Hancock, R. E., A. Nijnik, and D. J. Philpott. 2012. Modulating immunity as a therapy for bacterial infections. *Nat Rev Microbiol* 10:243-254.
178. Vandamme, D., B. Landuyt, W. Luyten, and L. Schoofs. 2012. A comprehensive summary of LL-37, the factotum human cathelicidin peptide. *Cell Immunol* 280:22-35.
179. Lau, Y. E., D. M. Bowdish, C. Cosseau, R. E. Hancock, and D. J. Davidson. 2006. Apoptosis of airway epithelial cells: human serum sensitive induction by the cathelicidin LL-37. *Am J Respir Cell Mol Biol* 34:399-409.
180. Schiemann, F., E. Brandt, R. Gross, B. Lindner, J. Mittelstadt, C. P. Sommerhoff, J. Schulmistrat, and F. Petersen. 2009. The cathelicidin LL-37 activates human mast cells and is degraded by mast cell tryptase: counter-regulation by CXCL4. *J Immunol* 183:2223-2231.
181. Chennupati, S. K., A. G. Chiu, E. Tamashiro, C. A. Banks, M. B. Cohen, B. S. Bleier, J. M. Kofonow, E. Tam, and N. A. Cohen. 2009. Effects of an LL-37-derived antimicrobial peptide in an animal model of biofilm *Pseudomonas* sinusitis. *Am J Rhinol Allergy* 23:46-51.
182. Sawa, T., K. Kurahashi, M. Ohara, M. A. Gropper, V. Doshi, J. W. Larrick, and J. P. Wiener-Kronish. 1998. Evaluation of antimicrobial and lipopolysaccharide-neutralizing effects of a synthetic CAP18 fragment against *Pseudomonas aeruginosa* in a mouse model. *Antimicrob Agents Chemother* 42:3269-3275.
183. Zhang, H., G. Porro, N. Orzech, B. Mullen, M. Liu, and A. S. Slutsky. 2001. Neutrophil defensins mediate acute inflammatory response and lung dysfunction in dose-related fashion. *Am J Physiol Lung Cell Mol Physiol* 280:L947-954.
184. Gronberg, A., M. Mahlapuu, M. Stahle, C. Whately-Smith, and O. Rollman. 2014. Treatment with LL-37 is safe and effective in enhancing healing of hard-to-heal venous leg ulcers: a randomized, placebo-controlled clinical trial. *Wound Repair Regen* 22:613-621.

185. Li, Y. 2011. Recombinant production of antimicrobial peptides in *Escherichia coli*: A review. *Protein Expr Purif* 80:260-267.
186. Nibbering, P. H., E. Ravensbergen, M. M. Welling, L. A. van Berkel, P. H. van Berkel, E. K. Pauwels, and J. H. Nuijens. 2001. Human lactoferrin and peptides derived from its N terminus are highly effective against infections with antibiotic-resistant bacteria. *Infect Immun* 69:1469-1476.
187. Hilpert, K., R. Volkmer-Engert, T. Walter, and R. E. Hancock. 2005. High-throughput generation of small antibacterial peptides with improved activity. *Nat Biotechnol* 23:1008-1012.
188. Hilpert, K., M. R. Elliott, R. Volkmer-Engert, P. Henklein, O. Donini, Q. Zhou, D. F. Winkler, and R. E. Hancock. 2006. Sequence requirements and an optimization strategy for short antimicrobial peptides. *Chem Biol* 13:1101-1107.
189. Wu, M., and R. E. Hancock. 1999. Improved derivatives of bactenecin, a cyclic dodecameric antimicrobial cationic peptide. *Antimicrob Agents Chemother* 43:1274-1276.
190. Scott, M. G., E. Dullaghan, N. Mookherjee, N. Glavas, M. Waldbrook, A. Thompson, A. Wang, K. Lee, S. Doria, P. Hamill, J. J. Yu, Y. Li, O. Donini, M. M. Guarna, B. B. Finlay, J. R. North, and R. E. Hancock. 2007. An anti-infective peptide that selectively modulates the innate immune response. *Nat Biotechnol* 25:465-472.
191. Yu, H. B., A. Kielczewska, A. Rozek, S. Takenaka, Y. Li, L. Thorson, R. E. Hancock, M. M. Guarna, J. R. North, L. J. Foster, O. Donini, and B. B. Finlay. 2009. Sequestosome-1/p62 is the key intracellular target of innate defense regulator peptide. *J Biol Chem* 284:36007-36011.
192. Nijnik, A., L. Madera, S. Ma, M. Waldbrook, M. R. Elliot, D. M. Easton, M. L. Mayer, S. C. Mullaly, J. Kindrachuk, H. Jenssen, and R. E. W. Hancock. 2010. Synthetic cationic peptide IDR-1002 provides protection against bacterial infections through chemokine induction and enhanced leukocyte recruitment. *J Immunol* 184:2539-2550.
193. Polewicz, M., A. Gracia, S. Garlapati, J. van Kessel, S. Strom, S. A. Halperin, R. E. Hancock, A. A. Potter, L. A. Babiuk, and V. Gerdts. 2013. Novel vaccine formulations against pertussis offer earlier onset of immunity and provide protection in the presence of maternal antibodies. *Vaccine* 31:3148-3155.
194. Garlapati, S., N. F. Eng, T. G. Kiros, J. Kindrachuk, G. K. Mutwiri, R. E. Hancock, S. A. Halperin, A. A. Potter, L. A. Babiuk, and V. Gerdts. 2011. Immunization with PCEP microparticles containing pertussis toxoid, CpG ODN and a synthetic innate defense regulator peptide induces protective immunity against pertussis. *Vaccine* 29:6540-6548.
195. Haney, E. F., S. C. Mansour, A. L. Hilchie, C. de la Fuente-Nunez, and R. E. Hancock. 2015. High throughput screening methods for assessing antibiofilm and immunomodulatory activities of synthetic peptides. *Peptides* 71:276-285.
196. de la Fuente-Nunez, C., F. Reffuveille, S. C. Mansour, S. L. Reckseidler-Zenteno, D. Hernandez, G. Brackman, T. Coenye, and R. E. Hancock. 2015. D-enantiomeric peptides that eradicate wild-type and multidrug-resistant biofilms and protect against lethal *Pseudomonas aeruginosa* infections. *Chem Biol* 22:196-205.
197. Kindrachuk, J., H. Jenssen, M. Elliott, R. Townsend, A. Nijnik, S. F. Lee, V. Gerdts, L. A. Babiuk, S. A. Halperin, and R. E. Hancock. 2009. A novel vaccine adjuvant comprised of a synthetic innate defence regulator peptide and CpG oligonucleotide links innate and adaptive immunity. *Vaccine* 27:4662-4671.
198. Hou, M., N. Zhang, J. Yang, X. Meng, R. Yang, J. Li, and T. Sun. 2013. Antimicrobial peptide LL-37 and IDR-1 ameliorate MRSA pneumonia in vivo. *Cell Physiol Biochem* 32:614-623.
199. Pane, K., V. Sgambati, A. Zanfardino, G. Smaldone, V. Cafaro, T. Angrisano, E. Pedone, S. Di Gaetano, D. Capasso, E. F. Haney, V. Izzo, M. Varcamonti, E. Notomista, R. E. Hancock, A. Di Donato, and E. Pizzo. 2016. A new cryptic cationic antimicrobial peptide from human

apolipoprotein E with antibacterial activity and immunomodulatory effects on human cells. *FEBS J* 283:2115-2131.
200. Achtman, A. H., S. Pilat, C. W. Law, D. J. Lynn, L. Janot, M. L. Mayer, S. Ma, J. Kindrachuk, B. B. Finlay, F. S. Brinkman, G. K. Smyth, R. E. Hancock, and L. Schofield. 2012. Effective adjunctive therapy by an innate defense regulatory peptide in a preclinical model of severe malaria. *Sci Transl Med* 4:135ra164.
201. Niyonsaba, F., L. Madera, N. Afacan, K. Okumura, H. Ogawa, and R. E. Hancock. 2013. The innate defense regulator peptides IDR-HH2, IDR-1002, and IDR-1018 modulate human neutrophil functions. *J Leukoc Biol* 94:159-170.
202. Pena, O. M., N. Afacan, J. Pistolic, C. Chen, L. Madera, R. Falsafi, C. D. Fjell, and R. E. Hancock. 2013. Synthetic cationic peptide IDR-1018 modulates human macrophage differentiation. *PLoS One* 8:e52449.
203. Mayer, M. L., C. J. Blohmke, R. Falsafi, C. D. Fjell, L. Madera, S. E. Turvey, and R. E. Hancock. 2013. Rescue of dysfunctional autophagy attenuates hyperinflammatory responses from cystic fibrosis cells. *J Immunol* 190:1227-1238.
204. Wieczorek, M., H. Jenssen, J. Kindrachuk, W. R. P. Scott, M. R. Elliot, K. Hilpert, J. T. J. Cheng, R. E. W. Hancock, and S. K. Straus. 2010. Structural studies of a peptide with immune modulating and direct antimicrobial activity. *Chem Biol* 17:970-980.
205. Steinstraesser, L., T. Hirsch, M. Schulte, M. Kueckelhaus, F. Jacobsen, E. A. Mersch, I. Stricker, N. Afacan, H. Jenssen, R. E. Hancock, and J. Kindrachuk. 2012. Innate defense regulator peptide 1018 in wound healing and wound infection. *PLoS One* 7:e39373.
206. Rivas-Santiago, B., J. E. Castaneda-Delgado, C. E. Rivas Santiago, M. Waldbrook, I. Gonzalez-Curiel, J. C. Leon-Contreras, J. A. Enciso-Moreno, V. del Villar, J. Mendez-Ramos, R. E. Hancock, and R. Hernandez-Pando. 2013. Ability of innate defence regulator peptides IDR-1002, IDR-HH2 and IDR-1018 to protect against *Mycobacterium tuberculosis* infections in animal models. *PLoS One* 8:e59119.
207. Choe, H., A. S. Narayanan, D. A. Gandhi, A. Weinberg, R. E. Marcus, Z. Lee, R. A. Bonomo, and E. M. Greenfield. 2015. Immunomodulatory peptide IDR-1018 decreases implant infection and preserves osseointegration. *Clin Orthop Relat Res* 473:2898-2907.
208. Bolouri, H., K. Savman, W. Wang, A. Thomas, N. Maurer, E. Dullaghan, C. D. Fjell, C. J. Ek, H. Hagberg, R. E. Hancock, K. L. Brown, and C. Mallard. 2014. Innate defense regulator peptide 1018 protects against perinatal brain injury. *Ann Neurol* 75:395-410.
209. Reffuveille, F., C. de la Fuente-Nunez, S. Mansour, and R. E. Hancock. 2014. A broad-spectrum antibiofilm peptide enhances antibiotic action against bacterial biofilms. *Antimicrob Agents Chemother* 58:5363-5371.
210. Wang, Z., C. de la Fuente-Nunez, Y. Shen, M. Haapasalo, and R. E. Hancock. 2015. Treatment of oral multispecies biofilms by an anti-biofilm peptide. *PLoS One* 10:e0132512.
211. de la Fuente-Nunez, C., F. Reffuveille, E. F. Haney, S. K. Straus, and R. E. Hancock. 2014. Broad-spectrum anti-biofilm peptide that targets a cellular stress response. *PLoS Pathog* 10:e1004152.
212. Chow, L. N., K. Y. Choi, H. Piyadasa, M. Bossert, J. Uzonna, T. Klonisch, and N. Mookherjee. 2014. Human cathelicidin LL-37-derived peptide IG-19 confers protection in a murine model of collagen-induced arthritis. *Mol Immunol* 57:86-92.
213. Madera, L., and R. E. Hancock. 2012. Synthetic immunomodulatory peptide IDR-1002 enhances monocyte migration and adhesion on fibronectin. *J Innate Immun* 4:553-568.
214. Madera, L., and R. E. Hancock. 2015. Anti-infective peptide IDR-1002 augments monocyte chemotaxis towards CCR5 chemokines. *Biochem Biophys Res Commun* 464:800-806.
215. Turner-Brannen, E., K. Y. Choi, D. N. Lippert, J. P. Cortens, R. E. Hancock, H. El-Gabalawy, and N. Mookherjee. 2011. Modulation of interleukin-1beta-induced inflammatory responses

by a synthetic cationic innate defence regulator peptide, IDR-1002, in synovial fibroblasts. *Arthritis Res Ther* 13:R129.

216. Liechty, W. B., D. R. Kryscio, B. V. Slaughter, and N. A. Peppas. 2010. Polymers for Drug Delivery Systems. *Annu Rev Chem Biomol Eng* 1:149-173.
217. Mardirossian, M., A. Pompilio, V. Crocetta, S. De Nicola, F. Guida, M. Degasperi, R. Gennaro, G. Di Bonaventura, and M. Scocchi. 2016. In vitro and in vivo evaluation of BMAP-derived peptides for the treatment of cystic fibrosis-related pulmonary infections. *Amino Acids* 48:2253-2260.
218. Zhang, L., J. Parente, S. M. Harris, D. E. Woods, R. E. Hancock, and T. J. Falla. 2005. Antimicrobial peptide therapeutics for cystic fibrosis. *Antimicrob Agents Chemother* 49:2921-2927.
219. Song, Z., H. Wu, P. Mygind, D. Raventos, C. Sonksen, H. H. Kristensen, and N. Hoiby. 2005. Effects of intratracheal administration of novispirin G10 on a rat model of mucoid *Pseudomonas aeruginosa* lung infection. *Antimicrob Agents Chemother* 49:3868-3874.
220. Bartlett, K. H., P. B. McCray, Jr., and P. S. Thorne. 2003. Novispirin G10-induced lung toxicity in a *Klebsiella pneumoniae* infection model. *Antimicrob Agents Chemother* 47:3901-3906.
221. Wangdi, T., L. A. Mijares, and B. I. Kazmierczak. 2010. In vivo discrimination of type 3 secretion system-positive and -negative *Pseudomonas aeruginosa* via a caspase-1-dependent pathway. *Infect Immun* 78:4744-4753.
222. Marden, J. N., M. R. Diaz, W. G. Walton, C. J. Gode, L. Betts, M. L. Urbanowski, M. R. Redinbo, T. L. Yahr, and M. C. Wolfgang. 2013. An unusual CsrA family member operates in series with RsmA to amplify posttranscriptional responses in *Pseudomonas aeruginosa*. *Proc Natl Acad Sci U S A* 110:15055-15060.
223. Liu, P. V. 1966. The roles of various fractions of *Pseudomonas aeruginosa* in its pathogenesis. II. Effects of lecithinase and protease. *J Infect Dis* 116:112-116.
224. Liu, P. V. 1966. The roles of various fractions of *Pseudomonas aeruginosa* in its pathogenesis. 3. Identity of the lethal toxins produced in vitro and in vivo. *J Infect Dis* 116:481-489.
225. Soscia, C., A. Hachani, A. Bernadac, A. Filloux, and S. Bleves. 2007. Cross talk between type III secretion and flagellar assembly systems in *Pseudomonas aeruginosa*. *J Bacteriol* 189:3124-3132.
226. Diaz, M. H., C. M. Shaver, J. D. King, S. Musunuri, J. A. Kazzaz, and A. R. Hauser. 2008. *Pseudomonas aeruginosa* induces localized immunosuppression during pneumonia. *Infect Immun* 76:4414-4421.
227. Kurahashi, K., O. Kajikawa, T. Sawa, M. Ohara, M. A. Gropper, D. W. Frank, T. R. Martin, and J. P. Wiener-Kronish. 1999. Pathogenesis of septic shock in *Pseudomonas aeruginosa* pneumonia. *J Clin Invest* 104:743-750.
228. Kukavica-Ibrulj, I., and R. C. Levesque. 2008. Animal models of chronic lung infection with *Pseudomonas aeruginosa*: useful tools for cystic fibrosis studies. *Lab Anim* 42:389-412.
229. van Heeckeren, A. M., and M. D. Schluchter. 2002. Murine models of chronic *Pseudomonas aeruginosa* lung infection. *Lab Anim* 36:291-312.
230. Hoffmann, N., T. B. Rasmussen, P. O. Jensen, C. Stub, M. Hentzer, S. Molin, O. Ciofu, M. Givskov, H. K. Johansen, and N. Hoiby. 2005. Novel mouse model of chronic *Pseudomonas aeruginosa* lung infection mimicking cystic fibrosis. *Infect Immun* 73:2504-2514.
231. Hoffmann, N., B. Lee, M. Hentzer, T. B. Rasmussen, Z. Song, H. K. Johansen, M. Givskov, and N. Hoiby. 2007. Azithromycin blocks quorum sensing and alginate polymer formation and increases the sensitivity to serum and stationary-growth-phase killing of *Pseudomonas aeruginosa* and attenuates chronic *P. aeruginosa* lung infection in Cftr(-/-) mice. *Antimicrob Agents Chemother* 51:3677-3687.

232. Sabet, M., C. E. Miller, T. G. Nolan, K. Senekeo-Effenberger, M. N. Dudley, and D. C. Griffith. 2009. Efficacy of aerosol MP-376, a levofloxacin inhalation solution, in models of mouse lung infection due to *Pseudomonas aeruginosa*. *Antimicrob Agents Chemother* 53:3923-3928.
233. Winstanley, C., M. G. Langille, J. L. Fothergill, I. Kukavica-Ibrulj, C. Paradis-Bleau, F. Sanschagrin, N. R. Thomson, G. L. Winsor, M. A. Quail, N. Lennard, A. Bignell, L. Clarke, K. Seeger, D. Saunders, D. Harris, J. Parkhill, R. E. Hancock, F. S. Brinkman, and R. C. Levesque. 2009. Newly introduced genomic prophage islands are critical determinants of in vivo competitiveness in the Liverpool Epidemic Strain of *Pseudomonas aeruginosa*. *Genome Res* 19:12-23.
234. Cheng, K., R. L. Smyth, J. R. Govan, C. Doherty, C. Winstanley, N. Denning, D. P. Heaf, H. van Saene, and C. A. Hart. 1996. Spread of beta-lactam-resistant *Pseudomonas aeruginosa* in a cystic fibrosis clinic. *Lancet* 348:639-642.
235. Al-Aloul, M., J. Crawley, C. Winstanley, C. A. Hart, M. J. Ledson, and M. J. Walshaw. 2004. Increased morbidity associated with chronic infection by an epidemic *Pseudomonas aeruginosa* strain in CF patients. *Thorax* 59:334-336.
236. Kukavica-Ibrulj, I., A. Bragonzi, M. Paroni, C. Winstanley, F. Sanschagrin, G. A. O'Toole, and R. C. Levesque. 2008. In vivo growth of *Pseudomonas aeruginosa* strains PAO1 and PA14 and the hypervirulent strain LESB58 in a rat model of chronic lung infection. *J Bacteriol* 190:2804-2813.
237. Darveau, R. P., and R. E. Hancock. 1983. Procedure for isolation of bacterial lipopolysaccharides from both smooth and rough *Pseudomonas aeruginosa* and *Salmonella typhimurium* strains. *J Bacteriol* 155:831-838.
238. Ray, A., and B. N. Dittel. 2010. Isolation of mouse peritoneal cavity cells. *J Vis Exp*.
239. Schilbach, K., K. Frommer, S. Meier, R. Handgretinger, and M. Eyrich. 2008. Immune response of human propagated gammadelta-T-cells to neuroblastoma recommend the Vdelta1+ subset for gammadelta-T-cell-based immunotherapy. *J Immunother* 31:896-905.
240. Skerrett, S. J., C. B. Wilson, H. D. Liggitt, and A. M. Hajjar. 2007. Redundant Toll-like receptor signaling in the pulmonary host response to *Pseudomonas aeruginosa*. *Am J Physiol Lung Cell Mol Physiol* 292:L312-322.
241. Applequist, S. E., R. P. Wallin, and H. G. Ljunggren. 2002. Variable expression of Toll-like receptor in murine innate and adaptive immune cell lines. *Int Immunol* 14:1065-1074.
242. Filewod, N. C., J. Pistolic, and R. E. Hancock. 2009. Low concentrations of LL-37 alter IL-8 production by keratinocytes and bronchial epithelial cells in response to proinflammatory stimuli. *FEMS Immunol Med Microbiol* 56:233-240.
243. Inomata, M., T. Into, and Y. Murakami. 2010. Suppressive effect of the antimicrobial peptide LL-37 on expression of IL-6, IL-8 and CXCL10 induced by *Porphyromonas gingivalis* cells and extracts in human gingival fibroblasts. *Eur J Oral Sci* 118:574-581.
244. Barlow, P. G., P. E. Beaumont, C. Cosseau, A. Mackellar, T. S. Wilkinson, R. E. Hancock, C. Haslett, J. R. Govan, A. J. Simpson, and D. J. Davidson. 2010. The human cathelicidin LL-37 preferentially promotes apoptosis of infected airway epithelium. *Am J Respir Cell Mol Biol* 43:692-702.
245. Horn, M., A. Bertling, M. F. Brodde, A. Muller, J. Roth, H. Van Aken, K. Jurk, C. Heilmann, G. Peters, and B. E. Kehrel. 2012. Human neutrophil alpha-defensins induce formation of fibrinogen and thrombospondin-1 amyloid-like structures and activate platelets via glycoprotein IIb/IIIa. *J Thromb Haemost* 10:647-661.
246. Li, Y., X. Li, H. Li, O. Lockridge, and G. Wang. 2007. A novel method for purifying recombinant human host defense cathelicidin LL-37 by utilizing its inherent property of aggregation. *Protein Expr Purif* 54:157-165.

247. Auvynet, C., C. El Amri, C. Lacombe, F. Bruston, J. Bourdais, P. Nicolas, and Y. Rosenstein. 2008. Structural requirements for antimicrobial versus chemoattractant activities for dermaseptin S9. *FEBS J* 275:4134-4151.
248. Aguzzi, A., and T. O'Connor. 2010. Protein aggregation diseases: pathogenicity and therapeutic perspectives. *Nat Rev Drug Discov* 9:237-248.
249. Bucciantini, M., E. Giannoni, F. Chiti, F. Baroni, L. Formigli, J. Zurdo, N. Taddei, G. Ramponi, C. M. Dobson, and M. Stefani. 2002. Inherent toxicity of aggregates implies a common mechanism for protein misfolding diseases. *Nature* 416:507-511.
250. Doig, A. J., and P. Derreumaux. 2015. Inhibition of protein aggregation and amyloid formation by small molecules. *Curr Opin Struct Biol* 30:50-56.
251. Tripodo, G., A. Trapani, M. L. Torre, G. Giammona, G. Trapani, and D. Mandracchia. 2015. Hyaluronic acid and its derivatives in drug delivery and imaging: recent advances and challenges. *Eur J Pharm Biopharm* 97:400-416.
252. Kainthan, R. K., and D. E. Brooks. 2007. In vivo biological evaluation of high molecular weight hyperbranched polyglycerols. *Biomaterials* 28:4779-4787.
253. Frey, H., and R. Haag. 2002. Dendritic polyglycerol: a new versatile biocompatible-material. *J Biotechnol* 90:257-267.
254. Jain, N. K., and I. Roy. 2009. Effect of trehalose on protein structure. *Protein Sci* 18:24-36.
255. Soscia, S. J., J. E. Kirby, K. J. Washicosky, S. M. Tucker, M. Ingelsson, B. Hyman, M. A. Burton, L. E. Goldstein, S. Duong, R. E. Tanzi, and R. D. Moir. 2010. The Alzheimer's disease-associated amyloid beta-protein is an antimicrobial peptide. *PLoS One* 5:e9505.
256. Salminen, A., J. Ojala, A. Kauppinen, K. Kaarniranta, and T. Suuronen. 2009. Inflammation in Alzheimer's disease: amyloid-beta oligomers trigger innate immunity defence via pattern recognition receptors. *Prog Neurobiol* 87:181-194.
257. Afacan, N., A. Hilchie, E. E. Gill, R. Falsafi, and R. E. W. Hancock. 2016. 2-Deoxyglucose modulates innate defence regulator peptide activity. *Cellular Immunology & Immunotherapeutics* 1:1-8.
258. Huang, L. C., D. Jean, and A. M. McDermott. 2005. Effect of preservative-free artificial tears on the antimicrobial activity of human beta-defensin-2 and cathelicidin LL-37 in vitro. *Eye Contact Lens* 31:34-38.
259. Haisma, E. M., A. Goblyos, B. Ravensbergen, A. E. Adriaans, R. A. Cordfunke, J. Schrumpf, R. W. Limpens, K. J. Schimmel, J. den Hartigh, P. S. Hiemstra, J. W. Drijfhout, A. El Ghalbzouri, and P. H. Nibbering. 2016. Antimicrobial peptide P60.4Ac-containing creams and gel for eradication of methicillin-resistant *Staphylococcus aureus* from cultured skin and airway epithelial surfaces. *Antimicrob Agents Chemother* 60:4063-4072.
260. Mugabe, C., P. A. Raven, L. Fazli, J. H. Baker, J. K. Jackson, R. T. Liggins, A. I. So, M. E. Gleave, A. I. Minchinton, D. E. Brooks, and H. M. Burt. 2012. Tissue uptake of docetaxel loaded hydrophobically derivatized hyperbranched polyglycerols and their effects on the morphology of the bladder urothelium. *Biomaterials* 33:692-703.
261. Kumar, P., R. A. Shenoi, B. F. Lai, M. Nguyen, J. N. Kizhakkedathu, and S. K. Straus. 2015. Conjugation of aurein 2.2 to HPG yields an antimicrobial with better properties. *Biomacromolecules* 16:913-923.
262. Konig, S., F. Nitzki, A. Uhmann, K. Dittmann, J. Theiss-Suennemann, M. Herrmann, H. M. Reichardt, R. Schwendener, T. Pukrop, W. Schulz-Schaeffer, and H. Hahn. 2014. Depletion of cutaneous macrophages and dendritic cells promotes growth of basal cell carcinoma in mice. *PLoS One* 9:e93555.
263. Flores-Langarica, A., J. L. Marshall, S. Bobat, E. Mohr, J. Hitchcock, E. A. Ross, R. E. Coughlan, M. Khan, N. Van Rooijen, I. R. Henderson, I. C. Maclennan, and A. F. Cunningham.

2011. T-zone localized monocyte-derived dendritic cells promote Th1 priming to Salmonella. *Eur J Immunol* 41:2654-2665.
264. van Dijk, E. L., H. Auger, Y. Jaszczyszyn, and C. Thermes. 2014. Ten years of next-generation sequencing technology. *Trends Genet* 30:418-426.
265. Evans, S. E., M. J. Tuvim, J. Zhang, D. T. Larson, C. D. Garcia, S. M. Pro, K. R. Coombes, and B. F. Dickey. 2010. Host lung gene expression patterns predict infectious etiology in a mouse model of pneumonia. *Respir Res* 11:101.
266. Lewis, C. C., J. Y. Yang, X. Huang, S. K. Banerjee, M. R. Blackburn, P. Baluk, D. M. McDonald, T. S. Blackwell, V. Nagabhushanam, W. Peters, D. Voehringer, and D. J. Erle. 2008. Disease-specific gene expression profiling in multiple models of lung disease. *Am J Respir Crit Care Med* 177:376-387.
267. Damron, F. H., A. G. Oglesby-Sherrouse, A. Wilks, and M. Barbier. 2016. Dual-seq transcriptomics reveals the battle for iron during *Pseudomonas aeruginosa* acute murine pneumonia. *Sci Rep* 6:39172.
268. Dobin, A., C. A. Davis, F. Schlesinger, J. Drenkow, C. Zaleski, S. Jha, P. Batut, M. Chaisson, and T. R. Gingeras. 2013. STAR: ultrafast universal RNA-seq aligner. *Bioinformatics* 29:15-21.
269. Anders, S., P. T. Pyl, and W. Huber. 2015. HTSeq--a Python framework to work with high-throughput sequencing data. *Bioinformatics* 31:166-169.
270. Huber, W., V. J. Carey, R. Gentleman, S. Anders, M. Carlson, B. S. Carvalho, H. C. Bravo, S. Davis, L. Gatto, T. Girke, R. Gottardo, F. Hahne, K. D. Hansen, R. A. Irizarry, M. Lawrence, M. I. Love, J. MacDonald, V. Obenchain, A. K. Oles, H. Pages, A. Reyes, P. Shannon, G. K. Smyth, D. Tenenbaum, L. Waldron, and M. Morgan. 2015. Orchestrating high-throughput genomic analysis with Bioconductor. *Nat Methods* 12:115-121.
271. Love, M. I., W. Huber, and S. Anders. 2014. Moderated estimation of fold change and dispersion for RNA-seq data with DESeq2. *Genome Biol* 15:550.
272. Xia, J., M. J. Benner, and R. E. Hancock. 2014. NetworkAnalyst--integrative approaches for protein-protein interaction network analysis and visual exploration. *Nucleic Acids Res* 42:W167-174.
273. Consortium, G. O. 2015. Gene Ontology Consortium: going forward. *Nucleic Acids Res* 43:D1049-1056.
274. Mudunuri, U., A. Che, M. Yi, and R. M. Stephens. 2009. bioDBnet: the biological database network. *Bioinformatics* 25:555-556.
275. Oliveros, J. C. 2007-2015. Venny. An interactive tool for comparing lists with Venn's diagrams. .
276. Xiao, L., Y. Zhang, S. S. Berr, M. D. Chordia, P. Pramoonjago, L. Pu, and D. Pan. 2012. A novel near-infrared fluorescence imaging probe for in vivo neutrophil tracking. *Mol Imaging* 11:372-382.
277. Frantz, C., K. M. Stewart, and V. M. Weaver. 2010. The extracellular matrix at a glance. *J Cell Sci* 123:4195-4200.
278. Lee, L. Y., and J. Yu. 2014. Sensory nerves in lung and airways. *Compr Physiol* 4:287-324.
279. Nasarre, P., V. Potiron, H. Drabkin, and J. Roche. 2010. Guidance molecules in lung cancer. *Cell Adh Migr* 4:130-145.
280. Greenlee, K. J., Z. Werb, and F. Kheradmand. 2007. Matrix metalloproteinases in lung: multiple, multifarious, and multifaceted. *Physiol Rev* 87:69-98.
281. Roos, A. B., and M. Nord. 2012. The emerging role of C/EBPs in glucocorticoid signaling: lessons from the lung. *J Endocrinol* 212:291-305.

282. Chadban, S. J., G. H. Tesch, R. Foti, H. Y. Lan, R. C. Atkins, and D. J. Nikolic-Paterson. 1998. Interleukin-10 differentially modulates MHC class II expression by mesangial cells and macrophages in vitro and in vivo. *Immunology* 94:72-78.
283. Sun, L., R. F. Guo, M. W. Newstead, T. J. Standiford, D. R. Macariola, and T. P. Shanley. 2009. Effect of IL-10 on neutrophil recruitment and survival after *Pseudomonas aeruginosa* challenge. *Am J Respir Cell Mol Biol* 41:76-84.
284. Durieu, I., S. Peyrol, D. Gindre, G. Bellon, D. V. Durand, and Y. Pacheco. 1998. Subepithelial fibrosis and degradation of the bronchial extracellular matrix in cystic fibrosis. *Am J Respir Crit Care Med* 158:580-588.
285. Gaggar, A., A. Hector, P. E. Bratcher, M. A. Mall, M. Griese, and D. Hartl. 2011. The role of matrix metalloproteases in cystic fibrosis lung disease. *Eur Respir J* 38:721-727.
286. Bergeron, C., and L. P. Boulet. 2006. Structural changes in airway diseases: characteristics, mechanisms, consequences, and pharmacologic modulation. *Chest* 129:1068-1087.
287. Kranenburg, A. R., A. Willems-Widyastuti, W. J. Moori, P. J. Sterk, V. K. Alagappan, W. I. de Boer, and H. S. Sharma. 2006. Enhanced bronchial expression of extracellular matrix proteins in chronic obstructive pulmonary disease. *Am J Clin Pathol* 126:725-735.
288. Parker, D., T. S. Cohen, M. Alhede, B. S. Harfenist, F. J. Martin, and A. Prince. 2012. Induction of type I interferon signaling by *Pseudomonas aeruginosa* is diminished in cystic fibrosis epithelial cells. *Am J Respir Cell Mol Biol* 46:6-13.
289. Decker, T., M. Muller, and S. Stockinger. 2005. The yin and yang of type I interferon activity in bacterial infection. *Nat Rev Immunol* 5:675-687.
290. Power, M. R., B. Li, M. Yamamoto, S. Akira, and T. J. Lin. 2007. A role of Toll-IL-1 receptor domain-containing adaptor-inducing IFN-beta in the host response to *Pseudomonas aeruginosa* lung infection in mice. *J Immunol* 178:3170-3176.
291. Carrigan, S. O., R. Junkins, Y. J. Yang, A. Macneil, C. Richardson, B. Johnston, and T. J. Lin. 2010. IFN regulatory factor 3 contributes to the host response during *Pseudomonas aeruginosa* lung infection in mice. *J Immunol* 185:3602-3609.
292. Wainwright, C. E., J. S. Elborn, and B. W. Ramsey. 2015. Lumacaftor-Ivacaftor in patients with cystic fibrosis homozygous for Phe508del CFTR. *N Engl J Med* 373:1783-1784.
293. Castellani, C., H. Cuppens, M. Macek, Jr., J. J. Cassiman, E. Kerem, P. Durie, E. Tullis, B. M. Assael, C. Bombieri, A. Brown, T. Casals, M. Claustres, G. R. Cutting, E. Dequeker, J. Dodge, I. Doull, P. Farrell, C. Ferec, E. Girodon, M. Johannesson, B. Kerem, M. Knowles, A. Munck, P. F. Pignatti, D. Radojkovic, P. Rizzotti, M. Schwarz, M. Stuhrmann, M. Tzetis, J. Zielenski, and J. S. Elborn. 2008. Consensus on the use and interpretation of cystic fibrosis mutation analysis in clinical practice. *J Cyst Fibros* 7:179-196.
294. Nizet, V., T. Ohtake, X. Lauth, J. Trowbridge, J. Rudisill, R. A. Dorschner, V. Pestonjamasp, J. Piraino, K. Huttner, and R. L. Gallo. 2001. Innate antimicrobial peptide protects the skin from invasive bacterial infection. *Nature* 414:454-457.
295. Gill, E. E., O. L. Franco, and R. E. Hancock. 2015. Antibiotic adjuvants: diverse strategies for controlling drug-resistant pathogens. *Chem Biol Drug Des* 85:56-78.
296. Craik, D. J., D. P. Fairlie, S. Liras, and D. Price. 2013. The future of peptide-based drugs. *Chem Biol Drug Des* 81:136-147.
297. Bruno, B. J., G. D. Miller, and C. S. Lim. 2013. Basics and recent advances in peptide and protein drug. *Ther Deliv* 4:1443-1467.
298. Illum, L. 2002. Nasal drug delivery: new developments and strategies. *Drug Discov Today* 7:1184-1189.
299. Casettari, L., and L. Illum. 2014. Chitosan in nasal delivery systems for therapeutic drugs. *J Control Release* 190:189-200.

300. De Jong, W. H., and P. J. A. Borm. 2008. Drug delivery and nanoparticles: Applications and hazards. *Int J Nanomedicine* 3:133-149.
301. Kumar, A., S. S. Kolar, M. Zao, A. M. McDermott, and C. Cai. 2011. Localization of antimicrobial peptides on polymerized liposomes leading to their enhanced efficacy against *Pseudomonas aeruginosa*. *Mol Biosyst* 7:711-713.
302. Allen, T. M., and P. R. Cullis. 2013. Liposomal drug delivery systems: from concept to clinical applications. *Adv Drug Deliv Rev* 65:36-48.
303. Serafini, N., C. A. Vosshenrich, and J. P. Di Santo. 2015. Transcriptional regulation of innate lymphoid cell fate. *Nat Rev Immunol* 15:415-428.
304. Keiser, N. W., and J. F. Engelhardt. 2011. New animal models of cystic fibrosis: what are they teaching us? *Curr Opin Pulm Med* 17:478-483.

Appendices

Appendix A Scoring sheet for in vivo *P. aeruginosa* lung model

Category	Grade	Description
Warmth	0	Normal
	1	Slightly cool to touch
	3	Cool to touch
	5	Cold to touch and/or pale extremities
Fur	0	Normal
	1	Lack of grooming
	2	Slight piloerection
	3	Moderate piloerection (around head/neck)
	4	Severe piloerection (entire body)
Eyes	0	Normal
	2	Dull or squinted
	3	Discharge
	4	Sunken
Hunching	0	Normal
	2	Hunching (mild, intermittent)
	3	Hunching (moderate, persistent)
	4	Hunching (severe)
Activity	0	Normal
	1	Possible reduced activity
	2	Reduced activity
	3	Lethargic (no movement when cage moved)
	4	Lethargic, moves only when touched
	5	Non-responsive and/or persistent shaking
Breathing	0	Normal
	2	Shallow/rapid breathing (intermittent)
	3	Shallow/rapid breathing (continuous)
	4	Increased respiratory effort
	5	Gasping, extreme difficulty breathing